General Disclaimer

One or more of the Following Statements may affect this Document

- This document has been reproduced from the best copy furnished by the organizational source. It is being released in the interest of making available as much information as possible.

- This document may contain data, which exceeds the sheet parameters. It was furnished in this condition by the organizational source and is the best copy available.

- This document may contain tone-on-tone or color graphs, charts and/or pictures, which have been reproduced in black and white.

- This document is paginated as submitted by the original source.

- Portions of this document are not fully legible due to the historical nature of some of the material. However, it is the best reproduction available from the original submission.

5

NASA CR-
144480

E 7. 6 - 1 0.2 07

Dynamics of Plankton Populations in Upwelling Areas

Final Report of Skylab EREP Investigation 518

DR. KARL-HEINZ SZEKIELDA
College of Marine Studies
University of Delaware

CMS-NASA-C-1-75

DR. K. SZEKIELDA
PRINCIPAL INVESTIGATOR

FEB 1976
RECEIVED
NASA STI FACILITY
PUT BRANCH

Project from
March 19, 1973 to July 31, 1975
Under Contract No. NAS 9-13344

DYNAMICS OF PLANKTON POPULATIONS IN UPWELLING AREAS

Number of Investigation:	Skylab EREP Investigation 518
Period Covered:	March 19, 1973 – July 21, 1975
Contract Number:	NAS 9-13344
Principal Investigations Management Office:	Lyndon B. Johnson Space Center
Technical Monitor:	Zack H. Byrns
Principal Investigator:	Dr. Karl-Heinz Szekielda
Sponsoring Institution:	College of Marine Studies University of Delaware
Type of Report:	Final Report

3

Table of Contents

Overview

Skylab, with its newly-developed sensors aboard, gave a very challenging opportunity to investigate oceanic areas, especially regions of upwelling, a major source for the world's fisheries. Due to many technical problems which had to be overcome during the space mission, much of the data necessary to meet the original objectives of the proposed studies could not be obtained, even with repeated coverage of the test site. Fortunately, additional coverage was obtained by ERTS-1, giving very good insight into the possible dynamics of color gradients in the oceans.

The planned cooperation with multiship cruises could not be scheduled simultaneously because of other priorities during the spacecraft's missions. However, significant results during aircraft missions and in laboratory experiments have led to a better understanding of the water mass structure recognized in the Skylab data. Many failures, such as useless recordings with the S191, led to waste of man power. On the other hand, we gained information which never could have been acquired by conventional methods.

Dr. Karl-Heinz Szekielda

PART I:

SKYLAB INVESTIGATION OF THE UPWELLING

OFF THE NORTHWEST COAST OF AFRICA

by

Karl-Heinz Szekielda
Dennis J. Suszkowski
Paul S. Tabor

College of Marine Studies
University of Delaware
Newark, Delaware 19711

Table of Contents

Titles of Figures

ABSTRACT

The upwelling off the NW coast of Africa in the vicinity of Cape Blanc was studied in February – March 1974 from aircraft and in September 1973 from Skylab. The aircraft study was designed to determine the effectiveness of a differential radiometer in quantifying surface chlorophyll concentrations. Photographic images of the S190A Multispectral Camera and the S190B Earth Terrain Camera from Skylab were used to study distributional patterns of suspended material and to locate ocean color boundaries. The thermal channel of the S192 Multispectral Scanner was used to map sea-surface temperature distributions off Cape Blanc. Correlating ocean color changes with temperature gradients is an effective method of qualitatively estimating biological productivity in the upwelling region off Africa.

INTRODUCTION

From a practical standpoint, phytoplankton is a very important life form in the ocean, since primary productivity can be directly related to potential production of commercial fish. In upwelling regions of the world, such as off the northwest coast of Africa, wind stress produces an offshore movement of surface waters which are replaced by cooler, nutrient-rich subsurface waters. These upwelled waters are an excellent medium for the propagation of phytoplankton. Though upwelling regions comprise only about one-tenth of one percent of the ocean surface, Ryther (1969) estimates that they produce about half of the world's fish supply.

When studying plankton over large areas of the ocean, oceanographers face serious logistics problems. Since it may take several days to several weeks to cover a large study area by ship, the best that can be hoped for is

a time-averaged picture of plankton distributions. The ship sampling program may miss patches of plankton of significant interest and the concentrations may be changing rapidly over time. Since large surface areas of the ocean can be easily seen from space, the possibility of synoptically determining plankton quantities and distributions from earth orbit is extremely attractive.

On September 4, 1975, the Skylab spacecraft passed directly over the Cape Blanc section of NW Africa. This report will summarize the interpretation to date of radiometeric data derived from Skylab as it pertains to plankton distributions off the African coast.

ATMOSPHERIC CONDITIONS

The NW coast of Africa can be effectively studied from space, since favorable meteorological conditions are present throughout most of the year. During winter in the Northern Hemisphere, a high pressure system is centered between the Canary Islands and the Azores. In summer, this system extends further to the north and west. Therefore, the coast of Africa experiences clear weather during most of the year with extremely good horizontal and vertical visibility.

The NE trade winds are responsible for the upwelling conditions off the NW African coast. During the summer months when the Trades are located between 15°N and 35°N latitude, the principal component of the winds is northerly, therefore giving rise to the most intense upwelling conditions. (Szekielda, 1973).

Figure 1 shows a Nimbus 5 thermal image of the NW coast of Africa taken September 2, 1973, two days prior to the Skylab overpass. The clear conditions surrounding Cape Blanc indicate the influence of the offshore anticyclone and the low-moisture NE trade winds. The band of thick clouds to the south represents the Intertropical Convergence Zone.

SPECTRAL PROPERTIES OF PLANKTON

Light penetration in water is affected by plankton, algae, and dissolved and suspended matter. As a result, the composition of backscattered light from the air-sea interface is determined by the nature of the constituents in the water column. In contrast to the absorption spectrum of chemically-pure chlorophyll in solution, algae suspensions absorb and scatter light more uniformly throughout the visible part of the electromagnetic spectrum. Because of the spectral absorption and scattering properties of plankton, its concentration can be estimated by measuring the spectral backscattered radiance over water.

When monitoring plankton or biomass from high altitudes, we must consider the fact that algae behave more like a suspension than a pure solution of chlorophyll. As a result, solar light will be scattered at the outer shell of the plankton organisms. The absorption of incident irradiance by the cells depends on their outer structure and the optical density inside the cell. Variation in the optical density or the configuration of the cells may change the intensity of backscattered light even if the incident solar irradiance, sun angle, and chlorophyll concentration per unit of volume remain constant. Yentsch (1960) found that the red absorption band of chlorophyll has little influence on water color. This means that the signal obtained with a red band sensor would record primarily the effect of backscattered light from the organisms.

The intensity of backscattered light caused by plankton and dissolved matter from the ocean as a function of wavelength is given in Figure 2. Gulf Stream water was used as a reference water assuming that the chlorophyll concentration of less than $0.02\mu g \cdot l^{-1}$ does not change significantly the backscattered

light compared to pure water. It was assumed, for the interpretation of the different spectra, the sky conditions, sun angle, and sea state were the same over both sites. The spectrum in Figure 2 is the difference in energy between the spectrum obtained in near-coastal water and the spectrum recorded over the Gulf Stream.

If both water masses had the same optical characteristics and oceanic conditions, the energy difference in both spectra should be equal to zero. Any differences between the two signals would thus be caused by dissolved and/ or particulate matter in the sea. If chlorophyll affected the backscattered light by its absorption properties in the shorter wavelengths, we would expect differences near the absorption bands of chlorophyll.

Chlorophylls have two main absorption maxima in the visible region of the electromagnetic spectrum. The main absorption peaks for pure chlorphyll α are at $0.446\mu m$ and $0.663\mu m$. However, the naturally occuring chlorophyll α types in plants have spectra with peaks near $0.673\mu m$ and $0.683\mu m$. Other forms show maxima near $0.690\mu m$ and $0.710\mu m$.

The spectrum in Figure 2 shows that the first and the second absorption bands of chlorophyll have only a minor influence on the total backscattered light. Strong absorption appears at about $0.72\mu m$, but the maximum of back-scattered light appears at $0.58\mu m$. Considering only the portion between the second absorption band and the near-infrared, it can be seen that only a linear decrease of backscattered light appears. This is an indication that in addition to the absorption of light by chlorophyll, backscattered light from the organisms themselves contributes to the total backscattered energy. Thus, the size and concentration of particles or marine organisms seem to be the important contributors to the changes in backscattered light intensity as measured

in the Skylab sensors. The scattering intensity of suspended particles is proportional to λ^{-n} where λ is the wavelength and n the Rayleigh value which may vary from 4 for pure water to 0 at high turbidity. In other words, the intensity of backscattered light increases with particle concentration. This shows the important influence of particles without chlorophyll on the backscattered light from below the sea surface. Lorenzen (1970) established a correlation between surface chlorophyll concentrations and primary productivity for different oceanic waters. Better correlations were found when chlorophyll and primary productivity data from the upwelling region off the NW coast of Africa were compared. This suggests that a significant relationship between the two parameters can be obtained when individual oceanic regions are studied, thus making surface chlorophyll measurements that much more valuable.

An often suggested algorithm of narrow band ocean color reflectances was employed in an aircraft mission for evaluation of its effectiveness in chlorophyll determination and in recognition of changes in regional ocean color distributions. A ratio of the 0.443μm to the 0.525μm reflectances has been discussed by Clarke and Ewing (1974) and Duntley (1972) as having the ability to determine chlorophyll concentration in near-surface waters from aircraft and satellite altitudes. From these observations Arvesen et.al. (1973) developed a differential correlation radiometric method to detect chlorophyll. Their measurements of ratio values, using the continuous recording differential radiometer, correlated well with real-time sea-truth measurements of surface chlorophyll concentrations. From the results of flights over various types of water masses, a calibration of the reflectance ratio to surface chlorophyll concentrations (mg/m^3) was constructed.

During February and March 1974 the differential radiometric (DR) method was used in an extensive oceanographic aircraft mission as part of the JOINT-I

project in a one square degree region (20° − 21° N latitude x 17° − 18° W long-
itude) offshore of Cape Blanc. In comparison with surface chlorophyll sea-truth,
the DR method was not effective in the determination of chlorophyll off Africa.
Interferences caused by suspended particulates of eolian origin in the surface
waters plus presumed concentrations of Gelbstoff, resulted in an "enhanced"
apparent chlorophyll signal. These interferences can be explained by the
following: 1) Increased backscattered radiance was caused by the high con-
centration of high refractive index (highly reflective) eolian and wave eroded
particulates; 2) Inherent optical properties including absorption by dissolved
Gelbstoff, attenuation of radiance by sea water and particulate scattering (in-
cluding multiple scattering) produced a spectral signal that the ratio method
could not differentiate from that of chlorophyll; 3) Selective scattering by
phytoplankton and high non-selective scattering by the additional particulates
in multiple events produced an increased backscattered signal to the DR which
was an "enhanced" chlorophyll signature. These apparent chlorophyll signals
were investigated in laboratory studies and were found to be principally attri-
buted to the scattering properties of both inorganic particles and algae in
suspension.

Although this color ratio did not effectively determine chlorophyll levels,
there was a strong correlation between sea surface temperature (SST) gradients
and the observed ocean color ratio gradients. Higher ratios were coincident
with low temperature, with only a few nearshore exceptions. A significant cor-
relation of this color ratio and total particulates from sea-truth measurements
does exist and, in addition, increased fishing was observed to be closely associ-
ated with the SST-DR ratio gradients (Tabc~ 1975). Therefore, ocean color
changes associated with sea-surface temperature gradients are indicative of pro-
ductive water masses off the NW coast of Africa.

CAPE BLANC

The hydrography between Cape Blanc and Cape Timiris can be described by the T-S[*] diagram based on 16 stations (Allain, 1970) where data were collected between 0 and 300 m. Two main formations of water masses can be recognized. The first is within the upper 300 m and can be considered a mixture of surface water and Central South Atlantic water with values of 12°C and a salinity of 35.35°/$_{oo}$ at 300 m. The layer between 400 m and 800 m consists mainly of Central North Atlantic water with temperatures between 12°C and 8°C. The influence of Antarctic Intermediate Water is shown by water with a salinity of 35.05°/oo and a temperature of 7°C. Upwelling in this area is limited for water types with temperatures between 18.5°C and 20.5°C and salinities between 35.8 and 35.95°/oo, which show that the upwelling has its origin in the upper 100 m.

The upwelling in the vicinity of Cape Blanc is persistant throughout most of the year and is evident by the high concentrations of chlorophyll noted in Figures 3 and 4. A survey of fish tonnages between Cape Blanc and Cape Timiris was made by Boley (1974) in July of 1973. High concentrations of fish were observed west of Cape Blanc while very high tonnages were noted near Cape Timiris. The tonnages of fish therefore, show some correlation with surface chlorophyll concentrations in this area.

During the September 4, 1973 overpass, Skylab collected radiometric data with the S190A Multispectral Camera, the S190B Earth Terrain Camera and the S192 Multispectral Scanner. The ground coverage provided by these sensors is shown in Figure 5. During the subsequent Skylab 4 mission, photographs were also taken of the study area with hand-held cameras.

Figure 6 is a high resolution color photograph of the Banc d'Arguin taken with S190B Earth Terrain Camera. The scale of the photograph is approximately

[*]Temperature-salinity

1:900,000 in covering an area of 110 km x 110 km. There is an obvious color gradient of blue to green from offshore to nearshore waters indicative of the presence of suspended material and Gelbstoff. Figure 7 is the green band S190A multispectral spectral image having a response region between 0.5μm and 0.6μm. The scale of this photograph is roughly 1:2.7 million covering an area of 157 km x 157 km. The patterns and patchiness of offshore suspended material are evident from this photograph.

The nearshore patterns of suspended material indicate a northerly flow of waters toward Cape Blanc. The "U-shaped" plankton patch southwest of the Cape indicates a southerly drift of waters from north of the Cape. Using dynamic topography, Fedoseev (1970) discussed the geostrophic circulation of surface waters in the shelf region and concluded that quasi-stationary gyres are formed in the eastern boundary of the Canary Current. The most stationary gyre south of Cape Blanc was observed throughout the year and the offshore patterns noted in the Skylab images are influenced by the flow of the gyre.

Szekielda (1974) reports that plankton patchiness varies especially with the change of seasons. A strong gradient of chlorophyll and/or plankton offshore of Cape Timiris is connected with the converging water masses from the Banc d'Arguin and has been detected in all four season. Figure 8 shows the location of offshore ocean color boundaries as derived from ERTS-1 and Skylab. The southern gradients show seasonal positions between 1972 and 1973. Besides small-scale fluctuations, the gradient shifts over a maximum distance of only about 16 km. This is an indication that the offshore gradient is a fairly permanent feature.

The enclosed lines south of Cape Blanc, are the relative positions of the "U-shaped suspended material patch observed from Skylab 3 and 4. Between

September 1973 and January 1974, the patch experienced a broadening and shore-
ward movement. This may be a result of a seasonal change in the circulation.

Channel 13, of the multiscanner scanner of Skylab, recorded emitted
thermal radiation from the surface of the earth. For the Cape Blanc over-
pass, the radiation data were converted to blackbody temperatures and a
histogram was generated by the Johnson Space Center as shown in Figure 9.
Classifications were chosen and a color-coded image was produced corresponding
to different temperature intervals. Figure 10 is a color-coded temperature
map of the waters off Cape Blanc. The temperatures have not been corrected
for atmospheric affects, however, the relative temperature gradients can
be used to locate the origin of upwelled waters. The cold patch of water
in Figure 10 is shown to be roughly between 7°C and 11°C. Coldest known
upwelling water off the African coast has only been reported to be as low
as 14°C. Therefore it is estimated that the calculated blackbody tempera-
tures are at least 4°C to 6°C colder than actually present. Since the cold
patch directly corresponds to the "U-shaped" suspended material pattern
observed in the imagery, this is undoubtedly a source of upwelled water.
In September of 1972, Dr. Ballaster (Szekielda 1974) observed a strong
gradient of temperatures and fluorescence to the southwest of Cape Blanc.
The temperature distribution is shown in Figure 11. The temperature gradient
off   Cape Blanc is located in the same area as the cold patch we observed
from Skylab.

As described previously, ocean color changes associated with sea
surface temperature gradients indicate productive watermasses in this region.
The Skylab spacecraft was effective in recording these gradients and it can
therefore be determined that an intensive area of upwelling was present in

September of 1973. By correlating the observed ocean color changes with the low temperature readings, an obvious area of productive waters was apparent offshore of Cape Blanc.

CONCLUSIONS

The spectral properties of th upwelled waters off the NW coast of Africa have been studied with observations derived from aircraft and Skylab. Results of the aircraft study indicate that the two-channel, ratio approach is ineffective in determining surface chlorophyll concentrations and should not be used in future studies. Ocean color boundaries and temperature gradients were found to be directly correlated with each other and also with fishing effort in the upwelling region. Photographic and scanner data derived from Skylab has been effective in locating ocean color boundaries and mapping temperature distributions. Both can be utilized in this region to qualitatively determine areas of biological productivity. This simple correlation may be applicable in future efforts toward fishery resource management in upwelling areas.

ACKNOWLEDGMENTS

REFERENCES

Allain, C. (1970). Les conditions hydrologiques sur la bordure Atlantique de l'Afrique du nord-ouest. Rapp, P. v.Cons. Explor. Mer. 159, 25.

Arvesen, J. C., Millard, J. P. and Weaver, E. C. (1973). Remote Sensing of Chlorophyll and Temperature in Marine and Fresh Waters. Astronautica Acta. Vol. 18, 229-239.

Boley, M. T. (1974). Compte-Rendu De La Mission Tassergal, Cap 73-11, 9 au 23 Juillet 1973. CINECA Newsletter, Inc. Council for the Expl. of the Sea, Charlottenlund Castle, Denmark, 62-67.

Clarke, G. L. and Ewing, G. C. (1974). Remote Spectroscopy of the Sea for Biological Production Studies. In Optical Aspects of Oceanography, Julva, N. G. and E. Steeman Nielsen, eds. Academic Press, New York, N.Y., 389-412.

Duntley, S. Q. (1972). Detection of Ocean Chlorophyll from Earth Orbit. 4th Annual Earth Res. Program Review, Vol. IV, NOAA and NRL Programs, January 17-21, 1972. NASA, Manned Spacecraft Center, Houston, Texas, 1-25.

Fedoseev, A. (1970). Geostrophic Circulation of Surface Waters on the Shelf of North-West Africa. Rapp. P. v.Cons Explor. Mer. 159, 32-37.

Lorenzen, C. J. (1970). Surface chlorophyll as an index of the depth, chlorophyll content, and primary productivity of the euphotic layer Limnol. & Oceanogr. 15, 479-480.

Ryther, J. H. (1969). Photosynthesis and Fish Production in the Sea. Science, Vol. 166, No. 3901, 72-76.

Szekielda, K.-H. (1973). Distribution Pattern of Temperature and Biomass in the Upwelling Area Along the NW Coast of Africa. ASP Fall Conv., Lake Buena Vista, Fla., 664-716.

Szekielda, K.-H. (1974). Observations of Suspended Material from Spacecraft Altitudes. Deutsche Hydrographische Zeitschrift, Jahrgant 27, 1974, Heft 4, 159-170.

Tabor, P. (1975). Evaluation of Chlorophyll Measurements by Differential Radiometric Remote Sensing. Master's Thesis, College of Marine Studies, University of Delaware, 194 p.

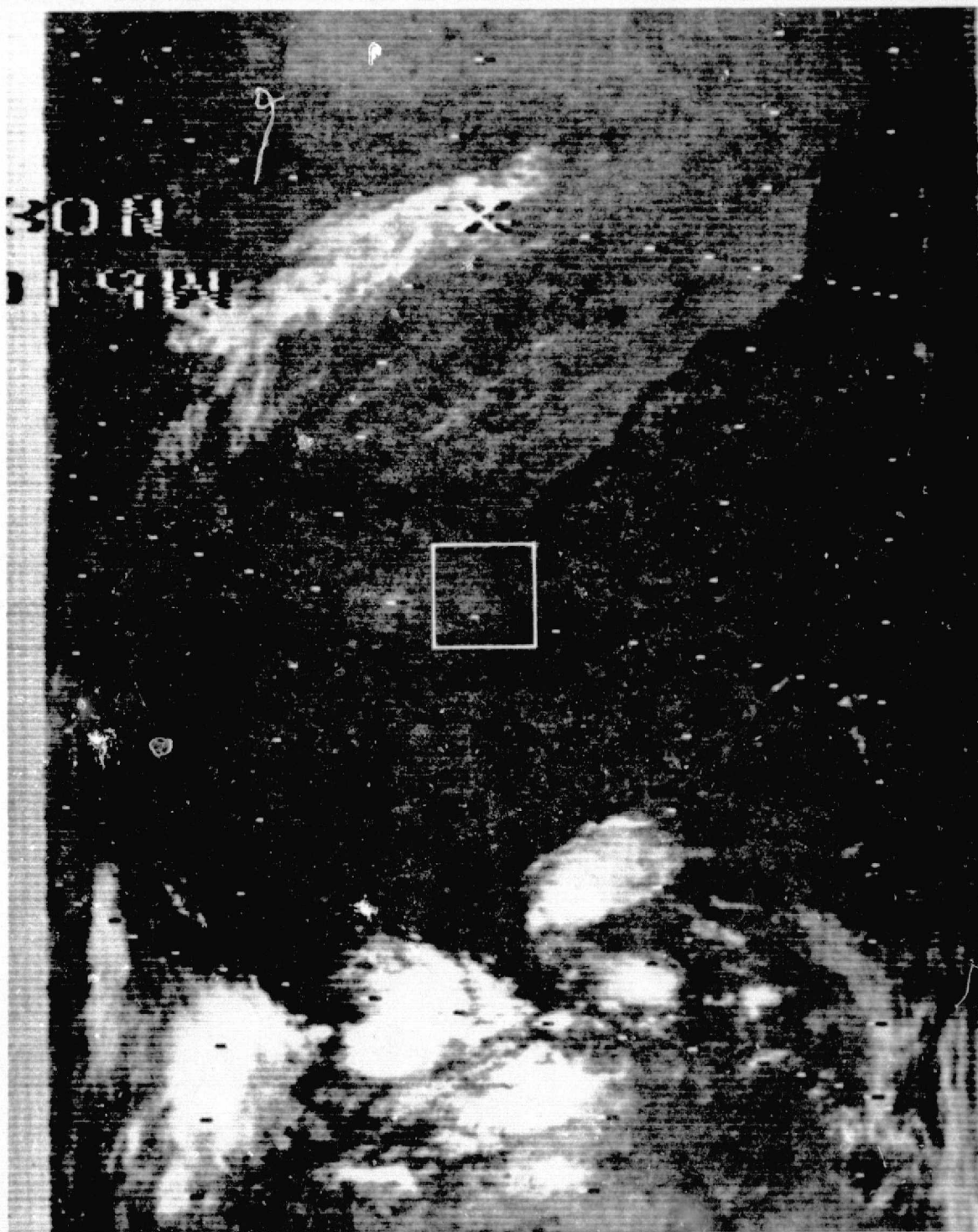Yentsch, C. S. (1960). The Influence of Phytoplankton Pigments on the Color of Seawater. Deep-Sea Res. 7, 1-9.

Figure 1. Nimbus 5 thermal image of the NW coast of Africa
taken 2 September 1973. Cape Blanc is located
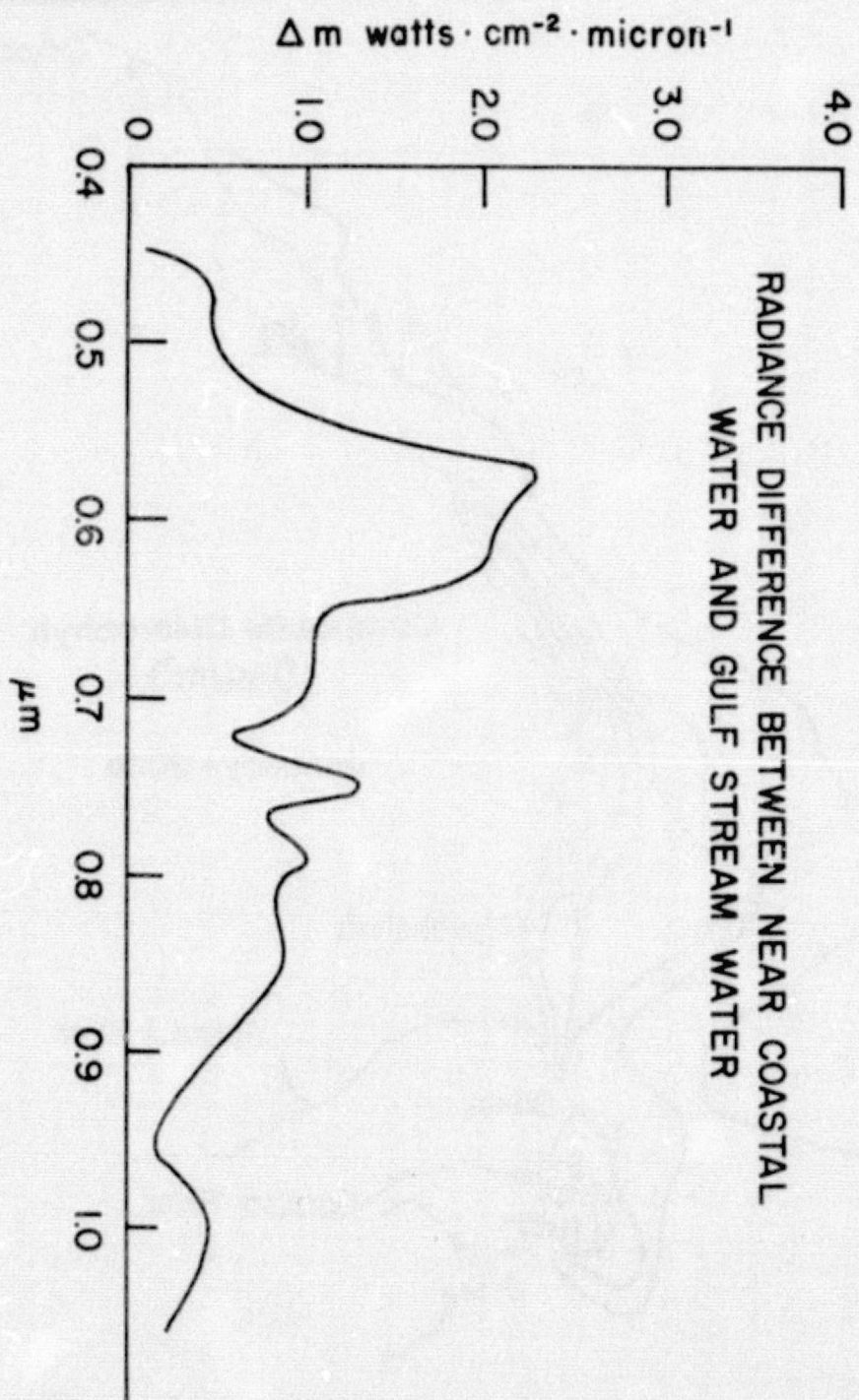within the enclosure.

Figure 2. Wavelength dependent radiance caused by particulate and dissolved matter. (from Szekielda (1974)).
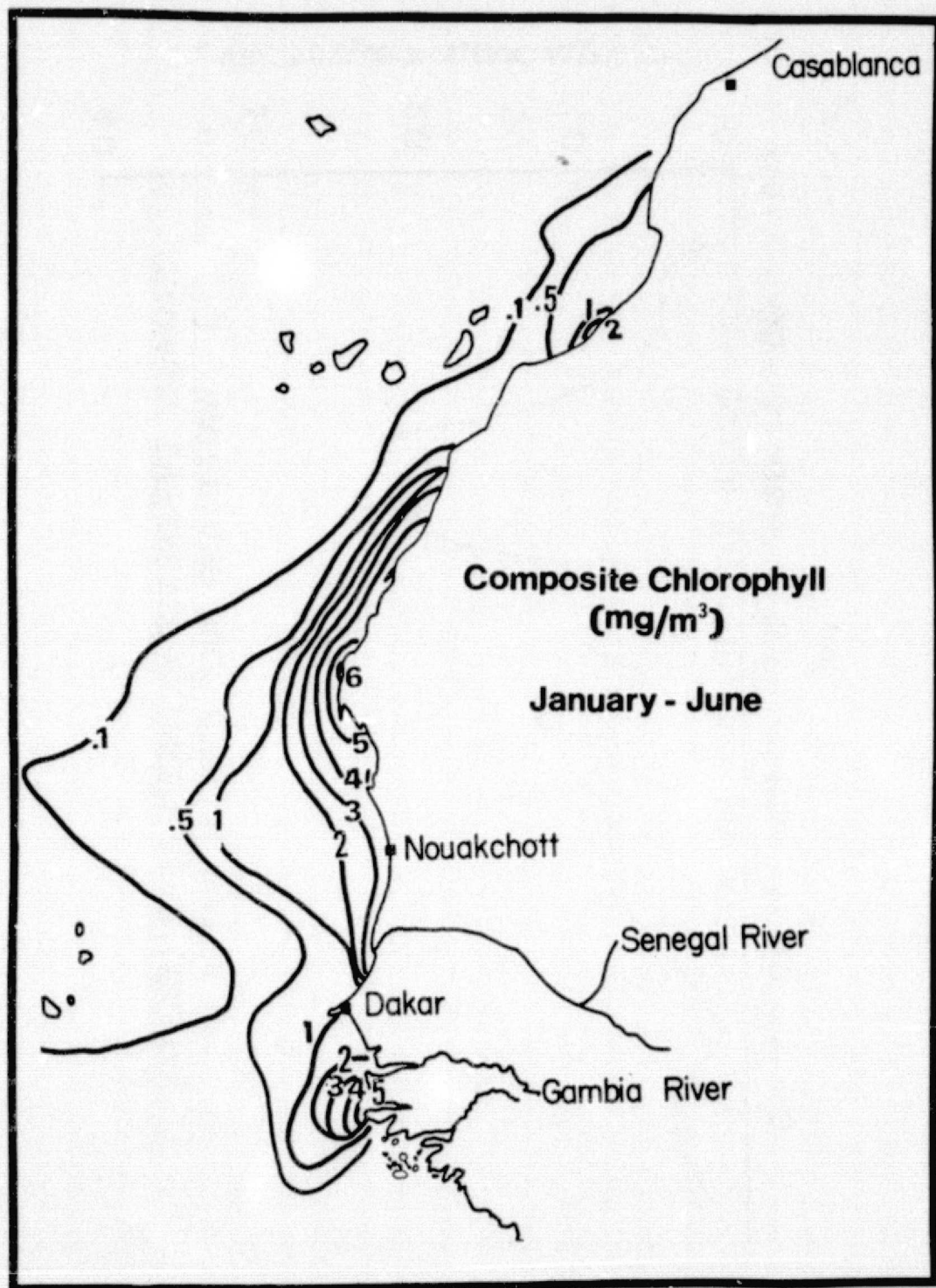
Figure 3. Composite of chlorophyll concentrations for the months January — June.
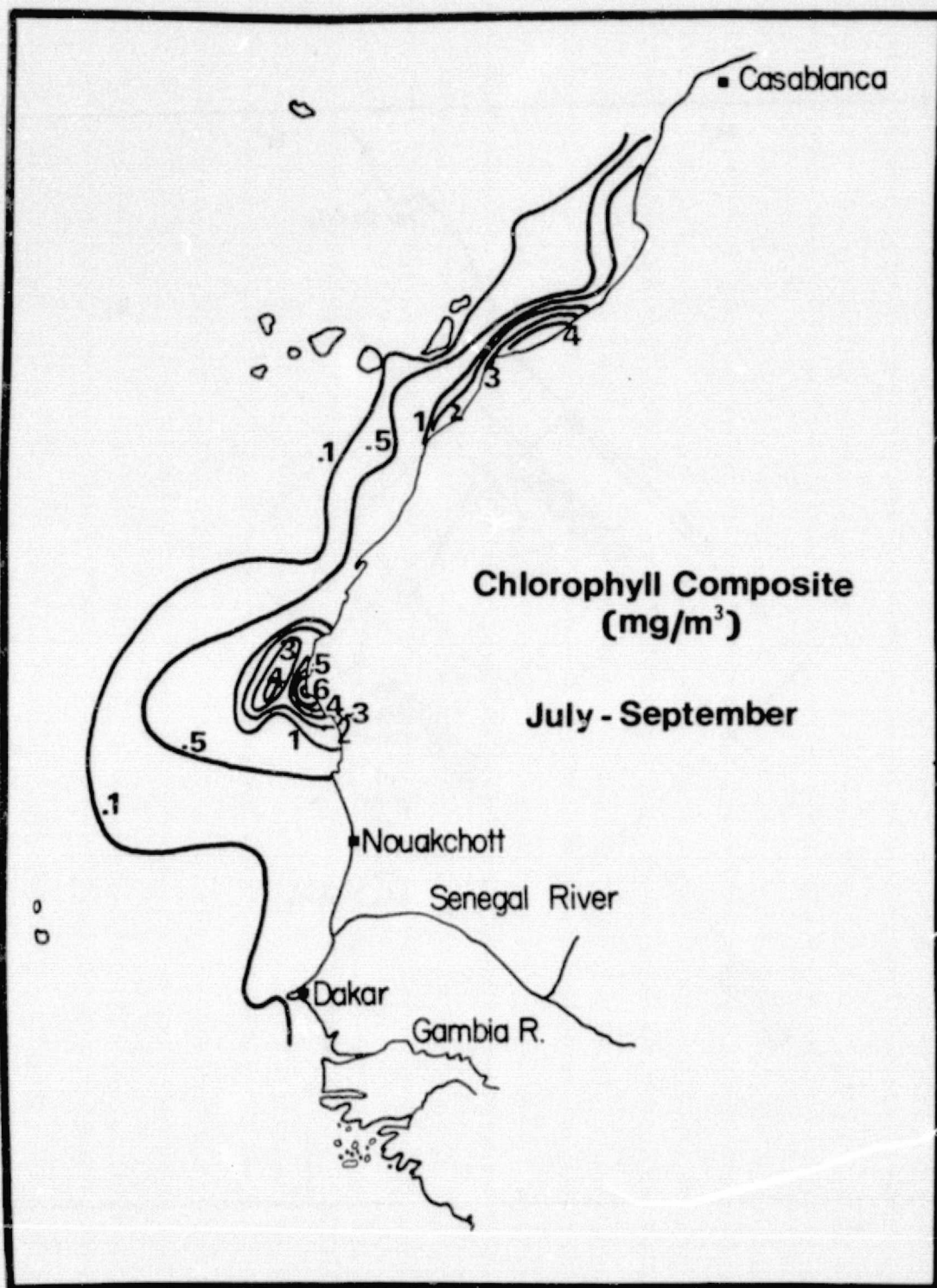
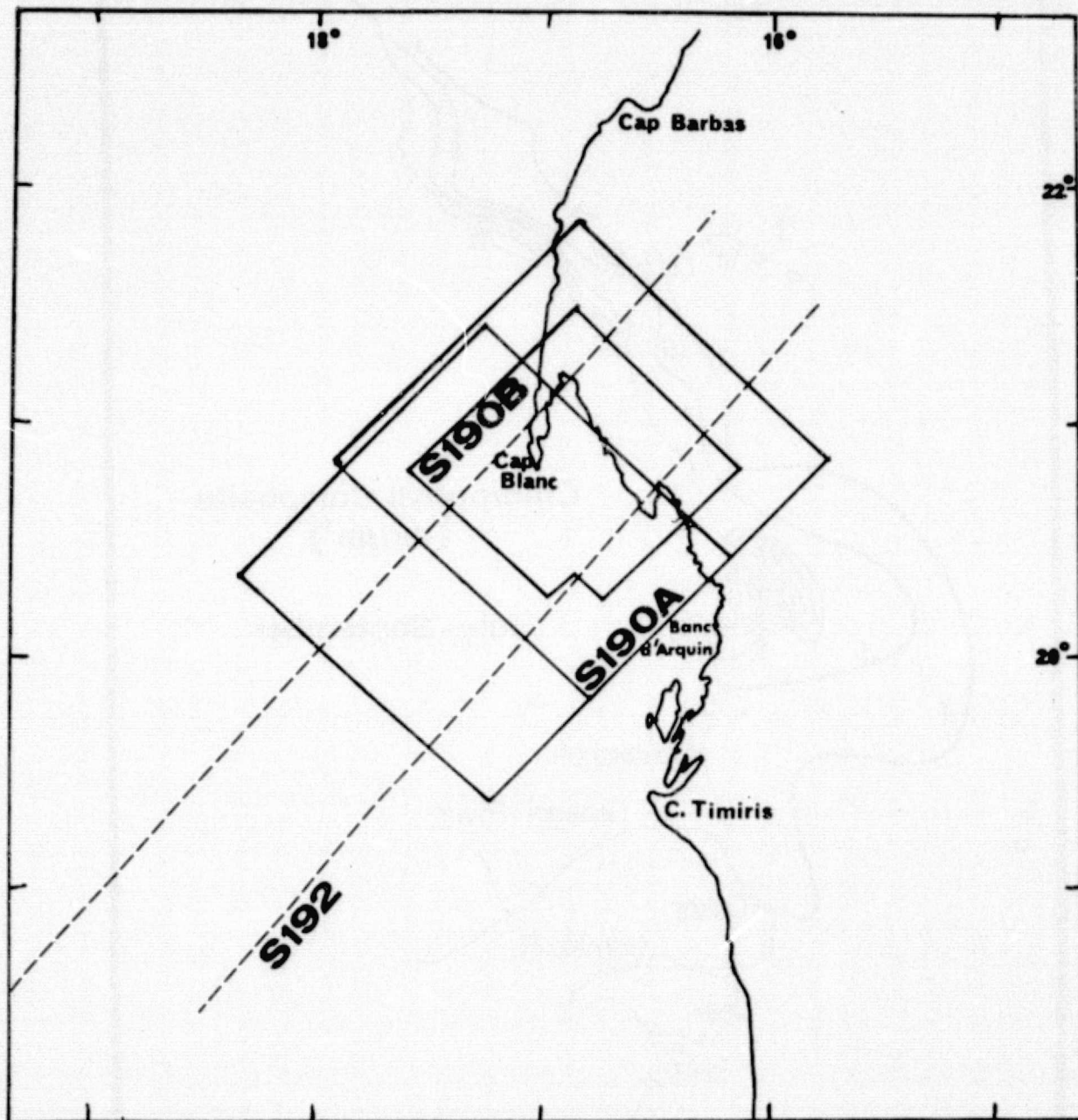**Figure 4.** Composite of chlorophyll concentrations for the months July — September.

Figure 5. Ground coverage provided by the Skylab sensors during the 4 September 1973 overpass.
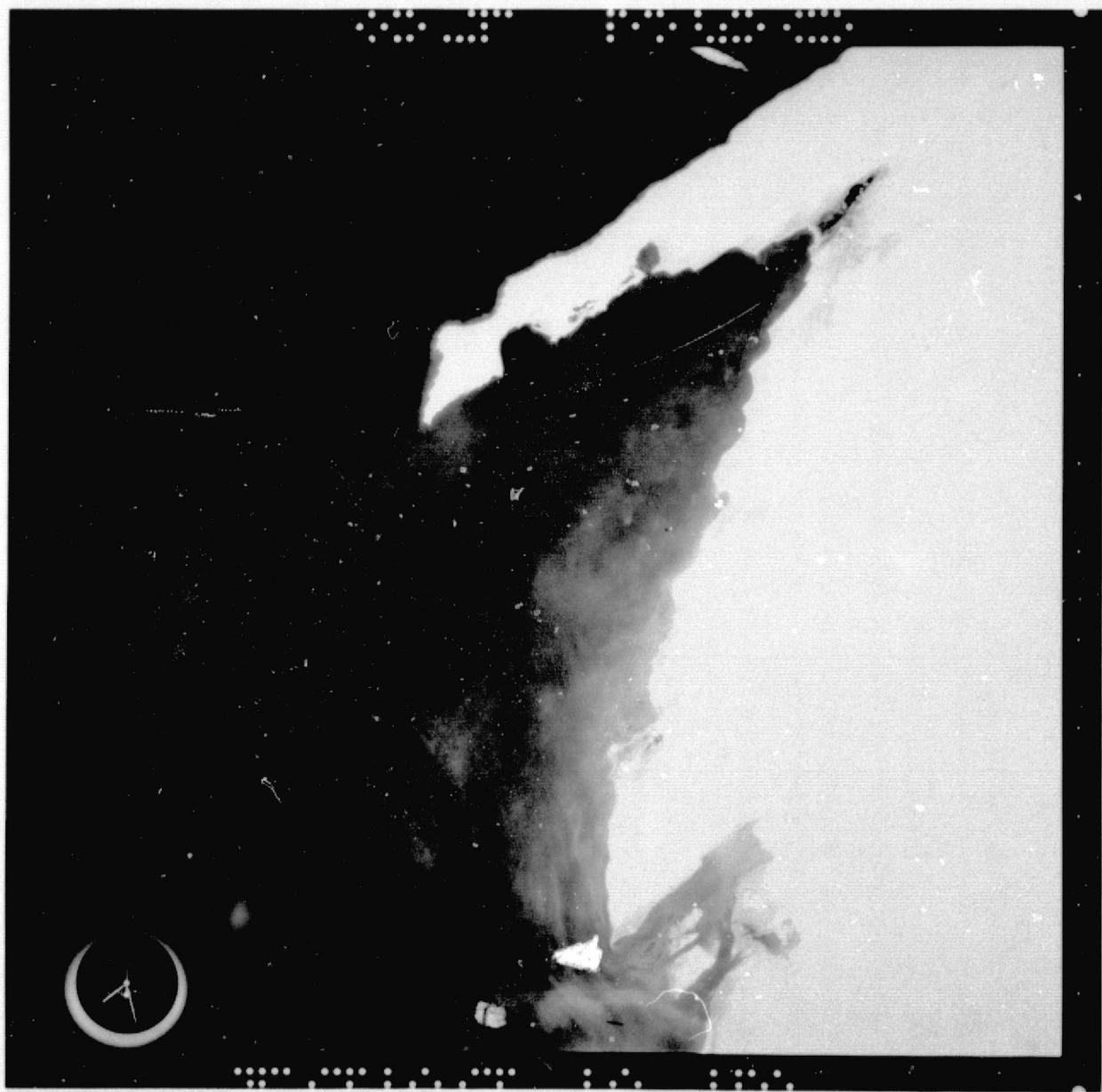
Figure 6. S190B color photograph of Cape Blanc.
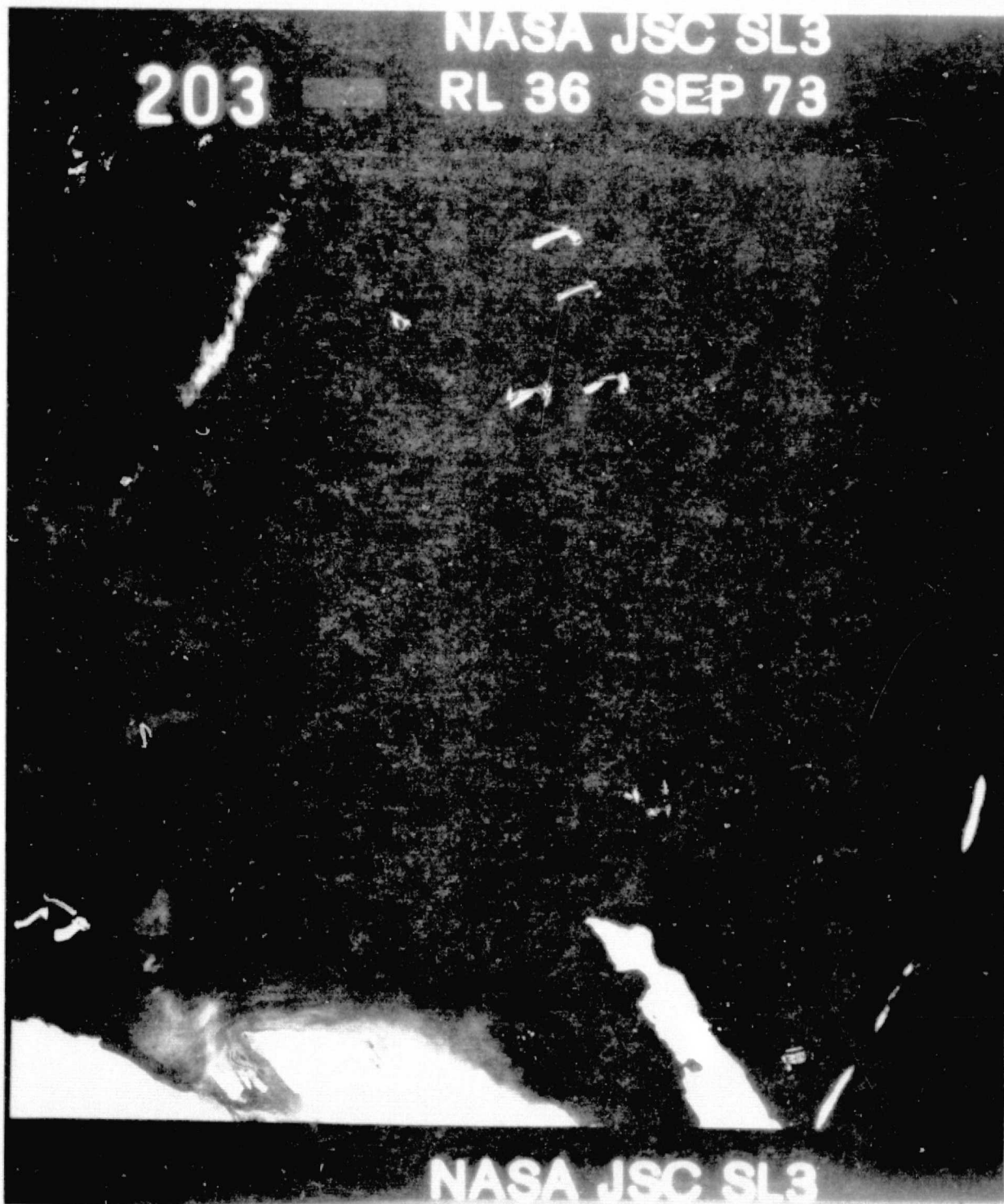
Figure 7. Green band S190A image of Cape Blanc.
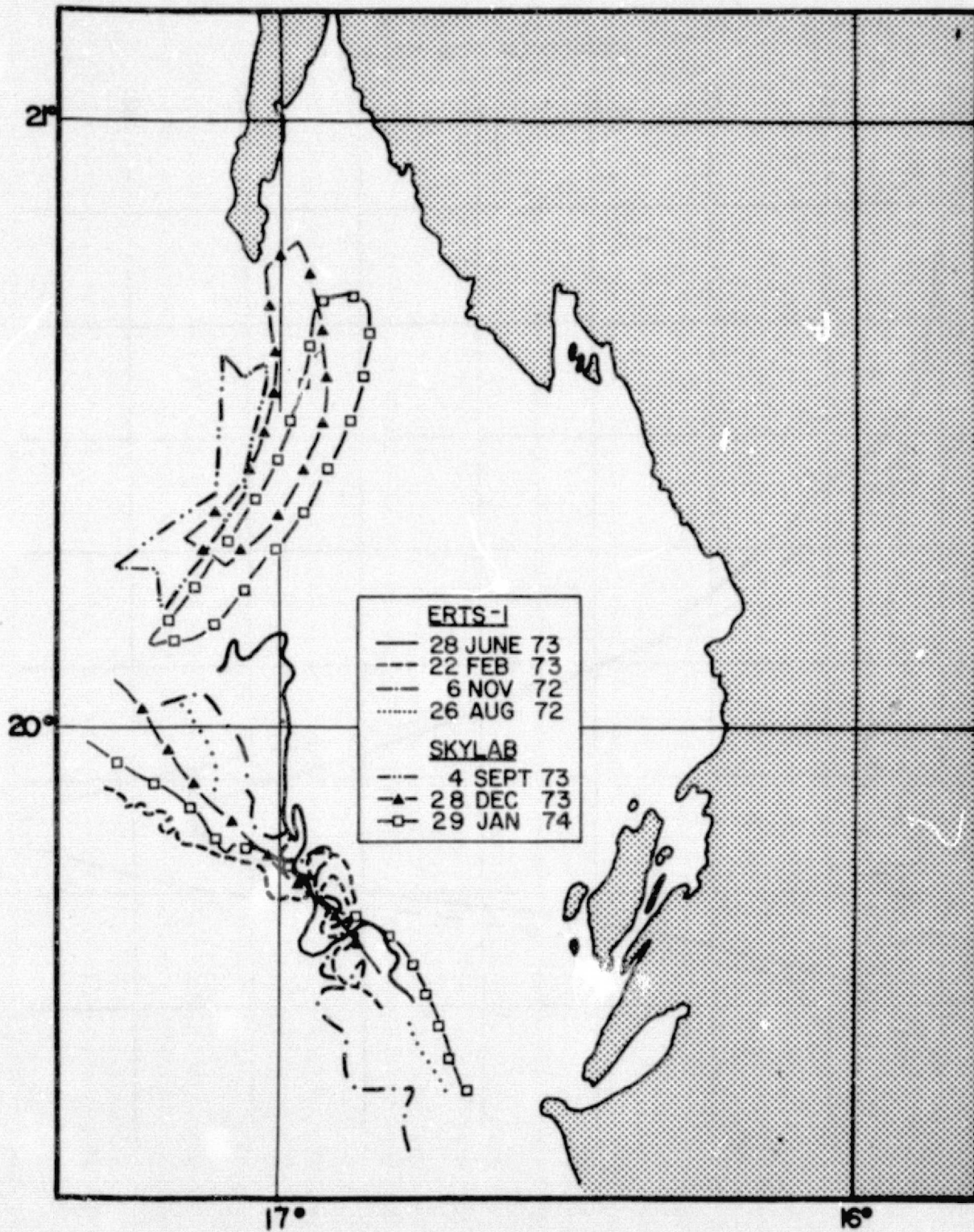
Figure 8. Offshore ocean color boundaries derived from ERTS-1 and Skylab.

Figure 9. Histogram of thermal data and color coding for S192 imagery.

Figure 10. Color-coded temperature distribution derived from channel 13 of the S192 multispectral scanner.

33

PART II:

EVALUATION OF CHLOROPHYLL MEASUREMENTS

BY DIFFERENTIAL RADIOMETRIC REMOTE SENSING

by

Paul Stephan Tabor

College of Marine Studies
University of Delaware
Newark, Delaware 19711

ABSTRACT

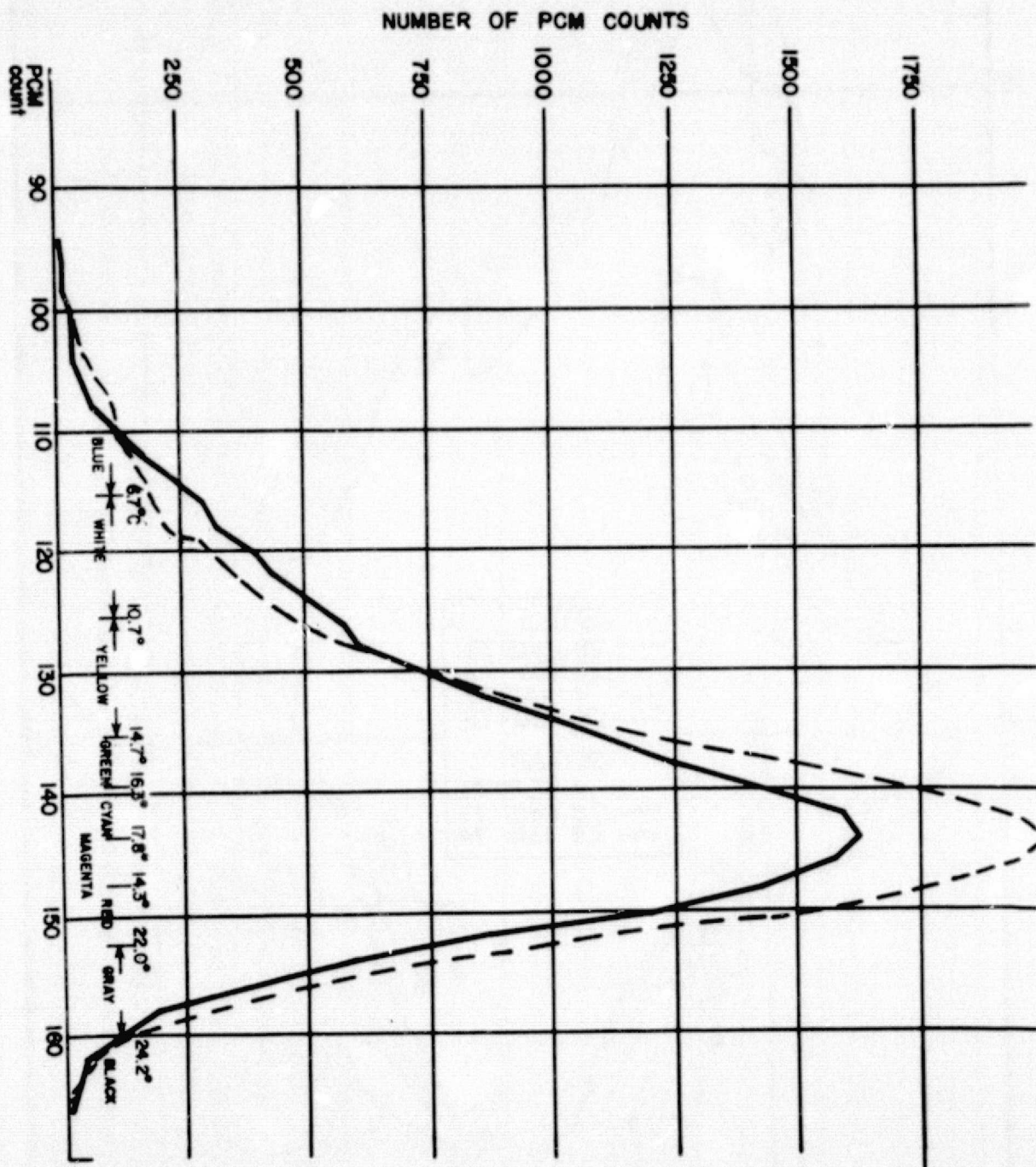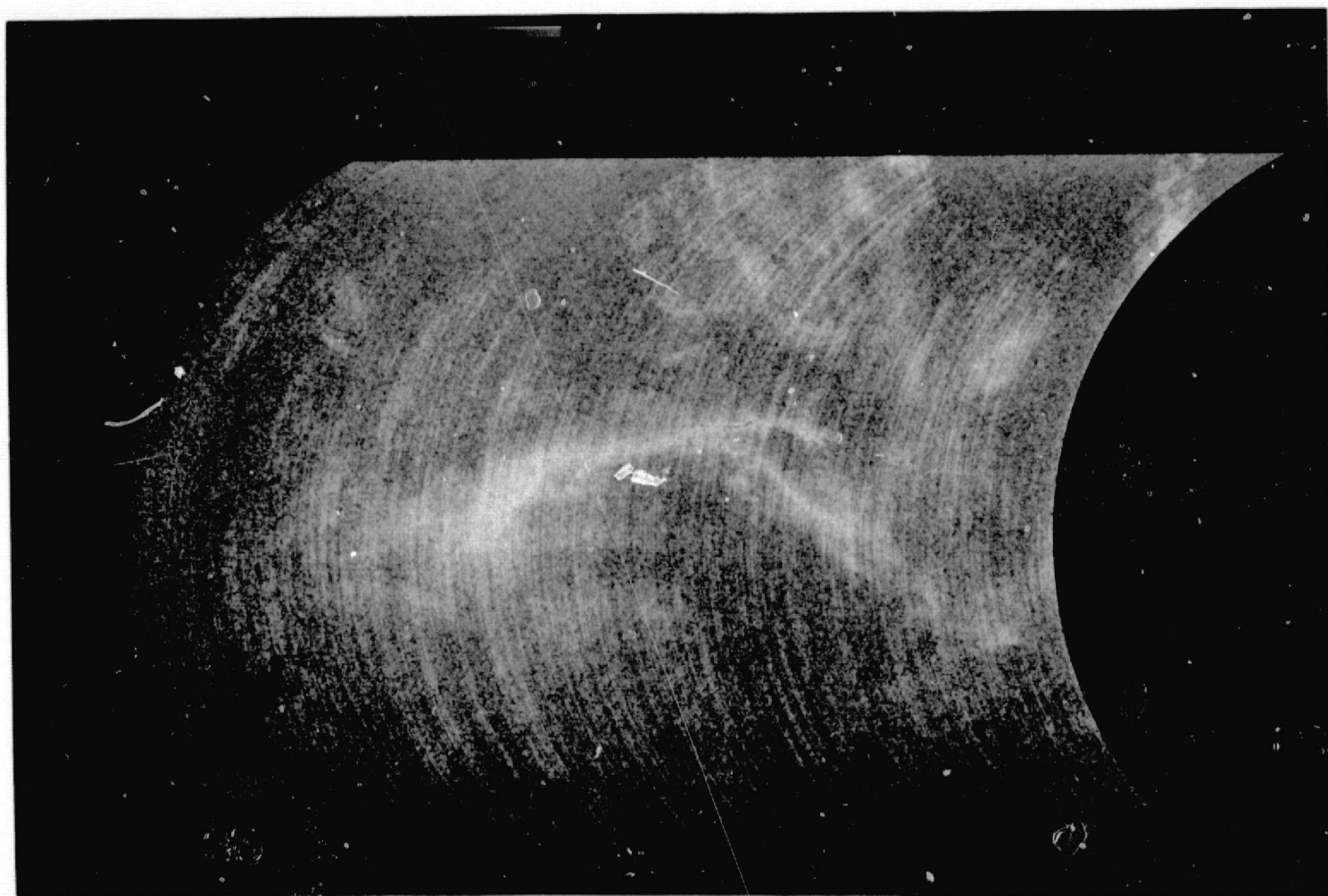A differential radiometric (DR) method for continuous determination of near surface chlorophyll levels from aircraft altitudes measures intensities of two narrow wavelength bands of the spectral reflectance from the sea. An evaluation of the effectiveness of the DR method for measuring and surveying the regional distribution of chlorophyll is given.

Two aircraft oceanographic research studies in a region of dynamic ocean color off the NW coast of Africa are described. The Sahara Upwelling Project (SUE) focused on a survey of apparent chlorophyll (Chl.) and radiometric sea surface temperature (SST) distribution in a 11,000 mi^2 region. Correlations of SST and Chl. gradients were found in the longshore and offshore directions. A constant onshore gradient of increasing Chl. as well as recognizable structures far offshore, including isolated features, were observed. The regional development of SST and Chl. structure was synoptically monitored from 18-26 August, 1973, with an expendable probe study on 21 August. Recordings of additional ocean spectral reflectance at yellow (576 nm) and red (663 and 723 nm) bands nearshore show correlations in intensity of response with the DR method, while often offshore SST and Chl. gradients do not correspond to any feature in the red or yellow signals.

Oceanographic research flights of the JOINT-I project are described and interpreted with available real-time sea truth measure-

ments. A partial description of the synoptic time-series of results is given for recognition of upwelling events. Analyses of apparent chlorophyll, SST and the DR ratio value (L_{443}/L_{525}) are presented for all flights. Gross differences between apparent Chl. and surface measurements are observed < 20 km offshore with apparent Chl. levels an order of magnitude greater than surface sea truth. In contrast, an inverse relationship exists offshore with sea truth an order of magnitude greater than Chl. A multi-comparison shows increasing particulates, decreasing 50% I_o depth, decreasing chlorophyll and decreasing ratio (443 nm/525 nm) values are positively correlated nearshore.

From preliminary interpretation of atmospheric effects on the DR method, the solar elevation is a far greater influence than atmospheric composition even in high eolian-load areas.

Laboratory investigations on the interference of chlorophyll-free particulates in suspension with algae employed multiple scattering samples which were spectrally scanned and interpretations of increased effective reflectance of the suspensions were made. When a multiple scattering situation exists the increase of photon survival in a algae-reflective clay suspension causes an enhanced chlorophyll signature to be produced. In an optically dense base water, successive additions of an algae standard and reflective particulates were related when sample particle counts were correlated to the change in reflectance ratio value (L_{443}/L_{525}). Successive additions of only

chlorophyll-free particles showed a similar relation of total counts

to ratio change, but the relationships of algae-only and algae-clay

suspensions were independent. The dissolved blue colorant and

non-selective particles were predicted to behave in the same manner

as Gelbstoff and reflective particulates do in high concentrations

in the ocean.

From the results and interpretation of this study the DR

method is evaluated not to be effective in determining concentrations

of chlorophyll even on a relative basis due to interferences,

predominately in the ocean, of additional wavelength selective optical

properties and particle multiple scattering conditions. The DR

method was effective in monitoring an ocean color parameter L_{443}/L_{525},

which had a distribution very closely identified with SST. Patterns

from the recordings of these sensors were recognized and their develop-

ment could be monitored in repetitive coverage. The parameter is

not well defined, but is strongly correlated to near surface

particulate concentrations. The 443 nm and 525 nm bands are concluded

to be inadequate alone as an algorithm for determination of chlorophyll

by ocean color measurements. Recommendations for directions of further

research on the backscattered spectral reflectance from the ocean are

made.

TABLE OF CONTENTS

TABLE OF CONTENTS (continued)

TITLE OF FIGURES

TITLE OF FIGURES (continued)

TITLE OF FIGURES (continued)

TITLES OF TABLES

1. INTRODUCTION

· This study is an extension of an area of research which is stimulated by the possibilities of using reflected signals of visible radiation to determine phytoplankton pigment concentrations in natural waters. The determination of color by remote methods is a very useful parameter to monitor because of its sensitivity to many properties in the ocean, thus giving estimates of biological chemical, and physical construction (Ewing, 1969). Research on ocean color reflected to an aircraft has shown, quite satisfactorily, correlations between spectral signals and chlorophyll concentrations in surface waters (Strickland, 1962; Duntley, 1963 and 1972; Clarke et al., 1970a; Arvesen et al., 1973; Mueller, 1974; and Pearcy and Keene, 1974).

The practical utility of these measurements, due to the coverage that can be gained in relatively short times has been recognized (Yentsch, 1971), and synoptic monitoring approaches have been initially developed (Pearcy, 1971; Pearcy, and Keene, 1974).

The strong relation between concentrations of green photo-synthesizing pigments of phytoplankton (especially chlorophyll a) and more tangible parameters in surface waters such as primary production, phytoplankton standing crop and total biomass, supports the use of the optical properties of this biochemical as a biological index (Riley, et al., 1971). Correlations between surface

1

chlorophyll concentrations and primary productivity measurements of a wide variety of marine waters were made by Lorenzen (1970). Historical data from a more defined ocean area (the upwelling region of the NW coast of Africa) shows a stricter correlation with an r^2 (correlation coefficient) range of 0.758 to 0.824 for individual cruises. Figure 1.1 shows the regression from the March-April 1971 CINECA-Charcot-II cruise.
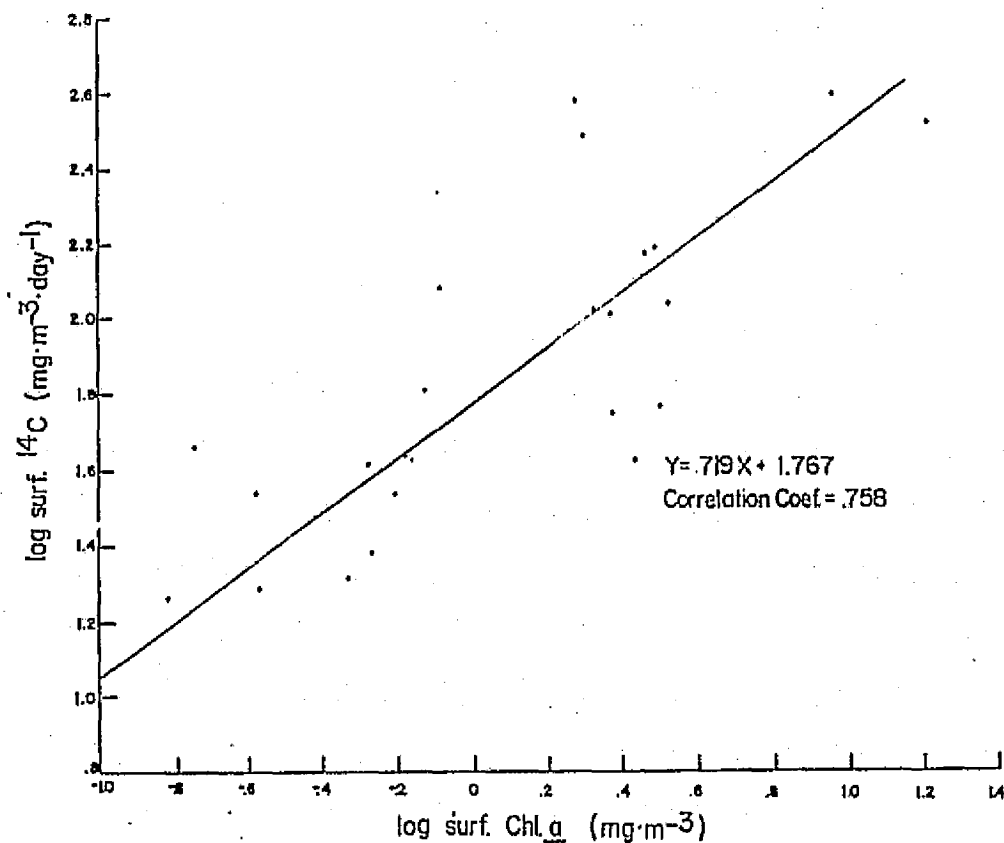
Figure 1.1 The Correlation Between Chlorophyll a (Chl.a) and

Primary Productivity (^{14}C uptake) off the NW Coast of

Africa from 30° 38'N to 17° 22'N During March-April, 1971.

2. OBJECTIVES

Continuous recording of measurements at two wavelengths
of the reflected spectral energy as ratio values has been
proposed as a method for determination of chlorophyll pigments in
natural waters (Clarke et al., 1970a; Arvesen et al., 1973; Duntley
et al., 1974). The objectives of the present study are to: 1)
evaluate a differential radiometric method proposed by Arvesen
(cit. loc.) for measuring chlorophyll and surveying its regional
distribution by defining the limitations of its effectiveness and by
identifying and investigating interferences in the method, and
2) also gain positive information on ocean feature patterns through
comparisons of the reflected wavelength ratio signal with sea truth
measurements.

3

3. BACKGROUND

In attempting to expand the use of chlorophyll measurements, radiometric methods were developed preceded by determination of optical properties of ocean features from measurements of radiance from the ocean.

3.1 Optical Properties of Ocean Features

As a prerequisite to the identification of ocean parameters of interest, it is necessary to identify the spectral signature produced by optical properties in the open ocean or varying coastal waters. A second, simplistic prerequisite is that the incident radiation is of suitable wavelength (λ) and intensity to produce a detectable spectral signature.

3.1.1 Significant Optical Processes in the Ocean

Very clear seawater has a well defined spectral signature (Clarke and James, 1939; Hulburt, 1945; Jerlov, 1968; and Morel, 1974). The processes of Rayleigh-like scattering in liquids (Einstein, 1910) and absorption is responsible for a low attenuation "window" in the 400-500 nm region. Below 250 nm in the UV and above 700 nm in the IR region, the absorption increases strongly by electron transitions and intra-intermolecular motions respectively. In addition, the volume scattering function for pure sea water, caused by dielectric

4

fluctuations of molecular movement, increases nearly ten fold from
600 nm to 360 nm (proportional to λ^{-4}) (Morel, 1966). Thus increased
scattering is found at the wavelength regions of least absorption.
The wavelengths of maximum reflected intensity, then, are between
460 and 480 nm in the clearest waters.

Dissolved organic materials (especially Gelbstoff) are the
greatest influence on the spectral character of sea water excluding
particulate effects. These melanodines described by Kalle (1966),
absorb strongly in the UV and carry over into the blue visible region.
In a region where plankton populations are continually fluctuating,
the backscattered spectra of the filtered "base" water is not that of
the very clearest blue sea water. The diffuse reflection coefficient
at 460 nm is 2-3 times lower in biologically active regions than in the
open ocean (Duntley et al., 1974). Yentsch and Reichert (1962)
observed that Gelbstoff concentration increases were proportional
to decomposition of phytoplankton pigments. Duntley et al., (1974)
suggest that base water spectral characteristics for the regions of
interest in remote optical studies be well defined. Jerlov (1964)
presents a relationship between the total scattering function and
the irradiance attenuation coefficient at 465 nm for optical classifica-
tion of many ocean regions. Areas of upwelling, including the NW
coast of Africa, have a far greater absorbance contribution than open
ocean areas. This further indicates that spectral signatures of base
waters should be defined.

Whereas with dissolved matter in sea water and sea water itself, absorbance predominates over scattering (excluding perhaps the 400-500 nm "window"), particulate scattering is two to three times greater than absorbance by particulates. In fact, except in clear, open ocean waters, particulate processes dominate the characterization of the optical signal (Kullenberg, 1974; Jerlov, 1974).

Backscattered light in the ocean is a process of interest for remote studies. Although the lack of reflected radiance can also aid in description of the optical properties of a region (e.g., implying a few, large, forward scattering particulates), only the backscattered portion of the light field radiance can describe features characterized by spectral signatures. Unfortunately, much scattering and transmittance research has used meters designed to measure forward and low backscattering angle propogation ($2° < \Theta < 165°$). A computation of particle scattering functions observed in situ is given by Kullenberg (1974). The water mass types measured range from turbid lakes and coastal waters to the low productive Sargasso and Mediterranean Seas. The largest difference in the functions is in the backscattered direction, and this is partially attributed to the variations in the scattering particles. This indicates, first, that Duntley's et al. (1974) suggestion of a well defined base water should be extended to include the identification of the particulate composition, especially including size distribution and indices of refraction associated with different fractions, that may commonly occur in regions of interest for remote optical studies. The use of optically

effective areas (Owen, 1974) of particulates is a good example of the
type of the basic knowledge needed. Secondly, if optical signals
backscattered and reflected from the sea are going to be used for
recognition of particulate frequency or composition, a more specifically
defined interpretation of the backscattering process is needed. And
this requires experiments designed for measuring scatterance,
including the contribution of multiple events, in the $120° \leq \Theta \leq 180°$
scattering cone as well as total scattering function.

The production of the optical signal backscattered to the
atmosphere is, of course, a combination of dissolved and particulate
properties in the ocean. The integration of contributions from all
processes that are studied in situ, and using these in a radiative
transfer (Preisendorfer, 1965) calculation to describe an observed
signal is a complex problem, especially when multiple scattering
is included. Although not yet fully utilized, the Monte Carlo
computer modeling approach as described by Plass and Kattawar (1969),
and used by Gordon and Brown (1973) for computation of diffuse
reflectance may be the only practical calculation solution.

The dependence of the optical properties of pure sea water
on changes in temperature, pressure, salinity was reviewed by
Morel (1974) and is very slight. Pure sea water, then, can be
assumed nearly constant. However, the particulate and dissolved
matter in the sea are not found to be conservative in distribution,
composition or in their inherent optical properties (i.e., volume

scattering function, absorption or attenuation).

The optical properties of phytoplankton have been recently described by Mueller (1974). He considers the chlorophyll signature from wavelength dependent scattering of the phytoplankton to be a much flatter spectral response than previous measurements by Yentsch (1960) and Shibata et al. (1954). The latter two investigators measured diffuse forward scattered light, while Mueller was concerned mainly with beam extinction and cross section scattering spectra. Optical remote sensors with specifications such as the differential radiometer (see Section 3.2.2) receive a signal of diffuse reflectance from the ocean closer to that described by Yentsch (cit. loc.).

3.1.2 Optical Processes at the Ocean's Surface

A boundary exists between incident irradiance from the atmosphere and backscattered irradiance from the sea itself. This boundary between the two optical media is the air-sea interface. Processes that occur at level surfaces such as refraction, reflection and transmission have been described by Jerlov (1968). In addition, the effects of wave action, whitecaps and foam, and slicks at the optical boundary are recognized (Cox, 1958; Cox and Munk, 1956; and Cox, 1974). The surface processes involving introduction of incident light into the sea, reintroduction of an optical signal from the sea to the atmosphere, and return of incident light to the atmosphere never having penetrated the surface are significant for the problem of detecting a backscattered signal from the ocean.

Direct radiant and diffuse skylight incident on the ocean's surface is partially reflected at the surface and returned to a remote sensor. This reflection is a function of the index of refraction of the water, the viewing angle, and the wind speed which governs the wave slope effect (Austin, 1974a), but is independent of wavelength of the light. The refraction of radiance passing upward through the surface will, in effect, spread the same amount of energy into a larger solid angle cone. The factor of decreased energy is 1/(refractive index of water)^2 or 0.555. The Fresnel reflectance at the surface (Jerlov, 1968) causes a loss of transmitted signal and is a function of the angle of observation and wind speed or wave slope (Austin, cit. loc). Wave action scatters light at the sea surface. Swells and waves of all sizes continually refract, reflect and even focus some light with varying distribution. The capillary waves generated by wind forces ≥ 7 m/s are responsible for surface reflectance that is observed as sea glitter (Wu, 1972). Larger gravity waves are critical in the angular reflectance that is observed outside of the sun's specular point. Natural slicks at sea are often monomolecular layers, much thinner than the wavelength of light. In these cases slicks have negligible effect on surface reflectivity or angles of refraction and reflection (Cox, 1974). They do however, have a wave dampening effect which drastically reduces this scattering process (Ewing, 1950; Garret and Bultman, 1963). Therefore, observations outside the increased reflection at the specular point will be free from the scattered light of capillary waves. Observation angles for reduced

reflected sun glint and sun glitter input to the signal are dependent
on the elevation angle and azimuth angle of the sun. Cox (1974)
also shows a dependence of observed glitter on direction of the wind.
The time-averaged effect by sea glitter is not as important however.

Studies of reflectance at the air-sea interface as a function
of observation angles (Cox, 1974, Austin, 1974a) show that parallel
polarized light will have no contribution to the reflected signal
at the Brewster's angle (where the angle of radiance in air = 53.1°).
However, observations at this angle include 1.67 times the optical path
length of sensors viewing in the nadir direction and this atmospheric
interference severely reduces the advantage gained. For optimum
viewing angles to avoid sea glitter (defined as glitter radiance
observed/glitter radiance max. = 0.01), Fraser (1971) has calculated
that at wind speeds of 10 m/s , the glitter pattern does not extend
to the nadir when the solar zenith angle is > 40°.

Austin (1974a) has developed the following equation for total
inherent radiance, N_o, leaving the surface

$$N_o = \frac{R_W}{\pi} H_{ToT} + r_d N_s \tag{3.1}$$

where R_W is the diffuse water reflectance (a ratio of the irradiance
propagated through the surface to the total irradiance incident at
the surface), H_{ToT} is the total incident irradiance (sun and skylight),
r_d is the Fresnel reflectance of the surface (a function of index of
refraction and incident radiant angle), and N_s is the zenith radiance.

This equation points out that N_o has a component $(\frac{R_w}{\pi} H_{TOT})$ which is independent of observation angle and contains the spectral signature of the water mass, and a component $(r_d N_s)$ which can be considered as glint or noise to the remote sensor and is dependent on the observation angle. The apparent signal that will be available to a sensor at some height above the surface, N_z, can be expressed as:

$$N_z = N_o Ta + N^*$$ (3.2)

where: N_o is from equation 3.1, and Ta is the transmittance of the atmosphere and is a wavelength dependent process that reduces the signal. N^* is the radiance contribution to the path of sight by atmospheric scattering processes.

3.1.3 Atmospheric Processes on Optical Signals from the Ocean

Atmospheric processes on signals reflected from the sea are studied mainly to discover the applicability of detection of these signals from orbital altitudes. The processing of insolating light by the atmosphere must also be considered in the production of a signal from the ocean. Depending on the altitude of flight, aircraft measurements of returning surface signals, to a varying degree, are effected by atmospheric processes.

The most important process in the atmosphere is scattering. Rayleigh scattering was mentioned in Section 3.1.1 Again, the scattering coefficient is proportional to λ^{-4} and in the visible

region the exponent is -4.08 (Ramsey, 1968). For particles with sizes
larger than the light wavelength, Mie theory is used to predict
scattering attenuation. The attenuation coefficient for Mie scattering
is a function of the number, radius of the particle, and wavelength
of light. Forward scattering predominates with aerosols (considered
to be Mie scatterers). Ramsey (1968) has pointed out from previous
research that sea salt particles in the atmosphere have a very uniform
size distribution from 1-2μm and exhibit a non-selective attenuation
of visible light, while the distribution of particulates which
originate from land sources (which influence coastal water measurements)
is of much more polydisperse composition and seems to show a higher
scattering coefficient for light in shorter λ regions.

Measurements of the contribution of radiance backscattered
from the atmosphere and that returning from the sea, (avoiding specular
reflection), for a variety of turbid atmospheres and at various
altitudes (in Ramsey, 1968), show that 1) the atmospheric signal
measured at 1 km is from one-fifth to equal to the returning signal
from the sea in turbid atmospheres and at a sun elevation angle of
45°; 2) in Rayleigh atmospheres the signal from the sea is only
∿ 10% greater in wavelength region 400-500 nm. and nearly equal at
higher wavelengths to that of the atmosphere; 3) the total radiance
signal from a turbid atmosphere is ∿ 40% greater than that from a
Rayleigh atmosphere.

The apparent signal to a remote sensor in the atmosphere can be

quantified in terms of the albedo of the surface by:

$$A_s = \pi\ I(\lambda)\ [\mu_o F_t(\lambda) + F_D(\lambda)] \qquad\qquad (3.3)$$

where $I(\lambda)$ is the wavelength dependent radiance leaving the sea, whether backscattered or surface reflected, $\mu_o F_t(\lambda)$ is the directly transmitted solar irradiance and a function of the cosine of the solar zenith angle, μ_o, and $F_D(\lambda)$ is a wavelength dependent diffuse incident component (Curran, 1972). The equation above does not consider the albedo contribution from the optical path of the atmosphere. Curran has calculated this contribution as a function of λ (460 nm and 540 nm) and found that increased aerosol optical depths (defined in terms of particle number density and the volume scattering coefficient) and varying solar zenith angles have a much larger effect than A_s alone. Comparisons of one standard deviation in the color ratio (540 nm/460 nm) observed at the sea surface versus one standard deviation in the aerosol optical thickness for a variety of optical thicknesses and solar zenith angles showed that aerosol scatters are the dominate influence on the color ratio at 1) optical depths only slightly above clear marine atmosphere conditions and 2) solar zenith angles > 60°.

A large number of albedo recordings made on a 30 m high platform above Buzzard's Bay, Mass. (Payne, 1972) under various solar elevation angles and atmospheric transmittance conditions showed again the strong relationship of solar angle and atmospheric transmittance (defined as the ratio of observed downward irradiance to

irradiance at the top of the atmosphere) to albedo, except in over-
cast (isotropic radiance distribution) instances.

From 0.9 km to 14.9 km flight altitudes, Hovis, et al. (1973)
found a factor of ten reduction in contrast in a 460 nm signal. It was
indicated that 1/2 of the light backscattered from the sea surface
was scattered out of the view of the sensor and that the atmospheric
addition to the radiance signal was 5 times as great at 14.9 km.

Generally the observed effects ($L_Z \equiv$ apparent signal) can be
represented by the equation given by Austin (1974a):

$$L_Z = (L_w + L_r)\, T_a + L^* \tag{3.4}$$

where L_w and L_r are the components of radiance from the sea and
radiance reflected from the surface respectively, T_a is the transmit-
tance of the atmosphere and is wavelength dependent, and L^* is the
scattered atmospheric light contributions and was considered only
20% of L_Z.

Clarke and Ewing (1971 and 1973) have observed the sequential
effects of an increased atmosphere on surface ocean color. Correlations
for the atmospheric contribution were made by substracting the change
in signal between observations at 305 m altitude and 152 m altitude
from the 152 m curve. The resulting surface curve approximates a
spectra of upwelling irradiance measured at 0.2 m below the surface.
The wavelength dependent T_a was not considered, and may have improved
the correlation of the ocean color curves.

In an ocean-atmosphere model by Kattawar and Humphrey (1973)
the optical depth made a negligible change in the radiance ratio
(upward radiance/downward radiance) only at measuring altitudes below
0.1 km.

Duntley et al. (1974) have studied the apparent orbital contrast
of computed apparent spectral radiance signals available at an orbital
altitude from a water mass without phytoplankton to one with 0.3
mg/m^3 distribution throughout the top 50 m from the equation

$$\text{Apparent orbital contrast (C)} = \frac{N_T - N_B}{N_B} \qquad (3.5)$$

where: N_T is the signal from the chlorophyll containing water mass, and
N_B is the signal from the water mass void of phytoplankton. Computations
were made for solar zenith angles from 24.3° - 70.6° and "clear" and
"hazy" atmospheric conditions. His results for both 560 nm and 465 nm
light show that > 0.001 apparent contrast can be obtained at all
angles up to ∿ 55° from nadir viewing, both toward and away from the
sun azimuth angle. The maximum contrast (> 0.003) was with the solar
zenith angle of 30.9°. At solar zenith angles > 42.0° the contrast
was greatly reduced.

3.2.1 Conclusions from Previous Investigations

A representative summary of conclusions from radiometric
studies developed for determination of chlorophyll in surface waters
is necessary for an idea of the state-of-the-art, success of the
methods, and the expectations and recommendations given for future

studies.

In general, three applications have been given for use of remote sensing of chlorophyll in natural waters. Before radiometric studies, fisheries scientists had observed increased fishing of migratory species at color boundaries noticed in the sea (Blackburn, 1969; Panshin, 1971; Pearcy, 1971). Interest and research in all types of radiometric approaches in the fisheries resource area has increased with developing techniques. An example of investigations on parameters considered for remote sensing in fisheries research, including chlorophyll by ocean color analysis, is the 1971 "Symposium on Remote Sensing in Marine Biology and Fisheries Resources" held at Texas A&M University. Blackburn (1969) has concluded that if aircraft and satellite sensors can determine chlorophyll at levels of significance for a biological activity index, the adequate relationship between surface chlorophyll concentrations and fish populations may present the most efficient approach to fisheries search activities. One of the most important aspects of remote monitoring of chlorophyll distribution is the short time space in which it may be accomplished. A dynamic condition such as upwelling, and the sequential response by the food chain, requires this capability of remote sensing to be useful in fisheries resource. The second application of remote chlorophyll determination is in assessment of pollution and eutrophication (Arvesen et al., 1971). The use of satellites for a routine coverage of large regions has been designated the most applicable

method for chlorophyll measurement (Szekielda and Curran, 1973).

If changes in chlorophyll concentrations (blooms or kills) in a specific locale can act as a judicious monitor of discharging activities of known pollutants, documented radiometric chlorophyll measurements could act as a powerful and efficient tool. Phytoplankton in water masses are a non-conservative parameter. This presents difficulties in using chlorophyll concentrations as a label in circulation and mixing studies. However, chlorophyll changes in a single water mass may be used to observe its development over time, and in response to other changing conditions. If remote studies by aircraft or satellite can routinely monitor the surface temperature and the chlorophyll concentrations of a region, systems, patterns, and cycles of systems of water masses may be identified and partially interpreted. This application is the most recent suggestion for radiometric measurements of chlorophyll in natural waters (Szekielda, 1972a).

Ramsey (1968) has quite thoroughly reviewed many processes which are considered factors affecting remote measurement of ocean color and chlorophyll determination at levels of 0.2 mg/m^3. Calculations were made of the contribution to a radiance signal from the ocean by water reflectance and the atmosphere under a variety of conditions. From the data presented, specifications for a spectrometer to determine chlorophyll concentration levels of 0.2 mg/m^3 are given. This reference has been used as the background for the spectrometer employed by Clarke et al. (1970a).

Pearcy and Keene (1974) used differences of normalized back-scattered signals at blue (450-470 nm), green (520-580 nm) and orange (580-650 nm) wavelength bands with additional spectra created from 7 signal band widths in the visible region and IR temperature measurements to identify changes in ocean color radiance with distance offshore from the coast of Oregon. Relationships of these measurements to the Columbia River plume, upwelling and open ocean water types were observed. The oceanic type was characterized by strong reflectance peak observed only in the blue band. The differences of blue-green intensities were largest of any water types. Differences of green-orange intensities were $\sim 1/3$ the blue-green differences. In addition the green-orange difference was very uniform in the oceanic water type. In regions near its mouth, the Columbia River plume was observed to have the lowest radiance in the blue and green, but a backscattered signal in the yellow, orange and red as high as the blue signal in the oceanic type (blue-green decreased) while the blue intensity was as high as oceanic water. A decreased slope in the spectra from the reflectance peak in the blue to yellow green was observed in this region compared to the similar slope in oceanic waters. The region of the plume has been identified as containing a small concentration and smaller sizes of particulates from the river discharge than the river mouth area. Also larger chlorophyll concentration are found in the plume offshore. The chlorophyll concentrations are larger in the offshore plume than in the oceanic water, but this feature can not

be observed by selective blue light attenuation by phytoplankton.
The water type designated as coastal upwelled water has spectra
that vary from maximum signal in the blue (450-470 nm) to maximum
signal in the green-yellow (550-580 nm). The average slope of the
spectra from 450 nm to 580 nm was least of any water type, with the
exception of the river mouth discharge. The difference in water
character between the offshore plume and the most near shore upwelling
region is the greater concentrations of physotplankton, phytoplankton
degradation products and dissolved Gelbstoff in the latter, while more
fine clays and Gelbstoff are contained in the river plume. Pearcy, and
Keene, (1974) have combined comparisons of individual backscattered
signal bands (in this case differences in intensity) with use of
the total spectra to successfully describe these water types. The
blue-green difference is a strong indicator of phytoplankton or,
moreover, biologically established (containing Gelbstoff in addition)
waters. Pigment concentrations were not estimated however. The
difference between green and orange band reflectance is an indicator
of turbidity (lower differences with increasing turbidity) generally
irregardless of chlorophyll concentration. Comparison of color
boundaries or sharp color difference gradients and surface temperature
distribution showed a more complex structure for the ocean color
patterns than temperature. At temperature gradients, color gradients
were always observed, while color gradients were observed independent
of temperature change.

Mueller (1974) has used ocean color spectra collected by
aircraft over open ocean, upwelling and Columbia River plume
regions for covariance analysis of the principle color components
contributing to the observed spectra. It was found that 4 principal
components were responsible for > 95% of the spectral variance. Ocean
parameters of pigment concentration (treated as an average of
chlorophyll and carotenoid pigments as a function of pigment absorp-
tion coefficients, vertical integrations of chlorophyll concentration
and Secchi depth) the volume scattering coefficient, Gelbstoff
concentration and phytoplankton size distribution were shown to create
a similar variance distribution as observed spectra when calculations
of their optical properties as eigenvectors in a radiative transfer
model were made. Phytoplankton was found to be the major source
of variation (76%) while similar variations by non-selective
particle scattering, Gelbstoff absorption and changing phytoplankton
size distribution could produce apparent pigment concentration changes
up to 1 mg/m^3. This large a variation could be calculated by assuming
low concentrations of Gelbstoff and chlorophyll-free particulates
and without considering multiple scattering or the incident light
spectrum. Empirically, the weighted pigment concentration and Secchi
depth were related to the principal components by multiple linear
regression equations with residual standard deviations of 1.6 mg/m^3
and 2.6 m respectively. The parameterization of principal components
as eigenvectors allows an accurate analysis of the ocean color
spectra. Relating ocean color spectra to eigenstructure for uniform
analysis and future reference is worthy of consideration. This would

be especially so if a principal component or components could, in
some way, physically characterize a water mass type. However, as
Mueller points out, an expanded model, which requires measurement
of more optical parameters at sea, must be used to estimate pigment
concentrations or other covariance parameters from ocean color spectra.

The research by Clarke et al. (1970a and b and 1973), Duntley,
(1972), and Duntley et al. (1974) have been the most direct considera-
tions in the differential radiometric method developed and used by
Arvesen et al. (1973).

Clarke et al. (1970a and b) employed a scanning spectrometer
with a spectral range from 400 to 700 nm, scan time of 1.2 seconds
and field of view of 3° X 0.5°. Normalization to incident light
spectrum was accomplished by scanning a horizontal "gray card",
although this standardization could not be accomplished in flight.
The view angle of the sensor for these studies was at the Brewster's
angle. This, plus the addition of polarized filter oriented at right
angles to the major polarization axis, eliminated the large
contribution of polarized surface reflected light to the signal which
has no ocean spectral information. A problem was caused at higher
altitudes of flight (> 305 m) by increased diffuse atmospheric
light to the sensor and loss of spectral detail due to the large
optical depth that the signal must transit. Differences between
spectra of differing chlorophyll regions were maintained at higher
altidudes. Spectral measurements of Buzzard's Bay, the Gulf Stream and

Sargasso Sea with surface chlorophyll measurements of 4 mg/m^3,

0.3 mg/m^3 and < 0.1 mg/m^3 respectively ($\sim$ 2 orders of magnitude)

showed very characteristic curves. Increased intensities at shorter

wavelengths (< 520 nm) with decreased chlorophyll concentrations

cor sponded with decreased intensities at longer wavelengths (> 520 nm)

causing an increasing slope in lower chlorophyll regions. The

inflection point in all spectra was $\sim$ 520 nm. The curves of various

spectral character "rotated" about this wavelength which seemed

insensitive to changes in chlorophyll concentration. Thus it was

called the hinge point. The average slopes correlate well to the

chlorophyll concentrations. Changes of phytoplankton concentrations

were considered the most important influence on the spectral measure-

ments. Szekielda (1974), has determined the difference spectrum of

intensity of backscattered light caused by phytoplankton and dissolved

matter. Gulf Stream spectral energy was used as a reference and was

subtracted from a near coastal water energy spectrum. The resulting

spectrum represents the similar spectral variations observed by

Clarke et al. (1970a). The encouraging results of this study for

chlorophyll determination from ocean color spectral character prompted

further investigation by Clarke and Ewing (1971 and 1973). Spectra

were obtained at altitudes from 150-4500 m over waters of the Gulf

of Mexico, the Pacific near the Panama Canal and along the Mexican

Pacific coast into the Gulf of California. Multiple recordings were

made of each target region at various nadir angles (0°-40°) and

employed different combinations of polarizing filters. In addition,

ship sea truth data for interpretation of spectra and expendable bathyphotometer probes as the aircraft's own sea truth was included in the research. These data and data collected over Buzzard's Bay were interpreted for the effects on the spectral characteristics by various chlorophyll levels, and the atmosphere at various flight altitudes. Comparison of measurements of upwelling light spectra from 20 cm below the surface and 500, 1000 and 2000 ft. altitudes revealed the addition of a predominately blue diffuse atmospheric light. The most drastic change in the spectral character is that from 150 to 300 m. A color ratio briefly described by Clarke et al. (1970b) and fully by Clarke and Ewing (1973) was used as an index to describe the character of spectra, and was related to the spectral effects of chlorophyll concentration changes. Light extinction profiles from bathyphotometers correlated well with the ratio of reflected radiance (540 nm/460 nm). Increasing extinction coefficients compared to increasing color ratio values. The research area of the Gulf of Mexico to the Gulf of California was mapped by the color ratio index and surface chlorophyll concentrations. Chlorophyll concentrations were not strictly related to the ratio. Clarke and Ewing could not discriminate color contributions of silt or sediments from chlorophyll in near coastal areas where the color ratio was > 0.7. In chief problems that remained to be investigated were: to assay varied incident illumination in flight, to better estimate and reduce diffuse atmospheric light interferences, and to identify the characterization of ocean color spectra by other materials in the sea.

Duntley (1972) and Duntley et al. (1974) were concerned with detecting chlorophyll changes at levels of 0.1 mg/m^3 which was considered the base of significant levels for commercial fisheries interests. However, their approach was designed for measurement from earth satellites. Radiative transfer calculations were made on the chlorophyll signal available at orbital altitudes from a backlog of data collected on optical atmospheric parameters, measurement of optical processes in the sea and measurements of varieties of phytoplankton cultures in the laboratory. The results presented represent the apparent optical signal contrast when passing from biologically poor water (Chl a < 0.1 mg/m^3) to higher selected chlorophyll concentrations. Data is presented as polar plots of the field of view and analyzed in apparent orbital contrast isopleths for green and blue wavelengths of returning light and at varying solar zenith angles. These plots indicate the areas of the field of view that sensors must focus in to distinguish chlorophyll changes. Solar zenith angles for best contrast were concluded to be 24° <Θ< 42°. Although most of the reflected visible spectrum was recommended to differentiate chlorophyll from other "ocean colorants", Duntley (1972) concluded that only phytoplankton cause a backscattered spectra to be increased at 560 nm, remain fixed at 523 nm, and be diminished at 450 nm although only pure laboratory cultures and biologically poor waters in situ were measured. Both blue and green wavelengths from ocean spectra were concluded to be of sufficient intensity to be detected through both clear and hazy atmospheres at earth orbit.

Duntley et al. (1974) further developed calculations of chlorophyll signal to an earth orbit by considering vertical distribution of chlorophyll, different species composition and differences in filtered base water composition. Radiative transfer calculations of two vertical profiles of chlorophyll distribution showed that the diffuse reflectance is only related to near surface concentrations (< 5 m) and integrated chlorophyll values through the water column and spectral diffuse reflectances are ambiguously related. Intensities of back-scattered light to ERTS-1 satellite in a 500-600 nm channel were determined to be proportional to near surface plankton (Szekielda, 1974). Calculations by Duntley et al. (cit. loc.) suggested that increases of sediments in suspension only increase the total diffuse backscattering coefficient and not the diffuse absorption. Thus the net result should be reflectance increase at all wavelengths in optically deep waters, and sediments can be distinguished from chlorophyll-bearing phytoplankton by the shapes of their respective spectra.

With the previous suggestions for chlorophyll determination by color ratio, Arvesen et al. (1973) studied a correlation method, based on differential radiometry to detect chlorophyll. The criteria he used for 443 nm/525 nm wavelength selections were based on independently observed characteristics of natural phytoplankton, Rayleigh-like seawater attenuation, and "white" Mie scattering by larger particulates. No theoretical treatment of the process of color ratio production or atmospheric transfer was considered. The

differential radiometric method did solve some of the previous problems described. A normalization of incident light intensity could be accomplished simply by adjusting the incident ratio (I_{443}/I_{525}) to unity. The difficulty in spectra analysis was removed and a continuous color index now could be more closely compared to continuous airborne radiation thermometer measurements. This also allowed an easy, real-time interpretation. The results of measurements over varied natural water types at an altitude of 150 m demonstrated the capability of this method to estimate surface chlorophyll levels.

Hovis et al. (1973) have continued studies using numerous reflected ratios at 11.3 km and 0.3 km altitudes over ocean areas off North Carolina and the Gulf Steam, San Francisco Bay, and NW Africa. Because satellite spectral data will be recorded as spectral bands and not complete spectra, color ratios-to-parameters comparisons were designed. A rapid scan spectrometer with a field of view of 3.8 X 3.8 milliradians was employed in this study. At low altitudes this narrow target resolved surface effects of waves. The spectra at the different altitudes were compared, and, in contrast to Clarke and Ewing (1973), there was severly reduced contrast. A factor of 2 reduction in contrast was observed even after the elimination of skylight from the high altitude signal. The conclusion was that this information had been scattered out of the radiance column viewed by the spectrometer. Hovis et al. (cit. loc), concluded that the use of ratios could minimize changing, broad spectral atmospheric effects by referencing to a spectral band that is insensitive to spectral changes in the ocean's

backscattered signal. Besides the 550 nm/443 nm ratio used previously, ratios of 600 nm/520 nm, 665 nm/520 nm and 550/600 nm measured at high altitudes also showed correlations to chlorophyll measurements. Under haze conditions the 550 nm/443 nm and 665 nm/520 nm ratios best correlated with chlorophyll concentrations. The calibration by Arvesen (Figure 3.1) was used by Hovis et al. for the NW coast of Africa data. Correlation of temperature changes simultaneous to color ratio changes supported the 443 nm/525 nm ratio as an index of chlorophyll because of the known response of phytoplankton to cold, upwelling waters.

3.2.2 The Differential Radiometer

The differential radiometer (DR) (Arvesen et al. 1973 and Arvesen, 1973) is an extension of the use of wavelength ratioing for determination of phytoplankton pigments in natural waters. In general, the instrument is designed to measure two narrow spectral regions of reflected (backscattered) light from water bodies at aircraft altitudes and produce a continuous signal which is a ratio of the two.

The reflected light is received in a sensor assembly through a fiber optics bundle. The field of view of the bundle is 30°. The bundle is then divided into four sections, each section having the same field of view. Behind each section is a spectrally narrow bandpass filter ($\Delta\lambda \sim 15$ nm) selected to allow transmittance of the spectral region of interest. Radiation passing through each selection filter is incident on a silicon photodiode detector (UDT 500).

Integral with each detector, a preamplifier produces an output voltage
signal proportional to the incident radiation. These signals can be
monitored directly. Two signals are further processed to produce
the following algorithm:

$$\text{Ratioed output signal} = 10\ \frac{(\text{Signal of detector \#2-Signal of detector \#1})}{\text{Signal of detector \#2}}$$

volts. Similarly, the signals from the remaining two fiber optic bundle
sections are processed and can yield a second ratioed output signal.
One output signal, developed for determination of chlorophyll in
water bodies, has selected filters which transmit a 443 nm band
(detector \#1) and a 525 nm band (detector \#2). The second output signal
was not used in this study because no other correlations of wavelength
ratios and features effecting ocean color have been proposed at present.

The objectives of the differential radiometer's design are to
provide a high resolution, continuous, real-time, remote determination
of chlorophyll pigment concentrations in near surface waters and still
be simple to operate. The principle of this method for remote sensing
of chlorophyll is a culmination of the conclusions from previous
research outlined in Section 3.3.1 First, the specific spectral
characteristics of chlorophyll in natural water were considered.
The proportional loss of reflected intensity in the 443 nm region is due
to the absorbance by increasing concentrations of chlorophyll pigments,
and the insensitivity of the reflection intensity at 525 nm to changes
in clear, natural waters (Duntley, 1972). The 443 nm intensity, then,

is the sample signal wavelength (λ), while the 525 nm exists as a background or reference λ. The interference to the sample signal (443 nm) and the reference signal (525 nm) by suspended sediments and the molecular attenuation of sea water was, from the preliminary research at the time, considered to have an equal effect on both wavelengths. Therefore, the algorithm would continuously compare the intensities of the reference wavelength and the sample wavelength to normalized interferences. From the algorithm it can be seen that the radiance ratio is linearly proportional to the voltage output.

A normalization of the incident light intensities (i.e., $I_{443}/I_{525} = 1$) at the flight altitudes can be obtained. Since the sensor is a flexible fiber optic bundle, direct viewing of solar radiation can be easily accomplished. A spectrally flat diffusor is placed over the sensor to decrease the intensity and also to increase the diffuse light to the sensor. Adjustment of a potentiometer varies the sample signal output so sample and reference intensity can be normalized. This solar zero operation can be accomplished periodically during flight with changes in sunlight conditions and changing solar zenith angle. Limiting skylight-sunlight intensities for instrument use have not been well established.

The sensor is mounted at an angle of 20° off nadir. Also, the mounted sensor may be rotated to any azimuth angle. The conclusions on optimum direction of sensing for the most valuable optical signal were followed in the design of this mounting apparatus (Duntley, 1972;

Duntley et al., 1974; Austin 1974a and b). A field of view
of 30° also gives a specular average signal large enough that sun
glitter contribution is negligible.

The calibration of the differential radiometer (DR) ratio system
in terms of chlorophyll concentration is the result of 50 measurements
over water bodies of various, known concentrations. This included
clear lakes, eutrophic lakes, marine water of varying chlorophyll
content and an estaury. The chlorophyll concentrations ranged from
< 0.03 to > 10.0 mg/m^3. The airborne measurements were made at an
altitude of 150 m. Arvesen (1973) shows a remarkable correlation
between sea truth and DR measurements along one 700 km track southwest
from San Diego. Arvesen's calibration (Figure 3.1) is also in agree-
ment with a well established principal in ocean color observations.
At very low concentrations of chlorophyll small changes in concentrations
correlate to large changes in the 443 nm/525 nm ratio. In water masses
of higher concentrations of chlorophyll, a far greater change of
concentration is needed to produce the same magnitude change in the
color ratio. The DR was shown capable of detecting chlorophyll
variations < 0.03 mg/m^3. Unfortunately, the total suspended particulate
distributions are not given for additional comparison.
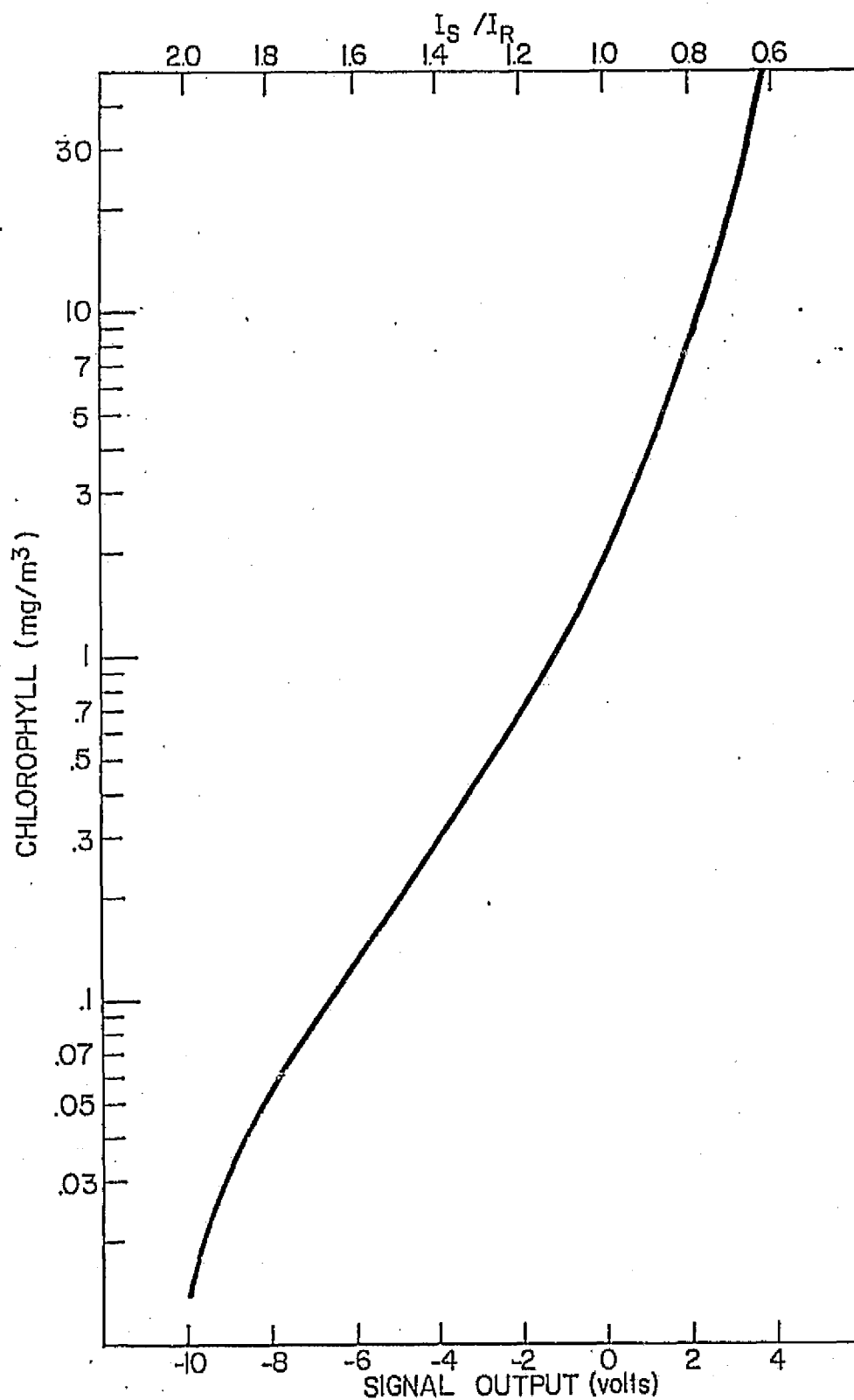
Figure 3.1 Calibration curve of DR ratio values (I_S/I_R) and proportion·l analog Signal Output (in volts) to Chlorophyll Concentration units (mg/m^3).

Additional considerations for effective use of the DR
followed in the present study are: The solar elevation angle should
be > 20° to insure adequate backscattered signal with respect to
background radiance. The direction of view was 20° from nadir oppos-
ing (180°) the solar azimuth angle to reduce sun glitter reflec-
tion 'o the sensor. As the solar azimuth angle changes in respect
to the aircraft, it is then necessary to correct the azimuth viewing
angle of the radiometer. The preliminary effective depth of measure-
ment was considered to be about one-half to one-third of the Secchi
depth (Arvesen, 1973). This limitation is more firmly defined by the
present study. Additional information on the DR is given by
Arvesen (1973).

A pre-study evaluation of the effectiveness of the color
ratioing method is difficult. A number of published aircraft ocean
color spectra with corresponding sea truth chlorophyll concentrations
(Duntley, 1972; Clarke and Ewing, 1973; Mueller, 1974; and Pearcy and
Keene,' 1974) allow development of a color ratio chlorophyll concen-
tration comparison. However, various altitudes of flight, chlorophyll
concentration ranges of most measurements within only two order of
magnitude, and individual analysis of the data make a cummulative
comparison impractical. Generally, from comparison of color ratios
to chlorophyll concentrations for each study individually, the scatter
is far more than that seen by Arvesen. Also, in the calibration of
very high chlorophyll values, the larger change in the color ratio

(compared to Arveson's calibration) is indicated for similar changes
in chlorophyll concentrations > 20 mg/m ^{3} . This is supported by
Curran (1972) in a comparison of chlorophyll concentrations and the
reflected color ratio 540 nm/460 nm.

4. FIELD METHODS

The NW coast of Africa has long been recognized as a region of upwelling. Smith (1968) has given a general review of the physical oceanographic processes which result in this phenomena observed at the Eastern boundaries of most oceans. Results of previous oceanographic exploration have been reported by Defant (1961), Furnestin (1959), Jones and Folkard (1970), Jones (1972), Fedoseev (1970), and Schemainda et al. (1972). Biological results including chlorophyll measurements have been reported by Furnestin (1970), Lloyd (1971) Ballester et al. (1972) and Margalef (1971 and 1972). Interest in better defining this upwelling area which led to the Sahara Upwelling Expedition and the JOINT-I project originated from the recognition of the upwelling area by the previous investigations cited.

4.1 The SAHARA UPWELLING EXPEDITION

In August, 1973, a joint project based on skylab investigations (Szekielda, 1972b) was conducted by the University of Delaware and NAVOCEANO. The area of operation was along the NW coast of Africa from Cabo Juby (28°N, 13'W) in the north, to Cabo Bojador (26°N, 14°30'W) in the south. The area of operation extended seaward 90 nautical miles to Fuerteventura. The bathymetry of this area is shown in Figure 4.1.

The Sahara Upwelling Expedition (SUE) was designed as an experimental mission with these three objectives: 1) to test from
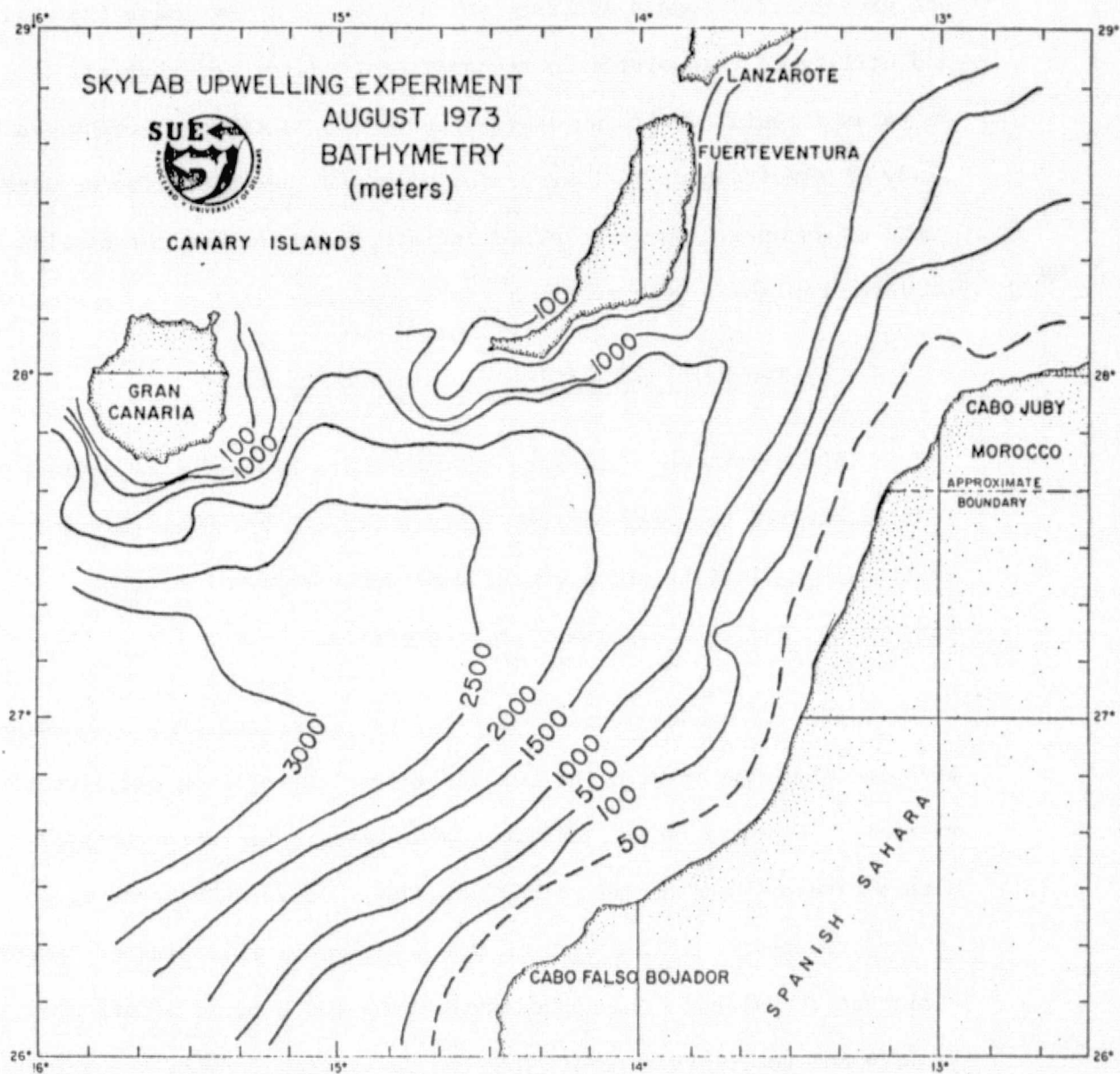
Figure 4.1 Bathymetry of the Sahara Upwelling Expedition research area.

aircraft altitudes a suite of experiments including expendable probes and experimental remote sensing instruments, 2) to evaluate the ability and utility of this system to recognize biological and physical patterns associated with an upwelling region, 3) to be a comparison study of simultaneous surface truth, aircraft, and satellite measurements in an upwelling area to aid in interpretation and correlation of data acquired by the remote sensors employed.

4.1.1 The Experimental Instrumentation Package

The experimental package of the Sahara Upwelling Experiment (SUE) contained both radiometric sensors for reflected visible and emitted IR radiation, and airborne expendable probes for light penetration and vertical temperature profiles.

The differential radiometer described in Section 3.2.2 and an airborne thermometer were the remote sensors employed on the aircraft missions. Continuous sea surface temperatures (SST) were recorded with a Barnes Airborne Radiation Thermometer 14320 (ART) operating in the atmospheric window between 9.5 - 11.5 μm. This band of infrared radiation is emitted from approximately the top 0.02 mm of the ocean's surface and therefore reveals only the sea surface's skin temperature (Clarke, 1964; Wilkerson, 1966). Aircraft thermal IR measurements have been discussed by Clarke (1967) and Saunders (1967a). The raw analog ART data were recorded on a strip chart recorder. Continual calibration and corrections for altitude (depth of air column) attenuation, air and lens temperatures from a format used by NAVOCEANO (Kerling, 1973) were applied to the raw ART signal so a corrected SST could be

recorded on a second two-channel recorder. The ART sensor head was mounted 50 cm above the main deck of the aircraft and 1.5 m above the aircraft skin in the viewing position normal to the sea surface plane. The normal viewing angle has minimum correction due to shortest optical depth and smallest influence by surface reflected solar energy (Saunders, 1967b). The field of view (f.o.v.) of the sensor was 2.2°. Extending this solid cone for 300 m, the operating altitude of the SUE mission, the target spot of the ART was 11.5 m in diameter. At an average ground speed of 108 m/s and an ART response time of approximately 1.0 second, the best spacial resolution available from this instrument system was 108 m. The target spot of the DR was 184 m in diameter with its f.o.v. of 30°.

Two expendable probes, a 300 m bathythermograph and a bathythermograph modified to record light penetration levels, were included in the SUE mission. The airborne bathythermograph (AXBT) is dropped from an aircraft and on impact at the sea surface an FM transmittor is activated by a sea battery. A carrier signal is transmitted which corresponds to a temperature measurement at the surface. Following the carrier signal, the probe falls through the water column in the same manner as a conventional expendable bathythermograph (XBT). The signal is transmitted to the aircraft where changes in frequency are recorded versus time and calibrated to °C. versus depth.

AXBTs were modified similarly to those used by Clarke and

Ewing (1973). The airborne expendable photometer (AXPM) has
incorporated a zenith viewing photocell replacing the temperature
sensor of the AXBT. The carrier signal is a measurement of light
incident at the sea surface. The profile, recorded as increasing
extinction of light penetration with depth, can be calibrated to
percent incident radiation (% I_0). Schematics of the expendable
probe operation and a description of signal evolution are presented in
Appendix A. AXBTs and AXPMs were dropped seconds apart so vertical
temperature profiles could be correlated with light attenuation pro-
files. Probes were dropped on parallel flight lines which ran
approximately normal to the coast. The profiles measured on these
lines were analyzed as two dimensional vertical slices.

4.1.2 Experimental Procedures and Data Collection

The date, time, and comments of four flights in the SUE
mission are shown in Table 4.1. Differential radiometer and narrow
band airborne radiation thermometer (ART) signals were recorded
simultaneously on a two-channel strip chart recorder. Time marks,
course changes, station marks, instrument adjustments and calibrations
were noted on the strip chart by the differential radiometer operator.
Visual observations of ocean and sea surface features, atmospheric
conditions and solar azimuth positions radioed by the pilot and front
and rear observers were noted as well. Complete weather observations
were logged every fifteen minutes during the flights. The continuous
differential radiometer and ART signals were immediately available
for interpretation of surface gradient structure and thus, were a

decision making input in the expendable probe experiments.

Fifty-seven Airborne Expendable Bathythermographs (AXBTs) and thirteen Airborne Expendable Photometers (AXPMs) were deployed in the SUE mission for vertical temperature and incident light penetration profiles respectively.

On August 22 and 26, additional reflected wavelength regions were recorded from the differential radiometer's secondary channels. The continuous reflected intensity of yellow and red optical energy from wavelength regions centered at 576 nm and 663 nm respectively was recorded for a major portion of the August 22 flight (see Table 4.1). The 576 nm yellow band and a substitute 723 nm red band were again recorded on August 26 for the entire six hour flight.

Table 4.1   Research Flights of the Sahara Upwelling Expedition

(SUE)

Date, 1973	Time	Comments[2]
		For all flights: ground speed 195-205 Knots Altitude: 1000 feet (305 m)
August 18	0640-1240	1 AXPM[1] deployed at end of leg 5, occasional haze and clouds below aircraft, > 70% cloud coverage overhead
August 21	1139-1753	Expendable probe mission, 11 AXPMs deployed during legs 8, 6, 5, and 2; > 80% cloud coverage during 20% of flight.
August 22	1159-1824	Additional reflected wavelength bands recorded (576 nm and 663 nm), 1 AXPM dropped at 1416 (between legs 4 and 9),

(continued)

Table 4.1 (continued)

Date, 1973	Time	Comments[2]
August 26	1143-1723	Additional reflected wavelength bands recorded (576 nm and 723 nm), haze to 90% overcast for 15% of flight.

(1) Airborne Expendable Photometer

(2) Airborne Expendable Bathythermograph deployment is given by

     LaViolette (1974).

4.1.3 Flight Planning

The coverage intensity and regional area chosen for the research

flights were designed to give a synoptic monitoring of an upwelling

region large enough for comparison studies with the resolution of

satellite data. After the morning flight of August 18, in which

research was partially hampered by cloudy and hazy conditions, the

remaining flights were scheduled in the middle of the day which also

allowed for use of same-day NOAA-2 satellite images for scheduling.

The average duration of the flights was 6.5 hours. The regional

area was the coastal to open ocean waters between the Canary Islands

(Gran Canaria and Fuerteventura) and the coast of Northwest Africa

from Capo Juby to South of Capo Bojador.

4.2 The JOINT-I PROJECT

The JOINT-1 project of the Coastal Upwelling Ecosystems Analysis

(CUEA) program was an intense oceanographic study of an upwelling area

approximately one degree square (17°-18°W, 21°-22°N) off Cap Blanc in northwest Africa for a three month period from mid February through mid May, 1974. JOINT-I incorporated a twin-engined aircraft from the National Center for Atmospheric Research (NCAR) with participating U.S. oceanographic vessels from NOAA, Woods Hole Oceanographic Institute and University of Miami. In addition the French research vessels Jean Charcot and Capricone, the Spanish research vessel Cornide de Saavedra; and the Mauritanian research vessel Almorivide participated in the project. Synoptic temperature coverage of the research area was performed by the NOAA-2 satellite.

4.2.1 Airborne Measurements

The aircraft's oceanographic mission was designed as an operational survey to support research vessel activities in the vicinity with the objectives of synoptically monitoring sea surface temperature and phytoplankton chlorophyll pigment concentrations in near surface waters by remote sensors. In addition, the aircraft was to study meteorological conditions related to upwelling regimes. It was designed that data acquired over the extended period of the aircraft's mission be transmitted daily in a hard copy form (as analyzed sea surface temperature (SST) and surface chlorophyll (Chl.) maps) via communication satellite to ships in the research area. The distribution of these surface parameters could then be used to locate upwelling events and as a decision-making input into selecting areas for intense investigation. On the other hand, the data collected by the differential radiometer (DR) and the radiation thermometer (PRT-5)

were supported by the sea truth obtained by the research vessels. This data includes surface chlorophyll measurements, sea surface temperatures, distribution of particulates and incident light penetration.

Specifications of the radiation thermometer and the twin engine Beechcraft "Queen Air" used in JOINT-1 are described in NCAR (1973). Pre-flight calibration was accomplished by sensor measurement of a water bath. Periodically during the flight, the solar standardization of the DR was accomplished (see Section 3.2.2). The mounting of the DR sensor in the aircraft allowed manipulation of the azimuth angle, while the viewing angle was 20° from nadir. The PRT-5 sensor head was mounted at nadir. The operating altitude of the aircraft was 500 feet (150 m). The f.o.v. of the DR is 30°, and at the operating altitude the target spot of the DR is ∿ 92 m in diameter. The PRT-5 sensor's view was unobstructed by the aircraft skin. The plexiglass window through which the DR viewed the sea surface was identical to the observation window material through which solar standardizations were made.

4.2.2 Flight Planning

Two types of oceanographic flight plans were devised to give periodic intense coverage of a small (1/2° longitude by 1° latitude) area and larger (1° square) area synoptic coverage. Occasionally, both types of flights were flown on the same day for comparison purposes. Intercepts in the flight tracts were designed to give

cross-referencing points for aircraft instrument checks. Oceano-
graphic flights as scheduled did not have more than a two day lapse
between consecutive flights.

. Meterological flights required a profiling of the air column
and no oceanographic data were obtained. On days when one oceano-
graphic flight was scheduled, the time of optimal sun elevation for
the differential radiometer was selected. This was between 1000-
1400 hr. local time. The average duration of flights was four
hours.

Whenever research vessels were in the vicinity of the flight
tract, the aircraft diverted to make several overpasses to obtain sea
truth measurements. The time "on course" in these passes over the
vessels was usually more than one minute. The amount of time insured
stability of differential radiometer adjustments after the
course change.

Experiences early in JOINT-I with days of high dust loading
and its detrimental effect on the aircraft's operation became a
safety factor in scheduling flights. The dust that eventually sifted
into the instruments, especially the Inertial Navigation System and
the NCAR Aris data collection system, caused frequent inflight failures
in the later flights and finally an early conclusion to the aircraft's
mission.

4.2.3 Aquisition Format and Data Handling

Thirty-five research flights from Feb. 17 to March 28, 1974 were accomplished. Table 4.2 shows the date, time, and type of each flight. Raw data available immediately were the precision radiation thermometer (PRT-5) and differential radiometer traces on the two-channel strip chart recorder. These recordings were annotated with time marks, visual observations of atmospheric and sea conditions by the rear observer who operated all instrumentation, and with observations of the pilot and front observer. This was particularly important for discrimination in the data of course changes, transition from cloud-free to clouded areas and visual observations of properties on the sea surface such as cloud shadows, large slick areas, slick streaks, color boundaries, color streaks, foam lines, and fishing vessels (Tabor, 1974). Besides the detailed strip charts, the front observer kept a log of times and positions of arriving and leaving stations and of features noted by him or the rear observer. The Inertial Navigation System (INS) allowed a direct, real-time readout of position, heading, distance to the next station and ground speed. These observations also were routinely noted with the specific observations made in the front observer's log.

All oceanographic sensor data were recorded via the Aircraft Recording Instrumentation System (Aris) data collection system on multichannel magnetic tape. This included the differential radiometer and PRT-5 data, the position data from the INS, and time. A description of the Aris system developed at NCAR is given in NCAR (1973).

Digital values were recorded on tapes at eight values per second

after computer processing. For oceanographic data usage at this time,

one second averages were considered sufficient and expediated the

processing of the twenty-six oceanographic flights. At NCAR in Boulder

Colorado, the data from the computer tapes were printed on microfilm

which gave fifteen-minute plots of the different parameters versus

time as well as the one second average listings of parameter values.

The best spatial resolution for the one second values at the average

aircraft speed of 140 knots was $\sim$ 78 meters.

Table 4.2 JOINT-I Oceanographic Research Flights

Flight #	Date, 1974	Local Time	Flight Pattern	Average Wind Direction/ Speed	Comments
1	Feb. 17	0835-1320	Small scale: N	060/40	light haze (dust) - top at 2000 feet
2	Feb. 18	0840-1300	Small scale: S	050/10-89	thick haze - top 4000 feet
3	Feb. 19	1230-1605	Large scale		scattered cumulus
4	Feb. 20	0800-1200	Small scale: N		occasional clouds
5	Feb. 20	1325-1630	Small scale: S	-/10-67	
6	Feb. 21	0815-1215	Modified small		light haze
7	Feb. 22	0810-1140	Large	-/02-68	Cloudy
8	Feb. 28	1335-1745	Small		occasional clouds, light haze-top 2000 feet
9	Mar. 4	1320-1630	Small	020/12	
10	Mar. 5	0800-1130	Large	050/18	few clouds, light haze-top 3000 feet
12	Mar. 6	0800-1145	Small	353/17	scattered heavy cloud cover
13	Mar. 6	1315-1700	Small	350/15	special flight for comparison with AM
16 *	Mar. 8	0950-1340	Small	002/14	light haze
17 *	Mar. 9	0800-1200	Small	045/22	Partially cloudy
18 *	Mar. 9	1330-1700	Large	025/23	
19	Mar. 12	0750-1035	Small	045/27	low visibility. (3-4 miles), flight cut short, no Chl. data
20	Mar. 12	1320-1640	Large	040/27	low visibility, heavy clouds and dust - top 3500 feet
23 *	Mar. 16	0740-1130	Small	035/25	light fog and dust - top 600 feet

Table 4.2 (continued)

Flight #	Date, 1974	Local Time	Flight Pattern	Average Wind Direction/ Speed	Comments
24	Mar. 16	1320-1450	Large	034/18	very dusty, flight cut short
29 *	Mar. 19	1000-1305	Small	036/21	
30	Mar. 20	0745-1130	Small	045/22	frequent clouds
31	Mar. 20	1315-1630	Large		
32	Mar. 21	1005-1450	Small	-/23	dust top 4500 feet
33	Mar. 28	0915-1015	Small		flight cut short - no data
34	Mar. 28	1345-1720	Small	359/16	occasional cumulus, light haze top 1500 feet no computer digital data, analyses from strip charts
35	Mar. 29	0815-0915	Small		scattered N-S cumulus, flight cut short

* Flights described in text.

5. RESULTS OF FIELD STUDIES

5.1 SAHARA UPWELLING EXPEDITION

5.1.1 Explanation of Data Analyses

Analog sea surface temperatures (SST) and differential radio-
meter (DR) voltages calibrated to chlorophyll (Chl.) values from the
calibration curve described in Section 3.2.2 and presented in Figure
3.1 were digitized in one minute averages, then plotted on flight
tracts mapped by the aircraft's navigator. The rationale of using
one minute average intervals of continuous data was: for a first
comparison with either continuous chlorophyll measurements from vessel
or spacecraft data, 6 km average values would be most useful and
convenient. The analog recordings existed as a reference if greater
resolution would be needed. The decision of which data were excluded
from analysis was made from the written comments on the airborne
recordings and distinctive features in the traces such as signal
spikes due to aircraft motion and loss or increase of normal low level
surface noise by cloud scatter processes or sun glint respectively.
Cloud contaminated regions were disregarded in DR data and excessive
sun glint, cloud cover and banking motions of the aircraft were
disregarded in both the DR and ART data. For example, the August 18
flight was the only morning flight of the SUE mission and the large
change in solar elevation throughout the flight and variations in
atmospheric conditions suggested some limiting conditions for the
radiometric method. The DR data before 0800 hours was rejected due to

insufficient solar incident light and skylight through the > 70%
cloud cover. Cloud contamination beneath the aircraft caused
features in the recordings which had similar appearance to actual
color boundaries. Loss of the background reflection noise from
constant sea state oscillations helped differentiate this interference
from actual features. Clouds and cloud shadows erratically increased
the ratio value of reflected light. An erratic ART signal supported
the DR signal under these conditions. Analysis of the data maps involved
contouring of SST in °C. and DR maps in mg/m^3 chlorophyll as per
calibration curve. The final forms of these maps are presented in
Figures 5.1 a-d. The flight path, divided into one minute intervals
on the SST maps and two minute intervals on the Chl. maps, is
indicated by discrete data points. The intervals of chlorophyll
contour are not equal and this caution in interpretation of gradient
structure should be observed. A representation more closely related
to ocean color changes can be exhibited by this presentation, but
again a cautious interpretation is needed.

Data received from the expendable probes were analyzed on
return to the laboratory. Amplification and normalization of the
Airborne Expendable Bathyphotometer (AXPM) recordings were
needed for interpretation as light penetration. Data of the routinely
used Airborne Expendable Bathythermographs (AXBT's) could be analyzed
immediately. The absolute accuracy of the temperature values given
in the results of the SST and AXBT data is not known. The relative
accuracy of these measurements, due to the intercomparisons of data

that were made, is reliable.

5.1.2 Description and Interpretation of Sensor and Probe Measurements

Results of the SAHARA UPWELLING EXPEDITION (SUE) include: 1) maps of the regional distributions of sea surface temperature (SST) and apparent chlorophyll values (Chl.) that were observed in an eight day period from 18-26 August, 1973 (Figure 5.1 a-d), 2) analyzed continuous recordings of DR and ART signals plus reflected intensities of yellow (576 nm) red (663 nm) and near IR (725 nm) bands which are presented for comparison of changes in the offshore and longshore direction (Figure 5.2 a-e), 3) simultaneous light penetration and temperature profiles of offshore sections on 21 August for identification of upwelling phenomena and for light penetration - surface ocean color comparison (Figure 5.3).

In figure 5.1 a-d, DR measurements indicate increased near-shore surface chlorophyll levels in all flights with maximum levels ranging from > 1 mg/m^3 on August 21 and 22, to > 5 mg/m^3 on August 18. Also common to all flights are the longshore paralleling contours which have differing degrees of offshore distensions, but consistently decrease in value moving offshore. The most dramatic changes in apparent chlorophyll levels are nearshore, but structure can be observed offshore in all flights as well. If the results of the four flights are observed in time sequence, a number of developments can be described and interpreted. The 18 August analysis shows

the most seaward-extending temperature structure and Chl. structure

of any date during SUE. Offshore distending isotherms indicate a

plume of colder water. From the sequential flights (21 and 22 August)

this feature appears to separate from the constant coastal

structure and move generally west by 21 August and then south by 22

August. On 18 August, the Chl. is apparently > 0.5 mg/m^3 in the position

of the plume < 19°. The Chl. analysis indicates that the plume feature

is already separated from the coastal region on 18 August. Through

21 and 22 August, the temperature difference between the plume and the

surrounding water is lost. Any Chl. difference between the surrounding

water and this migrating plume was not identified on 21 August. On

22 August, however a > 0.5 mg/m^3 feature which corresponds to the NW

temperature boundary is apparent south of Gran Canaria. Low Chl. and

> 21° SST are observed to the south of Fuerteventura. In reference

to the southerly Canary Current, this would be the leeward side of

the island. LaViolette (1974) interprets the isolated patches of

> 21° water (on 21 and 26 August) as surface eddies or an island wake

created by the expansion of the Canary Current south of the island

after the channelling between the African coast and Fuerteventura.

The > 21° feature was observed on all dates. This corresponded

to the clearest waters measured by the DR. Data from 18 August

demonstrate a very strict correlation between decreasing SST and

increasing Chl. The striking identity of location for both Chl. and

SST gradients in all areas and on all dates indicates a

significant dependence of the Chl. measurement on temperature structure.

The structure noted on the 21 August in the 0.5 mg/m^3 contour (the

third flight line from the south) is difficult to interpret. There
is a correlation between the SST and Chl. distribution. However,
these measurements were taken during observations of glint. This would
have the effect of cau... the chlorophyll values to be inaccurately
high. The signal reflected from the surface would approach the ratio
obtained during the solar zero procedure. Since the actual reflected
ratios from the sea in this locale were low compared to the solar zero,
sun glint received by the sensor would raise the values. This would
cause excessive noise in the DR analog signal if it was a significant
input to the sensor. The vertical section results (Figure 5.3), on
the other hand, support the surface temperature gradient. On August 22,
an isolated patch of < 0.2 mg/m^3 Chl. was observed to the southwest
of the structure of 21 August. This may be the development of an
isolated, very clear water parcel moving in the southerly Canary Current
offshore of coastal upwelling activity as indicated by the temperature
and apparent Chl. gradients. The distance which this feature and the
lower temperature offshore patch described above have moved in a one
day period is comparable with the ~ 1.5 knot speed of the Canary Current
(Fedoseev, 1970). On 21, 22 and 26 August, isolated patches of very
low Chl. were measured just offshore of strong temperature gradients.
The only high Chl. patch was measured on 26 August. The development
of the large Chl. plume extending to south of Gran Canaria can not
be interpreted due to the longer time interval between this and the
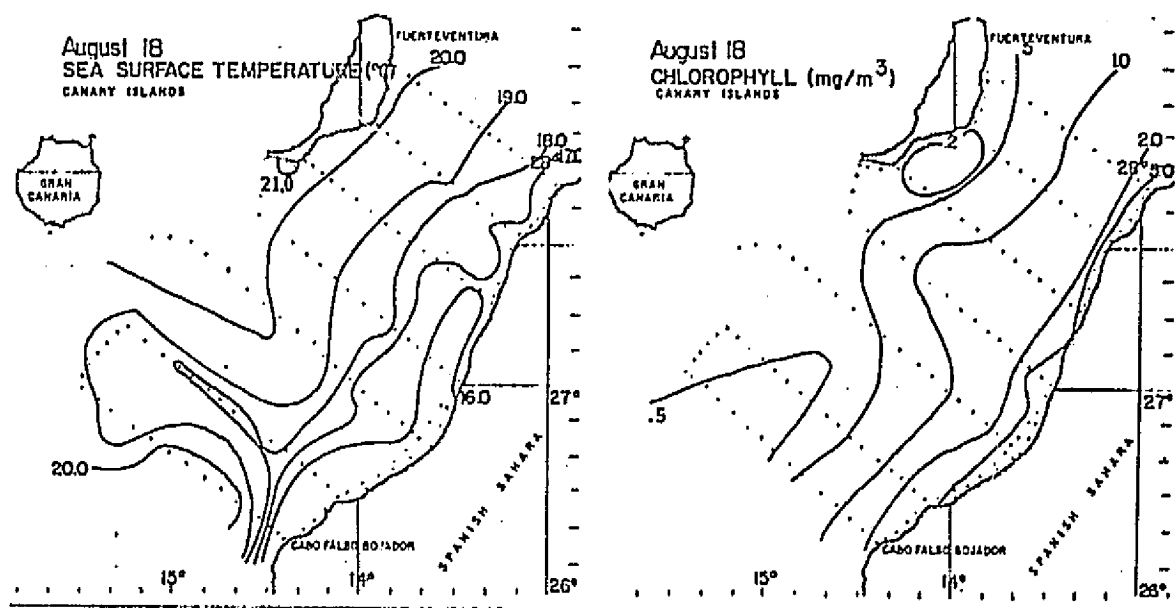previous flight.

Figure 5.1 a-d (continued on page 54).   Analyses of apparent Chlorophyll
(mg/m^3) and Sea Surface Temperature ($^\circ$C.) distribution on
18, 21, 22, 26 August, 1973.   The numbered solid lines (1-5)
on the 22 and 26 August flight   tract indicate the direction
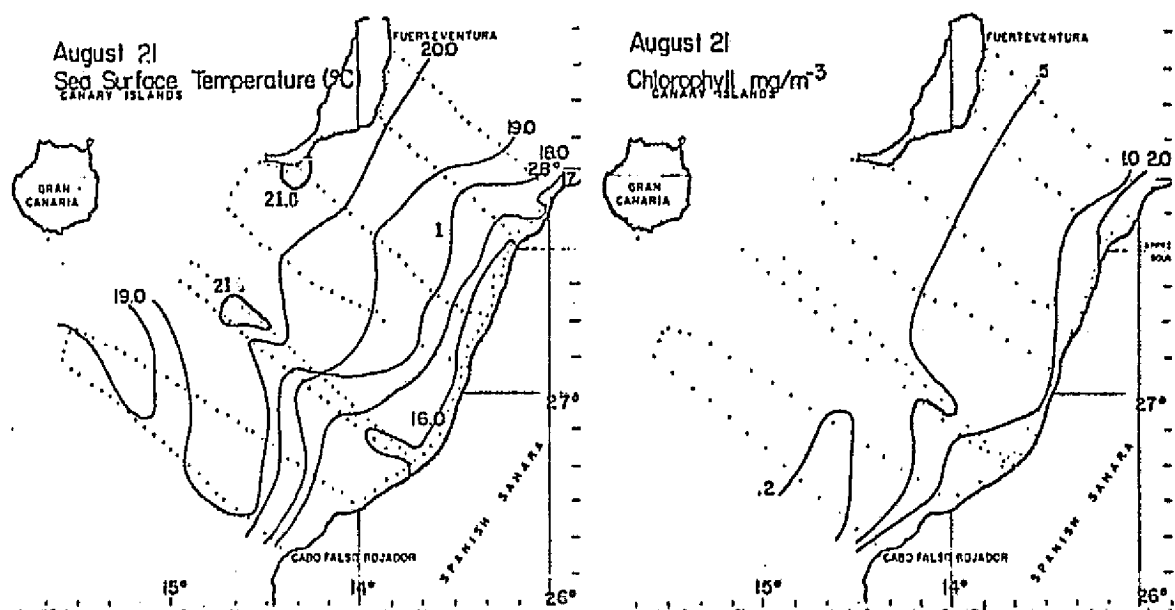and position of the continuous recordings presented in Figure
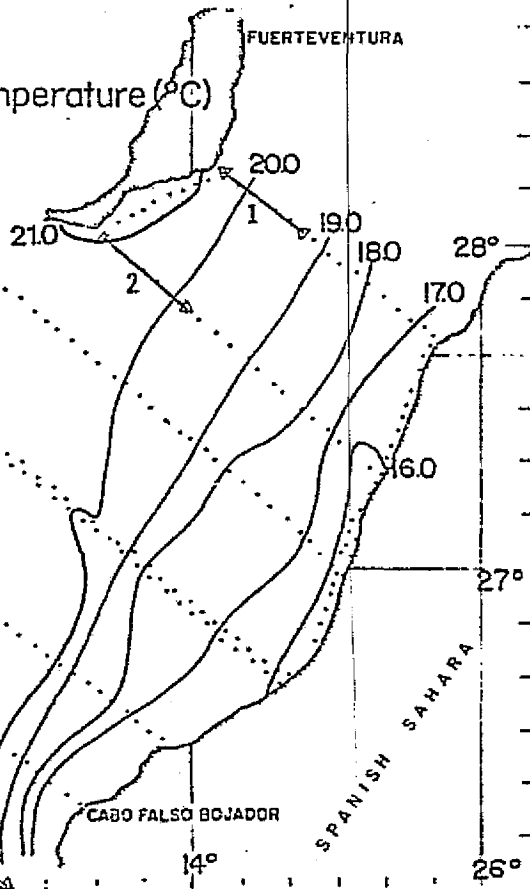5.2 a- 5.2 e respectively.

Figure 5.1b

August 22
Sea Surface Temperature (°C)
CANARY ISLANDS

August 22
Chlorophyll mg/m^3
CANARY ISLANDS
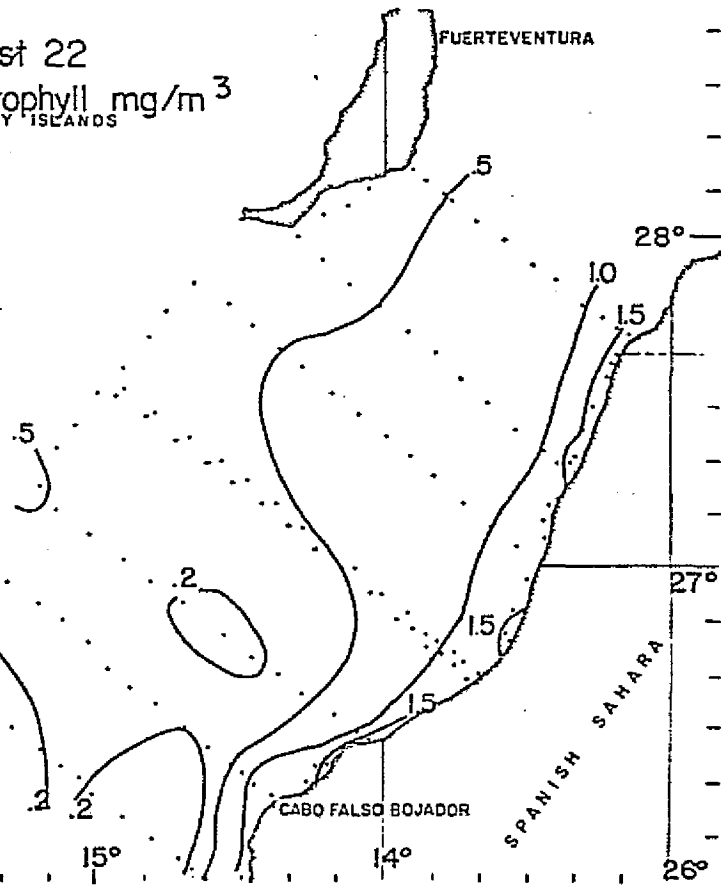
Figure 5.1c

In actuality, both SST and Chl. have more fine structure

variability or meandering than is shown because the analysis can only

be interpolated between flight lines. This can be exhibited where

flight lines are positioned nearer each other and thus the data

distribution concentrated. In all flights, the inshore legs running

parallel to the coast showed small, quite frequent plumes of apparent

chlorophyll. Two other observations tend to discount these as

measurements of actual chlorophyll. The SST of these plumes was

consistently higher in the plume and lower in contiguous areas. In

general, this is the converse of the results that showed decreasing

surface temperature with increases in apparent chlorophyll. This

feature could not usually be resolved in the one minute average

analysis, but it is observed in the continuous recording of

Figure 5.2c at time 1610. Photographs of the sea surface from the

aircraft showed plumes of sediment with the frequency and size of the

features indicated by the DR. The plumes can be interpreted as warmer,

surf zone water heavily laden with large sediment particles flowing

offshore and surrounded by colder, less reflective coastal water.

In this case, it was visually clear the DR measured particulate

load as increased chlorophyll levels. More disperse non-phytoplank-

ton particulates originating from coastal errosion and bottom distur-

bance are suspected to partially cause the general apparent chlorophyll

increases in all near shore areas.

On August 22 and 26, in addition to the DR and ART signals,
red (663 nm or 723 nm) and yellow (576 nm) channels of reflected
light were recorded. The four reproduced analog recordings of five
time intervals are presented in Figure 5.2 a-e. The position of each
recording is shown on the Chl. maps of 22 and 26 August
(Figures 5.1 c and d). The incorporation of measurements at these
wavelengths was designed to help interpret the effectiveness of the
DR method by having additional wavelengths which could support
the identification of the chlorophyll by its characteristic spectral
response. All large non-selective particulates should cause increased
scattered light from a clear ocean to the sensor at all wavelengths if
they are distributed in near surface waters. If phytoplankton are
present, the blue absorption and $\sim$ 525 nm insensitivity will be
measured as Chl. by DR. The yellow band should respond to the particle
scattering much as if phytoplankton were non-selective. The red bands
are expected to have a similar response as the yellow, with an increased
signal predicted for distributions closer to the surface. The 663 nm
band is close to the chlorophyll absorption maxima at $\sim$ 680 nm
in vivo, and may indicate high concentrations of phytoplankton near
the surface by decreased backscattered intensity at this wavelength.
With the composition of coastal water including phytoplankton,
Gelbstoff and observed sediment particulates, the response of the
yellow and red bands are complex to calculate. In general, the more
effective backscattering situation produced the largest response at
these additional wavelengths. In the 5.2 figures, increasing

voltages in red and yellow bands represent increasing reflected light
intensity. Positive voltage increases indicate a proportional decrease
in the DR ratio value. The SST trace is offset ten seconds behind
the other recordings. Visual comments are presented to help identify
features. The sensors recorded generally increasing reflectance in
both wavelengths and a decreasing 443 nm/525 nm ratio going onshore.
The features of both red (663 nm) far red (723 nm) and yellow (576 nm)
bands correlated well with nearshore DR features while offshore
the correlation was not this simple. In Figures 5.2 a, c and d, the
time intervals devoid of features in the red and yellow had the most
dynamic DR and temperature structure, but in Figures 5.2 b and e,
the opposite was true. Phytoplankton are believed to be responsible
for the former optical situations. The latter cases and the nearshore
areas of simple red-yellow-DR correlations are suggested to be obser-
vations of high concentrations of non-chlorophyll, highly reflective
suspended particulates in addition to phytoplankton. Pearcy and Keene
(1974) have identified water mass types in the Pacific off Oregon by
spectral variability. Their comparisons of blue to green and green
to orange in oceanic water, the Columbia River plume (high is suspended
particulates) and upwelling water (spectrally varying, but dense in
phytoplankton) support the interpretation suggested here. The
offshore, separated surface plume on 22 August (Chl. > 0.5 mg/m^3)
was observed to have decreased red (663 nm) signal in this area
(data not presented) in relation to the adjacent region. Pearcy and
Keene (cit. loc.) showed spectra obtained over upwelling water furthest

from the influence of the Columbia River plume was characterized by
the largest decrease in orange reflection of any water type. Although
the broad red spectral attenuation by clear sea water is usually consid-
ered to mask observation of chlorophyll absorbance at specific red
wavelengths, the decrease in the red intensity noticed in this example
in the SUE study and possibly in the Oregon study suggests that
chlorophyll absorption in the red was apparent. The vertical
temperature and light penetration profiles of 1524 hours on 21 August
(Figure A.3a in Appendix A) were located in this feature. They show
a more pronounced gradient at $\sim$ 30 m, but an extinction rate change
at $\sim$ 5 m. This suggests that the measurements made the following
day were of a near surface feature. Figure 5.2e is presented to show that
sharp boundaries were observed in the longshore direction as well as
onshore. This suggests the offshore extension of upwelling at the
surface into the waters of the Canary Current. Such a feature could
become separated from the coastal regime and develop as did the
upwelling plume to south from 18-22 August.

Table 5.1 lists the one percent light level depth and
the attenuation percentage in the first five meters recorded by the
expendable photometers, and the surface chlorophyll levels
indicated by the DR at the drop site. Generally, the greater
one percent light depths correlate with lower apparent chlorophyll
levels. Appendix A (Figures A.3a-h) shows the temperature and light
intensity profiles have deflections in the extinction rate toward
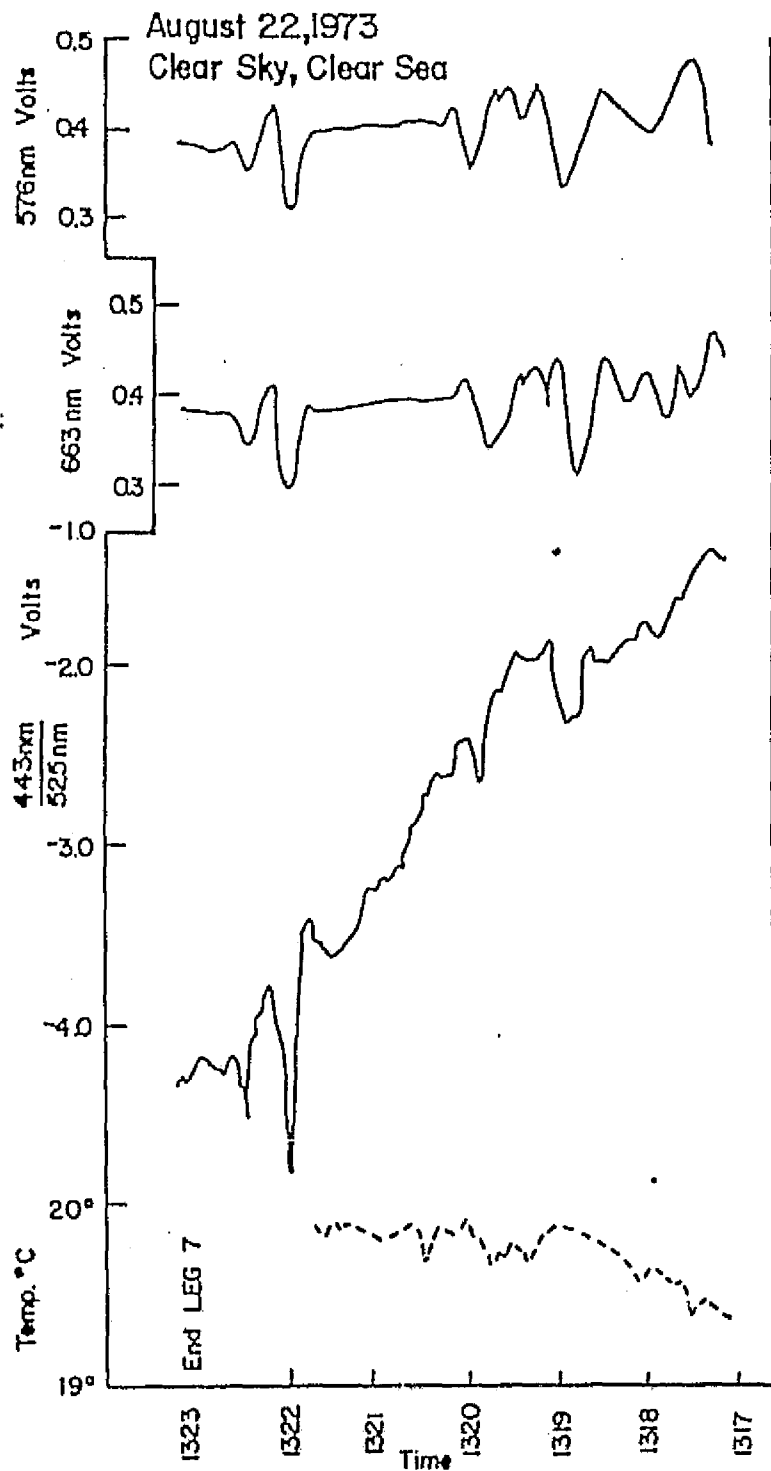decreasing extinction with depth at light levels from 80% to 15% and

Figure 5.2 a-e (continued through page 63). Comparison of continuous, simultaneous, Sea Surface Temperature (dashed line, °C.), DR ratio values, 443 nm/525 nm (in volts) and reflectance signals at two wavelengths (volts are proportional to intensity of reflected energy). Local time and visual comments are included. Positions and direction of the recordings are shown in Figure 5.1 c and 5.1 d.
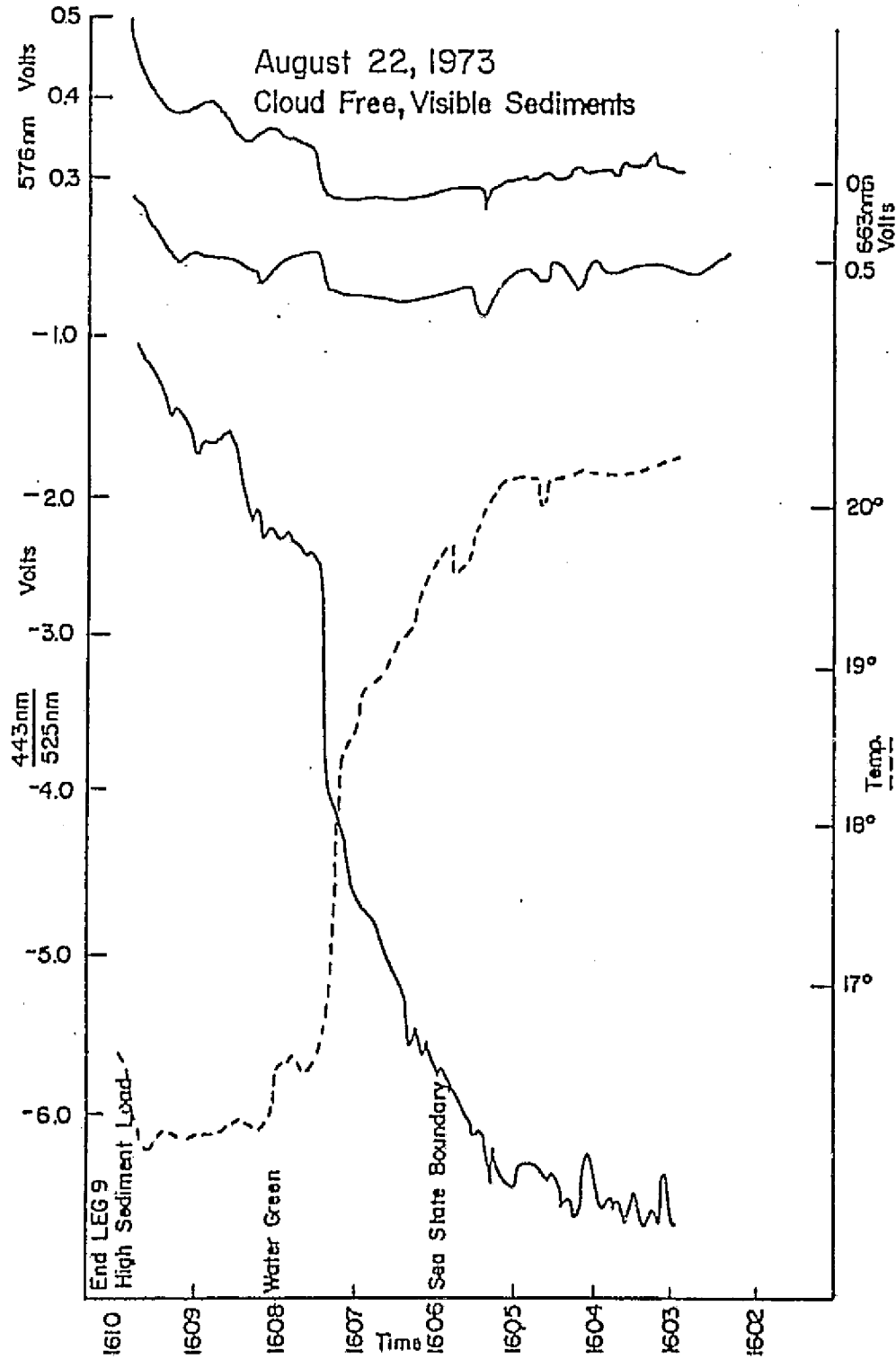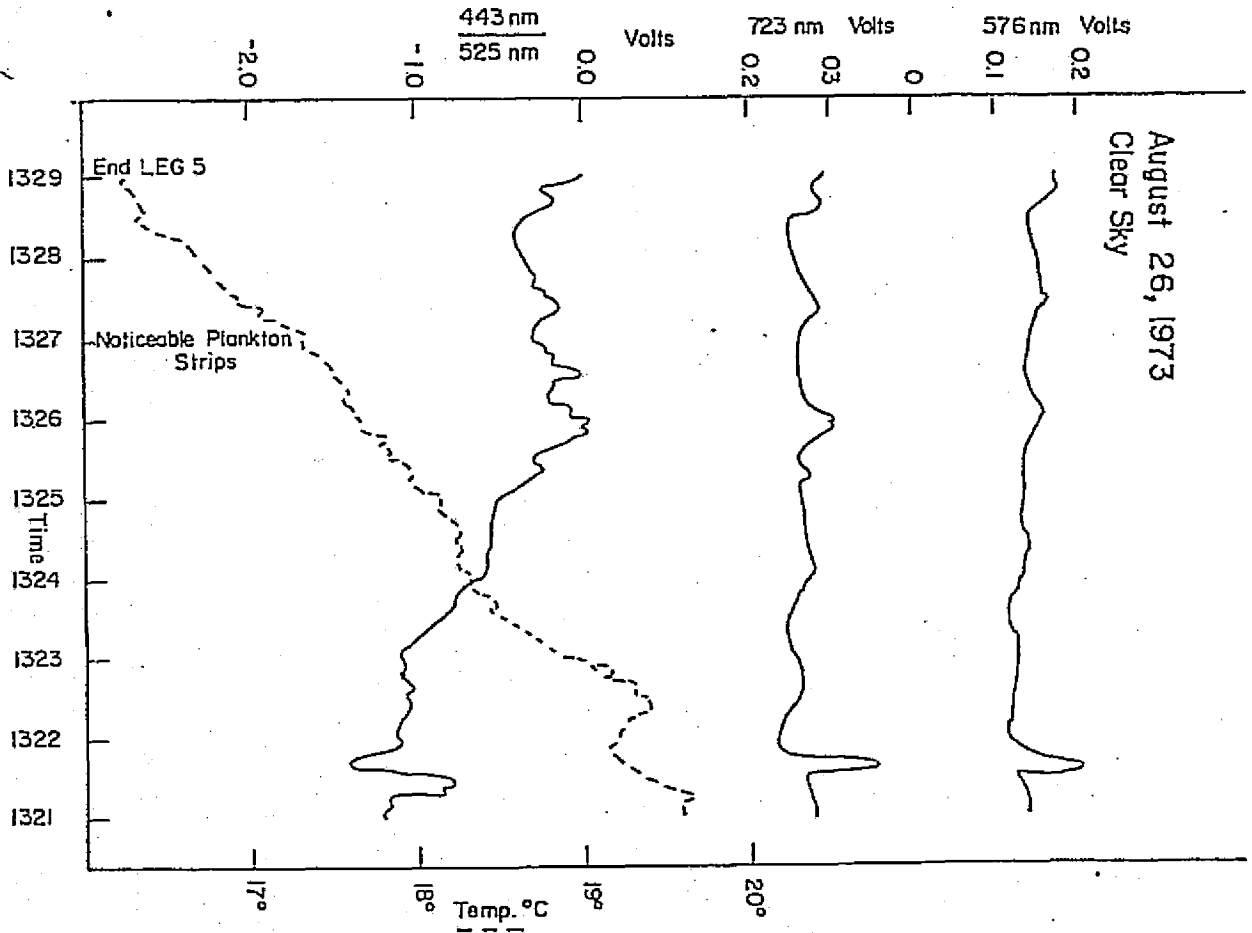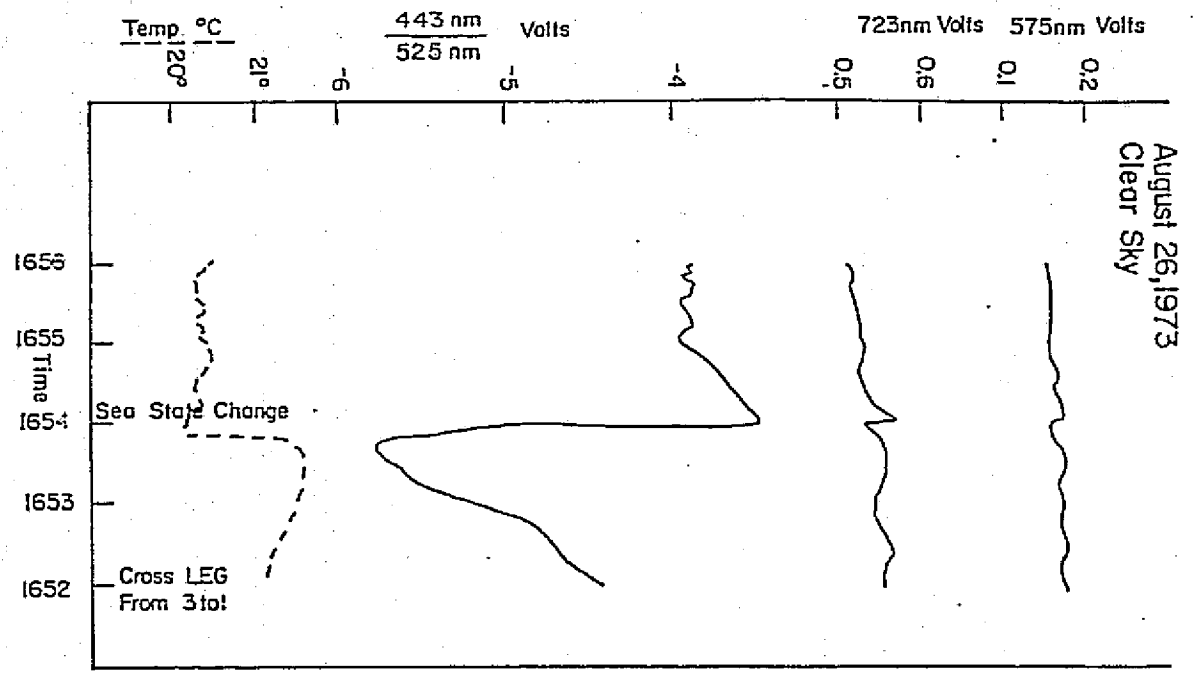
Figure 5.2b

August 22, 1973
Cloud Free, Visible Sediments
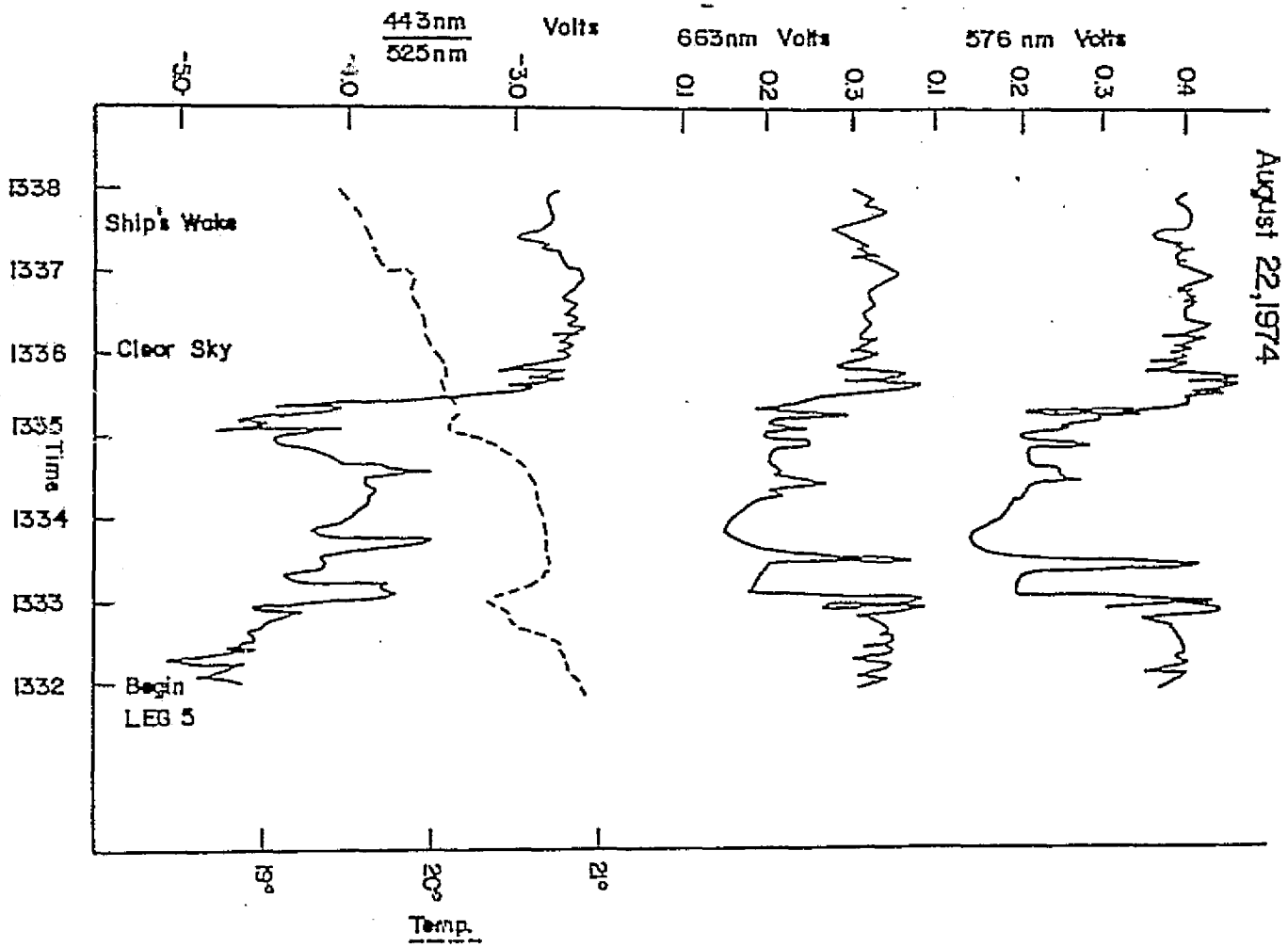
Figure 5.2c

Figure 5.2d

Figure 5.2e

August 26, 1973
Clear Sky

Table 5.1 Results of Airborne Expendable Photometer Study
August 21, 1973

	Position		1% Light Level[1] (m)	Attenuation %[2] (1st 5 meters)	DR Surface Chloro- phyll mg/m³	Comments
Local Time	Latitude (°N)	Longitude (°W)				
1152	27°34'	14°58'	23	3	0.4	SW of Gran
1155	27°27'	14°51'	17	4	0.4	Canaria
1204	27°09'	14°27'	38	7	0.5	Line 2
1215	26°44'	13°50'	19	8	1.7	
1308	28°29'	13°40'	NA[3]	4	0.3	
1309	28°27'	13°38'	NA	12	0.3	Line 4
1318	28°15'	13°24'	NA	5	0.9	
1332	27°35'	13°13'	.20	12	1.5	Line 3
1354	27°53'	14°08'	65	5	0.3	
1524	27°01'	15°24'	NA	19	0.3	Line 1
1548	26°21'	14°33'	NA	8	0.4	

(1) 1% of the initial Airborne Expendable Photometer (AXPM) carrier signal

(2) Attenuation percent of initial AXPM carrier signal

(3) Data was not available

at depths < 20 meters. This depth may represent the bottom of the euphotic zone —the vertical limit of distribution of a majority of active phytoplankton is stable water masses. Phytoplankton and the associated chlorophyll probably caused the increased attenuation in the indicated euphotic zone. The two nearshore profiles on lines 2 and 3 are sites of upwelling, suggested by the cold water originating at a depth of about 300 m. The well defined offshore euphotic zone boundaries were not found in nearshore profiles due to upwelling effects. Phytoplankton and non-phytoplankton suspended material from the coast, well distributed from the surface to depth, and causing high rates of light attenuation are indicated as causing the high apparent chlorophyll measurements. It must be pointed out that the percent light intensity given by the expendable photometers (AXPM) is calibrated with 100% being the first value measured below the surface after impact and stabilization of the probe or approximately 1 meter (see Appendix A). The Secchi depth observed off Cabo Bojador (just south of the 1548 probe on line 1 of Figure 5.3) ranged between 5 to 10 meters in April-May, 1973 (Cruzado and Manriquez, 1974). The levels of 1% light intensity recorded by all probes was consistently deeper than 20 m. Also, the 50% light level ranged from 2.8 m to as shallow as 1 m in similar coastal areas (JOINT-1). Therefore, the percentages indicated by the AXPMs are a fraction of the actual percent incident intensity (I_o).
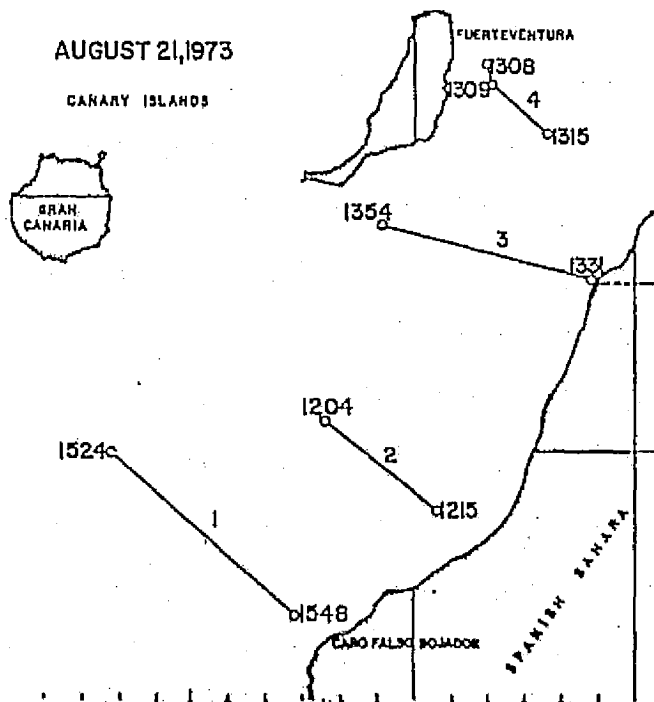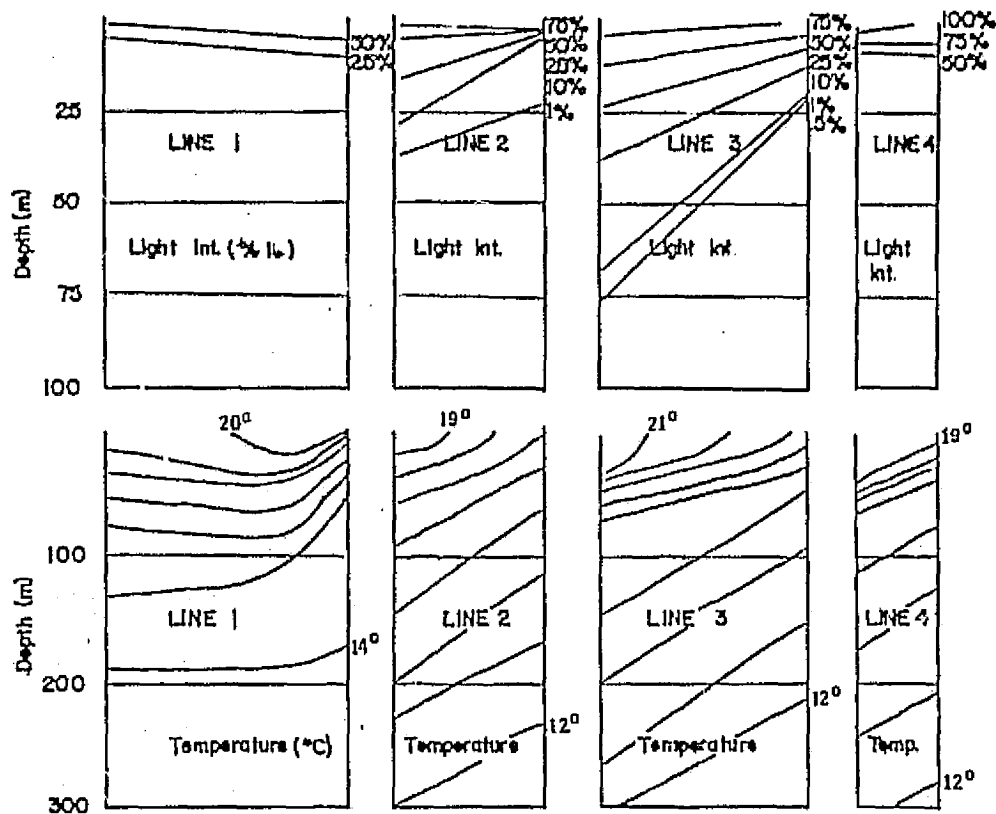
Figure 5.3 Offshore sections of vertical light penetration and temperature profiles on 21 August, 1973. Light intensity (Int.) is expressed in percentage of initial incident intensity. Temperature sections analysis include additional profiles between the two AXPM probe drops. Positions of the offshore lines of the sections are shown in the inset map.

5.2 JOINT-I Project

5.2.1 Data Analysis

The immediate analysis of the aircraft oceanographic data for distribution to research vessels (see Section 4.2) used the real-time strip chart recordings of DR and PRT-5 signals. This form of the data presented one minute averaged values mapped over the coverage area. The standard temperature analysis (SST) was 0.4°C. while the apparent chlorophyll (Chl.) analysis was made in intervals which more closely represented ocean color change. The calibration of the DR ratio (443 nm/525 nm) to Chl. units of mg/m^3 is described in Section 3.2.2 with the calibration curve presented in Figure 3.1. At the operational aircraft speed of 140 knots, the one minute averages translate to one value per 4.4 km. In July, 1974 the digital microfilm print-out of the sensor data at 1 second averages became available. The preliminary strip chart analog data was compared to the data recorded by the NCAR ARIS III data system (NCAR, 1973). The final form of the aircraft sensor data given in section 5.2.2 is from analysis of the ARIS digital output. In addition, an analysis of the data was made at NCAR. Data was presented as 15 minute, 1 value/s plots of parameter versus time. These graphs are on microfilm and offer a detailed comparison of parameters similar to the real-time comparison that was made from the analog traces. Preliminary sea truth surface chlorophyll and surface temperature values from direct aircraft over-flights of research vessels are included on the maps presented in Section 5.2.2, and in Appendix B. Neither the SST or Chl.

analyses are corrected to sea truth. At present, the data available allow an evaluation of the effectiveness of the DR for chlorophyll determination. Analysis of the solar radiation data recorded at coastal stations and on the Atlantis II (Figure 5.9) was accomplished by taking averages over one hour periods where voltages were converted to calories$\cdot$cm$^{-2}\cdot$min^{-1}.

5.2.2 Description and Interpretation of Sensor Measurements and Comparison with Preliminary JOINT-1 Sea Truth Measurements

Of the 26 oceanographic research flights of JOINT-I, six are described and interpreted in this study for determination of the effectiveness of the DR and for preliminary synoptic recognition of upwelling events. Table 5.2 presents basic information on the 26 flights and indicates those which are described here. Sufficient sea truth was available for specific comparison and interpretation with the results from these dates. A 14 day period was covered by the 6 flights. The intensity of coverage varied, with 3 flights flown in a 36 hour period on 8-9 March, a five day lapse, then the 3 final flights extending over 5 days (16-21 March). In an exception to this, the results presented in Figure 5.4 and 5.5 include all applicable sea truth data from stations made on 21° 20'N and 21° 40'N latitude during the period 8-21 March. The analyzed maps of the aircraft research are shown in Figures 5.6 a to 5.6 f. The NW coast of Africa, from Cap Blanc to Cabo Barbas, the bathymetry of the shelf and continental slope, and a distance scale are included in most maps for reference.
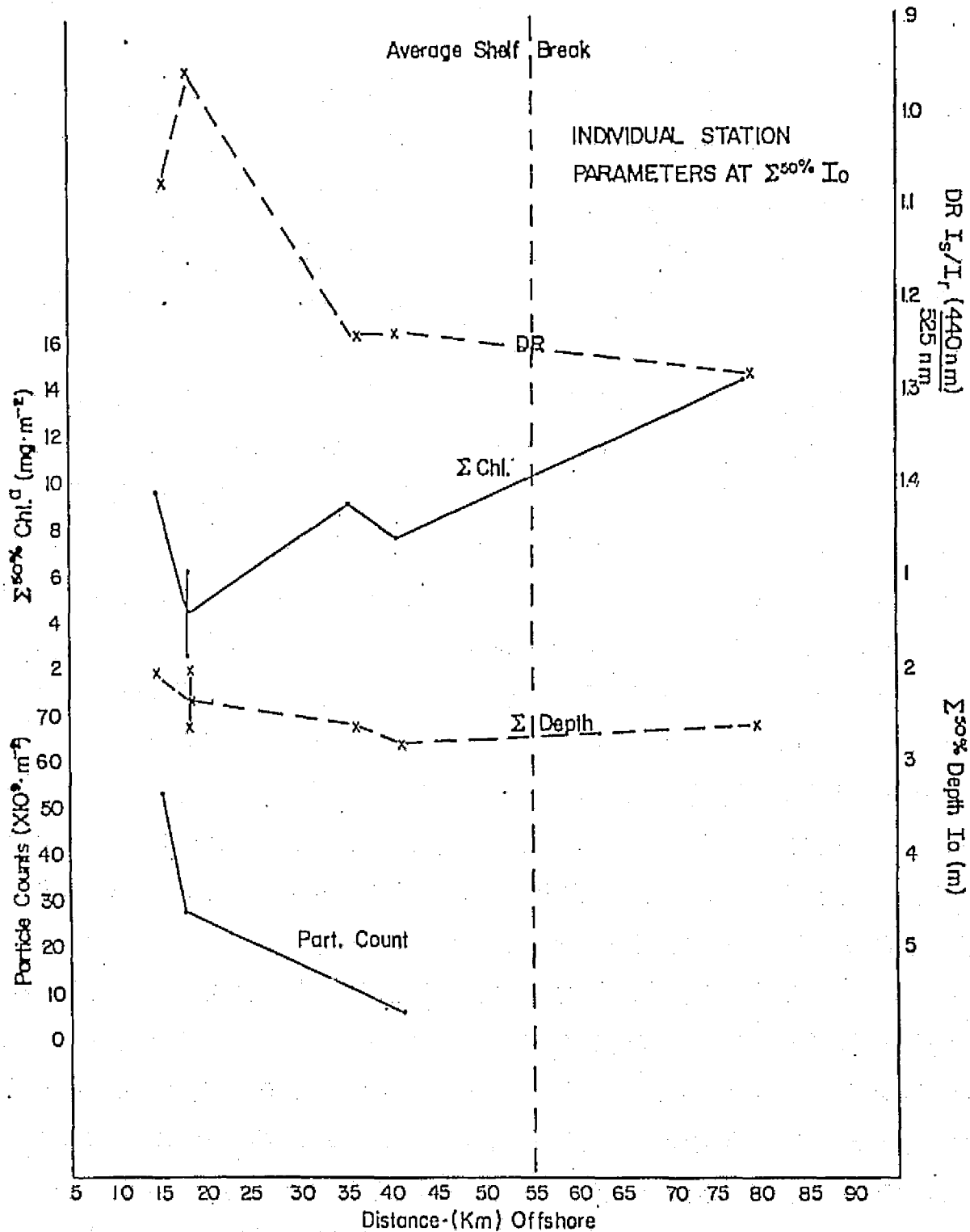
Figure 5.4 Specific comparison of values of the reflectance ratio at
the differential radiometer (DR I_S/I_R, I_S = 443 nm I_R = 525 nm)
and chlorophyll concentrations integrated to the 50% surface
incident light (I_0) depth (mg/m^2), particulate counts integrated
over the 50% I_0 depth and the 50% I_0 depth itself at
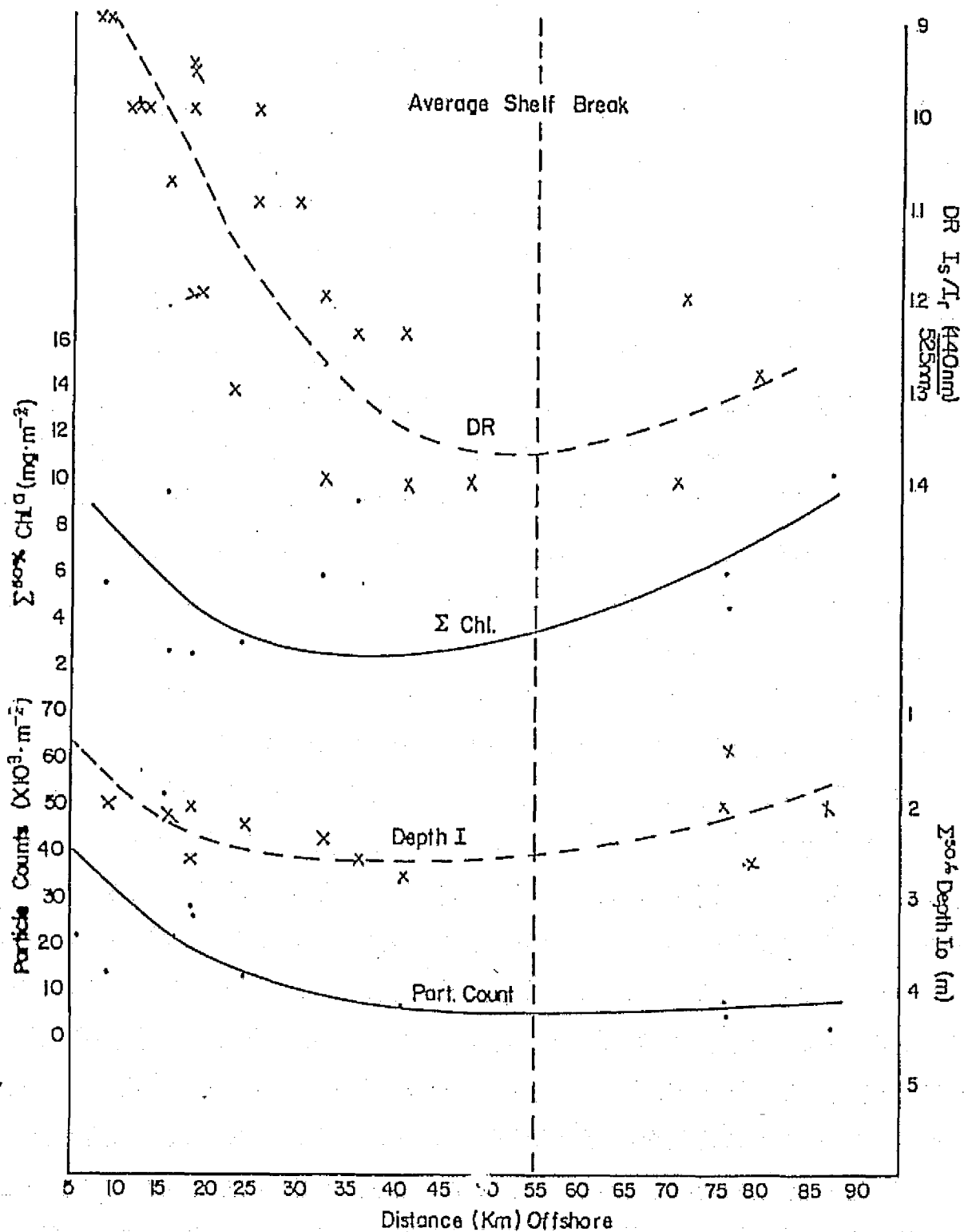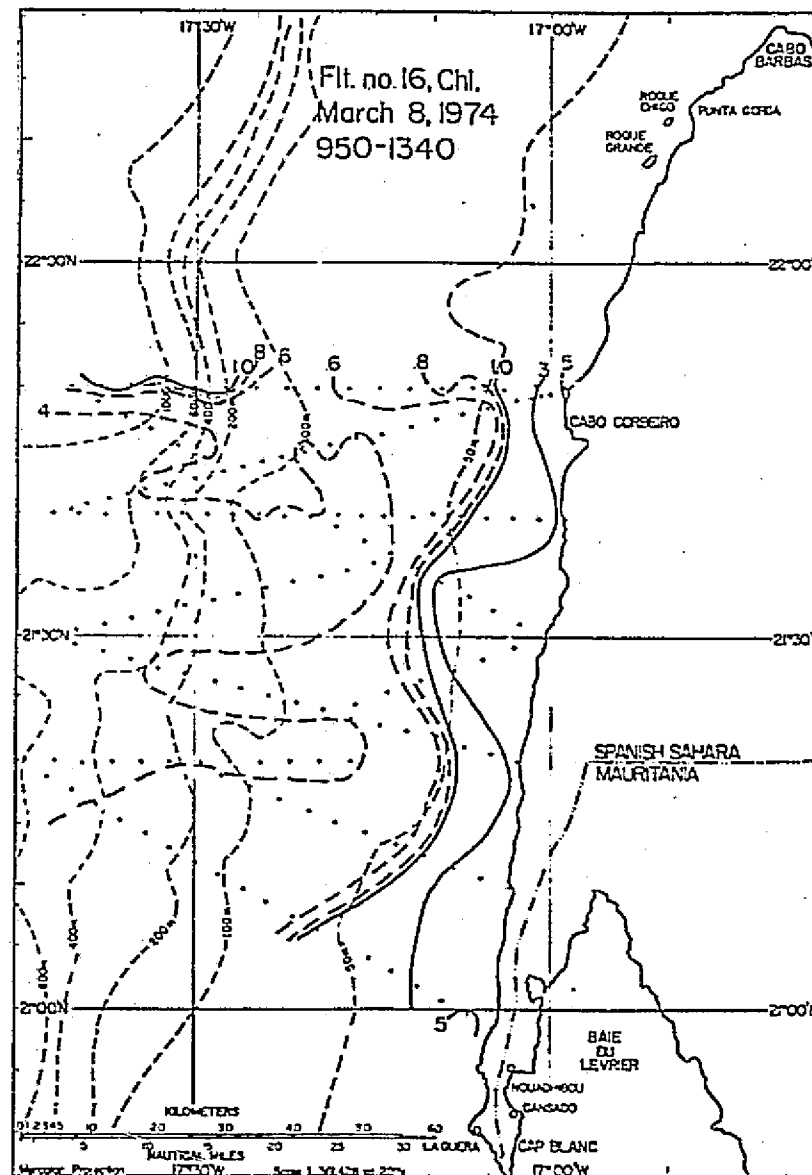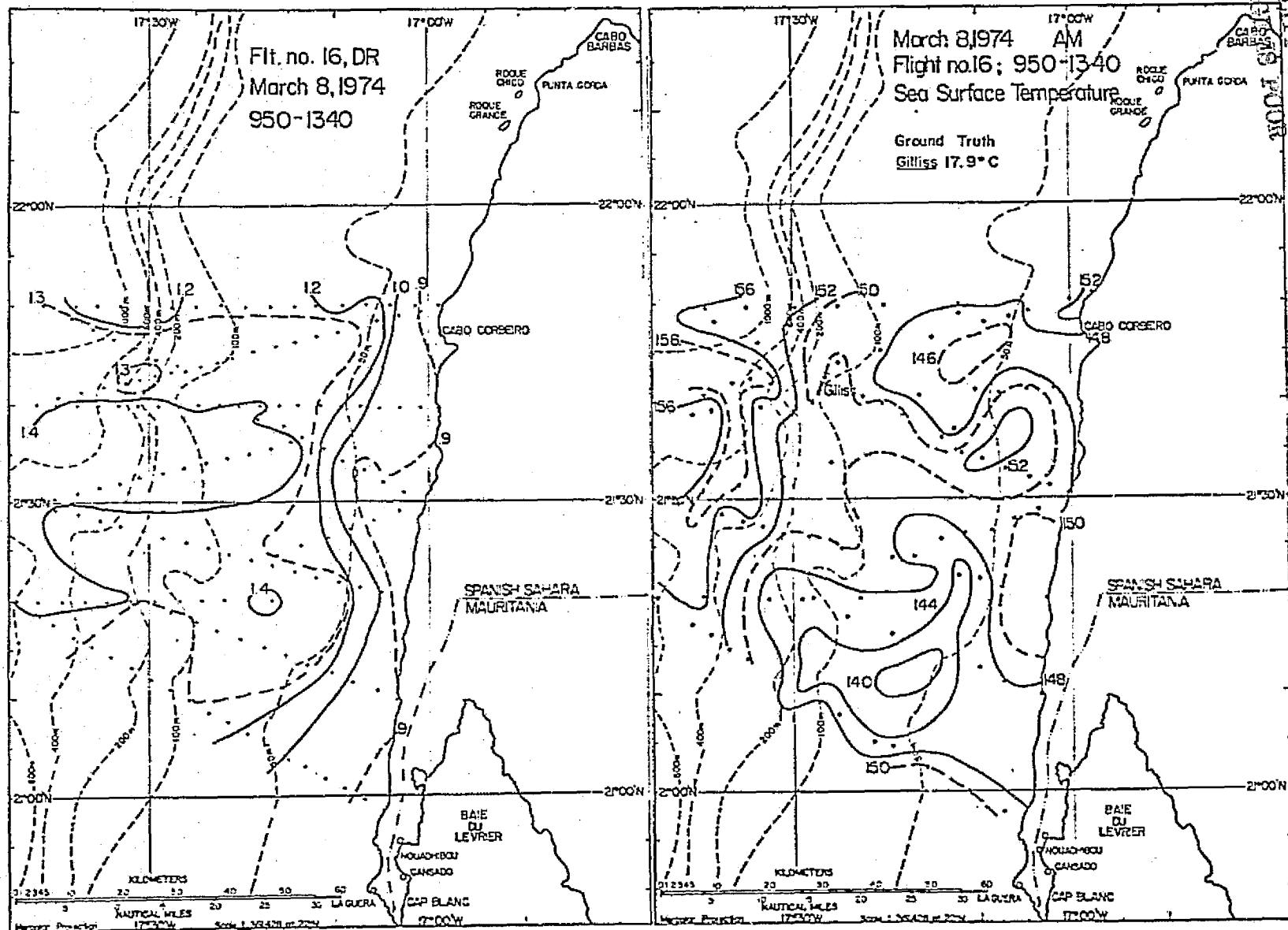individual stations versus offshore distance.

Figure 5.5 General comparison of values of the reflectance ratio at
the differential radiometer (DR I_S/I_R, I_S = 443 nm I_R = 525 nm)
and chlorophyll concentrations integrated to the 50% surface
incident light (I_0) depth (mg/m^2), particulate counts
integrated over the 50% I_0 depth and the 50% I_0 depth itself
versus offshore distance.

Figure 5.6 a-f (continued through page
82). A 14 day time-series analyses
of apparent chlorophyll (mg/m^3),
reflectance ratio value (L443/L525)
and sea surface temperature distribu-
tions from aircraft sensors. Each
is labeled with the date, flight
number and duration (in local
time to the nearest 5 min.),
and sea truth (ground truth)
measurements when available.

Fit. no. 16, DR
March 8, 1974
950-1340

March 8, 1974   AM
Flight no.16 ; 950-1340
Sea Surface Temperature

Ground Truth
Gitliss 17.9° C

Figure 5.6b

Flt. no. 17, DR
March 9, 1974
800-1200

March 9, 1974 am
Flight no. 17, 800-1200
Sea Surface Temperature

Ground Truth
Gilliss 17.7°C
Oceanographer 17.3°C
Atlantis II 17.0°C

Figure 5.6c

Flt. no. 18, Chl.
March 9, 1974
1330-1700
Ground Truth
AII 1.2-1.3 mg/m^3

Left panel:

Flt no. 18, DR
March 9, 1974
1330-1700

Labels on left panel: Capo Barbas, Capo Corboera, Spanish Sahara, Mauritania, Nouadhibou

Contour values: 1.3, 1.2, 1.0, .8, 1.2, 1.3

Right panel:

Ground Truth
Gilliss 17.8°C
Oceanographer 17.4°C
Atlantis II 18.0°C

Flt no 18
March 9, 1974 pm
1330-1700
Sea Surface Temp.

Labels on right panel: Capo Barbas, Capo Corboera, Spanish Sahara, Mauritania, Nouadhibou, GLS, OCN

Contour values: 16.0, 15.6, 15.2, 16.4, 16.4, 16.0, 15.6, 15.6, 15.2, 14.8, 15.2, 14.6

Figure 5.6d

Flight no. 23, D.R.
March 16, 1974
750-1130

March 16, 1974   AM
Flight no. 23 ; 750-1130
Sea Surface Temperature

Ground Truth
Atlantis II 15.9° C
Gilliss 15.96° C

Figure 5.6e

March 19, 1974
Flight no. 29, DR
1000-1305

March 19, 1974
Flight no. 29; 1000-1305
Sea Surface Temperature

Ground Truth
Atlantis II 17.0°C

Figure 5.6f

March 21, 1974
Flight no. 32, DR
1005-1450

March 21, 1974
Flight no. 32; 1005-1450
Sea Surface Temperature

Ground Truth
Oceanographer 17.1°C

The position of sea truth measurements is labeled with the
abbreviation of the research vessel. (Atlantis II - AII,
Oceanographer - OCN, James M. Gilliss - Gilliss). The flight tracts
are outlined by two-minute position points. Intervals where
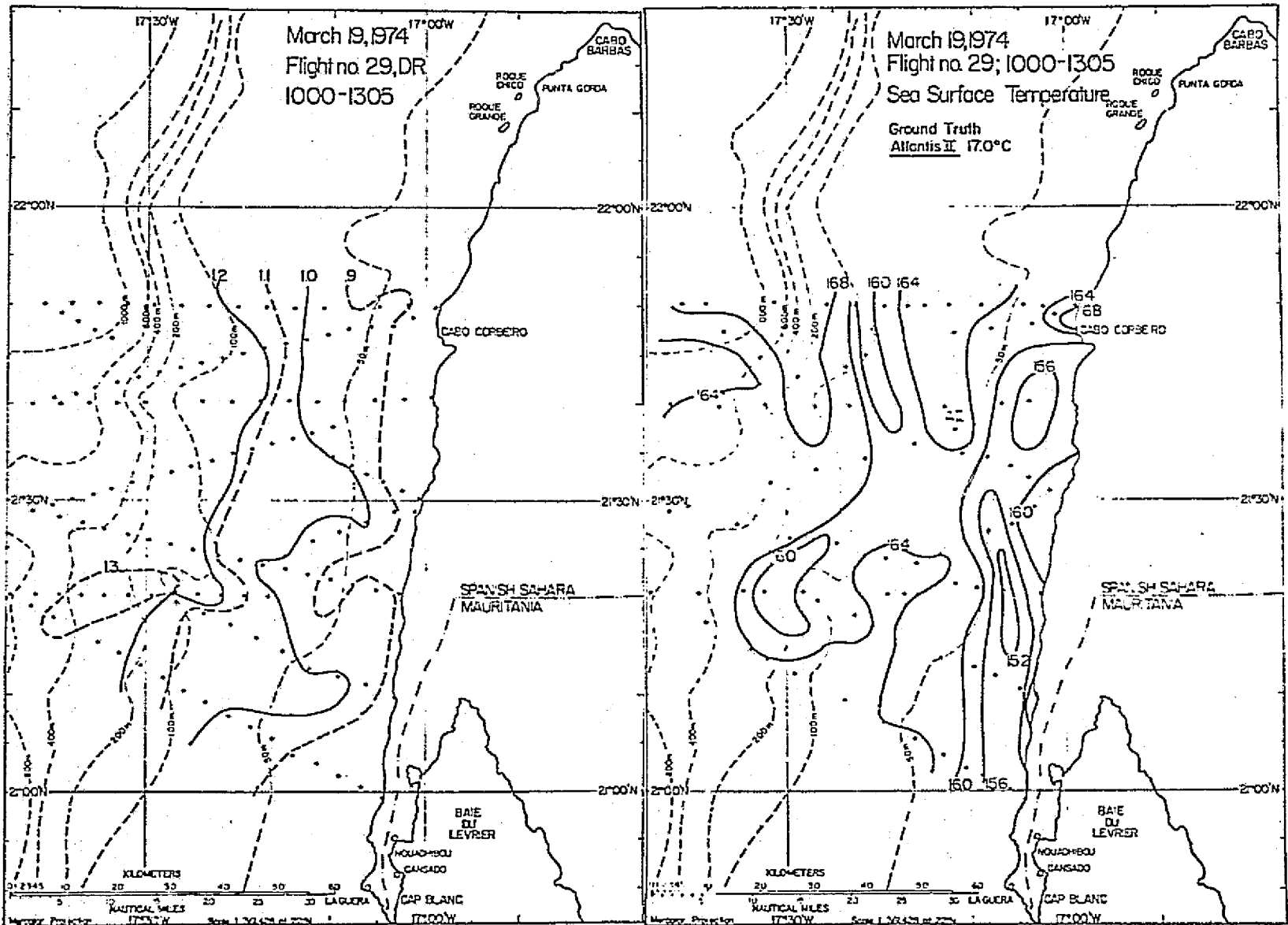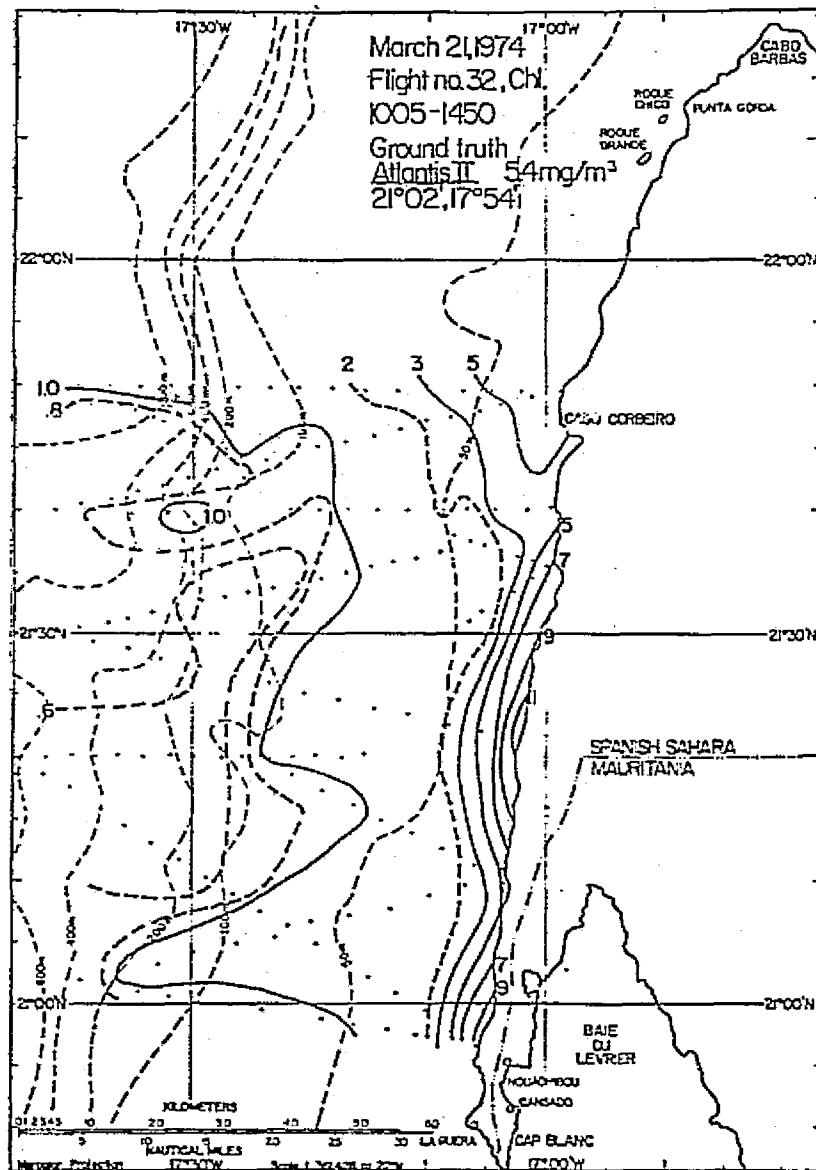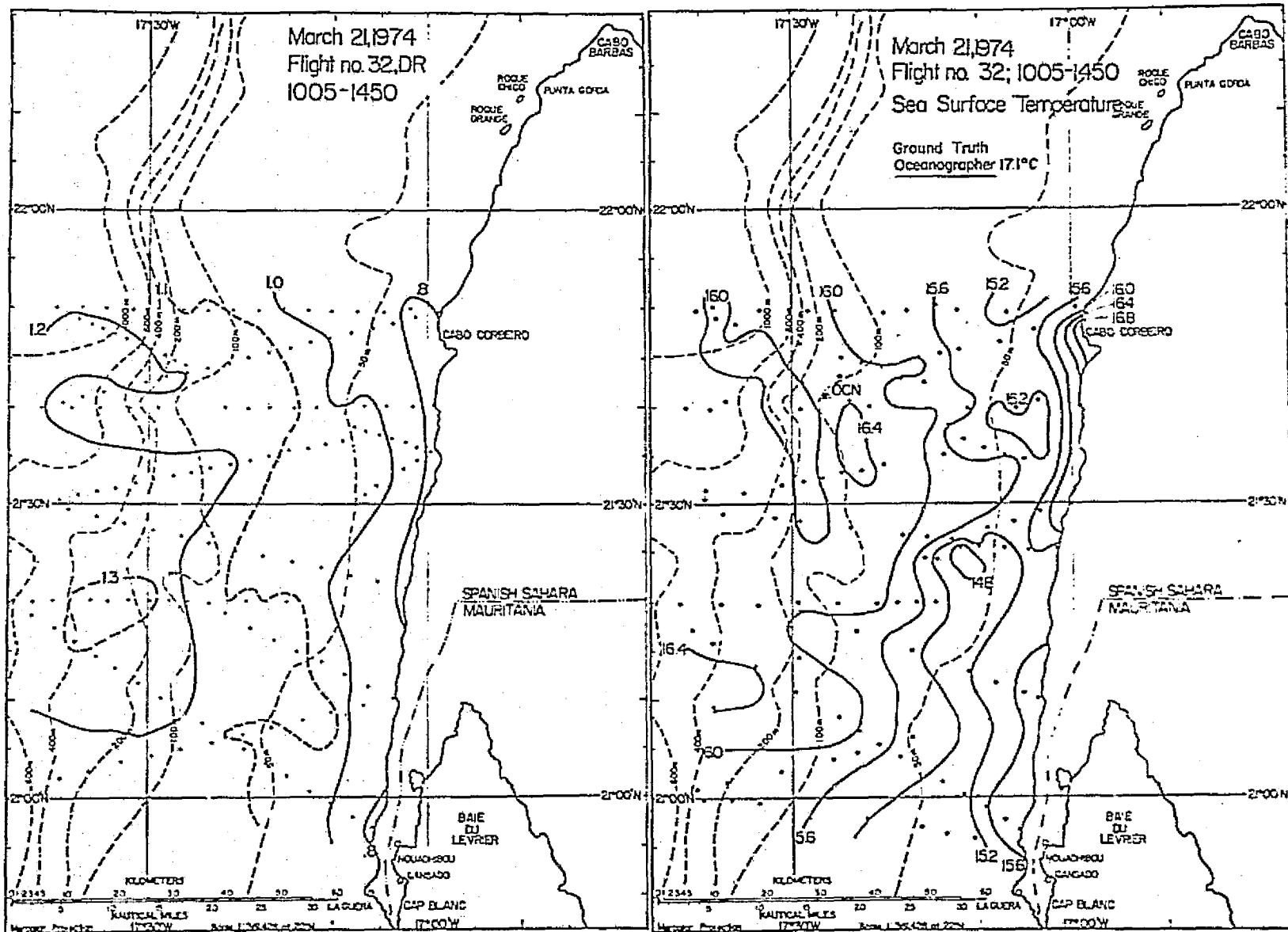meteo o rologic atmospheric soundings were made, and no oceanographic
data could be collected, have position points omitted. For
reference, the southern most flight line was the initial outbound leg,
the 21° 40' flight line was also outbound. Three analyses are
presented for each flight. The first is the differential radiometric
chlorophyll values (in mg/m^3 Chl.), determined from calibration of
the reflected ocean color ratio of intensities at a 443 nm band/525 nm
band (the ratio is normalized to incident ratio at the aircraft alti-
tude) to previously measured surface chlorophyll values by Arvesen
et al. (1973). The calibration curve is presented in Figure 3.1.
The two analyses presented together for comparison are the values of
the reflected ocean color ratio (L_{443}/L_{525}) mentioned above, and the
radiometric sea surface temperatures (SST) obtained from the aircraft,
not corrected for atmospheric effects or adjusted to actual surface
measurements. The total set of analyzed results from the aircraft
oceanographic research, with the exceptions of those presented in
this section, are found in Appendix B. A number of the maps are of
different scale due to occasional large-scale coverage and caution
should be used when identifying the same feature on successive dates.

A detailed description of the surface oceanography from
aircraft data is not attempted here. Generally, a maximum gradient of
apparent chlorophyll (Chl.) was in the offshore direction. The
distribution of Chl. farther offshore was of more variable structure.
The Chl. and DR analyses in Figure 5.6a show plumes distending offshore
from the generally longshore paralleling gradients. The larger ratio
values indicate particulate-free and low productive waters. Offshore,
approximately to the 50 m isobath, increased Chl. distribution
(or lower DR ratio) was associated very closely with that of warmer
SST regions. On the shelf, two separate centers of cold water
(14.6° at 21°45'N and < 14.0°.at 21°20'N) were observed. Low Chl.
and higher DR ratio values are associated with the center to the
north, while a low apparent Chl. feature was adjacent to the southern
cold center. A thermal gradient was identified at the shelf break
on 21° 45'N latitude. Here, increased apparent Chl. was
associated with an offshore boundary of upwelled water at the surface.
The line 21° 30'N latitude partitioned this feature to the north from
the low temperature cell on the shelf and the high DR value associated
(although not precisely) with it. This feature represented an
active upwelling location. The 9 March (AM) analyses identify March 8
features offshore of 50 m in precisely the same positions. Inshore of
50 m a slight southerly shift of ocean color and SST features was
observed. From a synoptic point of view, the patterns of the gradients
or boundaries have meandered, but the features have remained stationary
and gradient intensities have not developed or broken down. The large

scale March 9 PM flight gives additional coverage north to 22° 00' W

longitude. The increased area covered is compensated by a loss of

coverage intensity. This is why the higher Chl. region observed on

21° 40'N at the shelf break is not resolved in the large scale flight.

A better interpretation of the extent of the warm feature north of 21°

20'N and west of the shelf break is the trade-off gained by this large-

scale flight. Flight Number 23, on 16 March, (Fig. 5.6d) shows a

different type of situation. The coldest surface water was located

at the slope shelf boundary. Both seaward and shoreward there were

up to ∿ 1.5° thermal gradients. Beyond the shelf on 21° 30'N

a colder region was depicted. The warmest temperatures were observed

onshore but staggered between the locations where the cold coastal

upwelling was noticed on 8-9 March. Whereas the highest apparent Chl.

distribution compared to the lowest onshore temperatures on flights

of 8-9 March, on 16 March the highest apparent Chl., in levels similar

to 8-9 March, were coincident with the highest onshore temperatures. A

small area of high DR ratio was observed at 21° 20'N, 17° 17'W.

Thus far, all DR and Chl. analyses described this feature. Coverage

on other dates also confirmed a relatively constant feature of clearer

water or less apparent Chl. at this location (see Analyses in Appendix

B). On March 16 the thermal gradient at the shelf oreak and seaward

was in a region of very uniform ocean color. On March 19 and 21

(Figures 5.6e and 5.6f) a situation existed similar to 8-9 March.

Two, and perhaps three cold areas on the 50 m isobath were observed.

The 19-21 March, coastal upwelling was occurring in an even

narrower, nearshore band than on 8-9 March. These cold features

were associated with higher apparent Chl. values than surrounding
waters, although onshore the values continued to increase. This was
the constant, general observation of apparent Chl. distribution.
A distribution of cooler water at the shelf break coexisted with higher
DR values. Some ocean color fronts were visually observed,
as well as radiometrically, between 21° 21'N and 21° 31'N, 17° 30'W
on 21 March. A development at the shelf region located at 21° 40'N
was monitored from 19 to 21 March. A cooler water mass beyond the
slope was oriented normal to the slope on 19 March. It was also
identified in the apparent Chl. analysis (Figure 5.6e) as a shoreward
extending plume. The southern boundary of this feature can be
identified thermally and spectrally on 20 March at 21° 30'N
(see Appendix B). On 21 March more well defined offshore gradient
structures have developed. The ocean color analyses for 21 March
showed much the same orientation as 19 March and apparently no depen-
dence on the thermal development.

Preliminary results from investigators presented at a
JOINT-I workshop (Friday Harbor Workshop, 1974) were interpreted for
recognition of distinct upwelling types. Three types were discussed
and dates of the development of these events were given. Briefly,
8-9 March was in a period designated as classical, one-cell upwelling
occurring over the shelf. 16 March, was in a period of shelf break
upwelling, and 19 March was transitional type including two upwelling
cells. It can be seen that the aircraft results lend support to

these interpretations. The next step in interpretation of upwelling processes with the results presented here should include the time-sequence of the wind data.

More important to the objectives of this study is the interpretation of ocean color chlorophyll - surface chlorophyll differences. The constant feature of onshore increasing apparent Chl. is presented in Figure 5.7, with relationship to specific real-time sea truth measurements available. The plot expresses the difference of apparent Chl., measured by the differential radiometer (DR), and the ship measurements (ship ground truth) as a function of distance offshore. It can be seen from the preliminary data, that extraordinary discrepancies existed between measurements within $\sim$ 10 km offshore. The measurements correlated better at 20 km offshore (i.e., difference approaches 0), but diverged offshore of 20 km in a inverse manner from that observed nearshore (i.e., ship surface measurements > DR Chl.) The trend is clear although the statistical significance may be questioned with the paucity of comparisons - especially inshore of 20 km. For identification of interferences in the DR method, and to give a semi-quantitative comparison of ocean color and parameter distribution, Figures 5.4 and 5.5 are presented. DR ratio values from measurements on the 21° 40'N and 21° 20'N lattitude flight lines from March 8-21 are plotted versus offshore distance. In addition, the integrated chlorophyll for the 50% incident light (I_o) depth, the 50% I_o depth, and the integrated particle counts for 50% I_o depth are

$$y = 32.86\ X^{-.66}$$

Correlation COEF = -.907
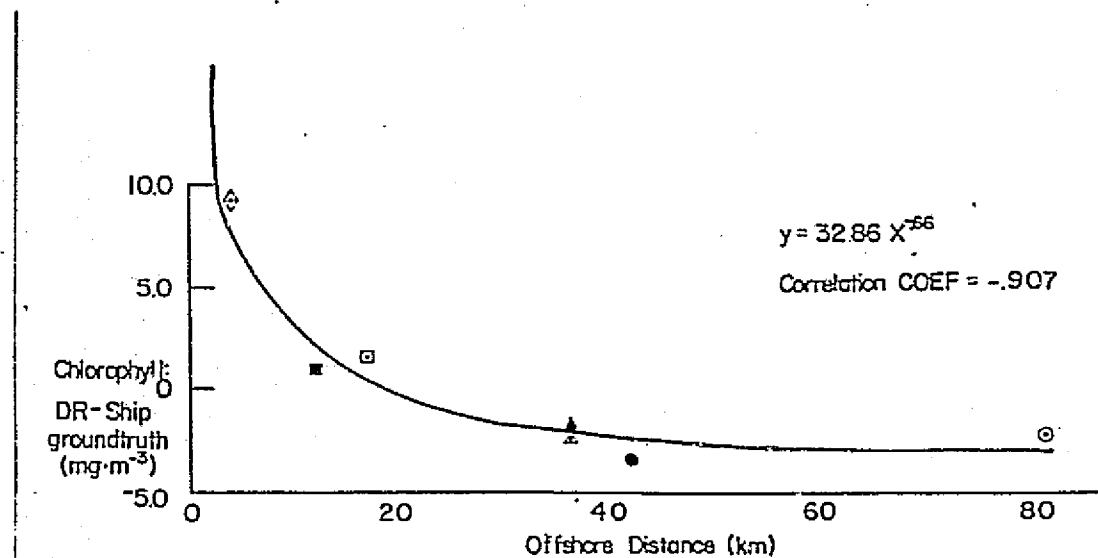
	Flight #	Date	Chlorophyll (mg/m³)		Distance Offshore (km)	Solar Zero	DR -Ship.	Local Time
			DR	Ship.				
▲	17	3/9	0.68	3.07	36.5	5.42	-2.39	0948
◊	18	3/9	9.8-11.0	1.2-1.3	4.0	4.58	+9.15	1337
●	23	3/16	0.58	3.88	42.7	6.28	-3.38	844
✹	29	3/19	2.5	1.62	12.0	5.96	+0.88	1036
▣	29	3/19	2.5	1.03	17.0	5.96	+1.47	
⊙	8	2/20	0.44	2.7	81.6	4.25	-2.26	1337
▲	30	3/20	0.2	2.0	36.5	>8.00	-1.80	752

Figure 5.7 Comparison of the difference between apparent chlorophyll and actual surface measurements versus offshore distance (DR - Ship ground truth). A tabulation of data for each composition is given and is identified by the symbols.

plotted versus distance offshore. The effective depth sensed by the
DR roughly corresponds to the $\leq 50\%$ I_o depth, from the preliminary
data. At the stations used for comparison with the DR signal, this
depth averaged 2 m. The 50% I_o effective depth was determined
by comparison of the DR response to the integrated particle counts for
100%, 50%, 30%, 15% and 1% I_o depths irrespective of actual
chlorophyll concentration. The comparison at the 50% I_o level was
determined to be the best correlated with DR values. The results of
Figure 5.4 are from specific DR-to-parameter comparisons, while
Figure 5.5 results are the general case of all measurements made at
these distances offshore. The relationship between apparent
chlorophyll diverging from actual measurements shoreward
(from Figure 5.4) is supported by the general case. The relationship of
DR ratio values and apparent chlorophyll has been described as a
log-linear function (Figure 3.1), with logrithmically increasing
chlorophyll concentrations required for a proportional decrease in
DR value. The relationship between individual comparisons shows an
inverse correlation between reflected intensity ratio values and
actual chlorophyll concentration to that ascribed. A positive
correlation in the individual comparisons exists between the increasing
443 nm/525 nm reflected intensity and decreasing particulate counts.
It may be established from the two figures that non-phytoplankton
particulates are responsible for the measured interference and
diminished effectiveness of the DR. At > 70 km offshore, the apparent
chlorophyll exhibits a positive correlation with the actual measurements.

The apparent Chl. analysis in the surface maps presented in Figure 5.6 often are observed to have increased values offshore. The 50% I_o depth decreases while the particulate counts remain generally constant with a slight decrease. It is suggested that the proportion of non-phytoplankton particles is decreasing.

The atmospheric processes that affect the differential radio-metric method can only preliminarily described at this time. Additional support materials including the satellite coverage imagery, meteorologic conditions, solar radiation measurements, solar standardization settings (solar zeros), aircraft photographs and collected eolian dust loadings must be compiled for conclusions on atmospheric interferences. Deliniation of the atmospheric interference is of prime importance in evaluation of IR thermal detection as well, and the corrections that can be introduced to the SST results presented here. Figure 5.8 compares the DR solar zero setting during periods of data collection by the aircraft and the incident solar radiation intensity measured by hemispherical pyranometers at the coastal meteorological stations (Station 6 at 21° 28'N, Station 4 at 21° 18' N). The plot shows a correlation between increased radiation and lower solar zeros. The solar zero is the offset potentiometer reading of the 443 nm signal. This offset is used to normalize the intensities of the 443 nm and the 525 nm used as the signal and reference wavelengths (respectively) by the DR. Lower solar zero settings are linearly proportional to lower 443 nm/525 nm ratio values. From this comparison it is seen that changes in the incident solar
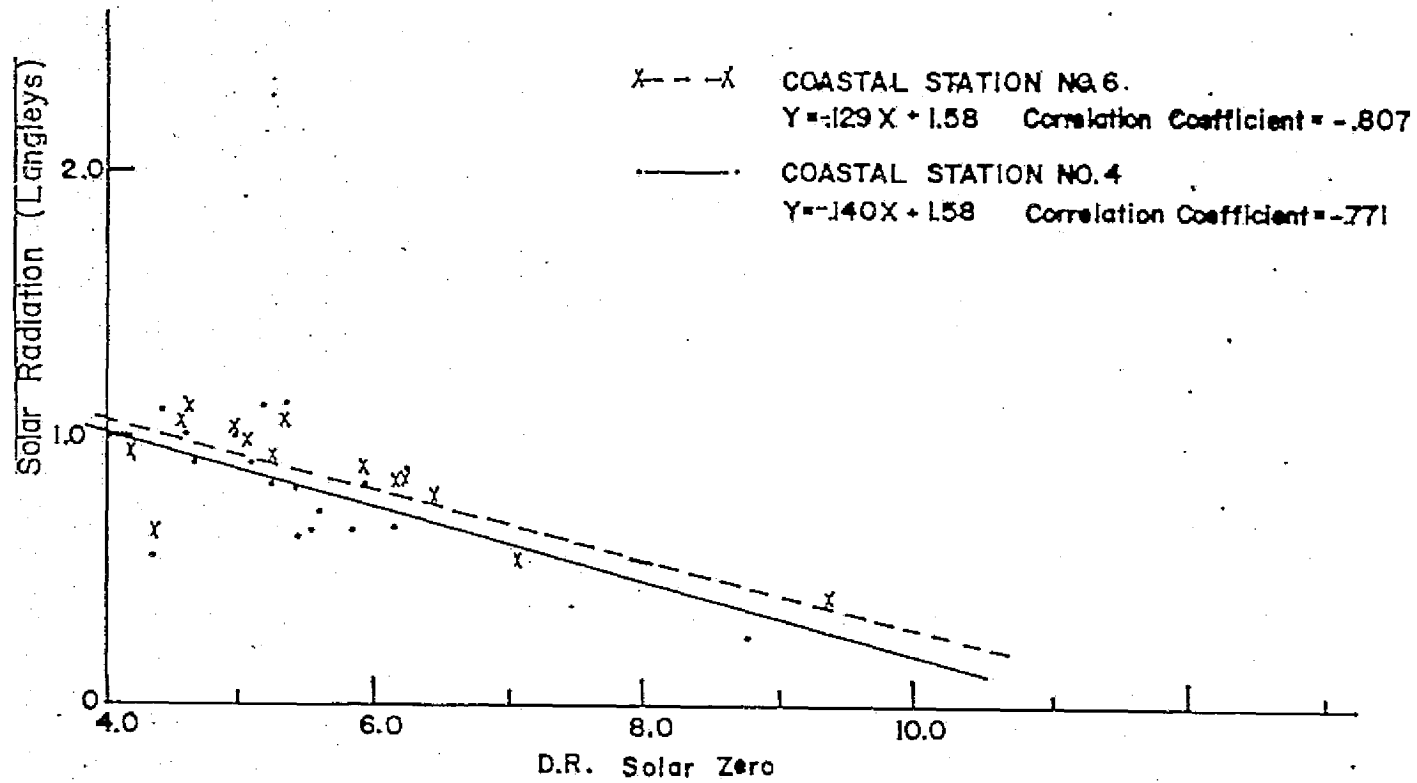
Figure 5.8 Relationship between the solar standardization setting
of the differential radiometer   (DR solar zero) and
the incident ratiation measured by two coastal pyranometers
(Langleys). See text for explanation of solar zero setting.

radiation were apparently linearly correlated to the ratio of intensities, I_{443}/I_{525} measured with a spectrally flat diffusor placed over the DR sensor and viewing the sun directly at its solar altitude. Thus, less diffuse scattering which is related to the decreased blue atmospheric signal was observed at higher solar radiation levels. This selective atmospheric contribution was normalized ($I_{443}/I_{525} = 1$) by the solar standardization. Therefore, the deviation of ratio values from 1.0 are assumed to be due only to the reflected ocean color signal. Also, the solar elevation has a far greater influence on daylight spectra than variations in atmospheric conditions at the same time on different days. This is recognized from Figure 5.9 a-c. Daytime pyranometer recordings from the coastal stations and from aboard the A II are presented for the time period of the flights discribed. The solar zero settings are also included and increased incident radiation was again observed to correlate to decreased solar zeros. The radiation curves on the coast are lower in intensity than the recordings at sea due to the eolian attenuation onshore. The variations in incident radiation from day to day were primarily due to atmospheric eolian loadings. The hourly irregularities observed were due both to clouds and eolian loading fluctuations. The description of eolian loadings collected during this period has been presented by Lepple (1974). The daylight spectra were dependent on atmospheric particulate distribution. High loadings of particulates caused increased extinction of the ocean color signal and increased contribution of atmospheric light to the DR sensor.

An interference in the infrared radiation thermometer
(observed as daily variations in radiation SST and actual SST differences)
was suspected to be due to changing particulate concentrations of wind
blown eolian material from the Sahara.   Differences between radiation
temperature measurements from 500 feet and actual SST versus offshore
distance with respect to the time of measurement and the solar radia-
tion intensity from either the coastal stations (if SST measurements
were from Gilliss or Oceanographer) or the All were investigated.   From
these correlations, interpretation of the eolian interference was
attempted.   It was thought that SST differences offshore would be
less due to the fall-out of particulates from the lower atmosphere
($\sim$ 500 feet).   However, no simple relationship exists between the
SST differences and either time of measurement or distance offshore.
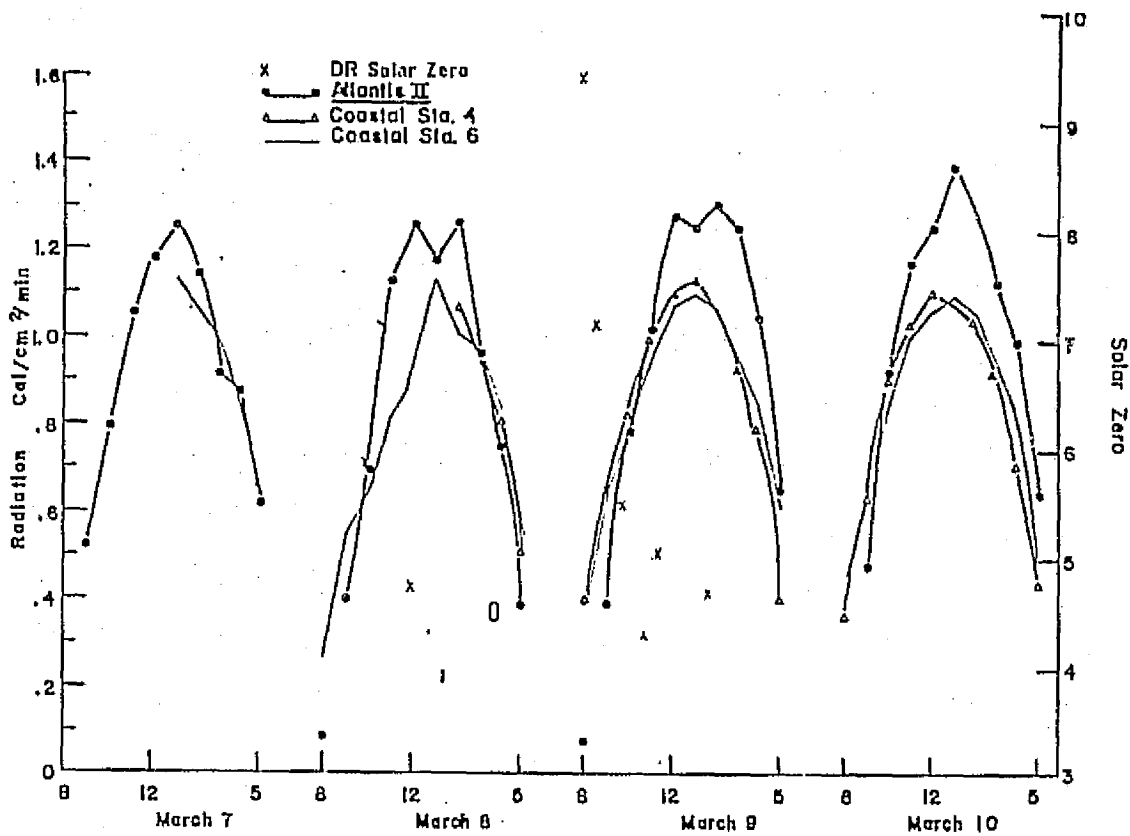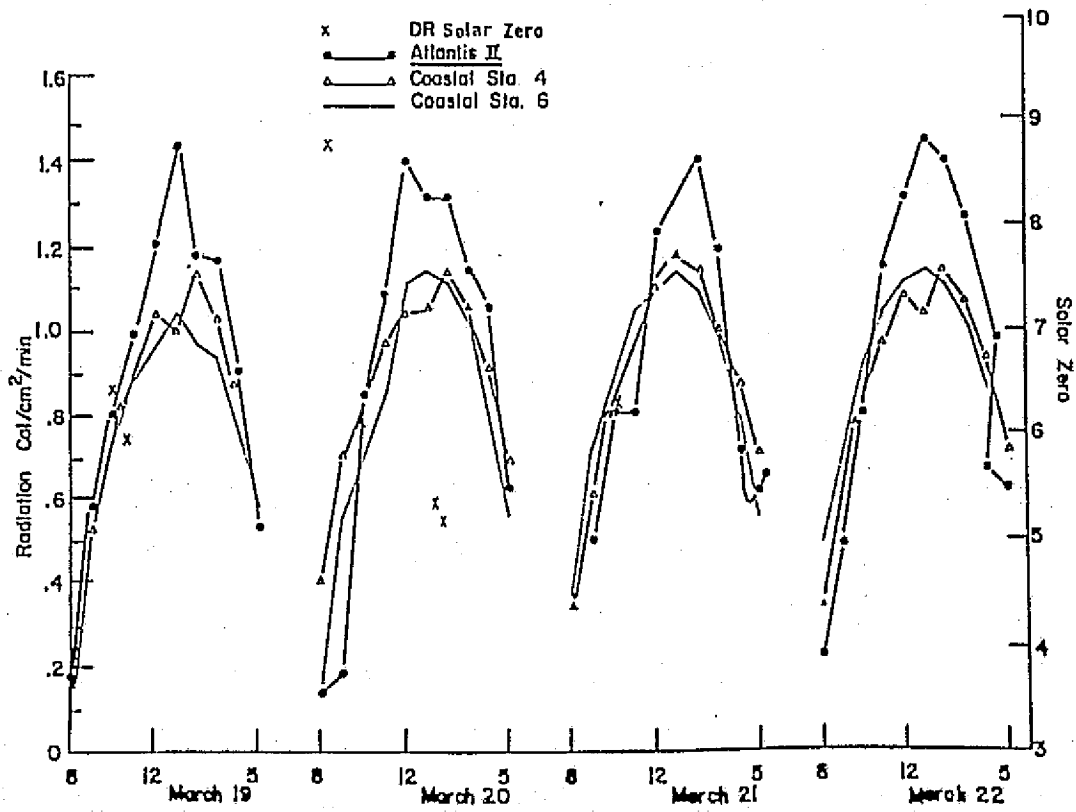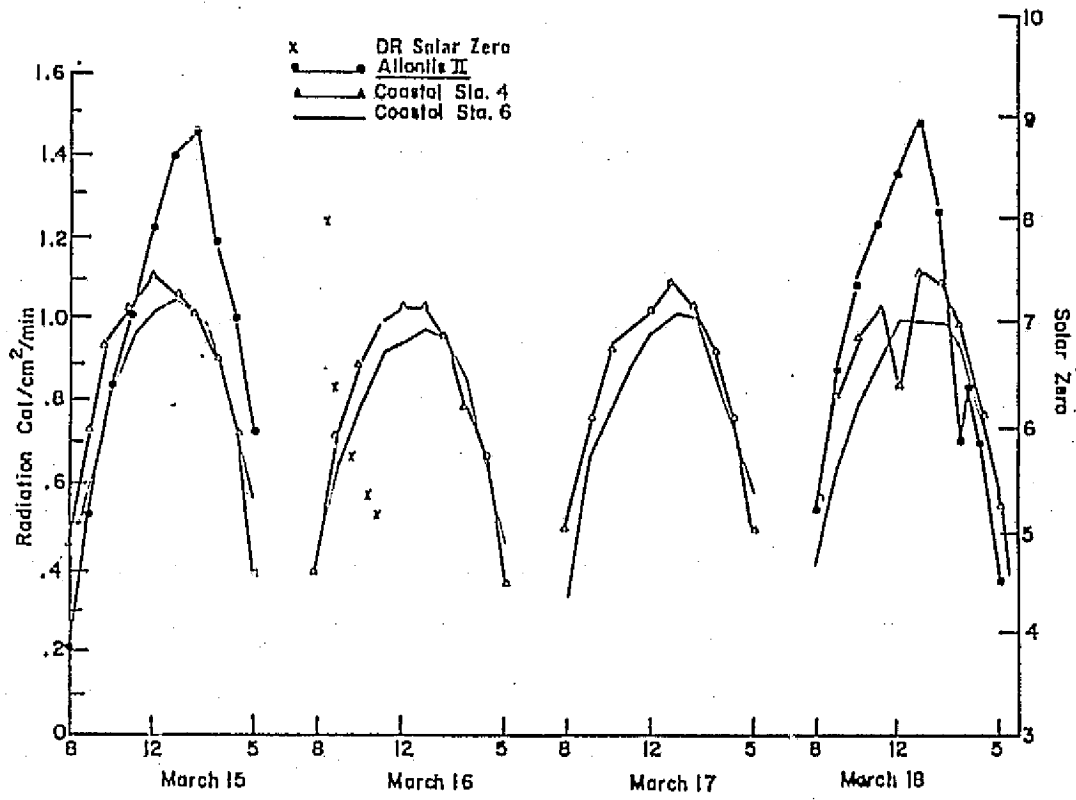
Figure 5.9 a-c (continued on page 95)   Solar radiation Curves
during 7-22 March recorded by pyranometers at
two coastal stations (positions given in text)
and aboard the AII.   Included are the solar zero
settings of the differential radiometer.

6. LABORATORY INVESTIGATIONS ON INTERFERENCES
IN RADIOMETRIC CHLOROPHYLL DETERMINATION

6.1 Reflective Spectroscopy of High Chlorophyll Concentrations and Chlorophyll-Free Particulate Suspensions

Field study results initiating this investigation were that the interference of suspended, chlorophyll-free particulates in the near coastal waters affected the radiometric measurement of phytoplankton chlorophyll pigments. Reflective scanning spectroscopy of varying phytoplankton and clay suspension concentrations was applied to detail the sediment effects on the spectral signature of chlorophyll. A spectral scan can delineate the full optical contribution of added clay particulate suspensions to a phytoplankton suspension and allow a more concrete interpretation of the combined effects than can the ratio of two wavelength bands from the differential radiometer.

From particle counts in the field, it is suggested that particle multiple scattering of light must be considered in this region. Study as to this consequence on the optical signal leaving the sea surface has been recommended by Jerlov (1974) and by Mueller (1974) in a similar study.

6.1.1 Design of the Reflection Spectrometer Experiment

For the initial investigation on the interference of suspended particulates, a Cary 14 Reflection Spectrometer (a prism-grating, double

monochromator) with better than 1 nm resolution was employed to measure

the reflected intensities of very dense, multiple scattering suspensions.

A phytoplankton sample was prepared by gently concentrating (via

centrifugation) 100 ml of healthy Carteria cells (obtained from

University of Delaware's Mariculture Project) to a 5 ml volume with a

final chlorophyll a concentration of 48,600 mg/m^3 and 11 X 10^9 cells

per liter by direct count. The concentration of the original cell

suspension was found too dilute for meaningful spectral information

to be gained. A fine potter's clay for a standard particulate suspension

was made by mixing clays and distilled water, allowing settling of

large particulates for one hour and pipetting off the remaining

suspension. Red and grey clay standards were mixed 1:1 by volume and

contained 124 X 10^9 particulates per liter with 95% of the particles

having diameter sizes between <1 μm and 51μm as determined

by a Coulter Counter (Model B). For compari... ...e size distribu-

tion of particulates from preliminary analys.. ... OINT-I data

showed 97% of the particulates ≤ 10 μm 4 nautical miles offshore

(Castiglione, 1974a). Because there is no river input into these

coastal waters and erosion of very reflective Sahara-type material via

wave and wind action was observed in nearshore areas, detrital

material of a higher, broad spectral extinction was not considered to

have a significant contribution to the reflected ocean signal. This

does not take into account phytoplankton remains that may

possibly be a significant influence in a short time period before

dispersion by mixing.

The incident source of the spectrometer was normal to the sample, and the 180° reflected signal, scanned at 2.5 nm/s, is referenced to the signal from a barium sulphate cell. The spectral region from 400 nm to 800 nm was scanned. The black sample cell itself is of nearly uniform 0.3% reflectance over the spectral range and has dimensions of 4.5 cm diameter by 1 cm depth.

6.1.2 Results and Interpretation

The reflection spectra resulting from this investigation are shown in Figure 6.1. Curve A is a record of the reflectance of distilled water (< 1 cm deep) in the black sample cell. This curve is approximately of uniform reflectance and thus no corrections of the following sample curves were made. Curve B represents the reflected spectrum of a 5 ml (∿ .3 cm deep), dense sus ension of Carteria (4.86 X 10^4 mg/m^3 Chl. a, 11 X 10^6 counts/ml.). This curve shows increased reflection in the visible region (λ_{max} ∿ 555 nm) outside of the pigment absorption bands. The small increased reflection at ∿ 450 nm was also observed in a spectrophotometric transmittance curve of the pigments extracted from Carteria. This indicates a decreased absorbance by pigments in this isolated wavelength region. Three reflectance minima are seen at ∿ 428, 475 and 672 nm. and correspond to the absorption maxima that were seen in the pigment extraction curve. Curves C_1 and C_2 are repeated scans of a suspension of sample B (5 ml algae suspension) with the addition of 1.0 ml. of the standard clay mixture (total volume = 6.0 ml., 29 X 10^6 total counts/ml.) described in 6.1.1. Curve D is the reflection spectrum of sample C plus 1.0 ml of the clay standard (total volume = 7.0 ml., 43 X 10^6 total c/ml). The spectra
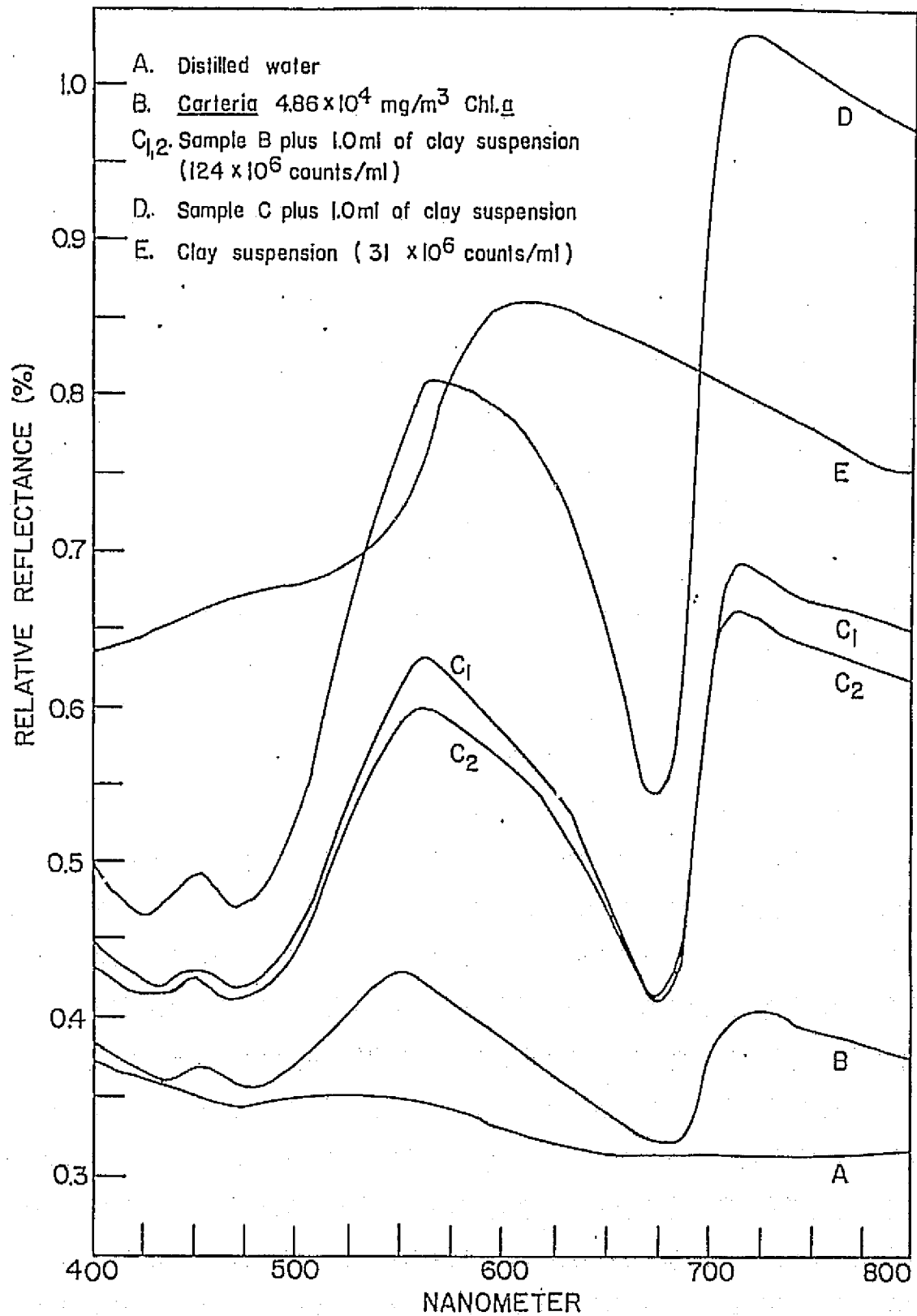
A. Distilled water

B. <u>Carteria</u> 4.86×10^4 mg/m^3 Chl.$\underline{a}$

$C_{1,2}$. Sample B plus 1.0ml of clay suspension (124×10^6 counts/ml)

D. Sample C plus 1.0ml of clay suspension

E. Clay suspension (31×10^6 counts/ml)

Figure 6.1 Reflection spectra of a dense algae sample
(Curve B), mixed algae-clay suspensions
(Curves C_1, C_2 and D) and a clay suspension (E).

of these samples appear as an _enhanced_ signal of the chlorophyll-containing phytoplankton in Curve B. A shift in the green reflectance maximum can be observed ($\Delta \sim 8$ nm) to a longer wavelength. A small shift towards longer wavelengths is seen for the ~ 450 nm reflection maximum as well ($\Delta \sim 4$ nm). The reflection minima in Curves C_1, C_2 and D are also shifted from Curve B. In the blue regions, the shift in the minima is towards shorter wavelengths ($\Delta \sim 6$ nm). The red spectrum minimum, due to chlorophyll absorption, is shifted to _shorter_ wavelengths in Curves C_1, C_2 and D also. More noticeable however, is the narrowing of the minimum reflection region at ~ 675 nm. With the increased addition of clay mixture, changes in the shape of the C and D curves are noticed. This is especially the case in the shape of the yellow-to-orange region (575 - 630 nm) where the maximum reflectance of the clay (Curve E) appears to be contributing to the color of the total suspension.

The effect of increased reflected radiance due to clays in suspension with the phytoplankton can be interpreted. The phytoplankton suspension (Sample B) contains the dominant light absorption characteristics contributing to the spectral signatures in all suspension samples. This is predominately due to selective absorption of chlorophylls which are solely responsible for the reflection minima at ~ 675 nm. A selective attenuance is observed for the mixed clay suspension in Curve E. However, the dominant optical property determining the spectral distribution in the phytoplankton-plus-clay suspensions is the absorption by chlorophyll. Backscattered light from single

scattering events is the consequence of reflection and refraction.
Refracted light acquires the spectral signal of chlorophyll through
the absorption by chlorophylls contained within phytoplankton scattering
layers. In a single scattering situation, the large flagellate
Carteria (> 10 μ dia.) would have a greater reflection/refraction
proportion at backscattering angles than if additional scattering
events occur. In the existing multiple scattering situation of sample B,
however, the signal at backscattered angles has optical contributions
from a very complex light field distribution. In general, the dominant
forward propogation of refraction scattering for large biological
particles of relatively low refractive index in single scattering
situations approaches a more isotropic distribution as the number
scattering events increase (Woodward, 1964). This increases the portion
of the refracted light at backscattered angles. Sample B is approach-
ing an optical situation where further increases in the concentration
of chlorophyll-containing cells will have little effect on
the spectral distribution by scattering processes. This is due
to the loss of the dominant radiance distribution by which the process
of forward scattering was able to selectively attenuate spectral contri-
butions. However, with isotropic scattering conditions, portions of
all spectral contributions by scattering are reflected to the sensor.
Also, the high, non-selective total spectral attenuance by
phytoplankton reduces reflection of an "enhanced" chlorophyll absorp-
tion signal.

The addition of suspended clays to sample B increases the total reflectance of the suspension. Compared to a similar addition of phytoplankton, the reflectance is increased because the effective refractive index of the suspension is higher. The chlorophyll in suspension with the clays is being exposed to more light per volume due to increased scattering by the clays. Moreover, the selective signal scattered by the phytoplankton is more effectively rescattered by the clay particles than by high, broad attenuance phytoplankton. Thus, the chlorophyll signal is enhanced in the reflected signal. In sample D, again, a higher effective refractive index per volume suspension creates an increased efficient transfer of more of the specific absorption portion of the phytoplankton extinction via clay scattering, and less of the non-selective extinction by decreasing the percentage of rescattering events by phytoplankton.

The spectral attenuance of the clay suspension is responsible for the spectral shifts at the reflection maxima and minima from Curve B to Curves C_1, C_2 and D. The maxima will shift to regions of lower attenuation coefficients, while the minima will shift to the highest attenuation coefficient regions of the suspension.

6.2 Coordination of Differential Radiometric and Spectroradiometric Measurements of Chlorophyll and Chlorophyll-Free Particulate Suspensions

A second laboratory investigation coordinated a spectroradiometer

modified for airborne use   from the Goddard Space Flight Center's,
New York Institute for Space Studies with the NASA differential radiometer
(DR). A comparison of the DR response to various phytoplankton and
suspended sediment concentrations with their reflected spectra was
designed to identify interferences in the differential radiometric method
in the laboratory.

6.2.1   Experimental Design

The spectroradiometer has 512 channels over a wavelength range
from 400-850 nm with a resolution of 0.20 nm. The experiment consisted
of a tungsten lamp as an incident source installed $\sim$ 1.5 m above a
12 liter, 20 m deep container painted with low reflectance black paint.
The spectroradiometer and DR were installed above the container and
focussed at the surface at a small angle (< 20°) from nadir to avoid surface
 glint, and to include only the sample and not the container walls
in the field of view of the sensors. The DR solar standardization was
modified for use of this field instrument in the laboratory. In this
study normalizing of the I_{443}/I_{525} incident intensities
(see Section 3.2.2) was accomplished from the reflection of the tungsten
lamp source on a standard white disc held horizontally at the surface
of the sample container. The standard disc also served as the reference
for the spectroradiometer.

The standard suspended clay mixtures described in Section 6.1.1 were used in this study as reflective sediment load. A chlorophyll standard (algae mixture) had a concentration of 7.93×10^2 mg/m^3 Chl. _a._ The algae contained in the mixture included Carteria, Phaeodactylum, Isochrysis and other marine diatoms. The total direct count of the algae standard was 138.5×10^7 cells/liter. The white clay standard had 140×10^9 counts/liter (c/l) with 95% of the size distribution in the < 1-42 μm range. The red clay standard had a total concentration of $.05 \times 10^9$ c/l with 95% in the < 1-60 μm range.

The base water used in this investigation was designed to be optically dense quasi-model of clear deep sea water. Water soluble food dyes (McCormick, U.S. Certified) were added until a transmittance curve of the water standard (from spectrophotometric measurements) was obtained, which was a close reproduction of the sea water transmittance curve presented by Jerlov (1968, p. 110) for clear Mediterranean Sea water. The transmittances at the 440 nm and 525 nm regions were proportional to the transmittances (in percent/meter) given by Clarke and James (1939) for clear ocean water.

Following the incident light source standardization, spectroradiometric spectra and DR ratios were recorded for each sample. The successive additions of standard mixture samples were kept uniformly suspended in the container by gentle stirring until the recordings were made. Measurements of a calm, clear surface with no bubbles were recorded.

6.2.2 Results and Interpretation

The particle counts and chlorophyll concentrations of samples measured by the DR-spectroradiometer is given in Table 6.1. Samples of the B_1-B_4 were made by successive volumetric additions of the algae (chlorophyll) standard. The C samples are volumetric additions of clay standards to Sample B_4. Sample D_1 is an initial addition .. to the clear optically dense base water and the remaining D samples are made by sequential additions. The diffuse reflectance spectra, referenced to the standard white disc and backscattered to the spectroradiometer, are shown for the majority of samples in Figures 6.2, 6.3 and 6.4. The lowest reflectance is exhibited by the deep blue base water void of particulates. The predominate scattering of the spectral signal is forward and lost to the non-reflectant container surfaces. Figure 6.2 reveals the increasing backscattered reflectance (R) with successive algae concentration. In the visible region, at wavelengths below 650 nm the absorption characteristics of the blue base water are still evident. This is pointed out when the signal from the algae standard (in a 4000 ml beaker) is compared to the samples in the deep blue base water (the % reflectance of the algae standard curve is reduced by a factor of 0.2 for closer comparison with the curves B_2-B_4). The standard algae curve and the curves B_2-B_4 are similar at wavelengths $> \sim 675$ nm, indicating little influence by dye absorption at these wavelengths. The algae standard does show lower relative reflectance at 680-690 nm than the B curves due to greater absorption by the denser chlorophyll suspension.

Table 6.1 The Differential Radiometer Laboratory Study

Sample #	Description of Sample	Total Chlorophylla (mg/m^3)	Total Concentration (counts/1	Total Phytoplankton (Cells/1)	Total Counts Phytoplankton + Clays
A	Optically modelled "blue" water	0	0	0	0
B_1	500 ml. standard algae mixture (SAM)	33.45	0	5.84×10^7	5.84×10^7
B_2	1000 ml. SAM	64.18	0	11.21×10^7	11.21×10^7
B_3	1500 ml. SAM	92.53	0	16.17×10^7	16.17×10^7
B_4	2000 ml. SAM	118.76	0	20.75×10^7	20.75×10^7
C_1	2000 ml. SAM + 50 ml. Gray Clay Standard (GCS)	118.31	52.22×10^7	20.67×10^7	72.97×10^7
C_2	2000 ml. SAM + 100 ml.GCS	117.87	104.05×10^7	20.59×10^7	124.64×10^7
C_3	2000 ml. SAM + 100 ml. GCS + 50 ml. red clay solution	117.44	143.65×10^7	20.52×10^7	164.24×10^7
D_1	Clear water + 25 ml. GCS	0	30.76×10^7	0	30.76×10^7
D_2	Clear water + 50 ml. GCS	0	61.38×10^7	0	61.38×10^7
D_3	Clear water + 100 ml. GCS	0	121.69×10^7	0	121.69×10^7
D_4	Clear water + 150 ml. GCS	0	181.74×10^7	0	181.74×10^7
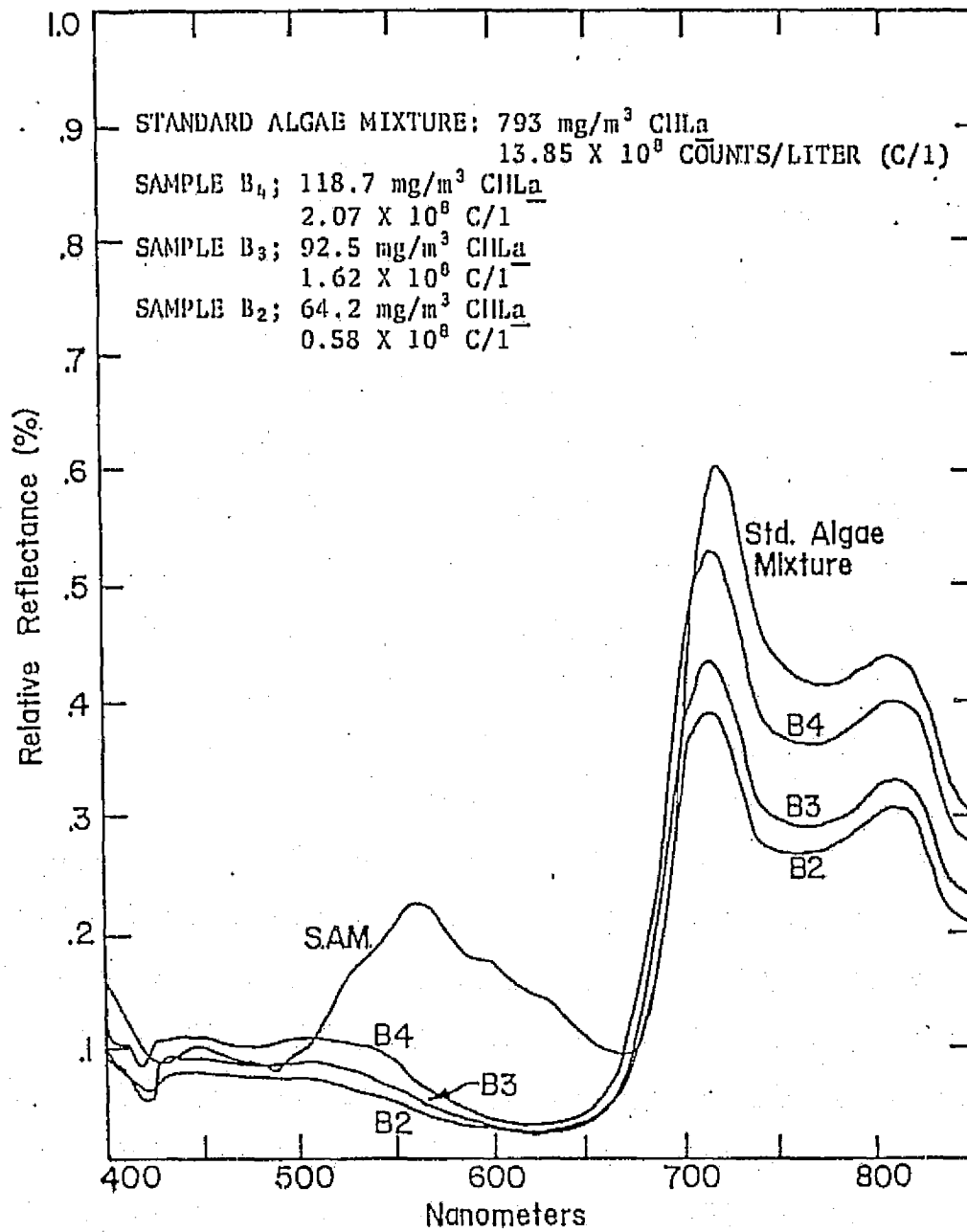
Figure 6.2 Reflectance Spectra of the Standard Algae Mixture and three Algae Samples of Various Concentrations. See Table 6.1 for composition of samples.

Comparison in the blue region (450-490 nm) between the standard mixture and samples B_2-B_4 shows that properties of the blue base medium do have an effect on the algae samples relative to the algae standard. In this case, the relative reflectance of the samples is increased in this region. The B curves show that on successive addition of algae the spectral reflectance at all wavelengths is increased in this region. They also show that on successive addition of algae the spectral reflectance at all wavelengths is increased although not proportionally at different wavelengths. This is caused by the wavelength dependence of the total attenuation coefficient which affects both primary and multiple scattered light. Increased chlorophyll is noticed by the changing shape of the spectral curves in the 440-550 nm region and an indentation in the slope between $\sim$ 665 nm and 690 nm. Figure 6.3 presents the spectral curves of samples B_3 and B_4 and the curves of algae-clay suspensions. Increased concentrations of particles are again responsible for increased diffuse backscattered reflectance. Spectra of samples C_1-C_2 appear brighter and are described by the same interpretation of the optical situation given in Section 6.1.2. Spectra of B, C and D samples are presented in Figure 6.4. The most noticeable differences in spectral signature are observed between D curves of chlorophyll-free particulate samples and algae-clay and algae-only suspensions. Decreased relative reflectance in the 410-450 nm range, increased R in 500 - $\sim$ 570 nm region and the decreased R at $\sim$ 675 nm due to chlorophyll-containing algae are best discerned from comparison of curves of samples D_3 and C_2 which had quite similar particle

SAMPLE B_3; 92.5 mg/m^3 CHLa
1.62 X 10^8 COUNTS/LITER
SAMPLE B_4; 118.7 mg/m^3 CHLa
2.07 X 10^8 C/1
SAMPLE C_1; 118.3 mg/m^3 CHLa
7.30 X 10^8 C/1
SAMPLE C_2; 117.8 mg/m^3 CHLa
12.46 X 10^8 C/1
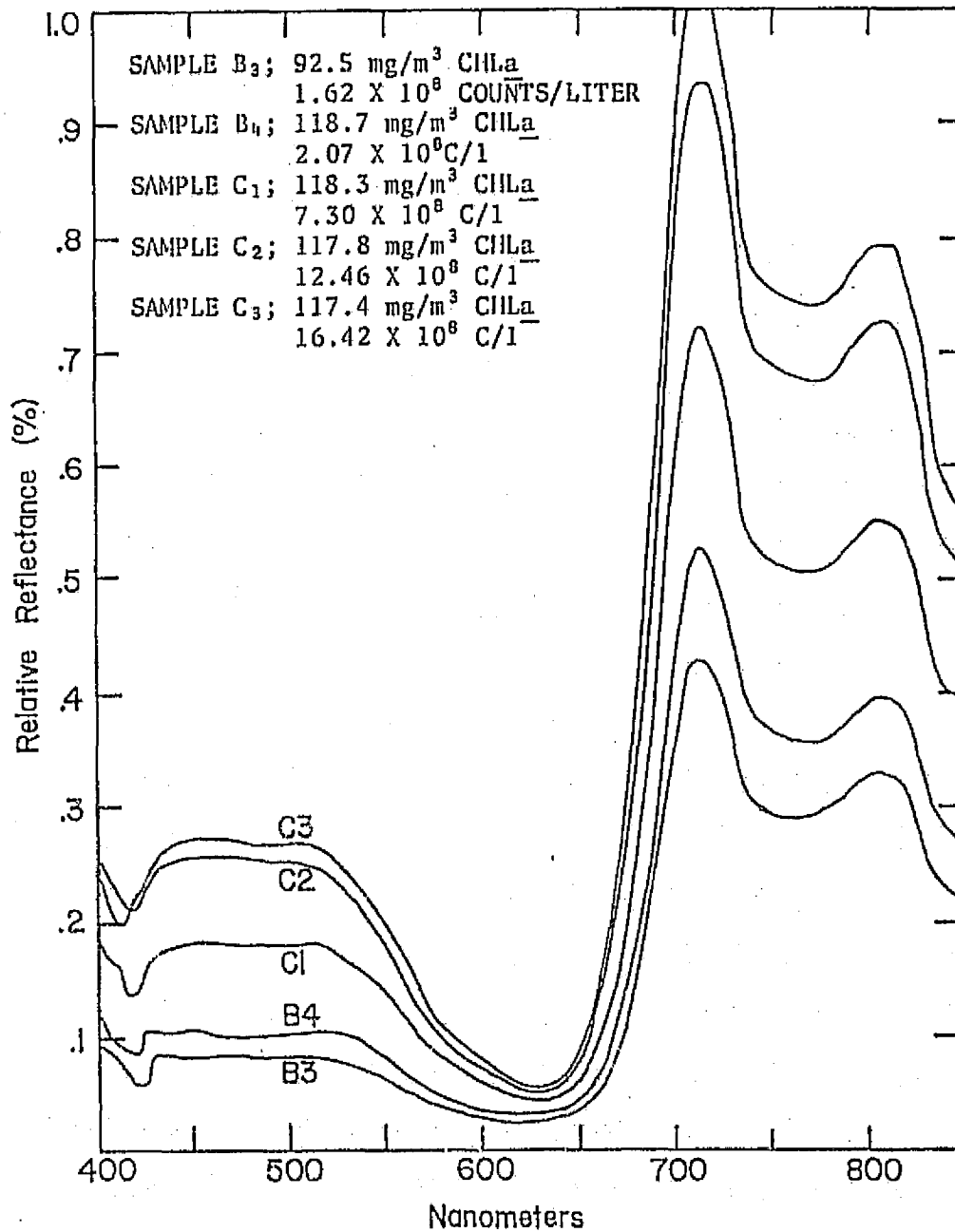SAMPLE C_3; 117.4 mg/m^3 CHLa
16.42 X 10^8 C/1

Figure 6.3 Reflectance Spectra of Algae Samples and Mixed
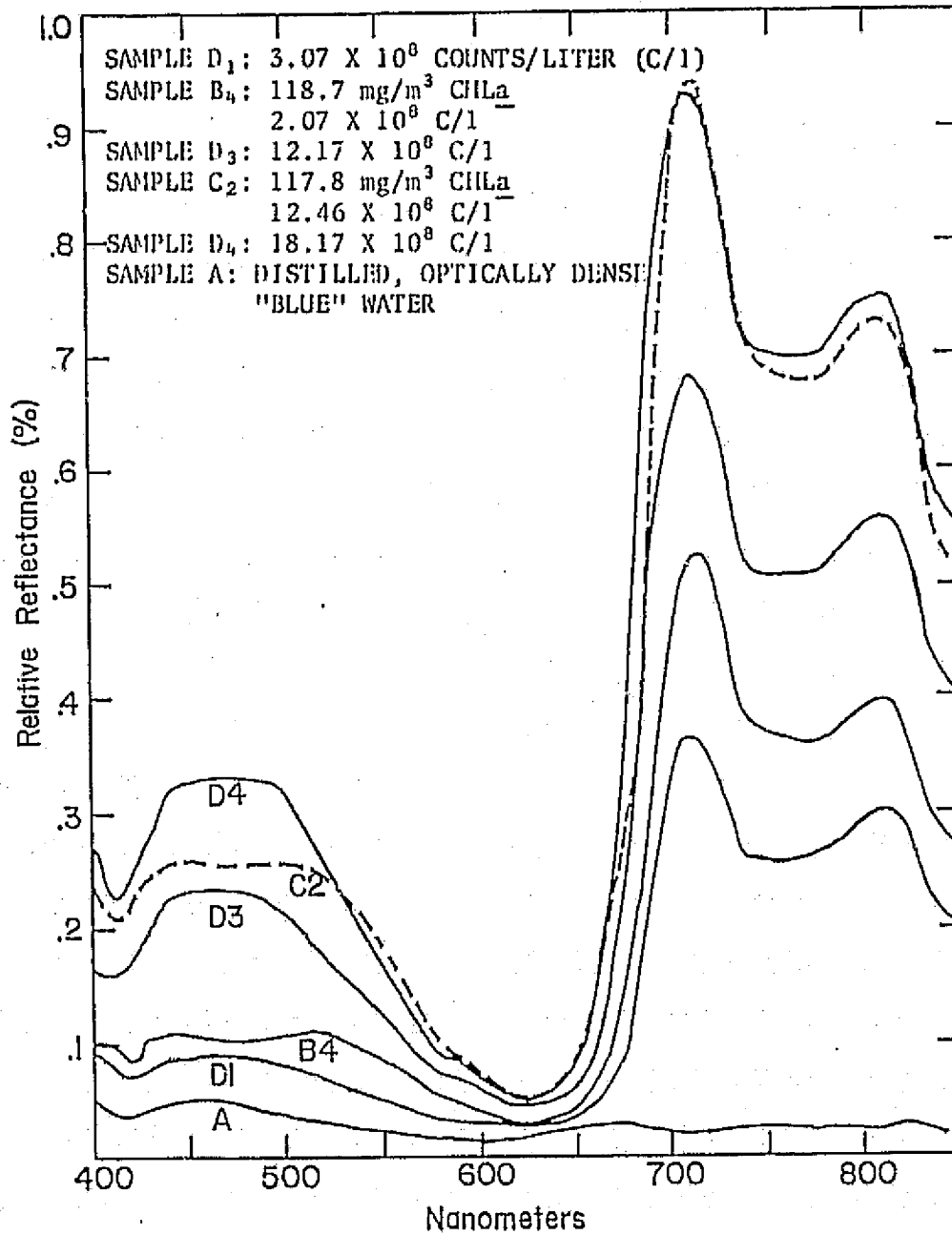Algae-Clay Suspensions. See Table 6.1 for
composition of samples

Figure 6.4 Reflectance Spectra of Algae Samples, Mixed Algae-Clay Suspensions and Clay Samples. See Table 6.1 for composition of samples.

.concentrations. Unlike the low refractive index of the flagellate algae suspension studied in Section 6.1, the algae standard in this study was predominately diatoms with higher indices of refraction resulting in greater effective scattering. The results presented in 6.5 are the correlations of measured DR ratio value of each sample with the particulate count of each sample. The solid data points represent the extreme of the ratio value for each sample with the open circles representing the mode average value. The range in ratio suggests that the suspensions are not stable or uniformly homogeneous. The averaging of a number of spectroradiometer spectra recorded at 32 scans per second has reduced this instability of the spectra presented for each suspension. Two results from this figure are the most significant: 1) The properties of the algae-only and algae-clay suspensions created spectral response that are related to the ratio value L_{443}/L_{525}. The spectral reflectance of the chlorophyll-free clay suspensions are not related to the spectral response of B and C samples. 2) With increased particle counts the L_{443}/L_{525} value decreased. The empirical relationships and correlation coefficients for both related samples sets are shown in Figure 6.5. It is predicted from this figure that the possibility exists for very high concentrations of particles that have non-selective reflectance in the sea to have ratio values which would indicate high apparent chlorophyll concentrations by the differential radiometric method. Also, it can be predicted that water masses in the sea will show a enhanced chlorophyll signal with the DR method when they are
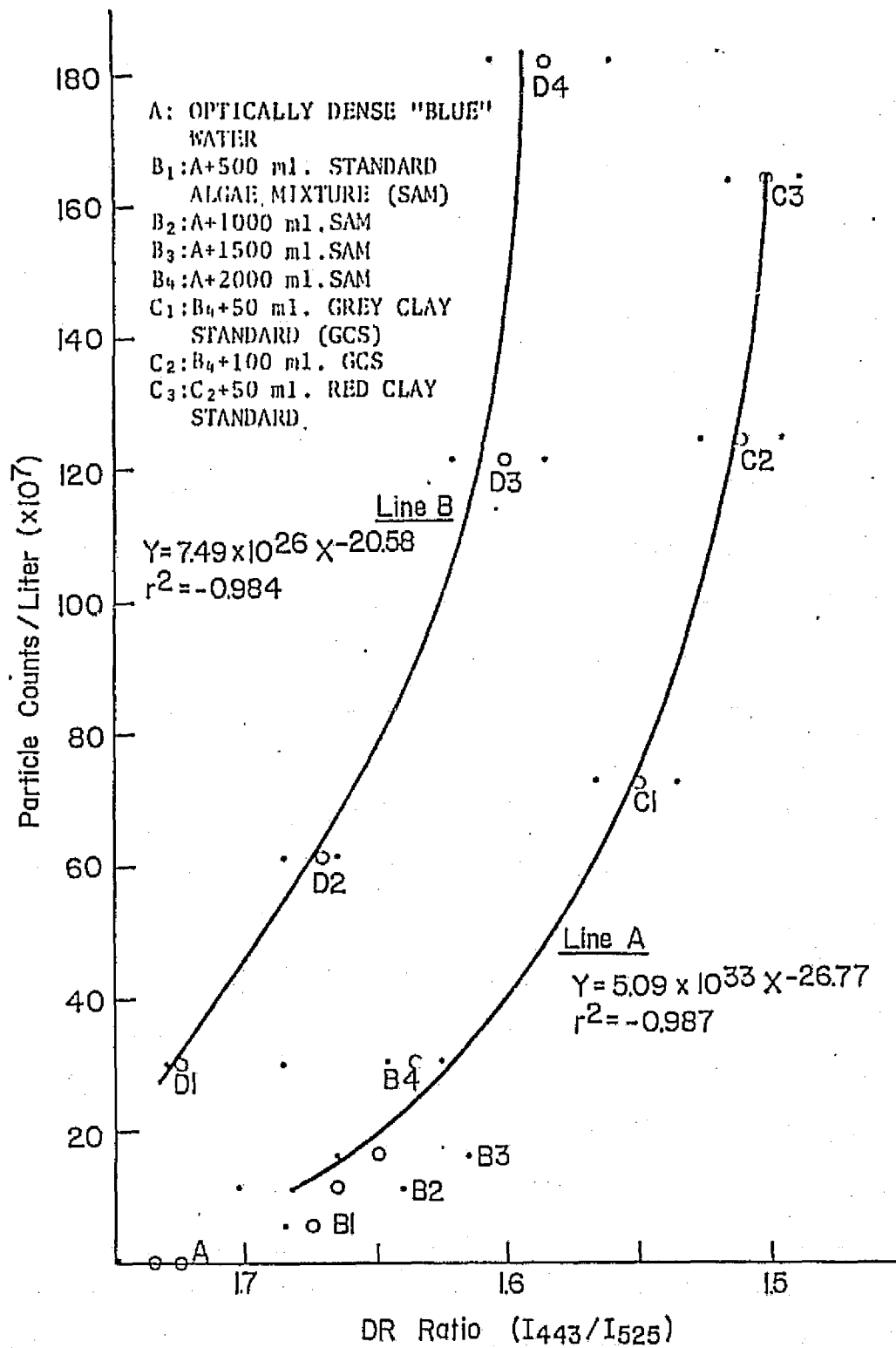
Figure 6.5 Relationships between Particle Counts and Reflectance Ratio Value *Change* for Chlorophyll-free Particulate Samples, and Algae only and Algae-Clay samples. See Table 6.1 for composition of samples

composed of phytoplankton and more reflective, chlorophyll-free
particulates in concentrations high enough for multiple scattering
events to occur. The enhanced chlorophyll signal will be proportional
to the total particulate counts. However, if the reflectance spectra
of these water masses are observed, the intensity of total backscattered
reflectance is a simple method to identify regions of chlorophyll-
containing particulate composition from those of chlorophyll-free
particulate composition. Even from their spectral signature, chlorophyll-
free particulates added to algae suspensions appear undifferentiable
from algae-only suspensions under the conditions of this investigation
and perhaps also in natural waters.

In addition to the results on chlorophyll enhancing by
particulate scattering, the use of the blue modelled water allowed an
interpretation of the combined effect of particulates and dissolved
compounds with specific optical characteristics of which Gelbstoff
is an example. It can be seen from the D samples that the addition of
clay suspension standard caused reflectance of a brighter blue.
The probability of photon backscattered reflectance to the sensor
χ, can be expressed as the ratio of total effective scattering
coefficient to total effective attenuation coefficient ($\chi = b/c$).
Specifically, the backscattered signal with the spectral characteristics
of the dissolved compound will be increased.

7. EVALUATION OF EFFECTIVENESS OF THE DIFFERENTIAL RADIOMETER FOR CHLOROPHYLL DETERMINATION

7.1 Comparison of Radiometric Measurements with Historical Data and Real-Time Sea Truth

Velasquez and Cruzado (1974) reported results of surface chlorophyll and surface temperature distribution from the SAHARA-I expedition of July, 1971. The 6-8 July cruise tract from 27.91°N, 14.29°W and 26.09°N, 14.76°W corresponded to the SUE coverage area from 18-26 August. The chlorophyll gradient structure onshore tends to confirm the DR effectiveness of chlorophyll survey. The surface values are comparable with the ocean color chlorophyll calibration. The surface temperature - chlorophyll relationship described in Section 5.1.2 is supported here as well. Many radiation temperature-apparent chlorophyll patterns were observed to be, essentially, reconstructed in these surface results. A consistently colder and apparently more productive region at the coast between 26° 20'N observed in during the Sahara Upwelling Expedition (SUE) was substantiated by the Sahara-I results. Cruzado (1974) reported the continuous underway fluorometric and surface temperature distribution of the same cruise from the method described by Ballester et al. (1972). Results were presented as parameters versus offshore distance and one tract, coincident with the onshore flight line at the southern tip of Fuerteventura, was available for comparison. Surface temperature values were in the same range of values as those

recorded by the IR radiometer and their distribution closely approximated that observed on 18 August, 1973 in SUE with a 0.5° temperature increase between 9 and 5 miles onshore. The lowest surface temperature (< 18.5°) was located 10 miles offshore and the increasing temperature distribution seaward had a small deflection toward cooler temperatures ($\sim$ 1.0°) between 22 and 46 miles offshore, then increases again far offshore. For chlorophyll, presented in fluorescence units, increasing fluorescence was inseparably identified with decreasing temperature nearshore (within 25 miles). In the offshore temperature pattern described, the fluorescence was observed to decrease with lower temperatures. In section 5.1.2, low apparent Chl. isolated patches were located just offshore of strong temperature gradients on 21-26 August and are comparable features in size and structure to the actual measurements. Again far offshore, fluorescence decreases accompanied increasing surface temperatures.

For similar reasons of sea truth comparison, Szekielda (1974) presented surface chlorophyll distribution analysis from the August 1972 NORCANARIAS Expedition. These more synoptic results showed surface values > 8.0 mg/m^3, but the same nearshore gradient structure and structure patterns offshore as noted in SUE were depicted here as well.

From the available, appropriate-season historical data, the DR method for determination of chlorophyll levels and surveying its distribution was apparently quite successful. Discrepancies in surface

chlorophyll-temperature correlations between historical data and the

results of the SUE study existed only in very nearshore areas

where visually sediment-laden water patches (< 3 miles across) had coinci-

dent higher temperatures. The significance of accompanying chlorophyll

and temperature regional discontinuities were discussed by Lorenzen

(1971). The lack of pronounced chlorophyll gradients with

temperature gradients suggested a biological "aging" of the two adjacent

water masses. In addition, the suite of sensor-probe experiments

tested in SUE was shown to be valuable in synoptic surveys for

recognition of upwelling patterns and monitoring development of these

patterns in a time-series such as the 18-22 August 1973

results interpreted in Section 5.1.2

Vertical chlorophyll distribution profiles of the NORCANARIES

Expedition presented in Braun and de León (1973)

supported the interpretation of euphotic zone boundary detection

in the light penetration profiles. Stations distributed coincidentally

to probe sites of SUE (see Table 5.3) showed maximum

distribution of phytoplankton above the depth of deflection in the

extinction rates noticed in expendable probe profiles. A discontinuity

in the comparable chlorophyll distribution profiles at depths < 50

meters would cause a similar decrease in extinction rate as shown in the

AXPM profiles at < 50 m.

During the JOINT-I project all chlorophyll (Chl.) and actual surface chlorophyll measurements showed extraordinary differences when compared. Nearshore ($\leq$ 10 km) differences showed an order magnitude higher apparent Chl. values than actual surface measurements. Offshore (> 36 km) an order of magnitude more actual surface chlorophyll was observed compared to apparent Chl. (see Figure 5.7). The DR method clearly was not effective, even in relative chlorophyll level determinations. No preliminary sea truth chlorophyll measurements available supported the DR method in the JOINT-I area. The multi-comparison of sea truth parameters vs. offshore distance (Figures 5.4 and 5.5) indicated that total particulate counts were in part responsible for the low DR ratio values (L_{443}/L_{525}) which corresponded to high apparent Chl. Only at distances > 70 km offshore were actual chlorophyll values positively correlated to any degree with apparent Chl. It should be pointed out again, that the relationship of apparent Chl. to DR ratio value is log-linear (i.e., a linear decrease in DR ratio value is proportional to a logarithmic Chl. increase).

High concentrations of particulates in the nearshore areas originated from blowing sand and dust off the Sahara. A complete study of atmospheric eolian loadings collected on the Cap Blanc coast and at sea has been presented by Lepple (1974). A size distribution gradient by atmospheric fall-out of these particulates is created in the offshore direction and a particle size zonation was considered by Castiglione (1974b) for this period of JOINT-I. A vertical structure in particle frequency shown in nearshore areas

indicated an atmospheric input or phytoplankton. Total particulates

did not have a significant component of phytoplankton however, as shown

by the general multi-comparison in Figure 5.5 and also in a statistical

correlation by Castiglione, in which logarithmic surface particle

counts/liter vs. surface chlorophyll had a linear regression correlation

$r = 0.8$. A particle number distribution offshore did not strictly

follow the size zonation of Castiglione or Figure 5.5 and the suggested

compositional change from predominately eolian to phytoplankton

is well considered. In support of a change in particulate

composition, comparisons were made between 1% surface incident

light (I_o) depths and integrated chlorophyll (to the 1% level)

concentrations for various zones determined by distance offshore.

For the nearshore (out to ~ 11 mi offshore) and shelf stations (out to

~ 23 mi offshore) increased 1% I_o (deeper euphotic zone) correlated

with increased chlorophyll concentrations when compared independently

by zones. For zones determined as outer shelf break and offshore,

the chlorophyll concentrations were an increasingly more important

factor in light extinction with distance offshore (i.e.,

increasing chlorophyll concentrations caused decreasing 1% I_o depths).

These calculations were made from preliminary data available from

Leg 1 (March-April, 1974) of the JOINT-I Project. More complete

integrated chlorophyll, 1% I_o depths and other productivity data was

presented by Huntsman and Barber (1974) and showed that Leg 1 data fit

the chlorophyll-light penetration relationship better than later Legs

(after April 1), although the trend was apparent for the whole

JOINT-1 period. This situation of inverse correlation of particulates

to chlorophyll was a rigorous test for the DR method. The historical
data available for comparison with the results presented here tended
to point out that such large quantities of chlorophyll-free particulates
over the shelf may have been an anamoly. Lloyd (1971) presented photic
zone depth and surface chlorophyll (mg/m^3) data for May and June, 1969
for   tions positioned on the shelf off Cap Blanc, which agreed with
the established increased light extinction with increasing chlorophyll
correlation made by Lorenzen (1972). An exception (shallow photic
zone and lower chlorophyll) was observed at $\sim$ 11 mi. offshore. Two
stations nearshore Cap Blanc studied during the CINECA-Charcot II
study (11-13 April, 1971) also show increased chlorophyll concentrations
with increasing 1% I_o. Margalef (1973) positively correlated total
particulates to increasing chlorophyll concentrations in upwelling regions
off NW Africa during March, 1973. Similarly, Lascartos (1974) found a
strict positive correlation of chlorophyll $\underline{a}$ and particulate concentra-
tions and also between total concentration of particulates and organic
particulates in the regions of upwelling off Cap Sim ($\sim$ 31° 30'N)
during CINECA-Charcot III (July-August, 1972). The volume percentage
of the mineral component in the most nearshore areas derived from the
coast (< 6 mi.) was $\sim$ 20%.

The particulate distributions during SUE might be concluded to
be closer to those described by the historical data, and therefore the
DR method $\underline{was}$ actually more effective for chlorophyll determination when
the concentration of high refractive index, mineral particulates was low

(an onshore limit in effectiveness still must be established). When
data from SUE are compared to those of JOINT-I, the discrepancy between
the magnitude of apparent Chl. values recorded nearshore was not
only an effect of the inherent backscattered reflectance from
the ocean, but also an effect of altitude of data collection. It was
seen from previous work (Clarke et al., 1971; and Duntley et al., 1974)
that investigators have recognized the increased diffuse atmospheric
light scattered into spectral signals of ocean color. The greatest
blue addition was going from 500 to 1000 feet altitudes and the color
ratio L_{540}/L_{460} was observed to decrease $\sim$ 6% with this increased optical
path. Since the JOINT-I aircraft operated at 500 feet while SUE flights
were at 1000 feet, the apparent Chl. signal would have appeared greater,
even over identical spectral areas, at the lower altitude.

7.2 Definition and Discussion of the Interference Processes in the
   Differential Radiometric Method Developed from Field Studies and
   Supporting Laboratory Investigations

With the preliminary results available from JOINT-I Leg 1
(March, 1974), the predominate interference to the DR method for chloro-
phyll determination can be defined. The unusual correlations of
increasing particulates with decreasing chlorophyll concentration and
decreasing depths of 1% surface incident light (I_o) with decreasing
chlorophyll (mg/m^2) nearshore and on the shelf, described in 7.1, point
out the fact that chlorophyll-free particulates, certainly a large
percent eolian in origin, govern important optical properties and

thereby the apparent chlorophyll signal measured by the differential

radiometer. The three-factor attenuation model presented by Lorenzen

(1972) which relates light extinction to phytoplankton, Gelbstoff and

undifferentiated particulate concentrations, and which was determined

from a wide variety of ocean waters including upwelling areas, did

not define the relationship of light penetration-to-extinction parameters

observed from JOINT-I, Leg 1 results. However, this did support the

unusual, if not anomolous, compositional and, thus, optical characteriza-

tion of this region. Recognition of the compositional change of suspended

materials from offshore to nearshore waters can be made from the continuous

recorded yellow, red and near IR reflectance signals. (Figures 5.2 a-e).

Areas of large increases in these reflected intensities and corresponding

small temperature changes represented a composition of predominately

coastal, highly reflective sediments. This was substantiated by

corresponding airborne photographs and visual observations. The

comparison of the continuous red and yellow reflectance with the

DR signal and SST's enabled a broader based interpretation of

apparent chlorophyll and SST features. However, for these spectral

measurements to support interpretation of optical properties, a

greater quantitative certainty of combined effects by these properties

on the spectral reflectance in particular optical situations is required.

This can only be accomplished by optical sea truth measurements in a

region of interest and semi-empirical modelling of these measurements

to describe a spectral signal. The same quantification of optical

properties is required for interpretation of light penetration profiles

such as those presented in Appendix A for support in defining spectral

signals. Not enough particulate frequency and area distribution data
are available now to do a semi-empirical modelling of optical properties
from actual observations to reconstruct the backscattered spectral
reflectance changes observed in JOINT-I. In addition to the information
above, the fluorescent particle distributions and morphology (which
can be then related to phytoplankton), the particulate organic carbon
distribution and some quantification of Gelbstoff concentration are
needed. There have not been any successful attempts to quantitatively
interpret backscattered signals by modelling radiative transfer
calculations of optical properties observed at sea. This is also due
to lack of essential optical property information. Simplifying models
have been presented for estimation of particulate Mie scattering properties
(Gordon and Brown, 1972) which consider an average refractive index
without absorption and compared well with observed scattering
functions in the Sargasso Sea. Maul and Gordon (1973) also attempted
to interpret qualitative changes in spectral reflectance in relationship
to ERTS-1 (Earth Resources Technology Satellite) spectral sensor signals.
The simplifying assumptions only consider wavelengths > 500 nm
and the effect of particulate concentration variability. This model
is not rigorous enough to interpret the observed variability of
numerous optical properties.

It was not apparent from the field studies if only sediment
suspensions would cause the high apparent Chl. values, or if phytoplankton-
sediment mixtures were required. Gelbstoff and particulates have
been previously recognized as producing a signal nearly indistinguishable

from chlorophyll by airborne spectral measurements in coastal areas
(Clarke and Ewing, 1973) and from radiative transfer
calculations (Maul and Gordon, 1973). A conclusion from Chapter 6
is that highly reflective suspended material, which are only to a small
degree selective, causes a measurement of significant enhancement of the
chlorophyll present in suspended mixtures. It is suggested that situa-
tions of multiple scattering in chlorophyll-clay suspensions were
observed by the changes in spectral structure. The non-phytoplankton
material in the NW African coastal waters is composed of highly
reflective material, because of the input from the Sahara. Similar
highly reflective suspensions of clays were used in the laboratory to
investigate the interference by spectral comparison of phytoplankton-
clay mixtures. In laboratory investigations, changes in the shapes
of the spectral curves were noticeable on successive additions of clays
to algae suspensions. In Section 6.1, the most concentrated particulate
sample (represented by Curve D in Figure 6.1) exhibits the contribution
of the selective optical properties of the clays. A partial differentia-
tion of sediment interference from chlorophyll signature in natural
waters could be accomplished if the concentrations and distribution with
depth of chlorophyll-free particulates and the entire diffuse reflectance
spectra were available. But the reflectance ratio from two wavelengths
can not differentiate the interference. In Section 6.1, two
processes were defined in multiple scattering suspensions of phytoplankton
and non-selective absorbing particulate that were applicable to explain
the DR measurements off NW coast of Africa. First, the field distribution

of radiant light is changed by the fact that more isotropic back-scattered light is "chlorophyll enhanced" because the proportion of refraction/reflection scattering is larger than in single particle scattering situations (the refraction contribution containing the signature of chlorophyll absorption). Secondly, by increasing the chlorophyll-free particulate concentration and thereby the effective "white" scattering of the suspension, an "enhanced" chlorophyll signature was produced by two means: 1) a greater number of "white" scattering events exposed the algae to more light which was effected by chlorophyll absorbance. 2) The processed signal scattered by the algae, having predominately the signature of pigment absorption, was rescattered and eventually reflected with a diminished probability of additional scattering events involving the high, broad spectral attenuance of phytoplankton.

If intermixed phytoplankton and chlorophyll-free suspended sediments were found in a near surface distribution in concentrations large enough to consider multiple scattering processes, the effects seen in the laboratory investigations could well be observed in the ocean. The lowest chlorophyll concentration (in the areas of highest particulate frequencies) still was > 1.0 mg/m^3, which can be considered a large enough fraction of phytoplankton/total particulates for chlorophyll-free particulate - phytoplankton multiple scattering events and thereby an enhanced chlorophyll signal. Perhaps more

significant to the production of the high apparent Chl. signal are the
interactions of Gelbstoff and particulate optical properties. These
interactions could be explained from the laboratory
investigation in Section 6.2 when chlorophyll-free particulate concen-
trations are high. The general conclusion from observations in
Chapter 5 and Chapter 6 investigations is that, besides chlorophyll,
the 525 nm and 443 nm wavelengths bands are not equally affected
optical properties in multiple scattering samples or in nature where
inherent properties process the incident radiance and the diffuse
reflectance is an apparent signal which may not be unique to any one
optical situation.

Sea surface effects could be identified in the analog
recordings (see Chapter 5) as an interference to the
effectiveness of the DR method. The 30° field of view, variable
azimuth angle control and 20° from nadir viewing angle reduced any
glitter or specular glint addition to the sensor.

The atmospheric interference on the signal backscattered to the
airborne sensor can not be adequately considered at present.
Additional available data plus historical measurements of
solar radiation attenuance by pyranometers and sun photometers such
as those made during BOMEX (Carlson et al., 1973) can be used to define
this interference in DR methology. Briefly, the haze and dust
frequent during JOINT-1 was considered to follow Mie theory; thus strong
forward scattering and low diffuse atmospheric (Rayleigh) scattering
should cause the incident radiance spectrum to more closely approximate
the solar spectrum than if the sky were clear and free of eolian material.

In these situations the increased aerosol scattering would reduce the fraction of parallel beam solar radiation and, in turn, reduce the intensity and frequency of specular reflectance from the ocean's surface.

Jerlov (1974) has reported the effect of solar elevation on a color index, L_{450}nm/L_{520} nm just below the surface and at various depths of the water column in differing water masses (see Section 8.3). His results showed that with sun elevation $< 15°$, the blue skylight significantly increased the value of the color index in a clear water mass at depths, while a considerably lower index in turbid water was less effected at all depths by the high percentage skylight with the sun near the horizon. The greatest effect in color change in the latter case was the attenuation by the water mass. In clear water, therefore, diffuse atmospheric light, predominately blue, contributes to the spectral character of ocean color at periods of lower solar radiation. The solar standardization procedure could be used to measure a defined limit of diffuse light. The solar zero was effective in normalizing the atmospheric selectivity of the reflected ratio L_{443}/L_{525} from the ocean as described in Section 5.2.2 Qualitatively, a limiting condition for DR effectiveness even with solar standardization was when haze in the atmosphere obscured the outline of the sun. This was determined by observations of discrepancies in apparent Chl. values when cross-points on flight tracts were crossed at low ($< 15°$) solar elevation angles and then again at higher ($> 30°$) solar positions.

8. CONCLUSIONS

8.1 Summary of Study

A differential radiometric (DR) method for continuous determination of near surface chlorophyll levels at aircraft altitudes continuously measured two narrow wavelength bands of the spectral reflectance from the sea as a ratio value. A wavelength highly influenced by phytoplankton attenuance (443 nm) has been correlated to change in chlorophyll concentration from aircraft measurements. A second wavelength (525 nm) was selected for an intensity-normalizing reference signal because of its insensitivity to changes in chlorophyll concentrations and the additional preliminary assumptions that optical properties of parameters other than phytoplankton do not effect the value of the reflectance ratio L_{443}/L_{525}. A chlorophyll calibration from the values of the spectral reflectance ratio was accomplished from aircraft and corresponding surface chlorophyll measurements in a variety of natural waters. Advantages of this method include real-time interpretation, airborne solar standardization and continuous recording capability.

In this study an evaluation of the effectiveness of the DR method for measuring and surveying the regional distribution of chlorophyll was made by defining limitations of successful use and by identifying and investigating interferences in the method.

Two aircraft oceanographic research studies in a region of dynamic ocean color as a partial function of upwelling off the NW coast of Africa are described. A regional survey was accomplished and allowed identification of interferences in chlorophyll determination.

The SAHARA UPWELLING EXPEDITION (SUE) was an experimental study designed. as a survey of surface waters with known optical variability due to high phytoplankton concentration in response to upwelling (Szekielda, 1973). Goals of this preliminary study were to establish the effectiveness of using a differential radiometer (DR) and an airborne radiation thermometer (ART) for simultaneous recording of surface parameters and synoptic analysis of a coastal region over a period of time. Expendable probe data and visual observations supported the interpretation of the system's effectiveness. The DR method for chlorophyll determination was preliminarily evaluated. The conclusion is that the method was effective in measuring changing apparent chlorophyll levels in the experimental conditions with support for visual observations of noticeable plankton strips (Figure 5.2) and a nearly constant dependence of apparent chlorophyll change with temperature (see surface maps of Figure 5.2). In addition to the evaluation, a valuable collection of oceanographic data was obtained, the results of which were preliminarily interpreted in Section 5.1.2. A full interpretation of the oceanographic processes identifiable by the data was not an objective of this study, but is a study that can now be made with more significance due to this prior evaluation. However, quantitative evaluation of chlorophyll determination was

not considered, nor the quantitative evaluation of what parameters were actually measured by the DR.

Six of 26 oceanographic research flights of the JOINT-I project are described and interpreted with preliminary available real-time sea truth measurements for defining the DR method's limitations and identifying interferences in its effectiveness in the $1°$ square operations area ($21°$-$22°$N, by 17-18°N) off Cap Blanc. In addition, a partial description of the synoptic time-series of results is given for recognition of upwelling events. Analyses of apparent ocean color chlorophyll, SST and the DR ratio value (L_{443}/L_{525}) are presented for all flights. As in SUE, a maximum gradient of Chl. in the offshore direction was located in the nearshore areas. Besides this constant nearshore gradient, Chl. distribution farther offshore had a more variable structure. There was a close identification between SST and Chl. gradients although at times it was an inverse relationship. Comparison of Chl. and surface chlorophyll levels raised immediate concern about the DR measurements. Gross differences between apparent Chl. and surface measurements were observed < 20 km offshore with apparent Chl. levels an order of magnitude greater than surface sea truth. An inverse relationship existed offshore with sea truth an order of magnitude greater than Chl. To identify the interferences in the DR method, a multi-comparison of ocean color ratio value (DR ratio value), chlorophyll concentrations and total particulate counts (both integrated to the 50% I_o depth) to distance offshore was made which showed increasing particulates, decreasing 50% I_o depth and ratio values positively correlated nearshore. Expected decreasing ratio with increasing

Chl. was observed to be the inverse. A positive correlation of Chl. and
DR ratio was observed > 70 km offshore. The effective depth of
measurement was not determined for all varieties of optical water
masses, but was about 50% I_o or $\leq$ 2 meters for this study as
determined by correlation of the integration of particulate counts
to various incident light penetration depths with the effects on DR
response.

Sufficient data were collected for interpretation of atmospheric
effects on the DR method and IR thermal measurements. When these
support materials become available, complete conclusions can be made.
From preliminary interpretation of atmospheric effects on the DR
method, the solar elevation was a far greater influence than
atmospheric composition even in high eolian-load areas.

Two laboratory investigations on the interferences of chlorophyll-
free particulates in suspension with algae employed multiple scattering
samples which were spectrally scanned. Interpretations were made of
increased effective reflectance of the suspensions. When a multiple
scattering situation exists the increased photon survival to the back-
scattered signal in the algae-reflective clay suspensions
causes an enhanced chlorophyll signature to be produced. In optically
dense (blue) base water, successive additions of an algae standard
and clay particulates were related when sample particle counts were
correlated to change in reflectance   ratio value (L_{443}/L_{525}).
Successive additions of only chlorophyll-free particles showed a
similar relation of total counts and ratio change, but was not related

to the algae-only and algae-clay mixed suspensions. The dissolved
blue colorant and particles were also predicted to behave in the same
manner as Gelbstoff and reflective particulates in high oceanic concen-
trations. It was concluded from this prediction that optical
situations could exist when Gelbstoff and particulates could be undifferen-
tiable from chlorophyll even with analysis of reflectance spectra.

8.2 Summary of Evaluation

From the results and interpretation of this study the DR
method was evaluated not to be effective in determining concentrations
of chlorophyll even on a relative basis due to interferences,
predominately in the ocean, of additional wavelength selective optical
properties and particle multiple scattering conditions. The DR method
was effective in monitoring an ocean color parameter, L_{443}/L_{525}, which
had a distribution closely identified to SST. The parameter was not
well defined but was strongly correlated to near surface particulate
numbers. The 443 nm and 525 nm wavelength bands are concluded to be
inadequate alone in an algorithm for determination of chlorophyll by ocean
color measurements.

An increased apparent Chl. gradient, which was not due to
actual increased chlorophyll especially within 20 km offshore of
the NW African coast correlated far better with the distribution
of total particulates. The gradient was a constant feature in the two
fields studies. The DR method did distinguish features offshore that
were known or suggested to be actual chlorophyll from historical data

and real-time sea truth. The atmospheric interference   beyond that
which could be normalized by the solar standardization procedure,
was minor compared to the interferences of processes in the ocean.
With the availability of support material, a full definition of the
atmospheric interference can be made.

Without measurement throughout the visible spectrum or at least
additional wavelengths that distinguish pre-quantified sediment influences
in spectral reflectance, the two wavelength DR method in this
study is limited in effective use for chlorophyll measurements.   To
be effective, the attenuation of the incident light signal must be
entirely due to phytoplankton. In addition, the cell concentra-
tion must be low enough that only single scattering occurs. Such
conditions are not the case in near coastal regions. In fact,
in productive areas, the detrital and other suspended materials may
exceed the amount of phytoplankton (as in JOINT-I). Detailed study
on multiple scattering processes and the influence on optical properties
is desperately needed. This process has been disregarded in light
attenuation and transmission studies in the sea because the small path-
length of water measured. The laboratory results of this study have
shown that spectral reflectance maxima and minima are shifted to
represent the effective scattering and attenuation coefficients of the
particular optical situation. Very narrow multiple spectral bands
or the entire spectrum are needed to recognize this shift. However,
in nature it may be impossible to recognize spectral shift effects due to

illdefined optical properties. A fact that must be recognized is; the more of the spectrum recorded, the better the ability to interpret it for identification of processes that created the spectral signal. Ratios of wavelength bands, on the other hand; 1) facilitate data reduction and presentation and 2) allow continuous recording from which small ocean color structures, sea state and atmospheric effects can be discerned and simultaneously compared with continuous sea surface radiation temperatures.

Although the evaluation of effectiveness of the DR method for its specific purpose was not encouraging, the synoptic coverage approach for support in oceanographic research of dynamic regions may be evaluated as important in the recognition of large-scale, time-sequence patterns developments as demonstrated by the results of the Sahara Upwelling Expedition and JOINT-I.

8.3 Recommendations for Further Research on Radiometric Chlorophyll Determination

Chapter 3 points out basic considerations for effective radiometric chlorophyll determination and will not be repeated here. The following list of recommendations were concluded from this study:

1) The total reflected intensity of the sea surface should be measured
along with the reflected intensity and spectra of the atmosphere
obtained by ground-based, upward oriented sensors for normalization
of the atmospheric effect and determination of the backscattered reflect-
ance for recognition of multiple scattering optical situations.

2) Detailed studies on multiple scattering processes and the influence
on optical properties are desperately needed. This process has been
disregarded in light attenuation and transmission studies
in the sea because the small path-length of water measured by the
instrumentation allows this simplification.

3) Two other basic evaluations are needed to allow significant
determinations to be made from the vast airborne data collections
from JOINT-I and SUE: the atmospheric processes and the
effectiveness of IR thermal measurements. They are seen to be compli-
mentary.

4) A reconsideration of the evaluation should be made when all
JOINT-I support data becomes available including semi-empirical
modelling of optical properties to the DR measured spectral reflectance.

5) The great difficulty of "fitting" reflectance spectra and inherent
optical properties (discussed in Section 7.2) for an interpretation of
dissolved and particulate composition of water masses may never prove a
satisfactory course of action although the Monte Carlo technique
may prove an exception to this (Gordon and Brown, 1973). One
alternative is recognizing an ocean color signal as a parameter itself,
for example, the relationship of the DR ratio values can be compared
much more easily to apparent optical properties. For example, Jerlov

(1974) showed inverse relationships between color index values defined
as the ratio:

$$F = \frac{L(180°)_{445nm}}{L(180°)_{520nm}} \qquad (8.1)$$

and the depth of 30% incident blue light and 10% surface irradiance
of quanta (350-700 nm). Bressette (1974) has also shown that
green and yellow-red backscattered reflectance to an aircraft
was inversely proportional to the Secchi depth in Chesapeake Bay. In
these cases a color index was used to optically classify water
masses and in an area where there is a limited range of variability.
6) The ultimate application of a differential radiometric correlation
method such as the one described in this study is routine coverage of
oceanic regions of interest and importance by earth satellites so
development of hydrographic parameters, recognized by semi-
conservative ocean color parameters, can be synoptically monitored.
It is recommended that further studies consider satellite application
in their design.
7) With all the radiometric sensing of Chl. work to date, it must
be realized that the correlation between any remotely measurable optical
signature of chlorophyll in the ocean, whether entire spectra or
color ratios, is far from established. It is recommended then, that
ground truth correlations always be included for radiometric
determination of chlorophyll.

BIBLIOGRAPHY

Arvesen, J. C., 1973. Operating manual for dual differential radiometer. NASA/AMES Research Center. 20p (Unpublished Manuscript.)

Arvesen, J. C., E. C. Weaver, and J. P. Millard, 1971. Rapid assessment of water pollution by airborne measurement of chlorophyll content. Amer. Institute of Aeronautics and Astronautics Paper No. 71-1097, 7p.

Arvesen, J. C., J. P. Millard and E. C. Weaver, 1973. Remote sensing of chlorophyll and temperature in marine and fresh water. Astronautica Acta. 18: 229-239.

Austin, R. W., 1974a. The remote sensing of spectral radiance from below the ocean surface, p. 317-344. In: N. G. Jerlov and E. S. Nielsen (eds.), Optical Aspects of Oceanography. Academic Press.

Austin, R. W., 1974b. Inherent spectral radiance signatures of the ocean surface. Ocean Color Analysis, Final Tech. Report, SIO Ref. 74-10. Scripps Inst. of Oceanog. 20p.

Austin, R. W. and S. Moran, 1974. Reflectance of whitecaps, foam, and spray. Ocean Color Analysis, Final Tech. Report, SIO Ref. 74-10. Scripps Inst. of Oceanog. 10p.

Ballester, A., A. Cruzado, A. Juliá, M. Manríquez, and J. Salat, 1972. Análisis automática y continuo de las características físicas, químicas y biológicas del mar. Publs. Técnicas Par. "J. Cierva". 1: 1-72.

Blackburn, M., 1969. Conditions related to upwelling which determine
distribution of tropical tunas off Western Baja, California.
Fish. Bull. 68: 147-176.

Brann, J. G. and A. R. deLeón, 1973. Primary production in waters
between the Canary Islands and the North West coast of
Africa. Bul. Inst. Espanol de Oceanografia.

Bressette, W. E., 1974. An optical filtering system for remote
sensing of phytoplankton and suspended sediment.
Earth Environment and Resources Conference,
Philadelphia, Sept. 10-12, p. 62-63.

Castiglione, L., 1974a. Report for the Friday Harbor Conference on
the Use of Laser Particle Counters off the N.W. Coast of Africa.
Univ. of Wash., Oct. 14. 30p.

Castiglione, L., 1974b. Preliminary abstract - JOINT-I, Leg 1.
JOINT-I Working Conference, Friday Harbor, Oct. 14-23. 1
6p. (Unpublished.)

Carlson, T. N., J. M. Prospero, and K. J. Hanson, 1973. Attenuation
of solar radiation by windborne Saharan dust off the West
coast of Africa. NOAA Tech. Memorandum ERL WMPO-7, 27p.

CINECA-CHARCOT II, Resultats de la campagne par le Groupe Mediprod,
March 15-April 29, 1971. Program de la RCP-247 du C.N.R.S.
58p.

Clark, H. L., 1967. Some problems associated with airborne radiometry
of the sea. Applied Optics 6: 2151-2157.

Clark, J., 1964. Techniques for infrared survey of sea temperature. U.S. Dept. of the Interior, Bureau of Sport Fisheries and Wildlife, Bureau Circ. 202, 142p.

Clarke, G. L. and G. C. Ewing, 1971. Use of visible region sensors for ocean data acquisition from spaceborne and airborne platforms. Woods Hole Oceanographic Inst., WHOI-71-74, 43p. (Unpublished Manuscript.)

Clarke, G. L. and G. C. Ewing, 1973. Application of spectrometry to biological oceanography. Woods Hole Oceanographic Inst., WHOI-73-8, 13p.

Clarke, G. L., G. C. Ewing and C. J. Lorenzen, 1970a. Spectra of backscattered light from the sea obtained from aircraft as a measurement of chlorophyll concentration. Science. 167: 1119-1121.

Clarke, G. L., G. C. Ewing and C. J. Lorenzen, 1970b. Remote measurement of ocean color as an index of biological productivity. Proc. Sixth Int. Symp. Remote Sensing in the Environment, Ann Arbor, Oct. 13-16, 1969. 2, 991-1001.

Clarke, G. L. and H. R. James, 1939. Laboratory analysis of the selective absorption of light by sea water. J. Opt. Soc. Am. 29: 43-55.

Cox, C. S., 1958. Measurement of slopes of high frequency wind waves. Jour. Mar. Res. 16(3): 199-225.

Cox, C. S., 1974. Refraction and reflection of light at the sea surface; p. 51-76. in: N. G. Jerlov and E. S. Nielsen (eds.), Optical Aspects of Oceanography. Academic Press.

Cox, C. S. and W. Munk, 1956. Slopes of the sea surface deduced from photographs of sun glitter. Bull. Scripps. Inst. Oceanog. Univ. Calif. 6: 401-488.

Cruzado, A. 1974. Resultados del análisis continuo en Africa del NW entre 23°N y 28°N. Res. Exp. Cient. B/O Cornide. 3: 117-128.

Cruzado, A. and M. Manriquez, 1974. Datos hidrográficos de la campaña "Atlor III" en la región de afloramiento entre cabo Bojador y Punta Durnford. Res. Exp. Cient. B/O Cornide. 3: .89-115.

Curran, R. J., 1972. Ocean color determination through a scattering atmosphere. Applied Optics. 11(8): 1857-1866.

Defant, A., 1961. Physical Oceanography, vol. 1. Pergamon Press, N.Y., 729p.

Duntley, S. Q., 1963. Light in the sea. J. Opt. Soc. Am. 53: 214-233.

Duntley, S. Q., 1972. Detection of ocean chlorophyll from earth orbit. Annual Earth Resources Program Review, 4th, Houston, 4 (sec. 102): 1-25.

Duntley, S. Q., W. H. Wilson and C. F. Edgerton, 1974. Detection of ocean chlorophyll from Earth orbit. Ocean Color Analysis, Final Tech. Report, S10 Ref. 74-10. Scripps Inst. of Oceanog. 37p.

Einstein, A., 1910. Theorie der Opaleszenz von homogenen Flüssigkeiten und Flüssigkeitsgemischen in der Nähe des kritischen Zustandes. Ann. Physik. 33: 1275.

Ewing, G. C. 1950. Slicks, surface films and internal waves. Jour. Mar. Res. 9(3): 161-187.

Fedoseev, A., 1970. Geostrophic circulation of surface waters
    on the shelf of north-west Africa. Rapp. P.-v. Cons. Explor.
    Mer. 159: 32.

Fraser. R. S., 1971. Sea glitter during ocean color measurements.
    Private communication, April 28.

Furnestin, J., 1959. Hydrologie du Maroc Atlantique. Rev. Trav. Inst.
    Pêches Marit. 23:7

Furnestin, M. -L. 1970. Rapport sur le plankton. Rapp. P.-v. Cons.
    Explor. Mer. 159:90

Garrett, W. D. and J. D. Bultman, 1963. Capillary-wave damping
    by insoluble organic monolayers. J. Colloid. Sci. 18:
    798-801.

Gordon, H. R. and O. B. Brown, 1972. A theoretical model of light
    scattering by Sargasso Sea particulates. Limnol. Oceanog.
    17(6): 826-832.

Gordon, H. R. and O. B. Brown, 1973. Irradiance reflectivity of a
    flat ocean as a function of its optical properties.
    Applied Optics. 12(7): 1549-1551.

Hovis, W. A., M. L. Forman, and L. R. Blaine, 1973. Detection of ocean
    color changes from high altitudes. Goddard Space Flight
    Center. 25p.

Hulburt, E. O., 1945: Optics of distilled and natural water. J.
    Opt. Soc. Am. 35 (11): 698-705.

Huntsman, S. A. and R. B. Barber, 1974. Primary productivity off
    the coast of NW Africa. JOINT-I Working Conf., Friday Harbor,
    Oct. 14-23. 1:9p. (Unpublished.)

Jerlov, N. G., 1964. Optical classification of ocean water,
p. 45-49. In: N. G. Jerlov (ed.), Physical Aspects of Light
in the Sea. Univ. Hawaii Press.

Jerlov, N. G., 1968. Optical Oceanography. Elsevier, Amsterdam.

Jerlov., N. G. 1974. Significant relationships between optical
properties of the sea, p. 77-94. In: N. G. Jerlov and E. S. Nielsen
(ed.) Optical Aspects of Oceanography. Academic Press.

JOINT-I Working Conference, Partial Preliminary Abstracts, Vol. 1
Friday Harbor. Oct. 14-23, 1974. (Unpublished)

Jones, P. G. W., 1972. The variability of oceanographic
observations off the coast of north-west Africa. Deep-Sea
Res. 19: 405-431.

Jones, P. G. W. and A. R. Folkard, 1970. Chemical oceanographic
observations off the coast of north-west Africa, with special
reference to the process of upwelling. Rapports et Procès Verbaux,
Conseil International pour l'Exploration de la Mer. 159: 38-60.

Kalle, L., 1966. The problem of Gelbstoff in the sea. Oceanog. Mar.
Biol. Ann. Rev. 4: 91-104.

Kattawar, G. W. and T. J. Humphreys, 1973. Theoretical study for the
remote sensing of chlorophyll in an atmosphere-ocean
environment. Texas A&M Univ. 40p.

Kerling, 1973. Private Communication

Kullenberg, G., 1974. Observered and computer scattering functions,
p.25-49. In: N. G. Jerlov and E. S. Nielsen (eds.) Optical Aspects
of Oceanography. Academic Press.

Lascaratos, A., 1974. Contribution à l'Etude Granulometrique
    des Particules en Suspension dans l'Eau de Mer. Ph.D. Thesis,
    l'Univ. de Paris VI, Paris, 89p.

LaViolette, P. E., 1974. A satellite-aircraft thermal study of the
    upwelling waters off Spanish Sahara. J. Phys. Oceanog. $\underline{4}$:
    676-684.

Lepple, F. K., 1974. Eolian dust over the North Atlantic Ocean.
    Ph.D. Thesis, Univ. of Delaware, Newark, 270 p.

Lloyd, I. J., 1971. Primary production off the coast of North-West
    Africa. J. Cons. int. Explor. Mer. 33 (3): 312-323.

Lorenzen, C. J., 1970. Surface chlorophyll as an index of the depth,
    chlorophyll content, and primary productivity of the euphotic
    layer. Limnol. and Oceanog. $\underline{15}$: 479-480.

Lorenzen, C. J., 1971. Continuity in the distribution of surface
    chlorophyll. J. Cons. int. Explor. Mer. 34(1): 424

Lorenzen, C. J., 1972. Extinction of light in the ocean by
    phytoplankton. J. Cons. int. Explor. Mer. $\underline{34}$(2) 262-267.

Margalef, R., 1971. Una campaña oceanográfica del "Cornide de Saavedra"
    en la región de afloramiento del noroeste africano. Inv. Pesq.
    $\underline{35}$ (supl.):1-39.

Margalef, R., 1972. Fitoplancton de la región de afloramiento del
    noroeste de Africa. Res. Exp. Cient. B/O Cornide. $\underline{1}$:23-51

Margalef, R. 1973. Distribution du Seston dans la region d'affleurement
    du N.W. de L'Afrique en Mars de 1973. Analyse de l'ecosysteme
    des upwelling, Second conference, Marseille, May 28-30, 1973.

Maul, G. A. and H. R. Gordon, 1973. Relationships between ERTS
    radiances and gradients across oceanic fronts. Earth Resources
    Technology Satellite-1 Symp, 3rd. 1(B):1279-1308.

Morel, A., 1966 Étude expérimentale de la diffusion de la lumiére
    par l'eau, les solutions de chlorure de sodium et l'eau
    de mer optiquement pures. J. Chim. Phys. 10: 1359-1366.

Morel, A., 1974. Optical properties of pure water and pure sea water,
    p.1-24. In: N. G. Jerlov and E. S. Nielsen (ed.)
    Optical Aspects of Oceanography, Academic Press.

Mueller, J. L., 1974. The influence of phytoplankton
    on ocean color spectra. Ph.D. Thesis, Oregon State Univ.,
    Corvallis, 223 p.

NCAR, Atmospheric Tech., National Center for Atmospheric
    Research. no. 1 (March), 76 p.

Owen, R. W., Jr., 1974. Optically effective area of particle
    ensembles in the sea. Limnol. and Oceanog. 10(4): 584-590.

Panshin, D. A., 1971. Albacore tuna catches in the Northeast Pacific
    during summer, 1969, as related to selected ocean conditions.
    Ph.D. thesis, Oregon State Univ., Corvallis, 110 p.

Payne, R. E., 1972. Albedo of the sea surface. Jour. of the Atmos. Sci.
    29(5): 959-970.

Plass, G. N. and G. W. Kattawar, 1969. Radiative transfer in an
    atmosphere-ocean system. Applied Optics. 8(2): 455-466.

Pearcy, W. G., 1971. Remote sensing and the pelagic fisheries
    environment off Oregon. Proceedings of Symp. on Remote Sensing
    in Marine Biology and Fishery Resources, Texas A&M Univ.,
    p.158-171.

Pearcy, W. G. and D. F. Keene, 1974. Remote sensing of water color
    and sea surface temperatures off the Oregon coast. Limnol.
    and Oceanog. 19(4): 573-583.

Preisendorfer, R. W., 1965. Radiative Transfer and Discrete Spaces
    Permagon Press, Oxford, 462 p.

Ramsey, R. C., 1968. Study of the remote measurement of ocean color.
    Final Report, TRW, NASW-1658, 89 p.

Riley, J. P. And R. Chester, 1971. Introduction to Marine Chemistry.
    Academic Press, N.Y., 465 p.

Saunders, P. M., 1967a. Areal measurements of sea surface temperatures
    in the infrared. J. Geophys. Res. 72: 4109-4117.

Saunders, P. M. 1967b. Shadowing on the ocean and the existence
    of the horizon. J. Geophys. Res. 72: 4643-4649.

Schemainda, R., S. Schultz and D. Nehring, 1972. Beiträge der DDR
    zur Erforschung der küstennahen Wasserauftriebsprozesse
    im Ostteil des nördlichen Zentralatlantiks. Teil I: Das
    ozeanographische Beobachtungsmaterial der Meßfahrt 1970.
    Geod. Geophys. Veröff. R. 4, H.7, 57S.

Shibata, K., A. A. Benson and M. Calvin, 1954. The absorption spectra
    of suspensions of living micro-organisms. Biochim. et
    Biophys. Acta. 15: 461-470.

Smith, R. L., 1968. Upwelling. Oceanogr. Mar. Biol. Ann. Res. 6:
    11-46.

Strickland, J. D. H., 1962. The estimation of suspended matter
    in sea water from the air. (Unpublished Manuscript.)

Szekielda, K. H., 1972a. Upwelling studies with satellites. J. Cons.
int. Explor. Mer. 34 (3): 379-388.

Szekielda, K. H., 1972b. Dynamics of plankton populations
in upwelling areas. NASA Headquarters Proposal # 518,
Manned Spacecraft Center, Houston.

Szekielda, K. H., 1974. Observations of suspended material from
spacecraft altitudes. Deutsche Hydrographische Zeitschrift.
4: 159-170.

Szekielda, K. H. and R. J. Curran, 1973. Biomass in the upwelling
areas along the northwest coast of Africa as viewed with
ERTS-1. Symp. in Sign. Results obtained from ERTS-1,
March 5-9, Goddard Space Flight Center, NASA. p. 1385-1401.

Tabor, P. S., 1974. Exploration of fishery resources with a
new monitoring approach. Earth Environment and Resources
Conference, Philadelphia, Sept. 10-12, p. 138-139.

Velásquez, Z. R. and A. Cruzado, 1974. Distribución de biomasa
fitoplactónica y asimilación de carbono en el NO de África. Res
Exp. Cient. B/O Cornide. 3: 147-168.

Wilkerson, J. C., 1966. Airborne oceanography. Geo. Marine Tech.
2(8): 9-15.

Woodward, D. H., 1964. Multiple light scattering by spherical
dielectric particles. J. Opt. Soc. Am. 54: 1325-1331.

Wu, J., 1972. Sea-surface slope and equilibrium wind-wave spectra.
Phys. of Fluids. 15 (5): 741-747

Yentsch, C. S., 1960. The influence of phytoplankton pigments on
the color of sea water. Deep-Sea Res. 7: 1-9.

Yentsch, C. A., 1971. Absorption and fluorescence characteristics
: of biochemical substances in natural waters. Proc. Symp.
of Remote Sensing in Marine Biology and Fishery Resources
Texas A&M Univ., 75-97.

Yentsch, C. S. and C. A. Reichert, 1962. The interrelationship between
water-soluble yellow substances and chloroplastic pigments in
marine algae. Botan. Marina. 3: 65-74.

APPENDIX A

Corresponding Vertical Temperature and Light Penetration Profiles

From the SAHARA UPWELLING EXPEDITION

The analyzed profiles of the near-simultaneous recordings of air-
borne expendable bathythermographs (AXBTs) and photometers (AXPMs) for
21 August, 1973 are presented in this section. These results, plus
additional temperature profiles were used in the comparison of the
vertical-plane sections presented in Figure 5.3. The profiles can be
identified with the positions in Figure 5.3 by the time labels.

Figure A.1 is a schematic of the expendable probe operation after
deployment from the research aircraft. During the drop the probe is
stabilized by a rotochute. On impact at the sea surface the stabilizing
apparatus is released and the antenna emerges. After activation of a
sea battery the sensor probes begins its descent with signal from the
probe assembly transmitted via a single cable. The probe, with its
zenith viewing photocell descends at a rate of 1.5 m/s for a maximum
cable length of 300 m. It is observed from the position of the probe
and buoy at time of probe release that the initial recording of light
incident on the detector is that at a depth of 1 m. Figure A.2 describes
the evolution of the signal by the probe. The photocell converts incident
downward irradiance to a resistance via the probe electronics. This
signal is carried by the cable to the surface and changing resistance
will cause a change of frequency produced by an audio oscillator. The
resulting audio frequency modulates a VHF transmitter and the signal

is received in the aircraft and either recorded directly on tape
(much as an FM radio broadcast), or the frequency is converted and
recorded as an analog signal for real-time interpretation. Further
details on the conversion of the expendable probes from bathythermo-
graphs to photometers are described in a University of Delaware
C.M.S. technical report. No absolute calibration of frequency to
light intensity was accomplished in this experimental study.

The profiles of AXPMs and AXBTs are presented in Figure A.3 a-h
with   light intensity expressed as % I_n, where n = depth of initial
probe recording, and temperature as a function of depth in meters
respectively.
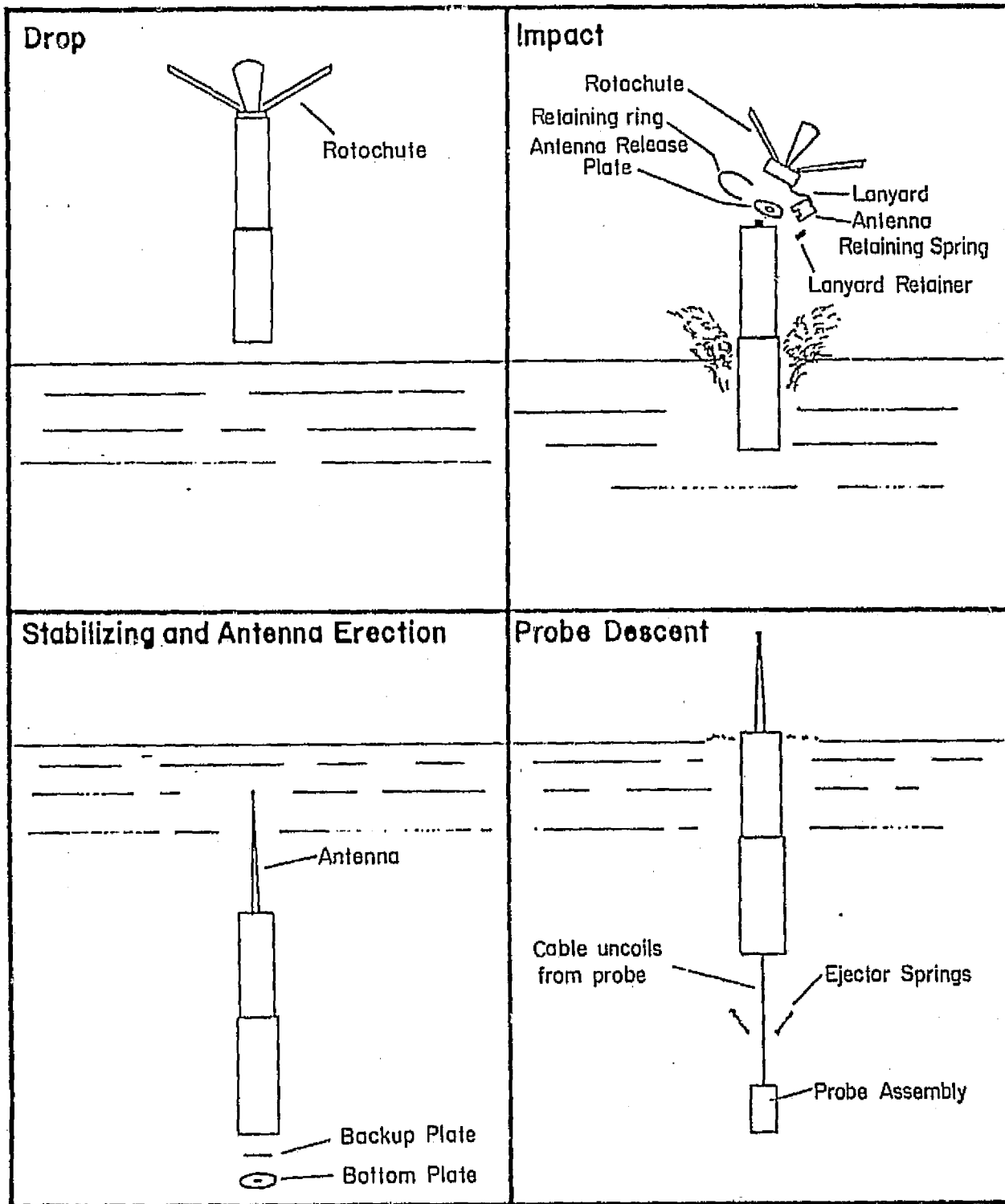
Figure A.1 Schematic of Expendable Probe Operation

Modified AXBT's

Photocell

Probe Electronics → / / → Modulator → V.H.F. Transmitter

Data Acquisition

V.H.F. Receiver → Frequency to D.C. Converter → Stripchart Recorder

Tape Recorder
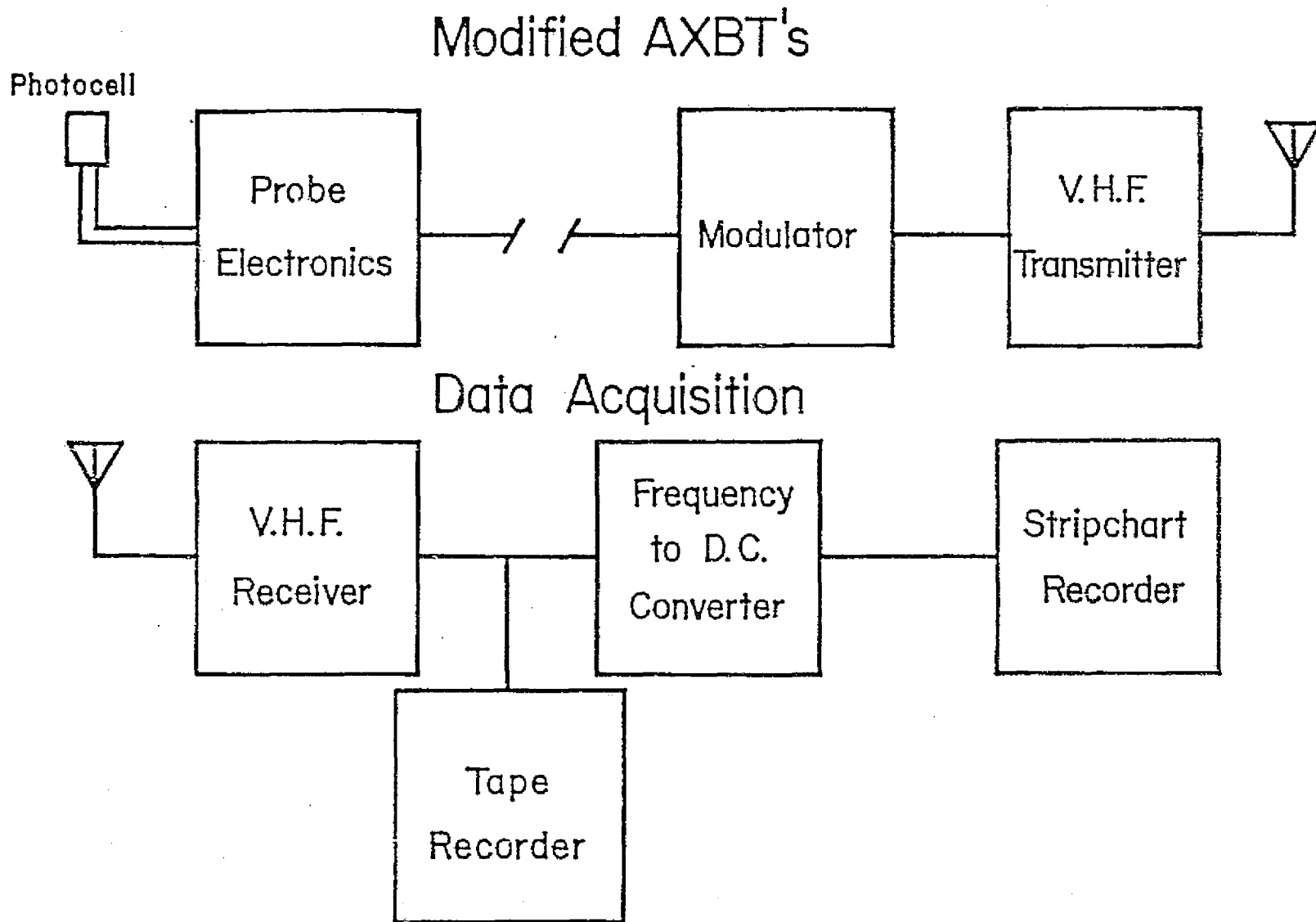
Figure A.2 Evolution of the Signal from an Expendable Probe
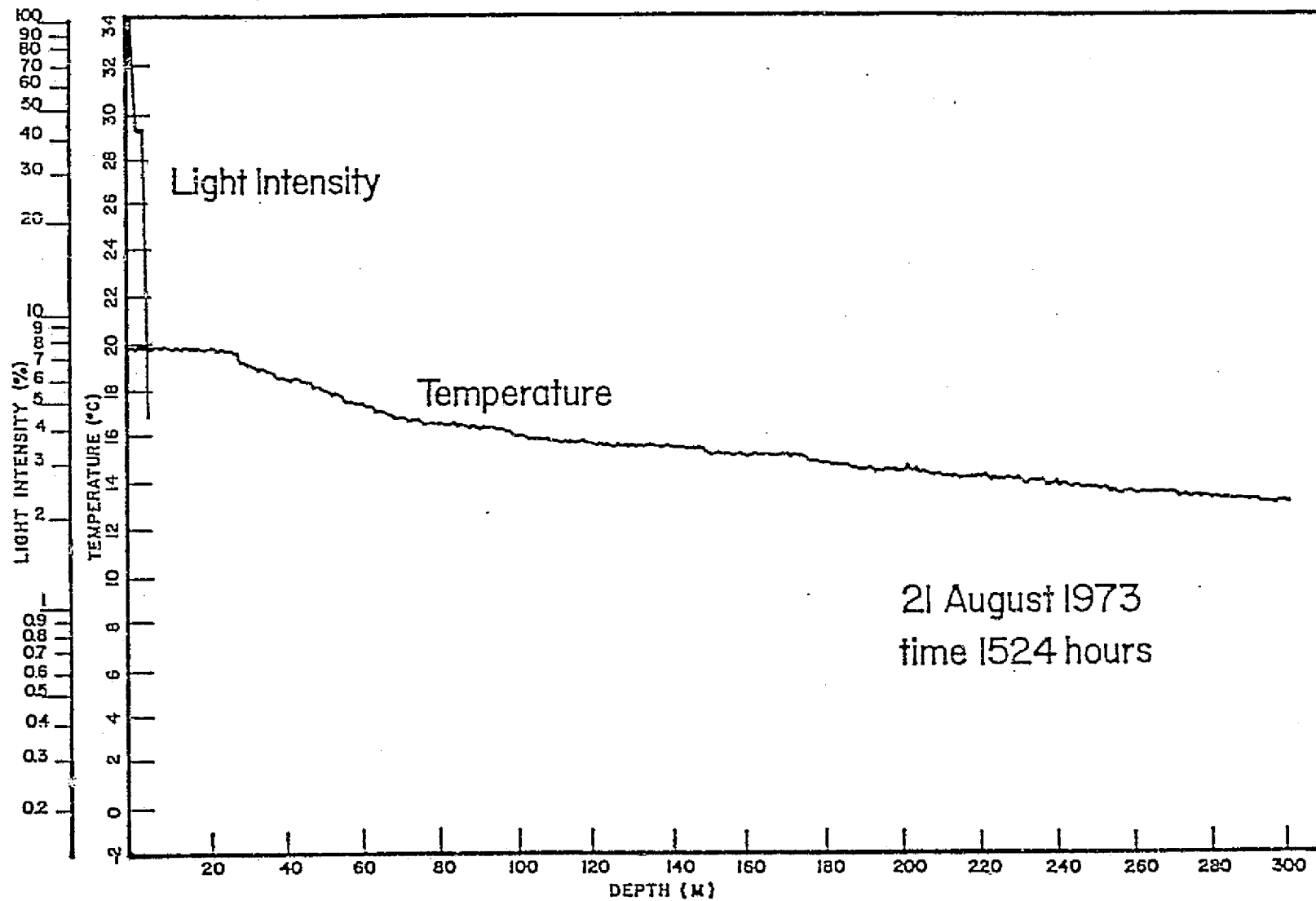
Figure A.3a-h   Profiles of Light penetration and Temperature from Airborne Expendable
Photometers and Airborne Expendable Bathythermographs during SUE, 21 August, 1973

Figure A.3b

Figure A.3c

Figure A.3d

Temperature

Light Intensity

21 August 1973
time 1354 hours
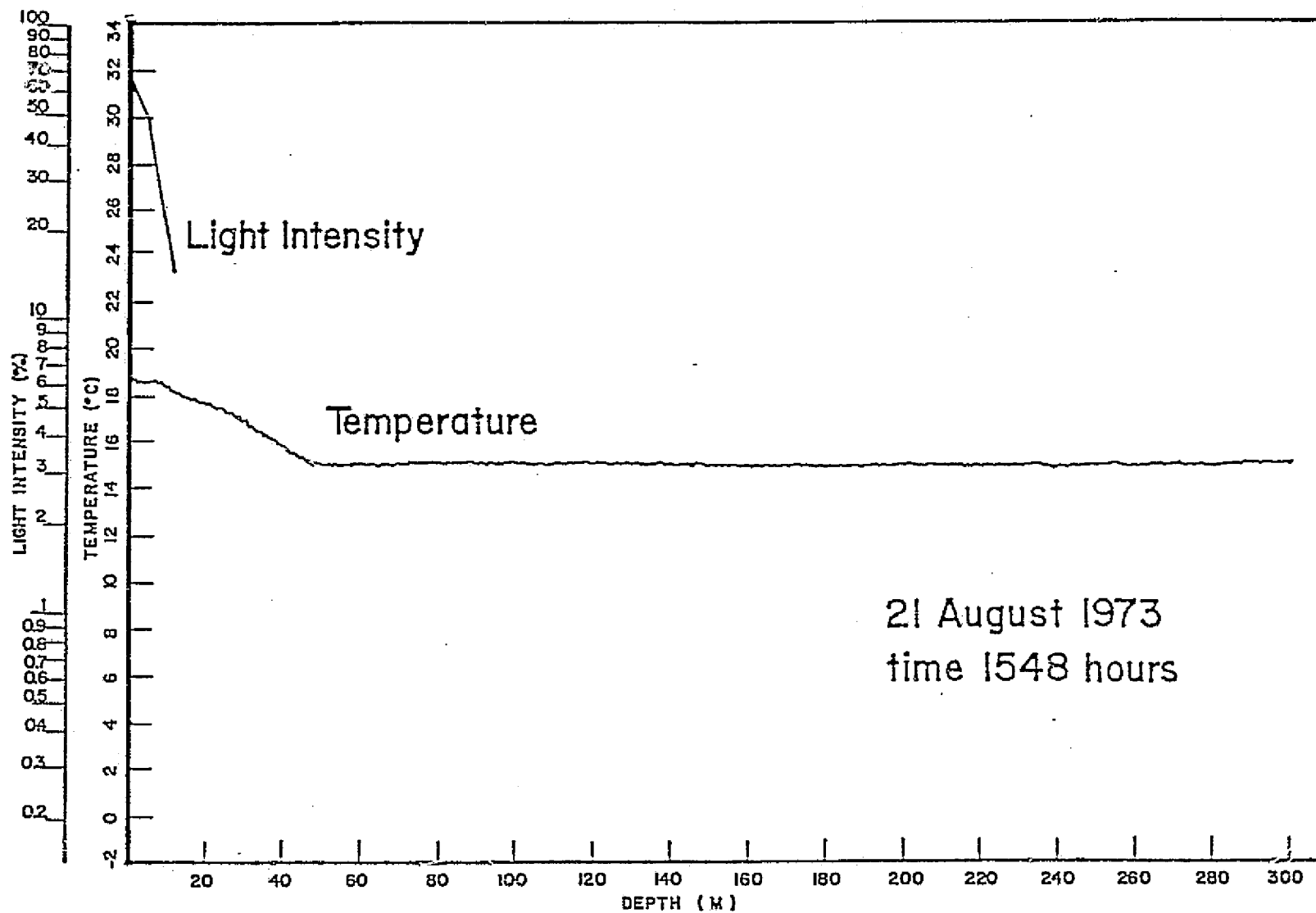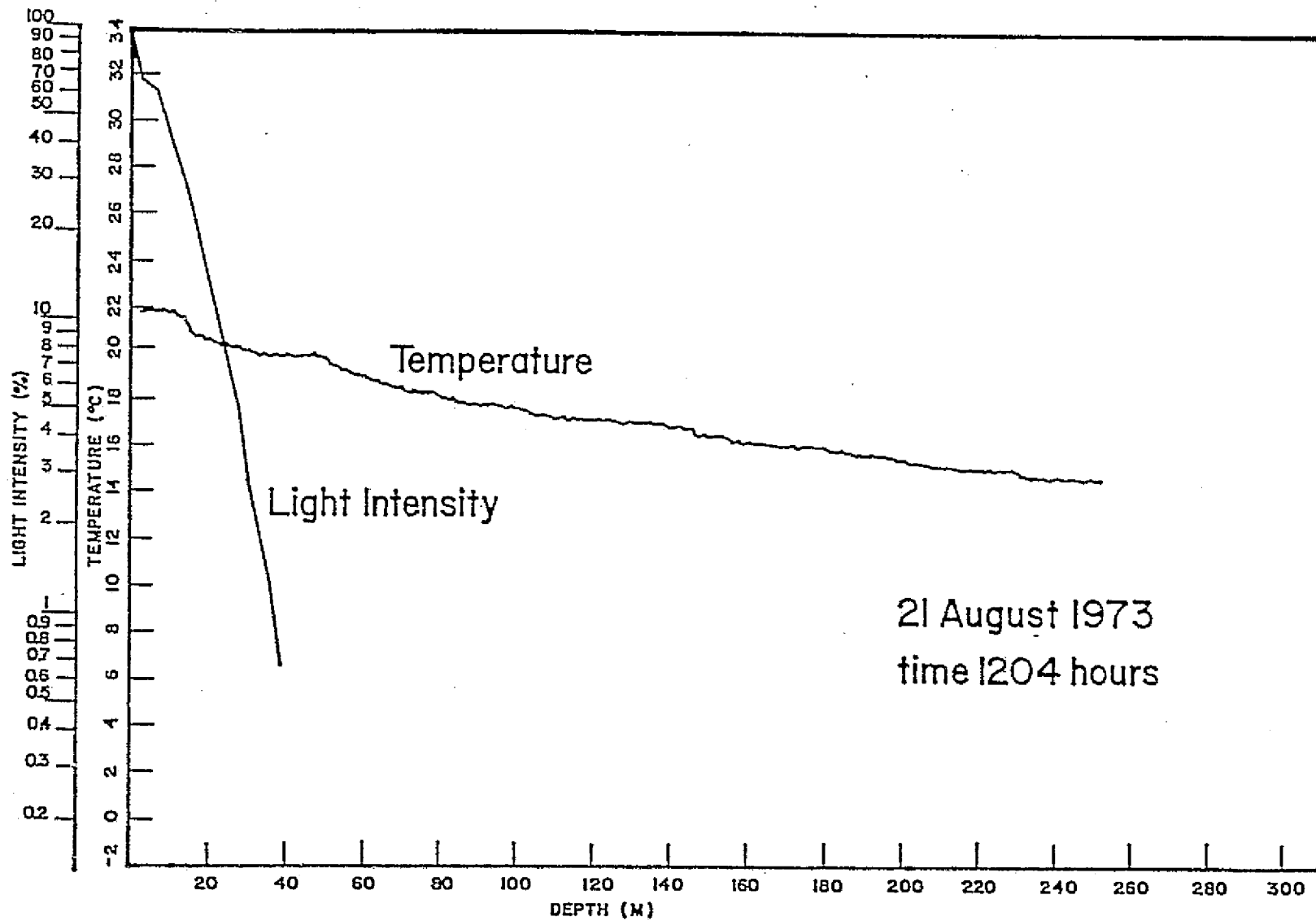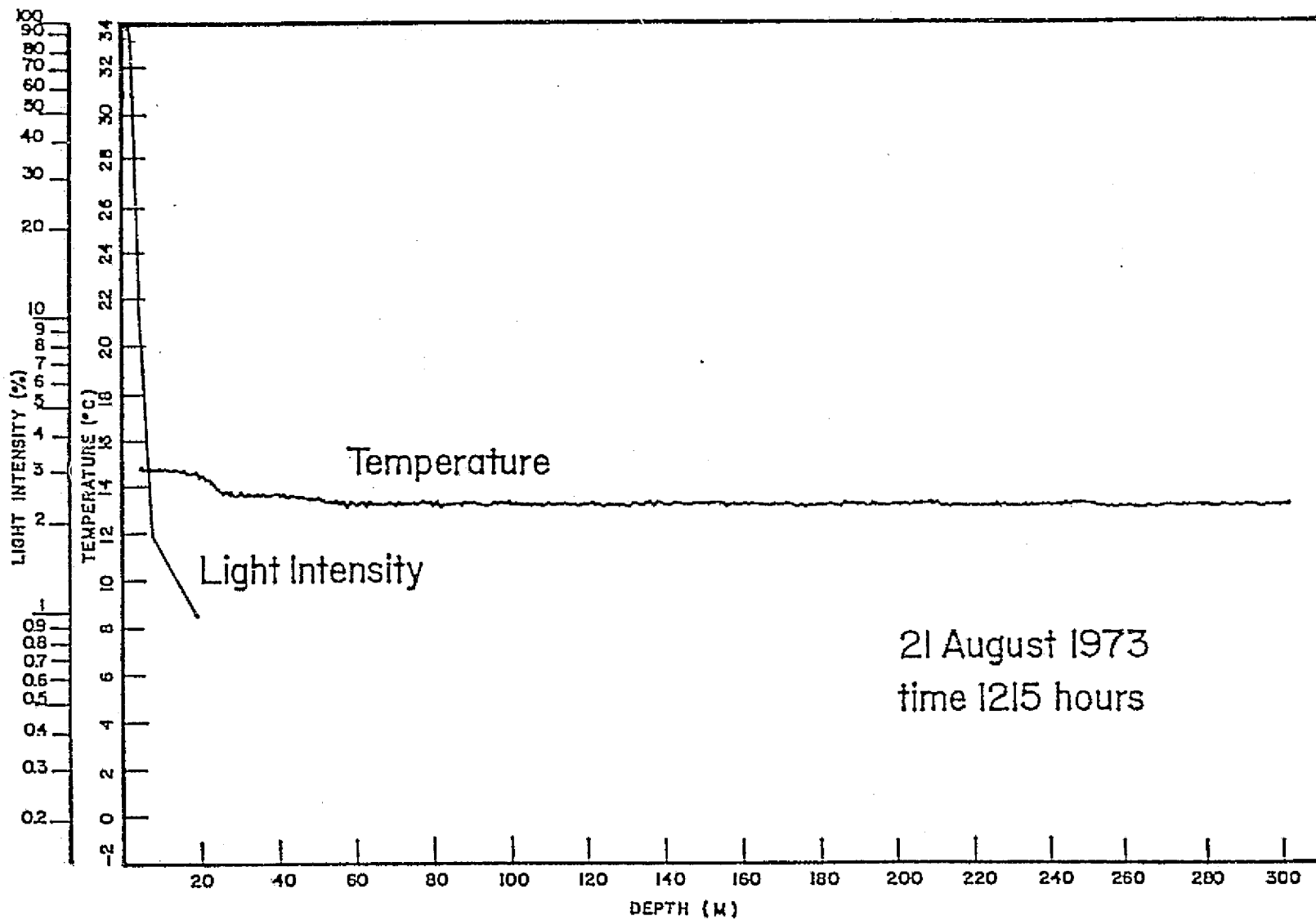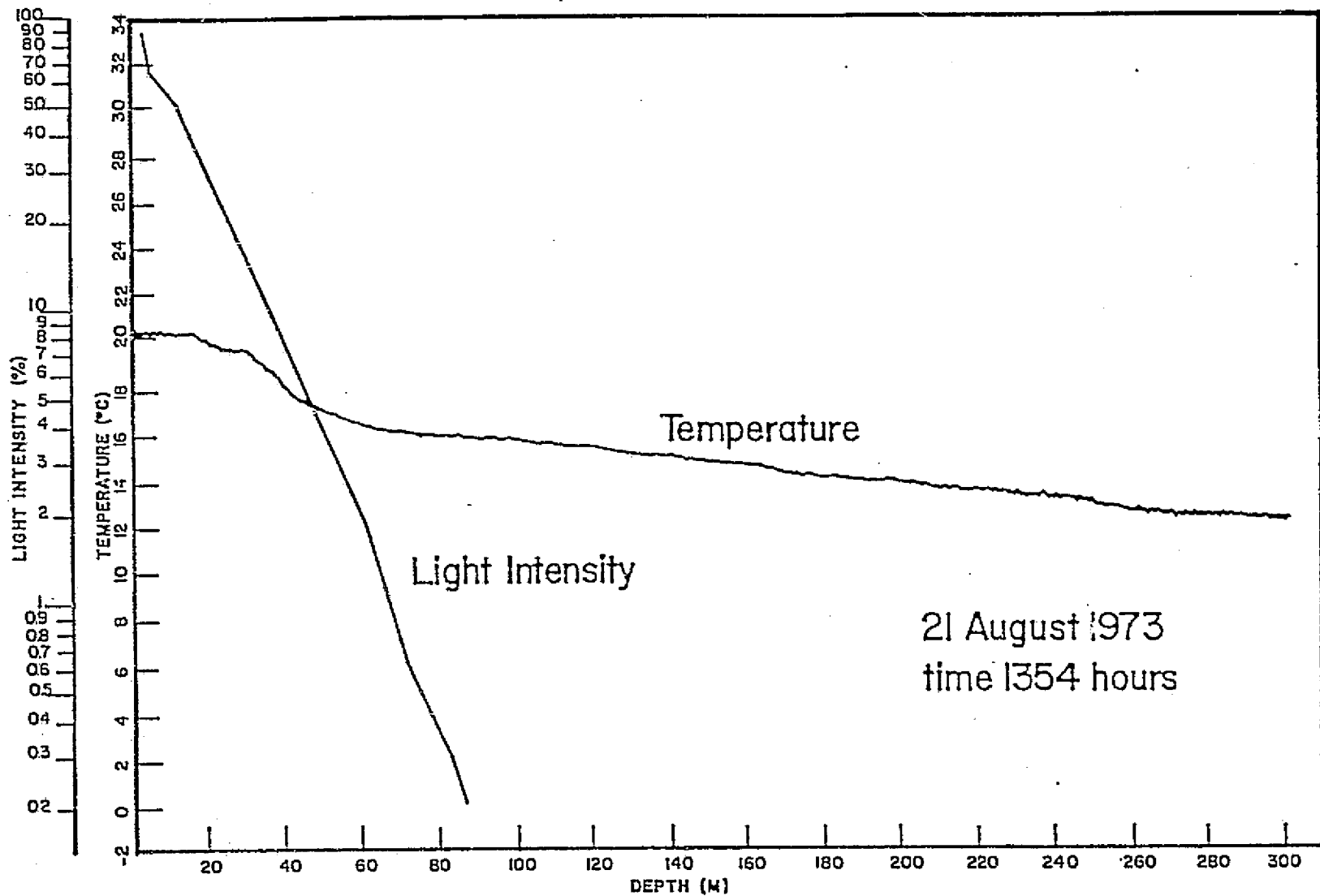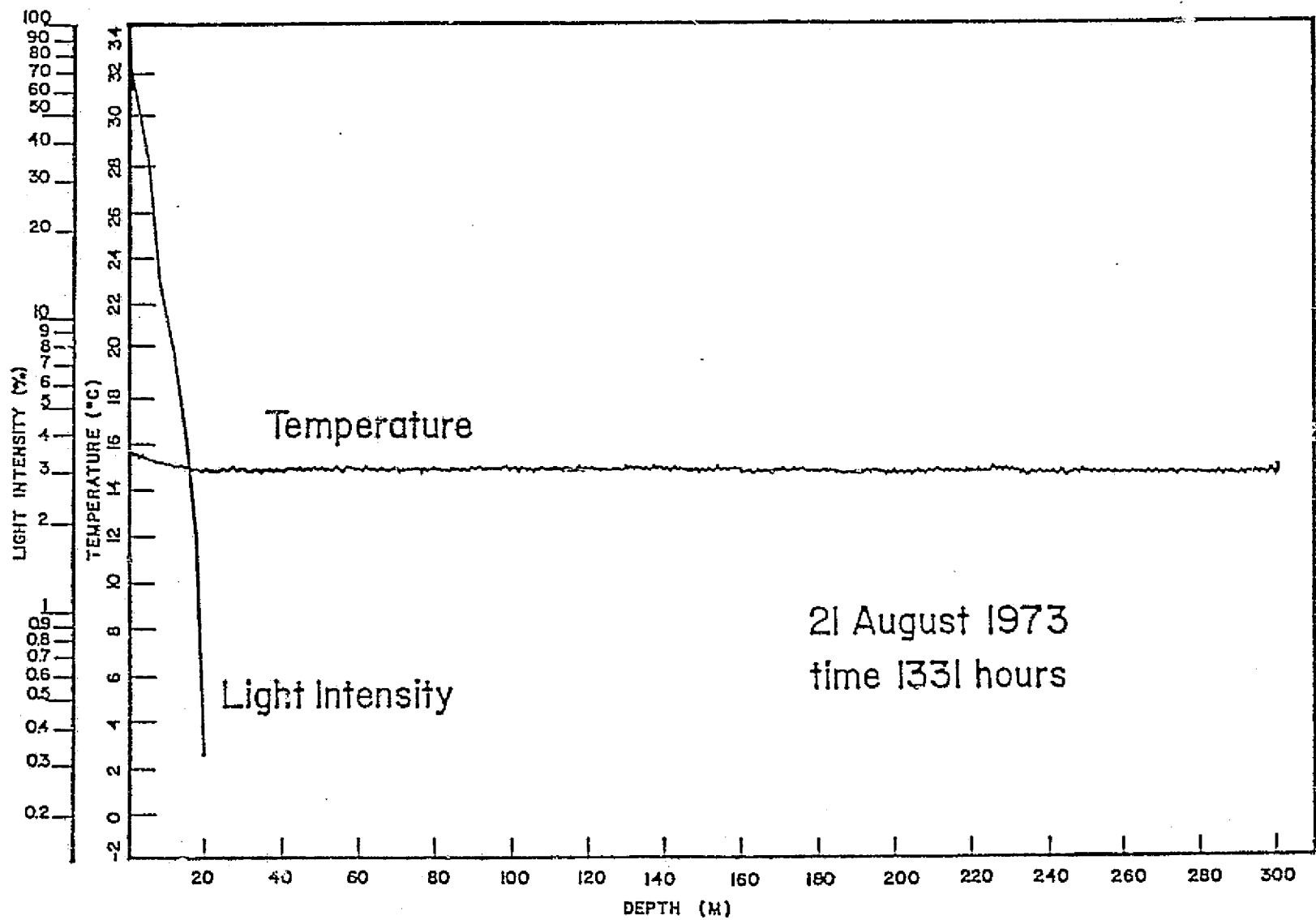
Figure A.3e
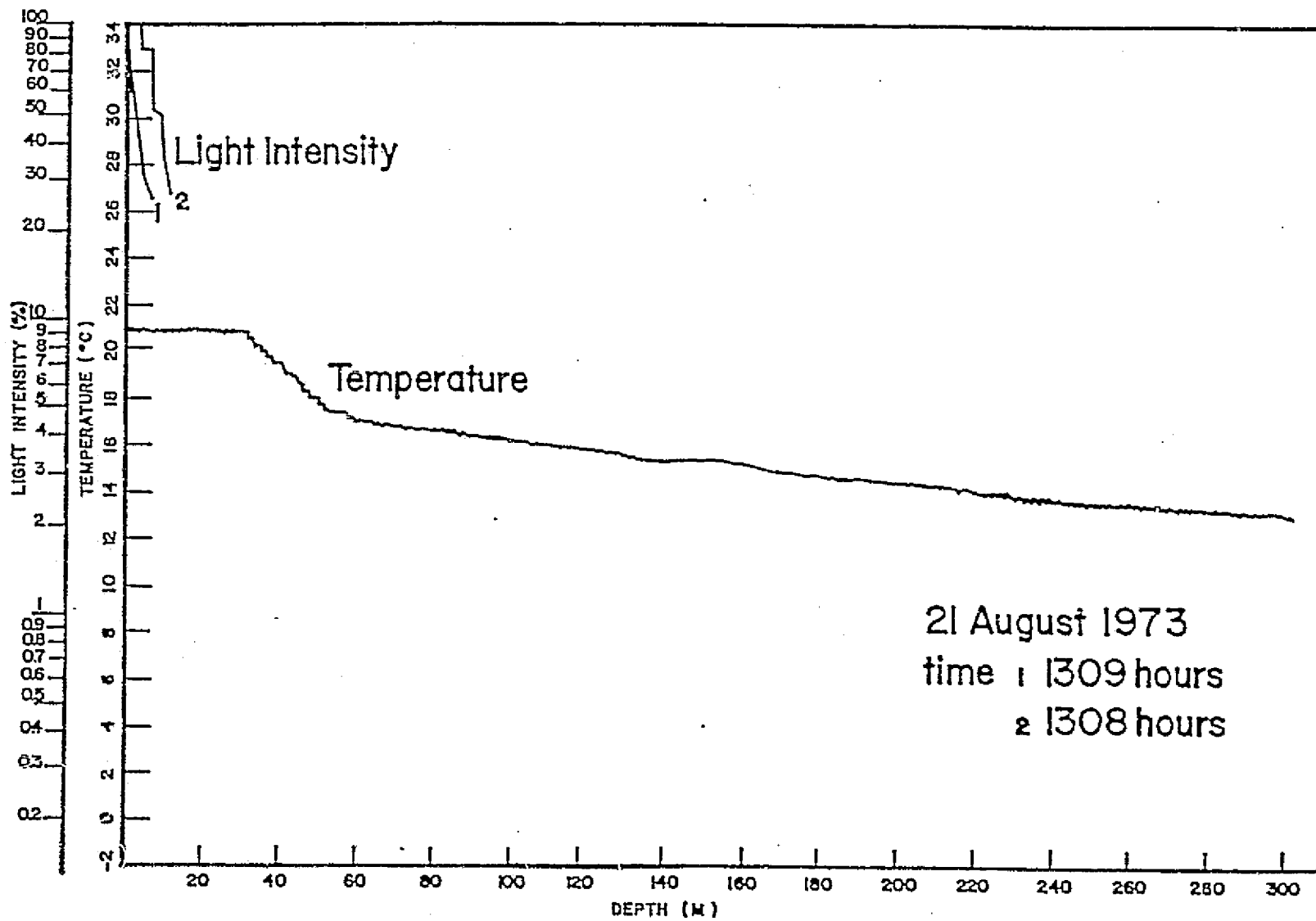
Figure A.3f

Figure A.3g
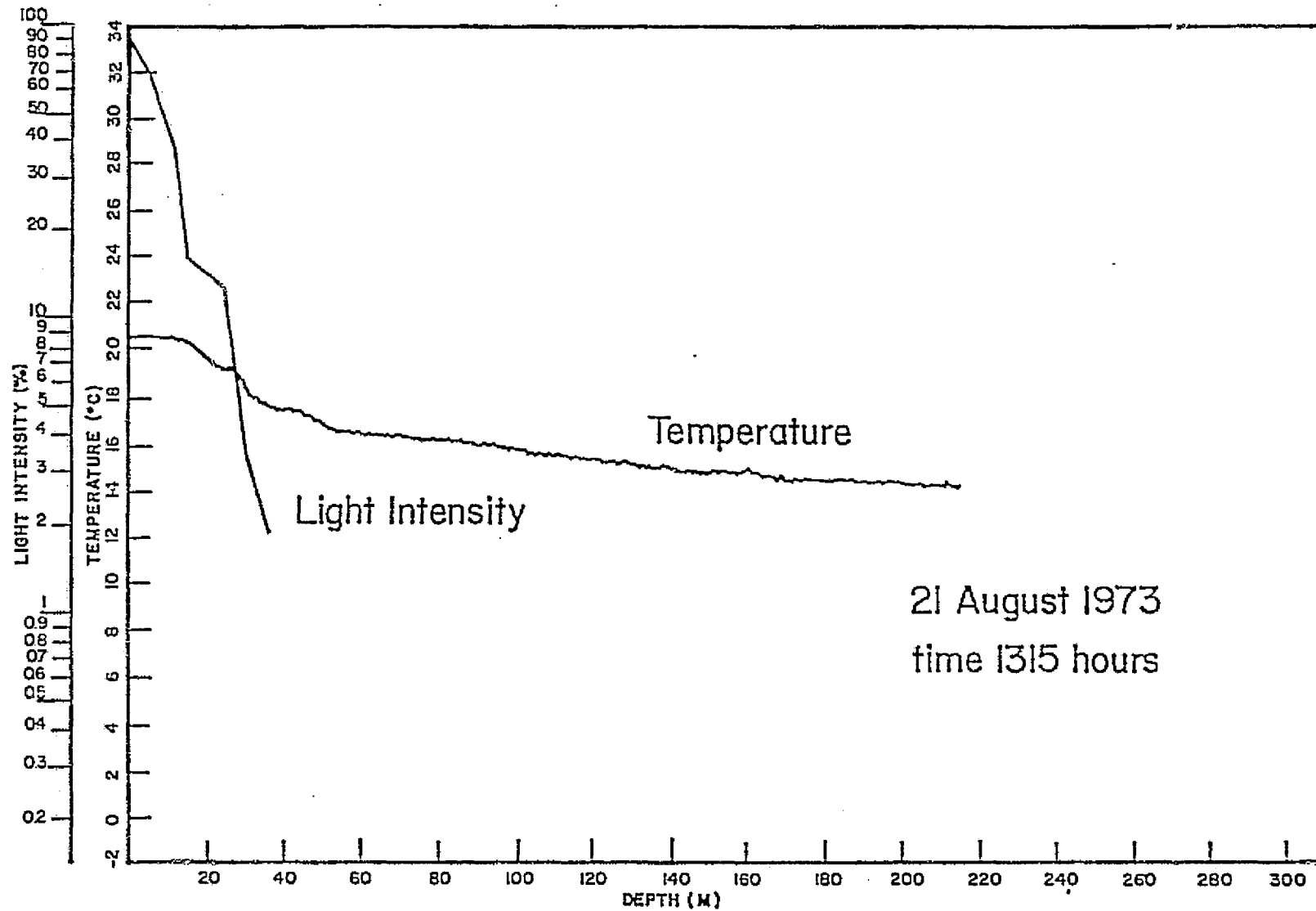
Figure A.3h

APPENDIX B

Analyzed Radiometric Sea-Surface Temperature, Differential Radiometer

Ratio and Apparent Ocean Color Chlorophyll Concentration Maps from the

JOINT-I Oceanographic Aircraft Mission

This section presents the analyzed data of the JOINT-I flights
with the exception of six flights appearing in the text of this
paper (Section 5.2.2). Each figure number includes three analyses
of the same flight. The first is ocean color chlorophyll concentration
(mg/m^3) followed on the next page by differential radiometer (DR)
ratio values at the left and sea surface temperature (SST) in °C.
on the right. The flight tracks are shown by two minute position
points on each map. The approach to the analysis of the data is given in
Section 5.2.1. A representative description of these 3 analyses for
6 flights is given in Section 5.2.2   Table 4.2   gives additional
basic information of each flight.

These results are included with those of the text for a
report of the complete time-series of the JOINT-I oceanographic
aircraft mission.

Figure B.1 a-c through B.18 a-c

Analyses of Apparent Chlorophyll, Reflectance Ratio value and Sea Surface Temperature Distributions from Aircraft Sensors during the JOINT-I Project, 17 February, to 28 March, 1974.
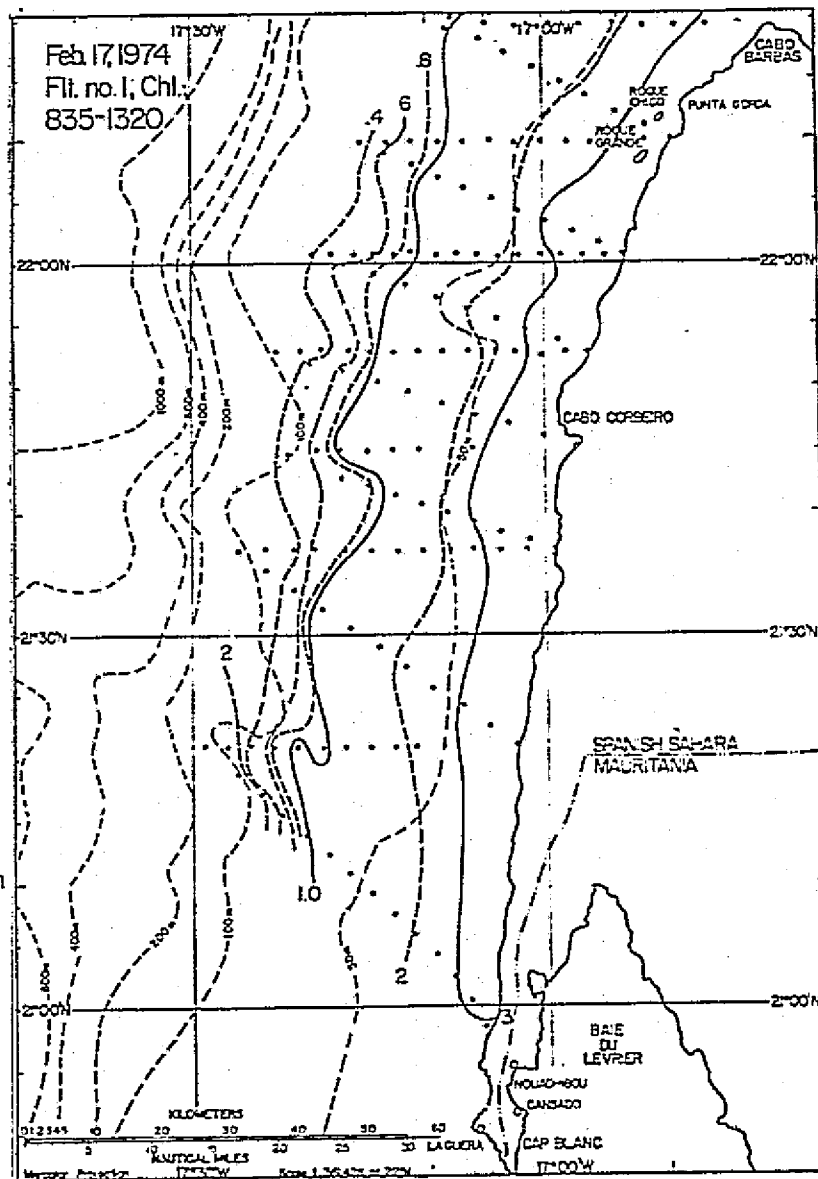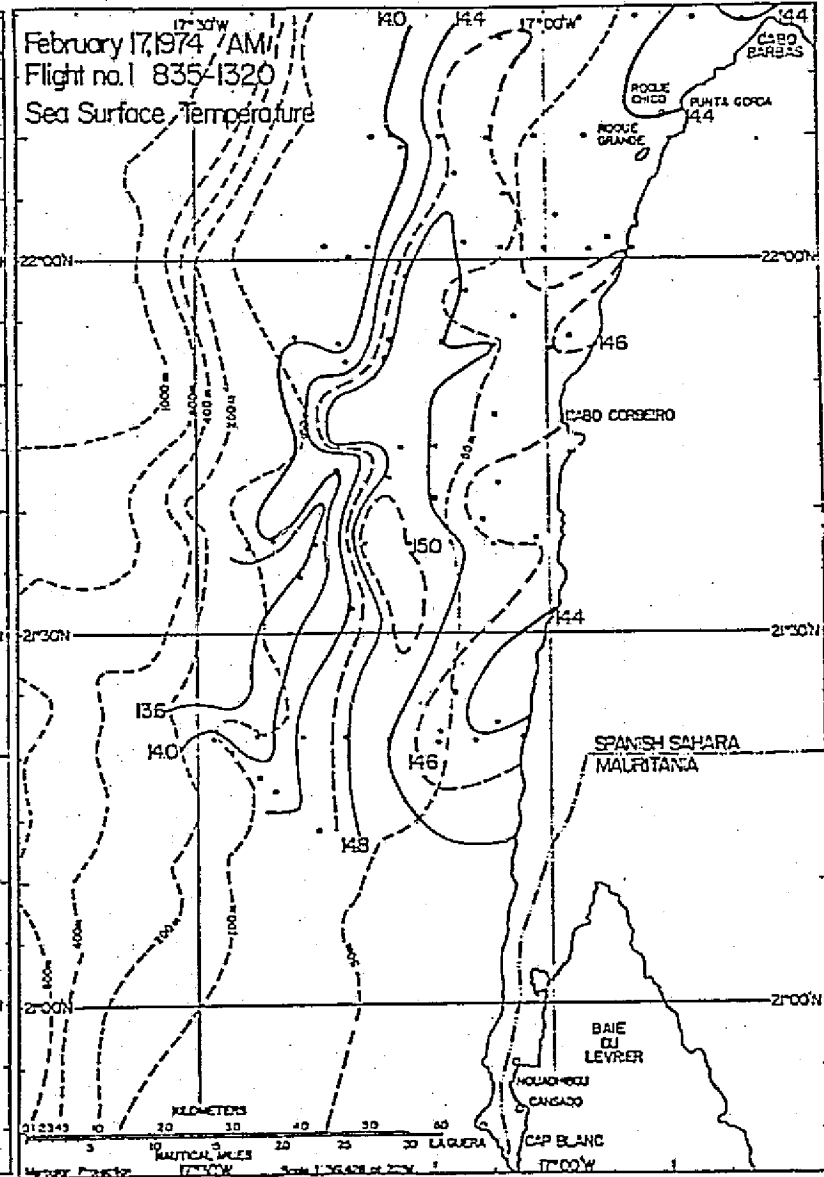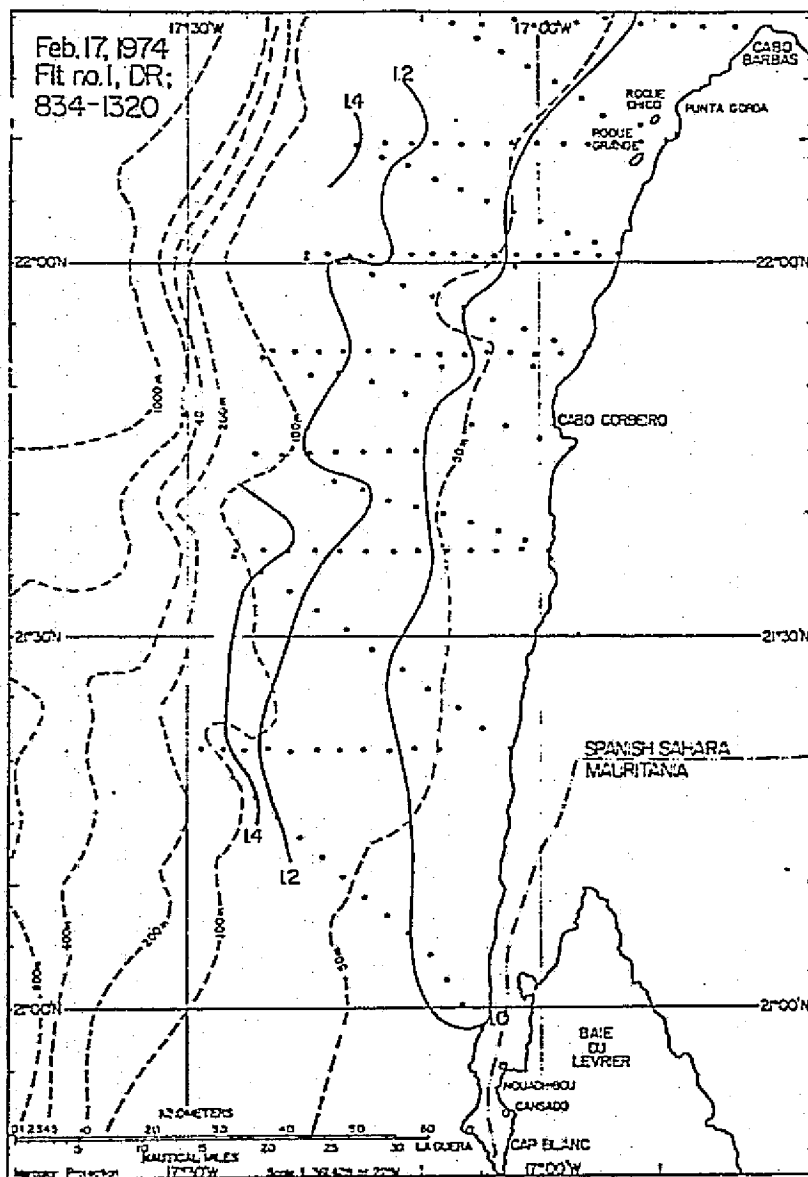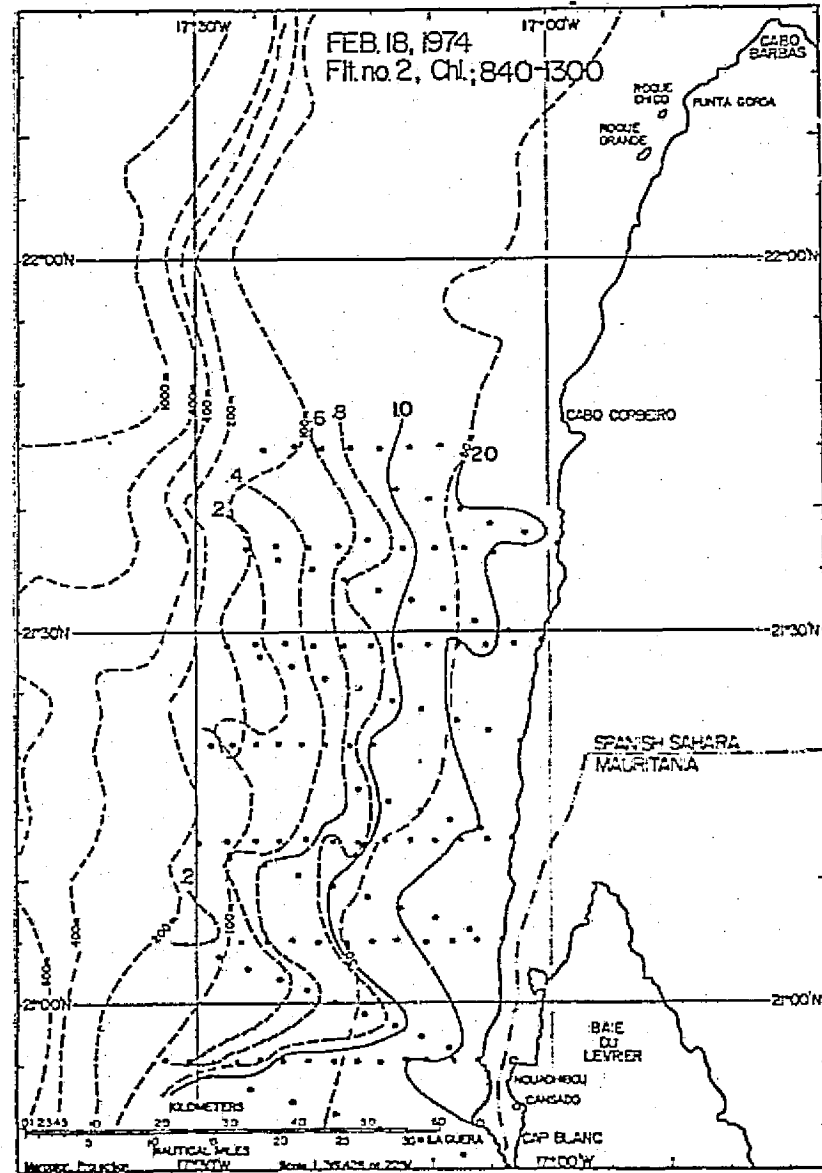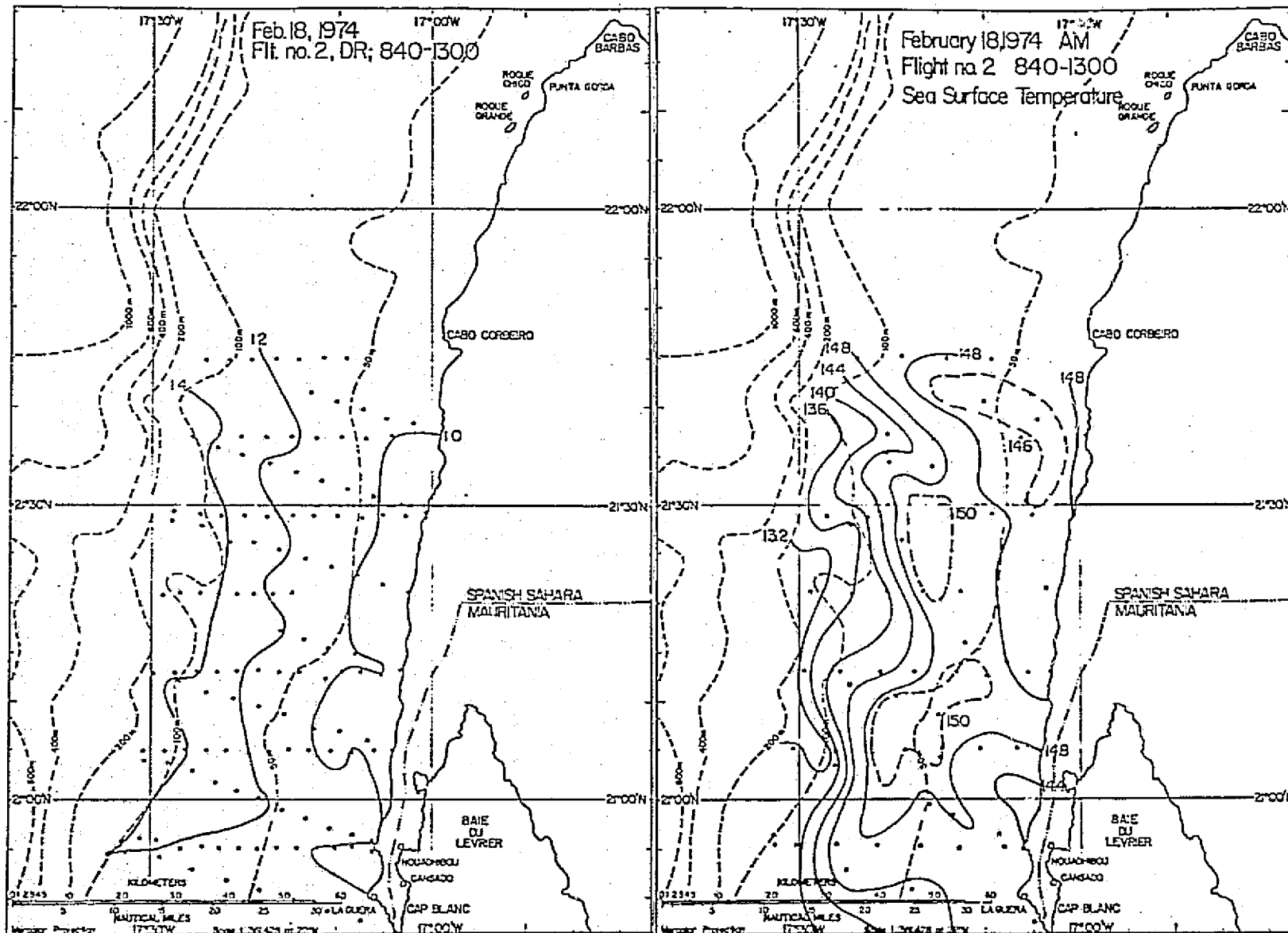
Figure B.2a-c

Feb. 18, 1974
Flt. no. 2, DR; 840-1300

February 18,1974 AM
Flight no. 2   840-1300
Sea Surface Temperature

Fit. no 3, Chl.
Feb. 19, 1974
1230 - 1695

Figure B.3a-c

Flt. no. 3, DR
Feb. 21, 1974
1230-1605

Flt. no. 3
February 19, 1974
(pm) 1230-1605

Sea Surface Temperature

Figure B.4a-c

211

Figure B.5a-c

Feb. 20, 1974
Flt. no. 5, DR; 1325-1630

February 20, 1974 PM
Flight no. 5; 1325-1630
Sea Surface Temperature

CABO BARBAS
ROQUE CHICO
PUNTA GORDA
ROQUE GRANDE

CABO CORBEIRO

SPANISH SAHARA
MAURITANIA

BAIE DU LEVRIER

NOUADHIBOU
CANSADO

LA GUERA
CAP BLANC

17°30'W 17°00'W
22°00'N
21°30'N
21°00'N

KILOMETERS
NAUTICAL MILES

Mercator Projection   Scale 1:750,425 at 22°N
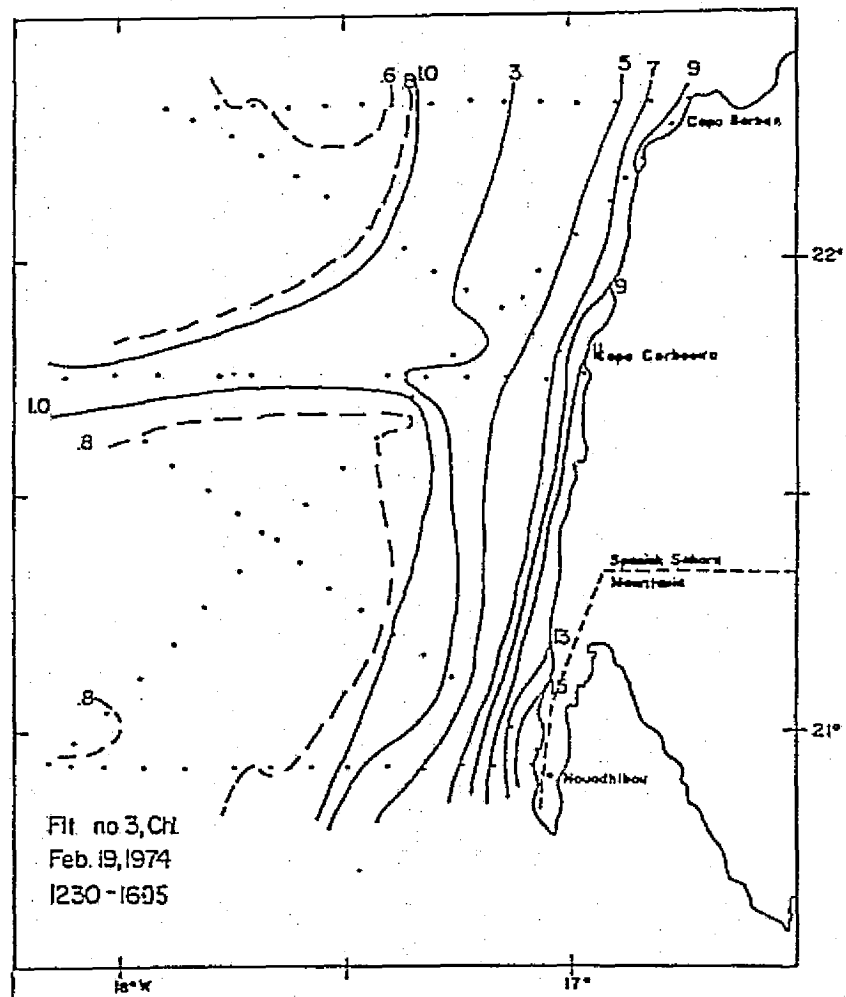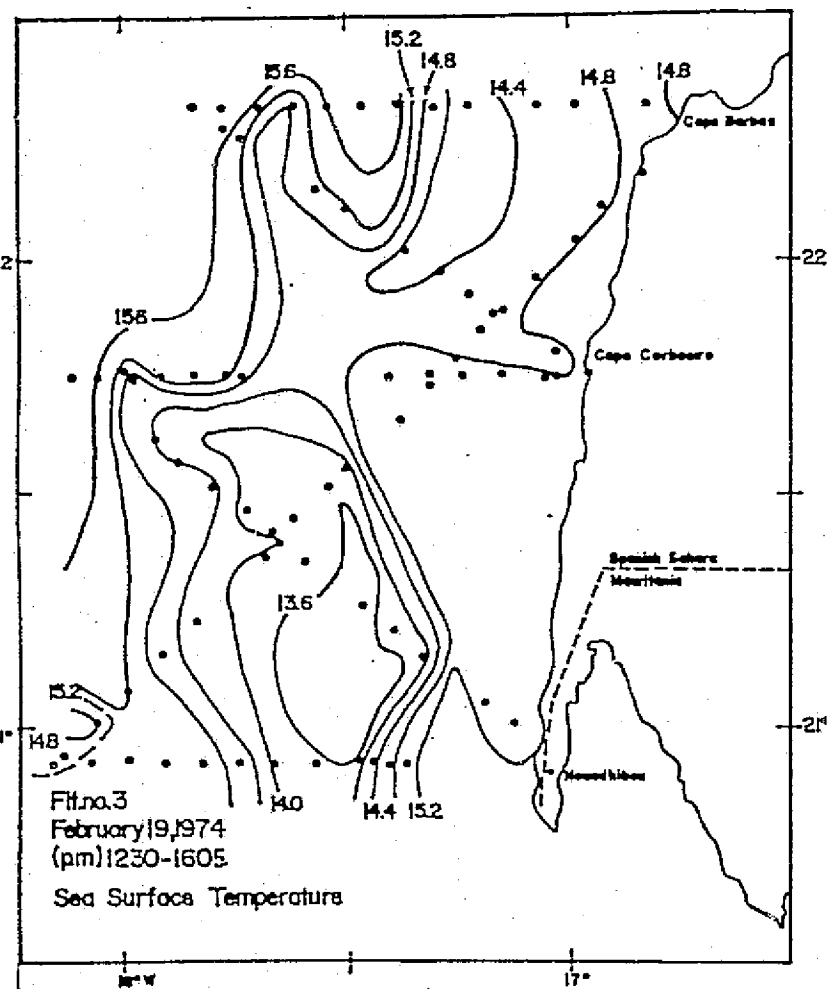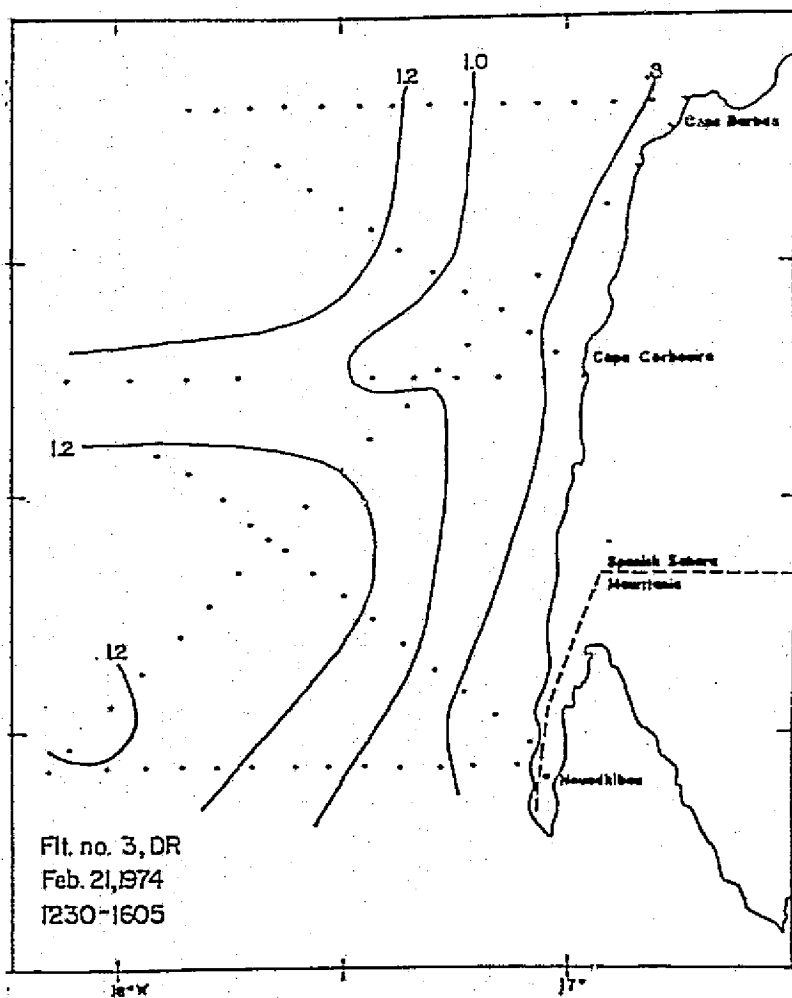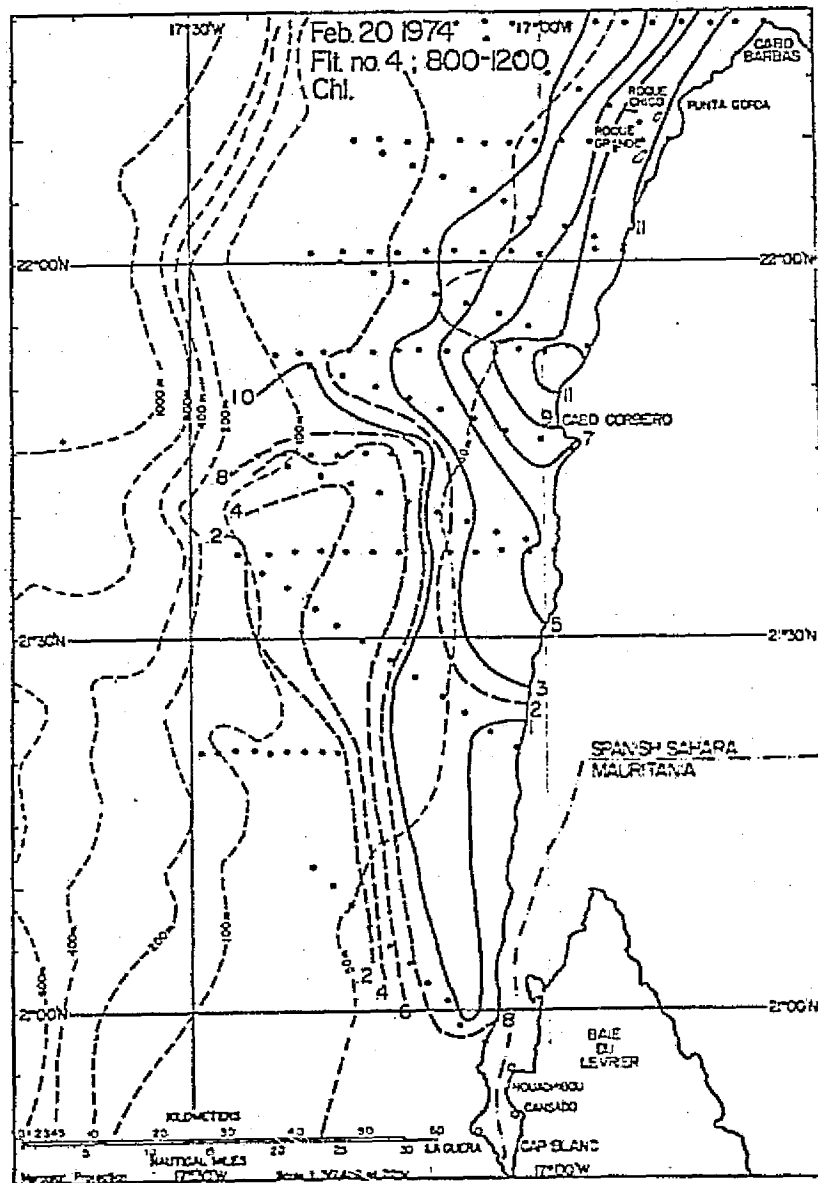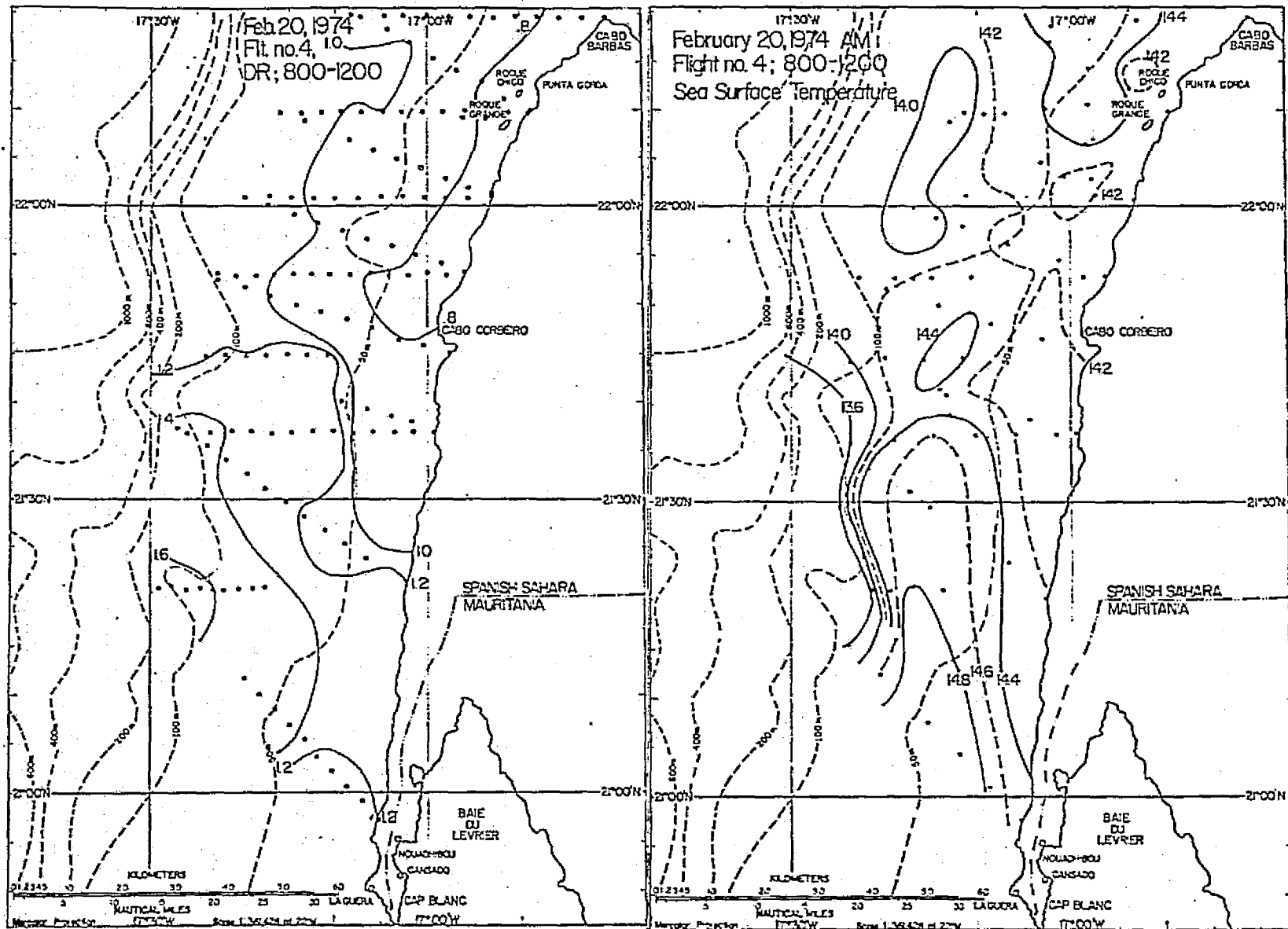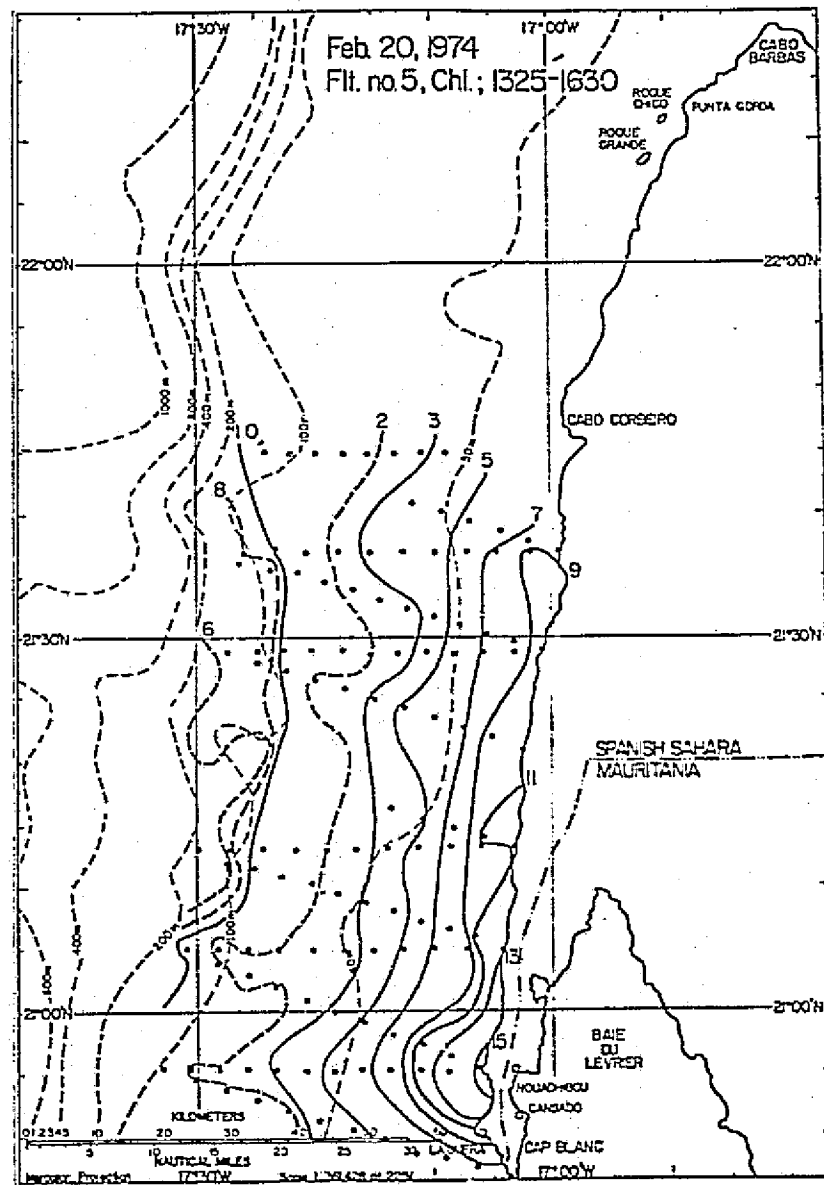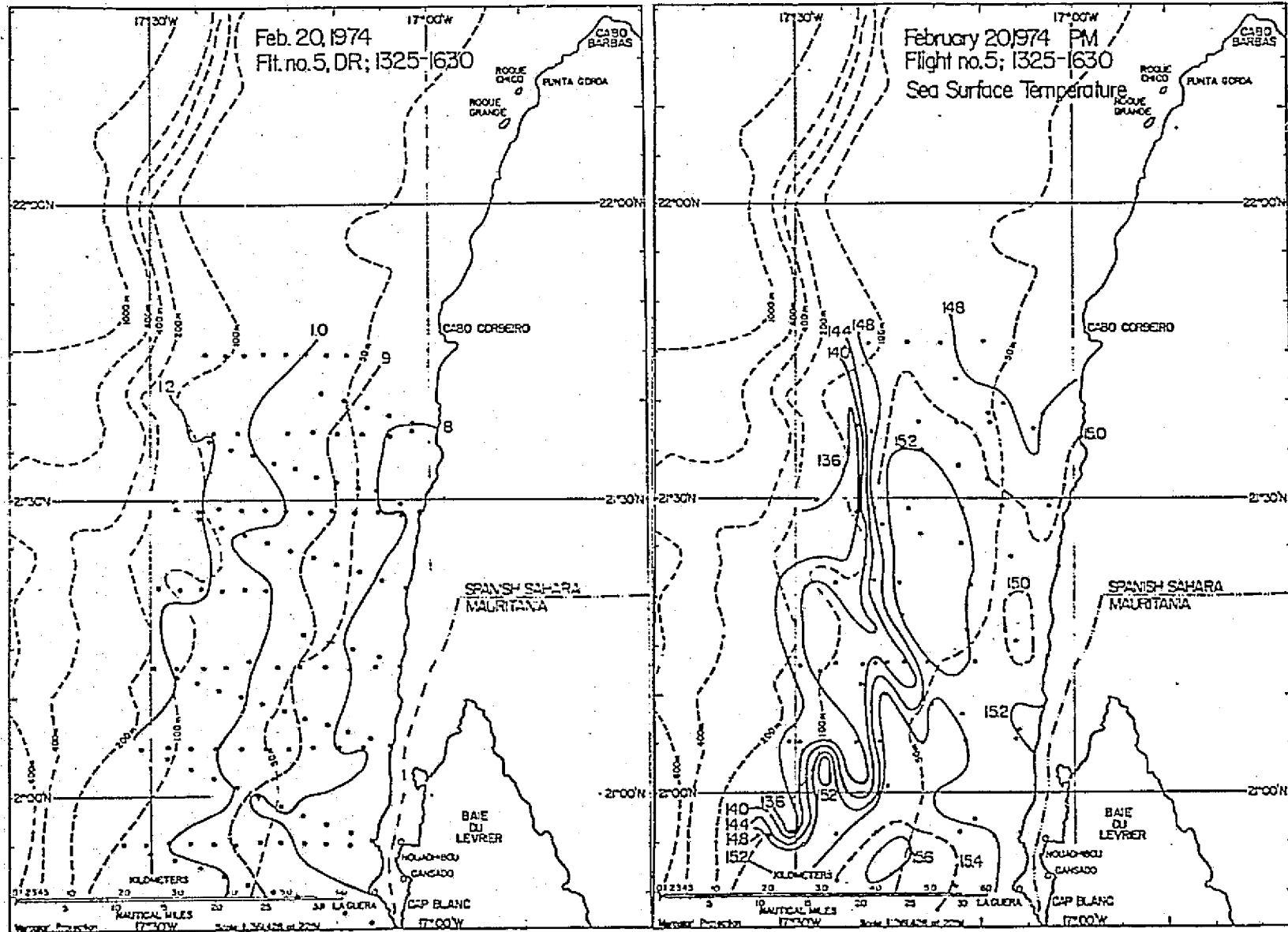
Figure B.6a-c
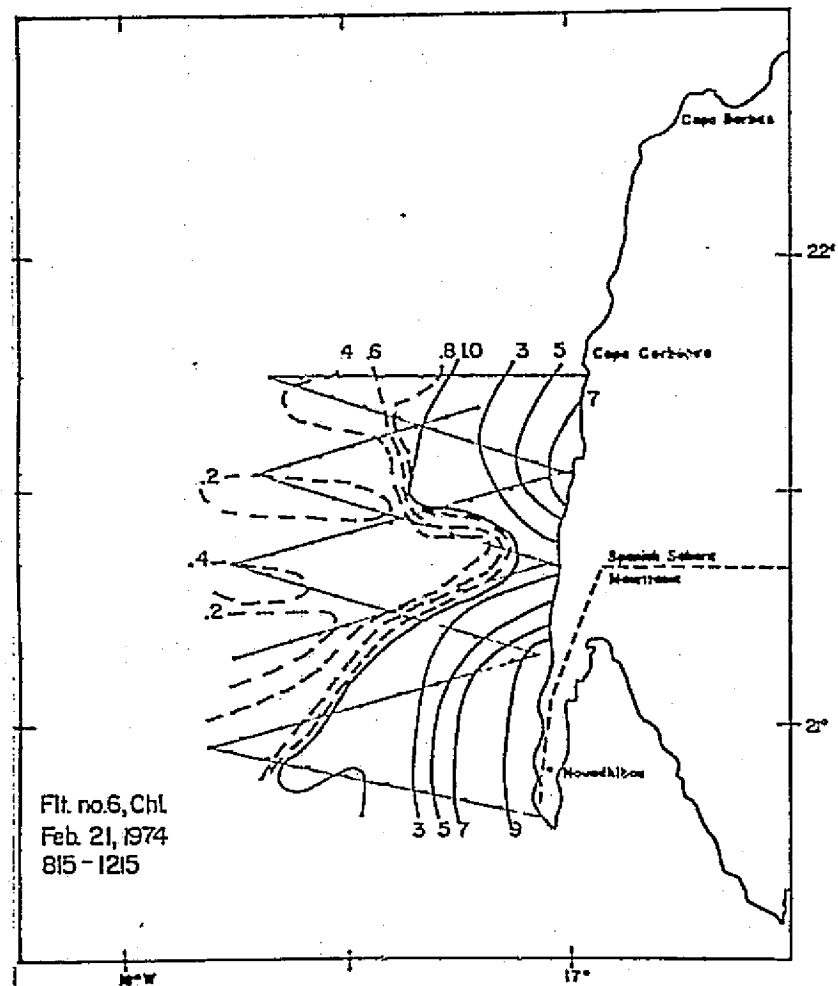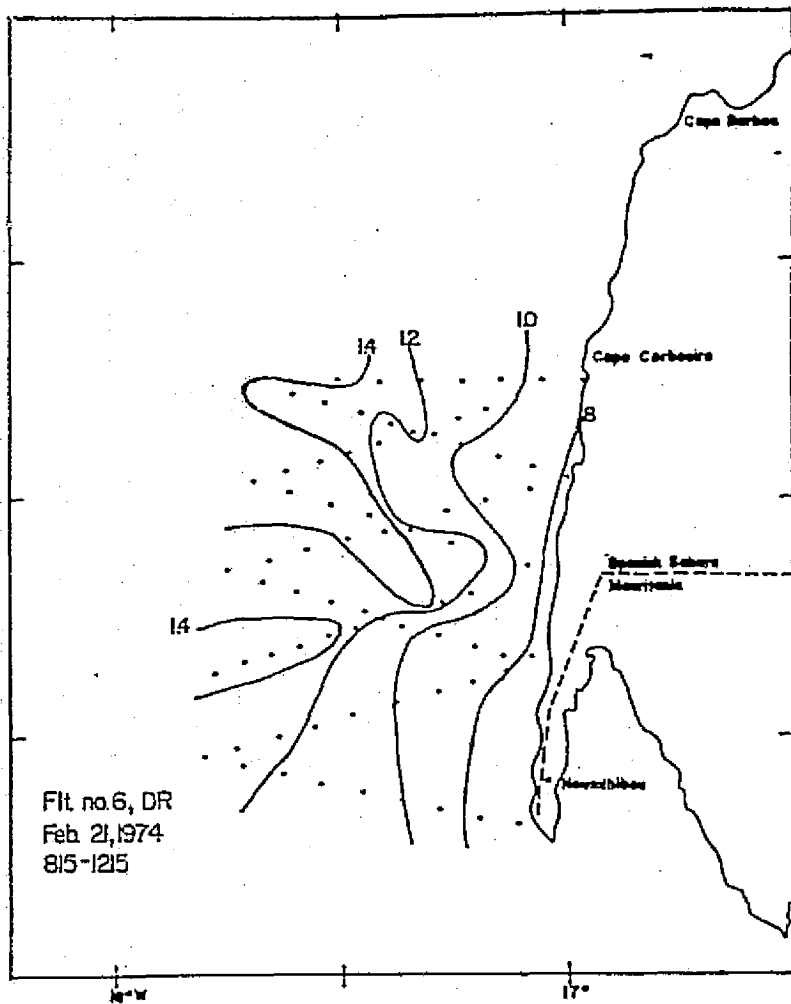
Flt. no.6, DR
Feb. 21,1974
815-1215

February 21,1974 AM
Flight no.6 815-1215
Sea Surface Temperature

Fit. no. 7, Chl.
Feb. 22, 1974
810 - 1140

Figure B.7a

Figure B.7b

February 22,1974 (am)
Flight no. 7 810-1140
Sea Surface Temperature
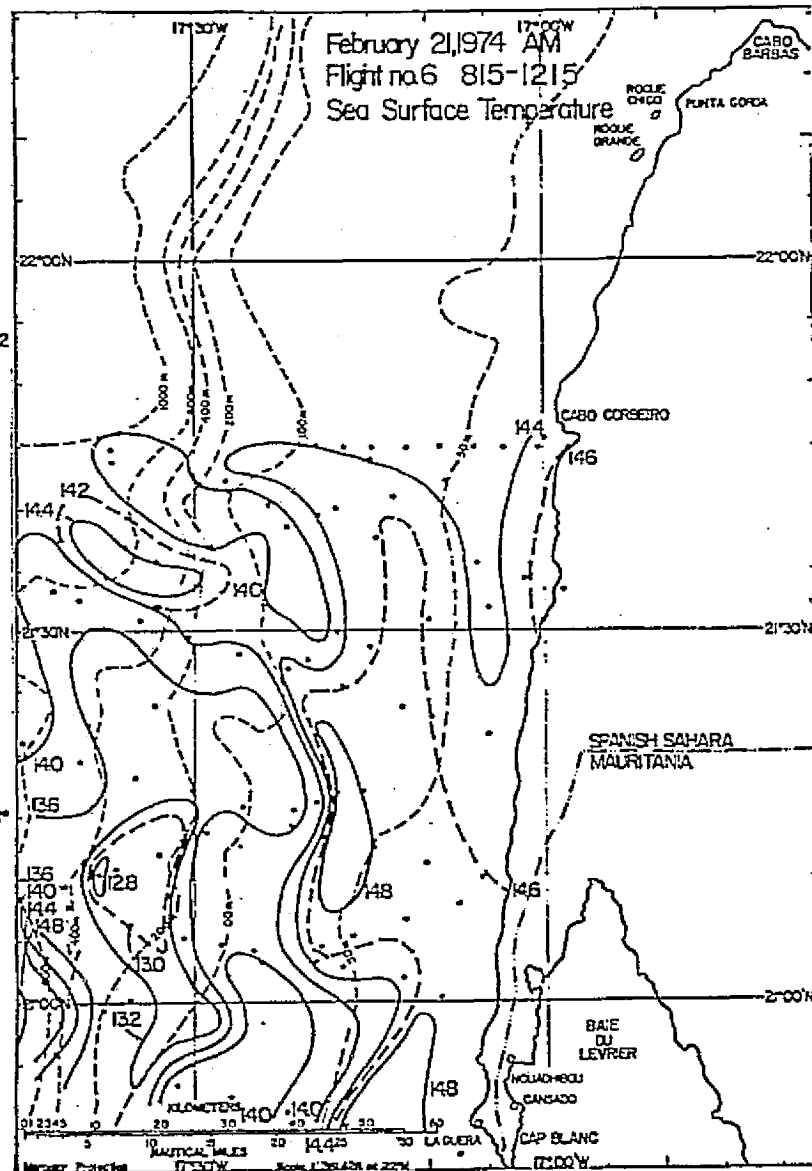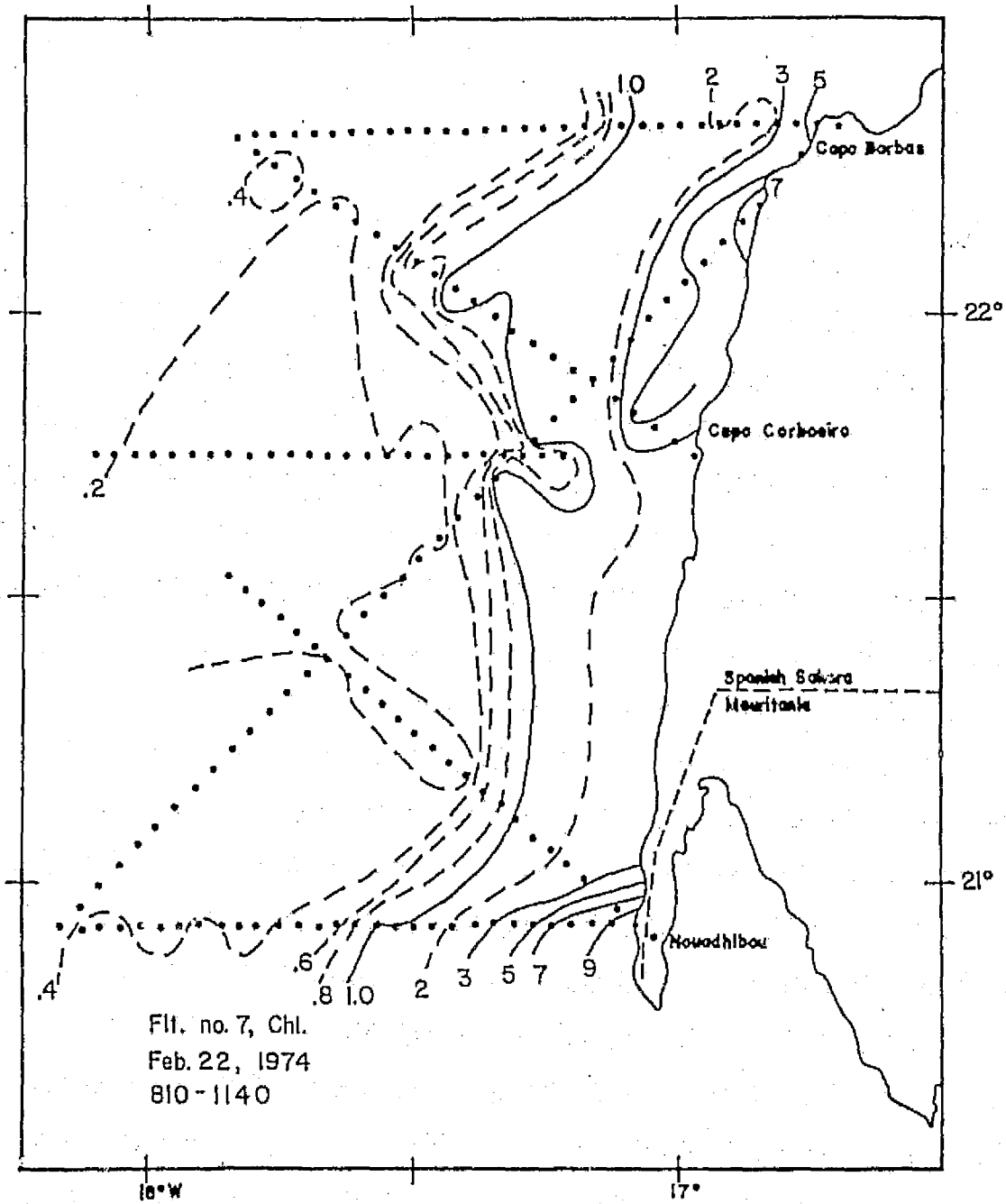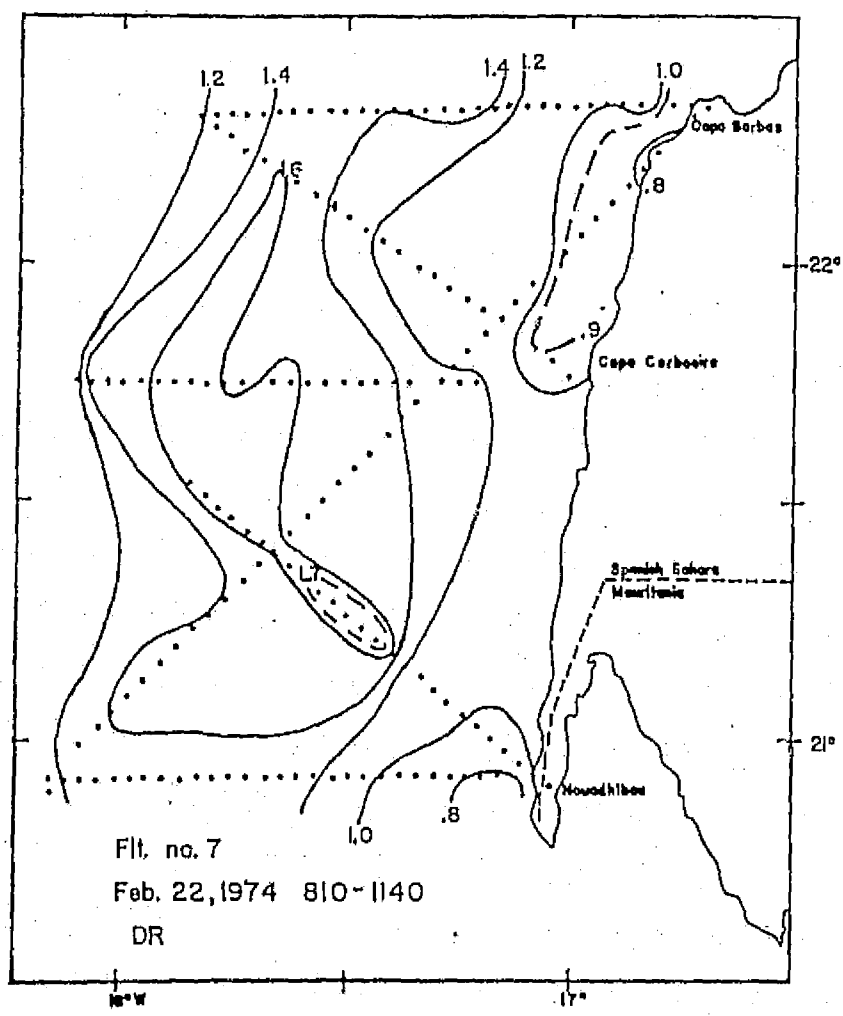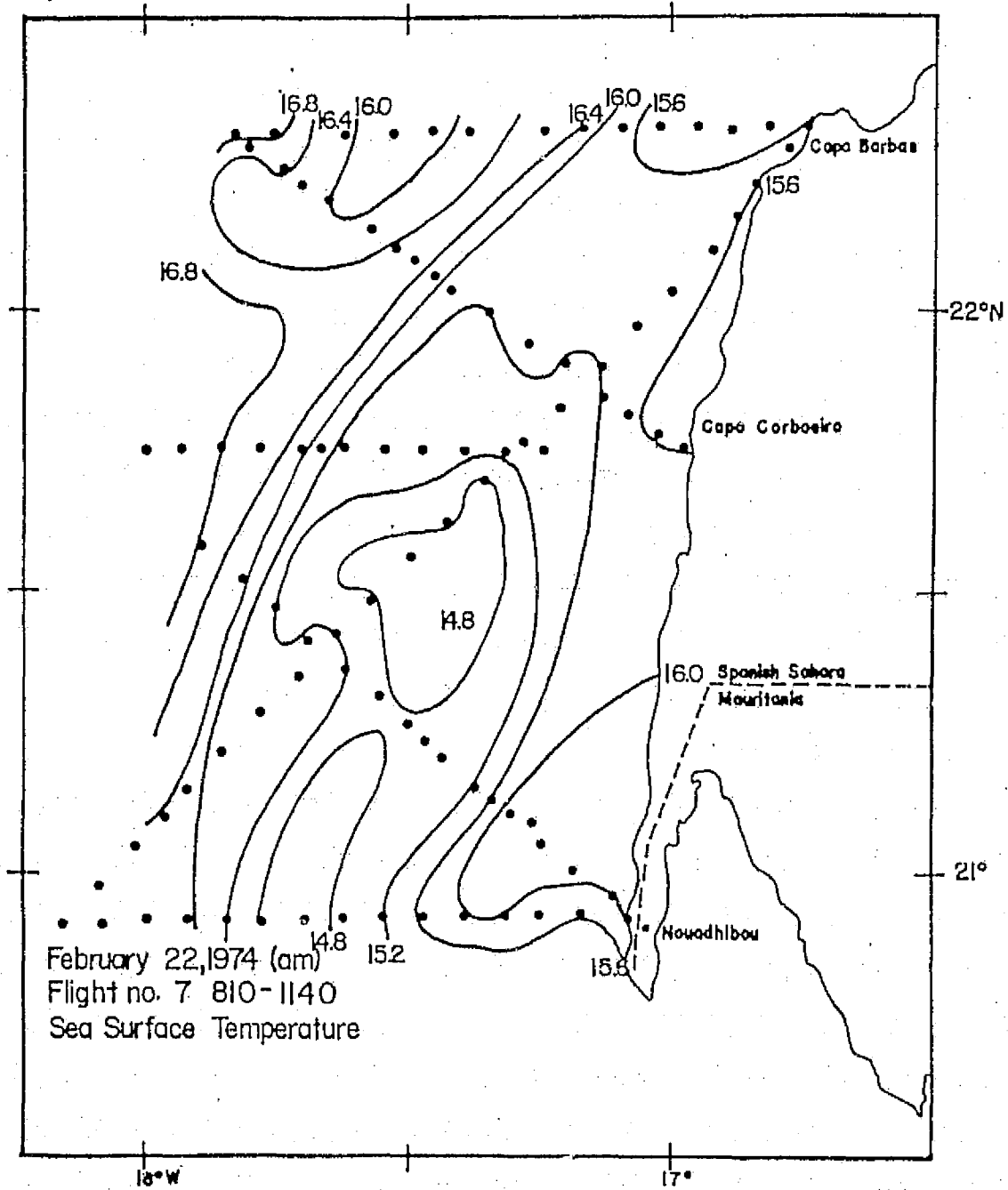
Figure B.7c

Figure B.8c

Figure B.9a-c

March 4, 1974
Flt. no. 9, DR; 1320-1630

March 4,1974   PM
Flight no. 9 ; 1320-1630
Sea Surface Temperature
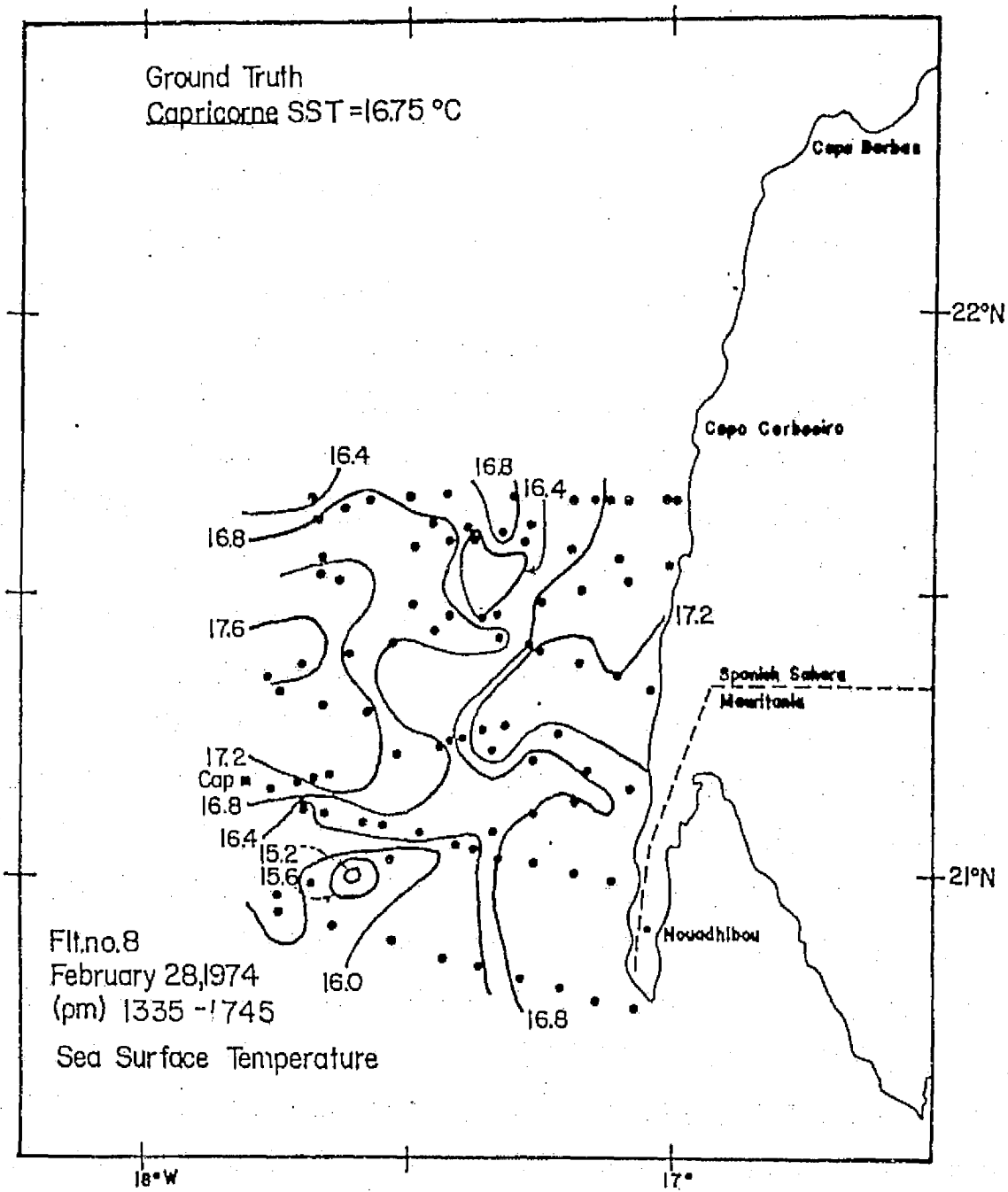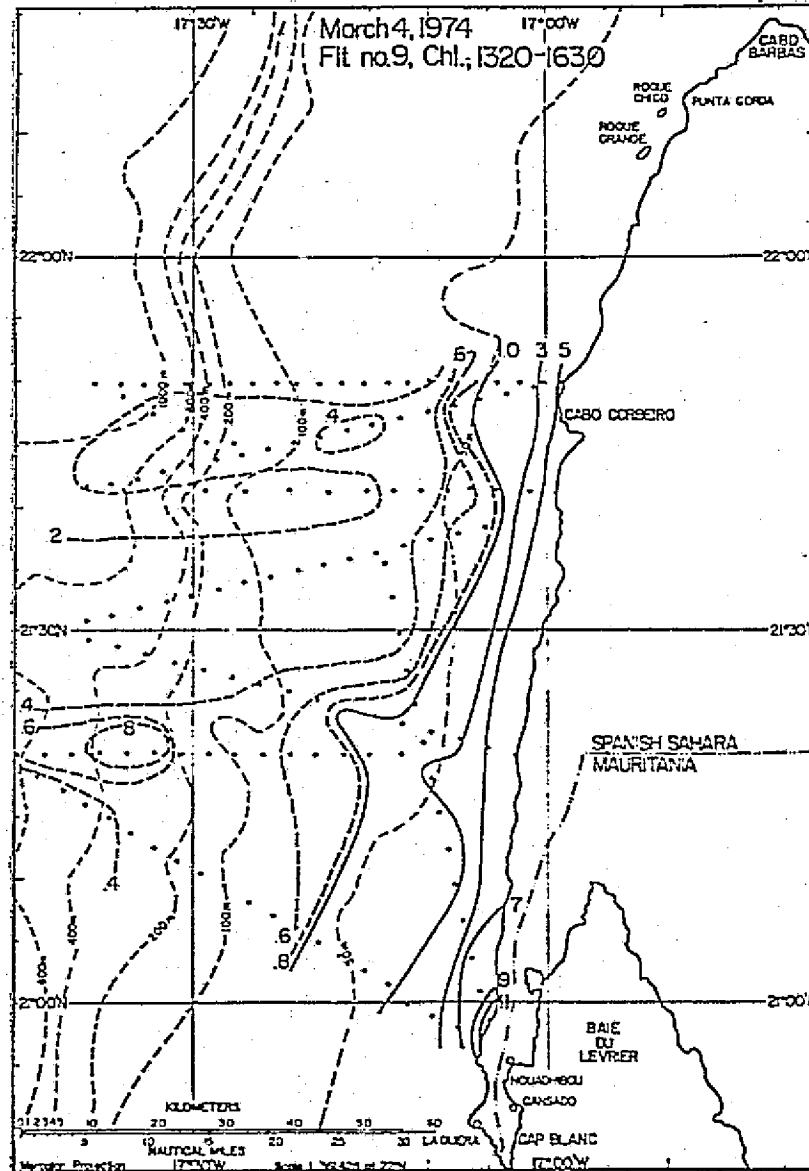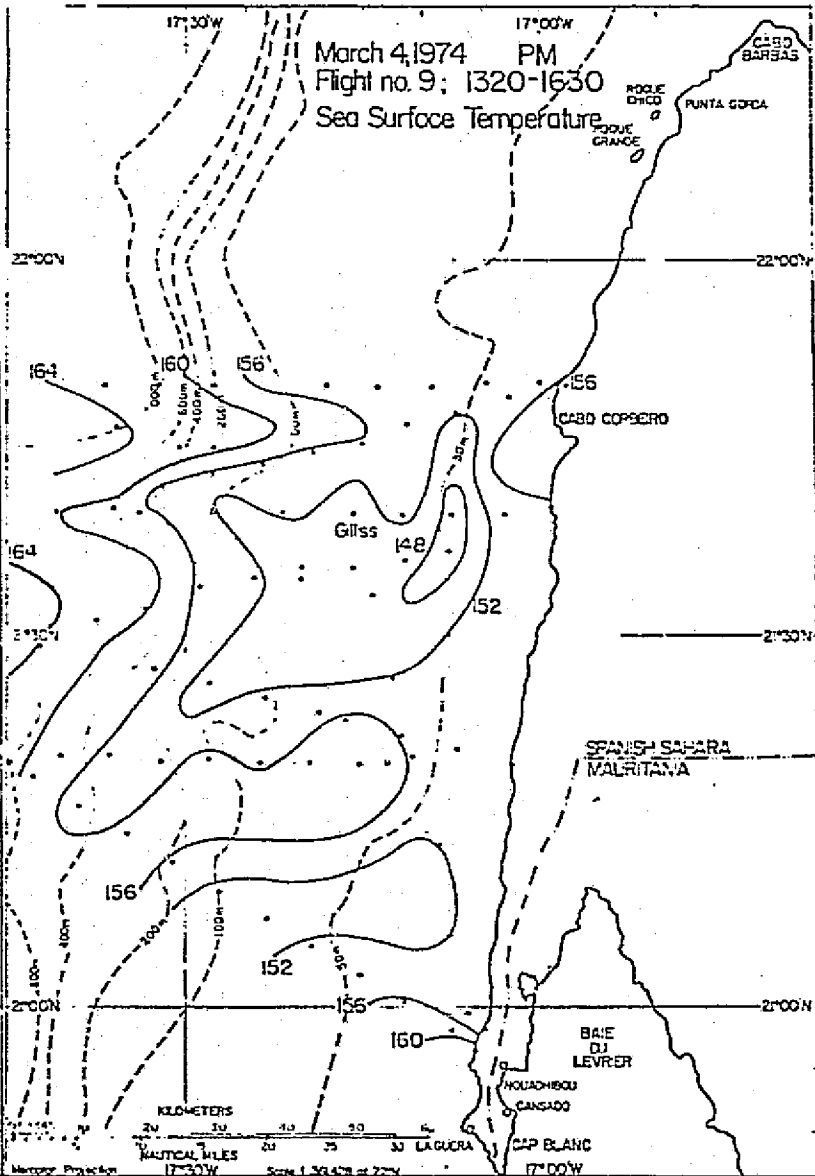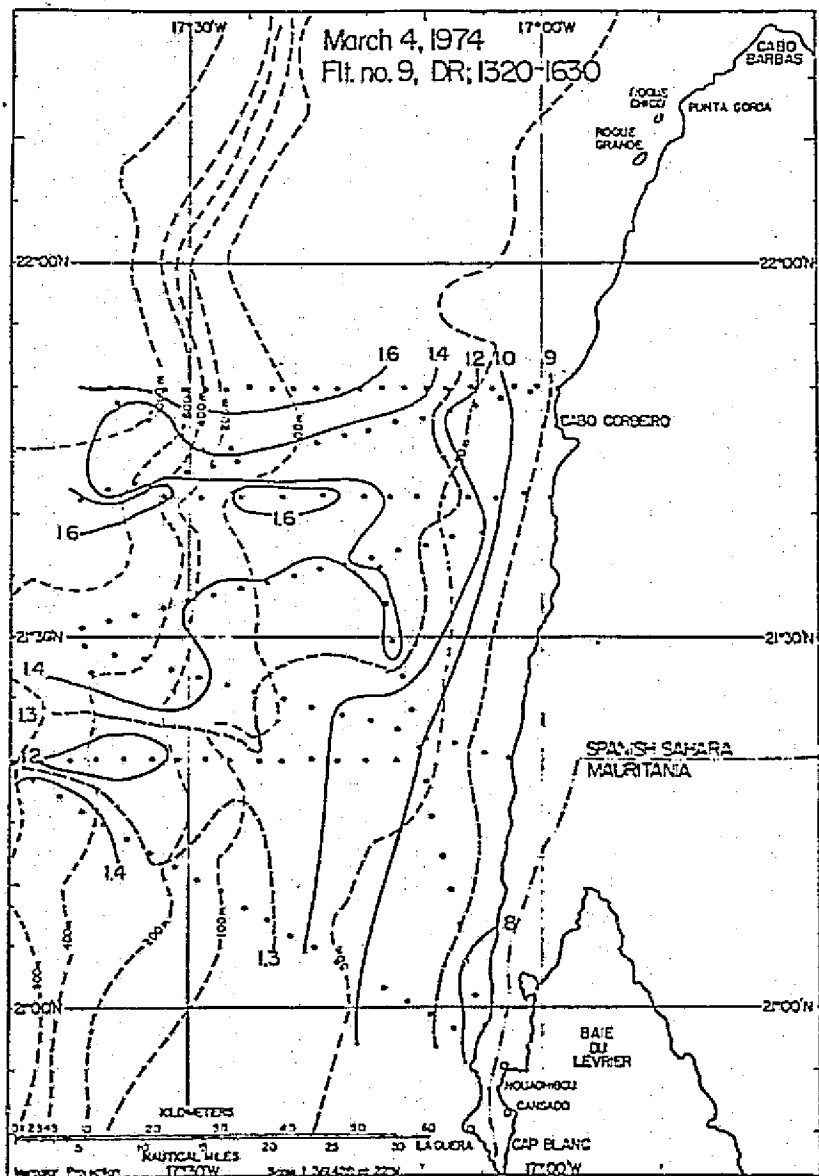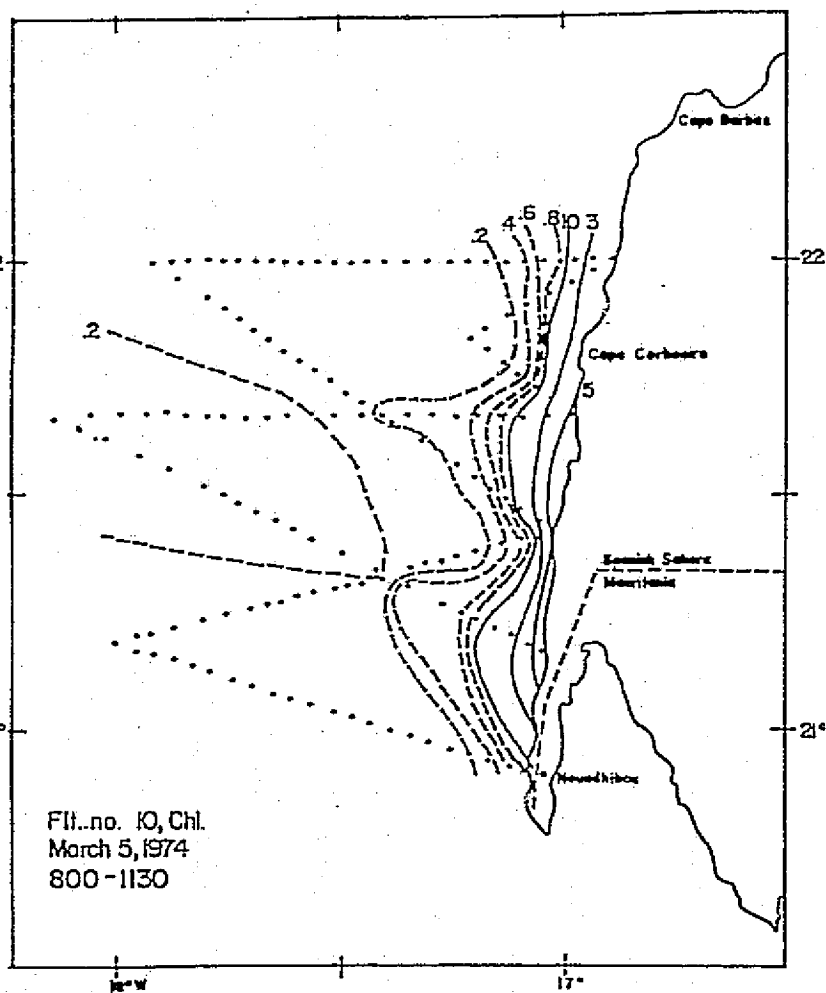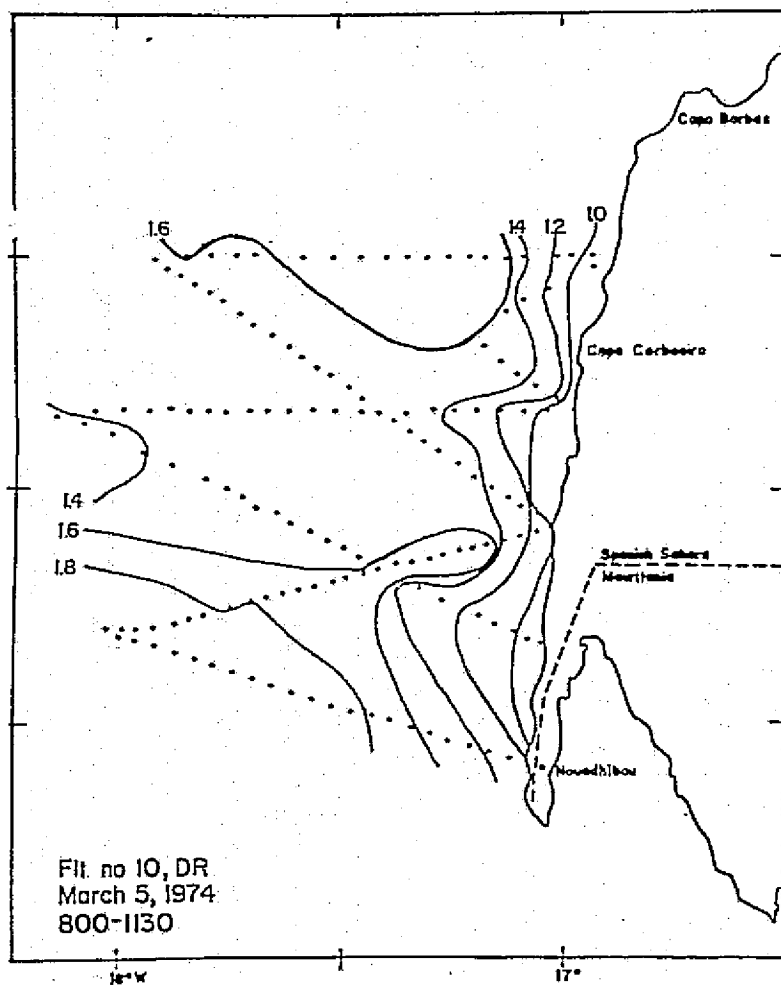
Figure B.10 a+b

Figure B.10c

March 6, 1974
Flt. no 12, Chl. 800-1145

Figure B.11a-c

March 6, 1974
Flt. no. 12, DR 800-1145

March 6, 1974   AM
Flight no. 12, 800-1145
Sea Surface Temperature

Ground Truth
Gilliss 16.97° C

Figure B.12a-c

Flt. no.13, Chl.
March 6,1974
1315 – 1700
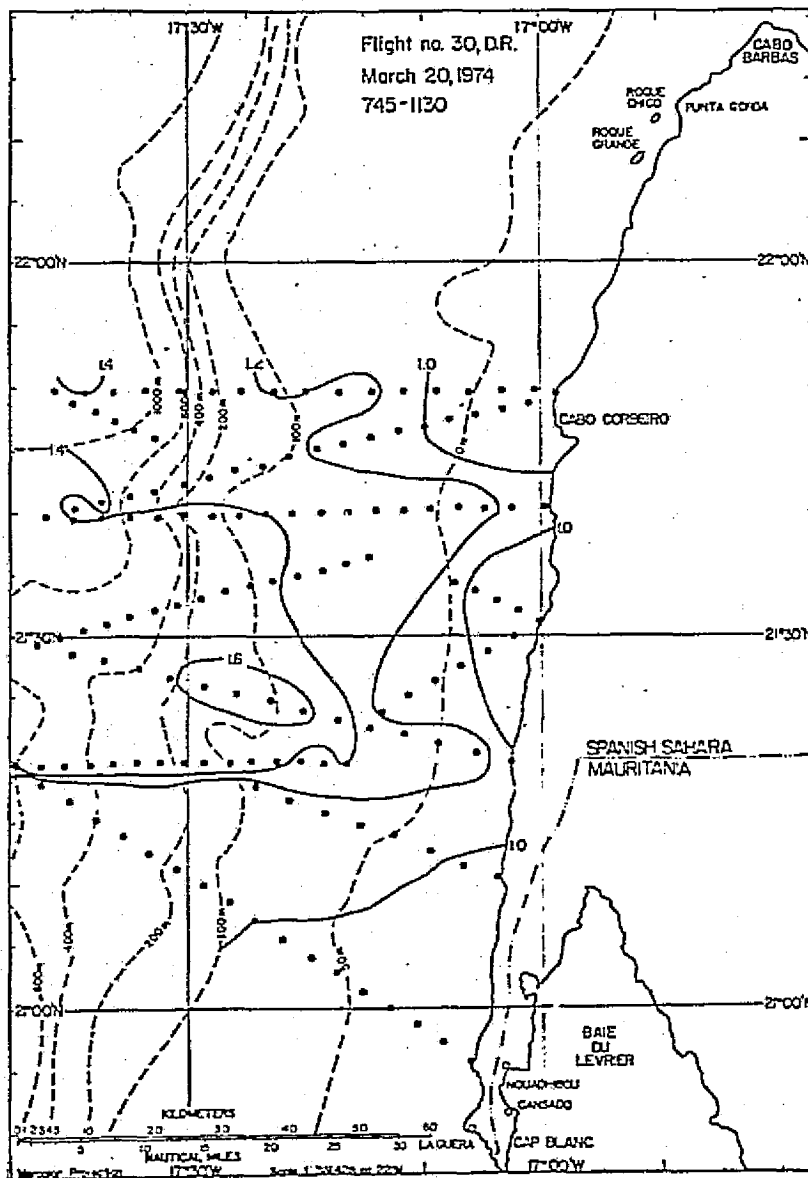
Flt. no. 13, DR
March 6, 1974
1315–1700

March 6, 1974   PM
Flight no. 13; 1315–1700
Sea Surface Temperature
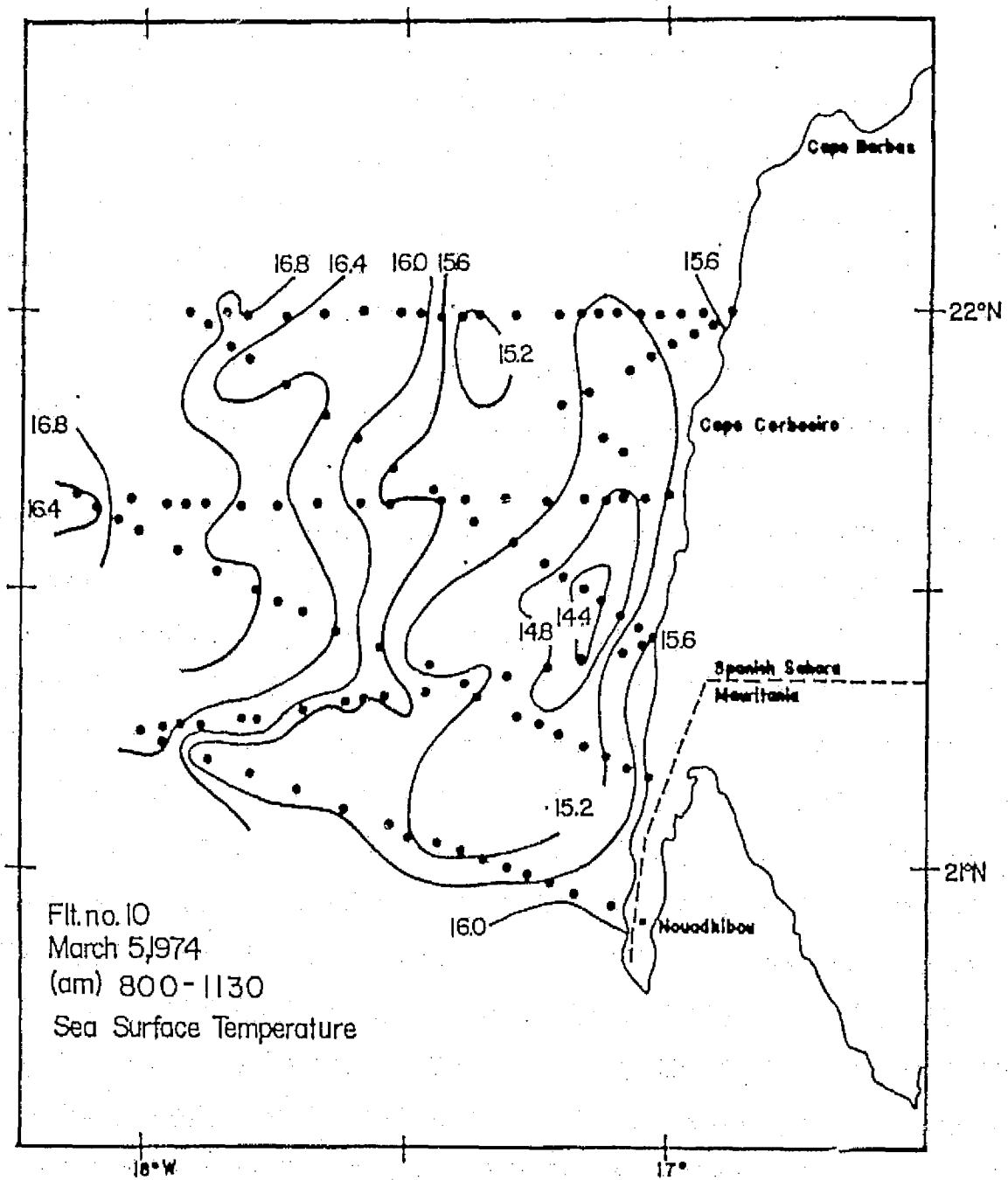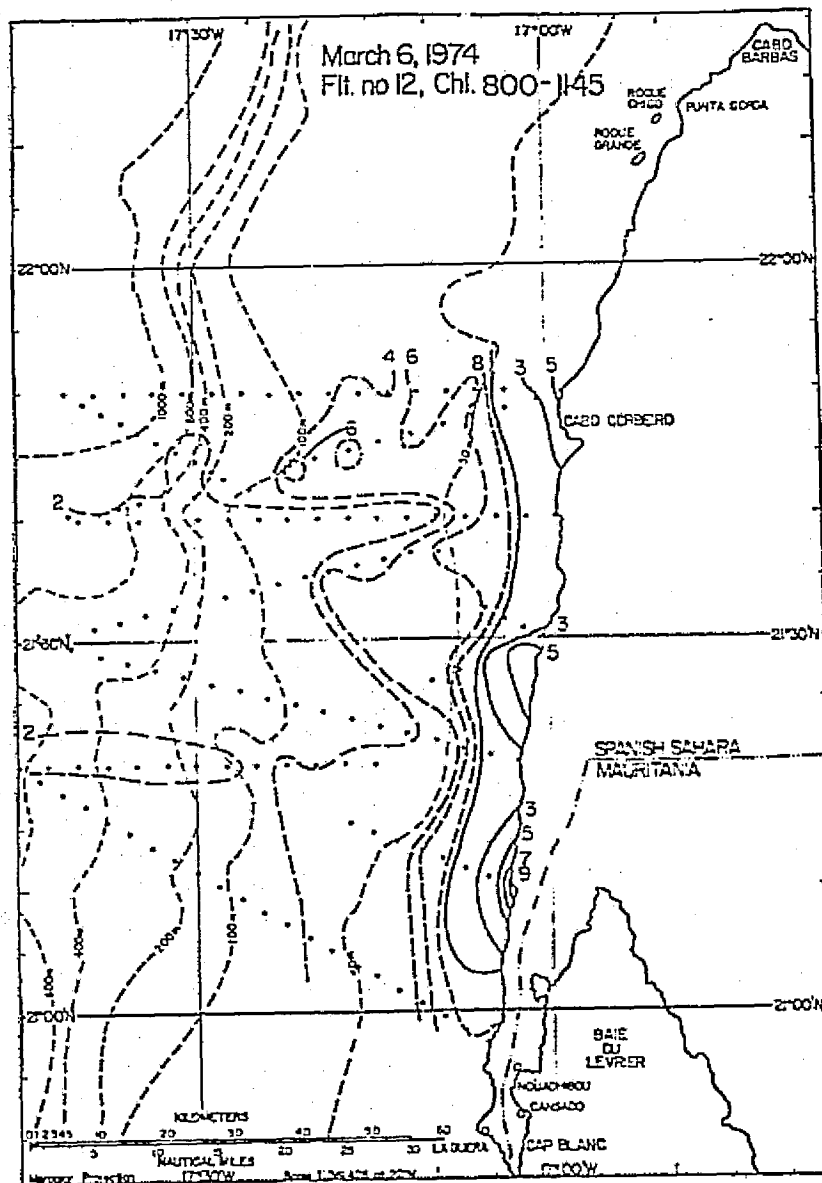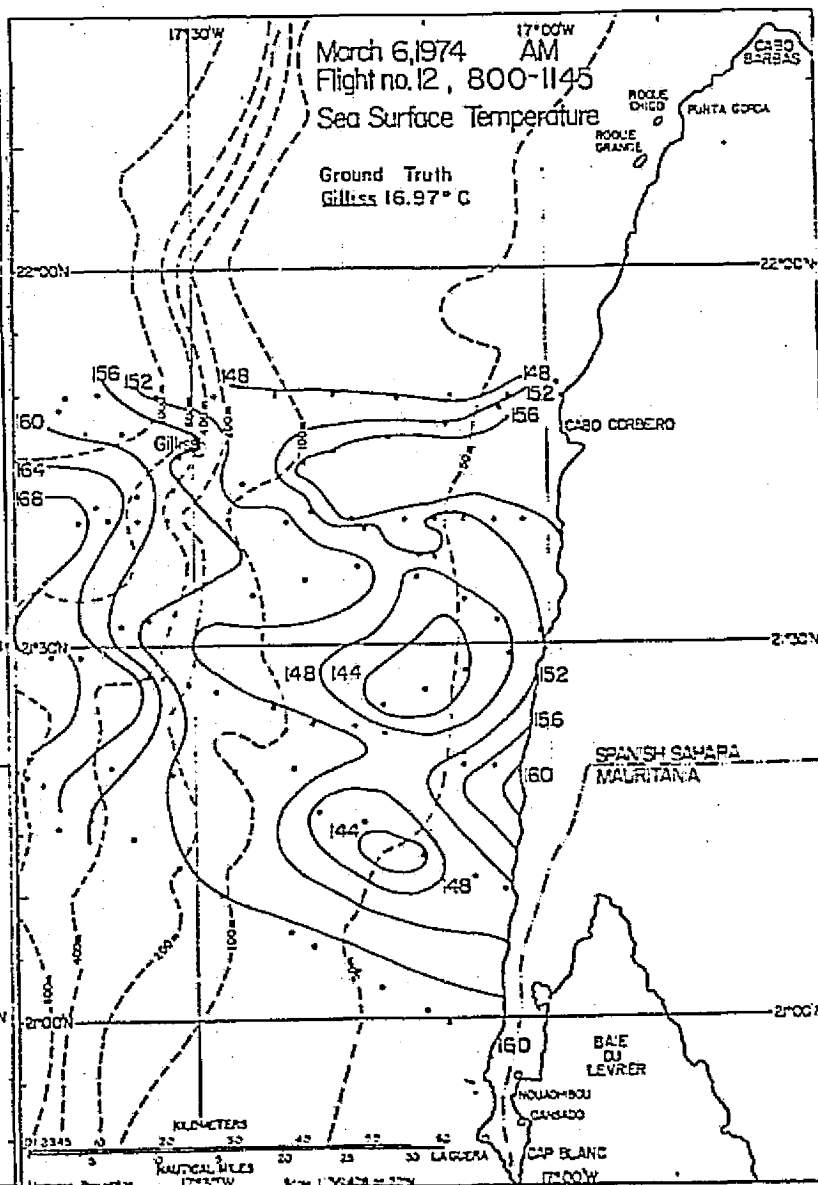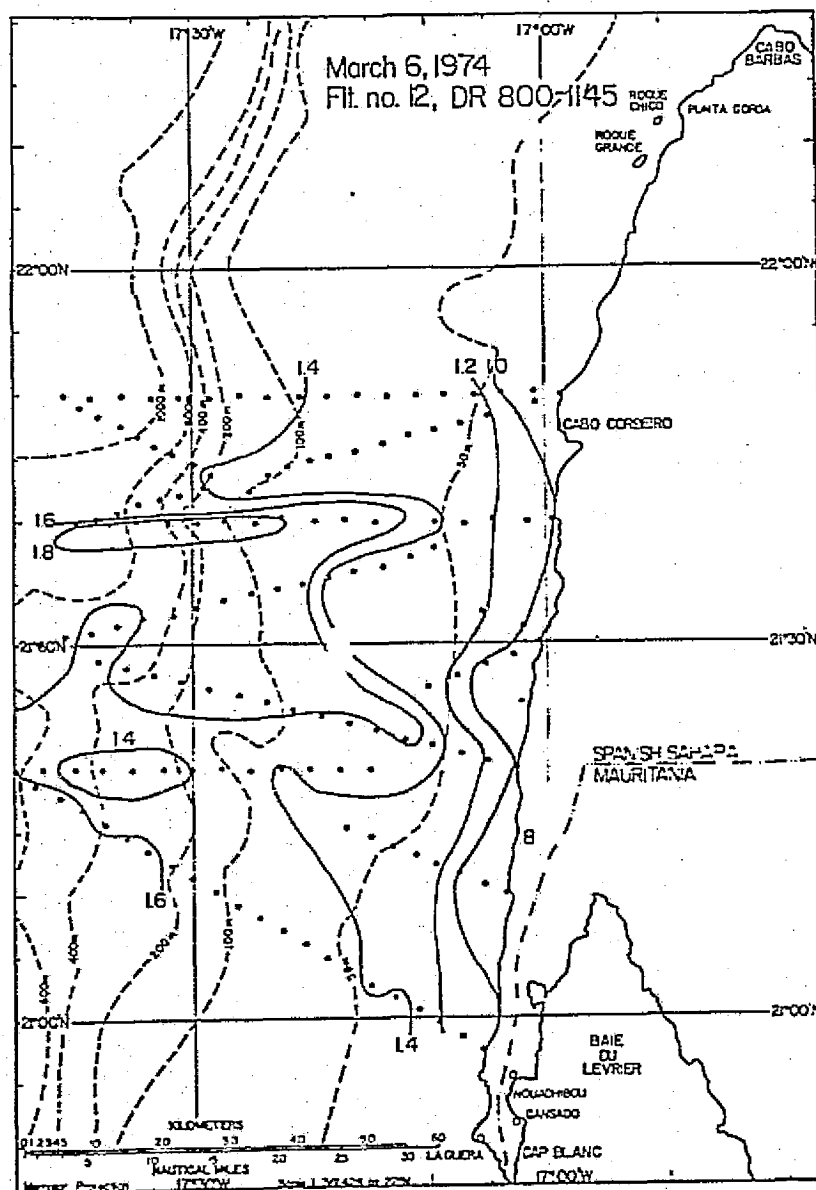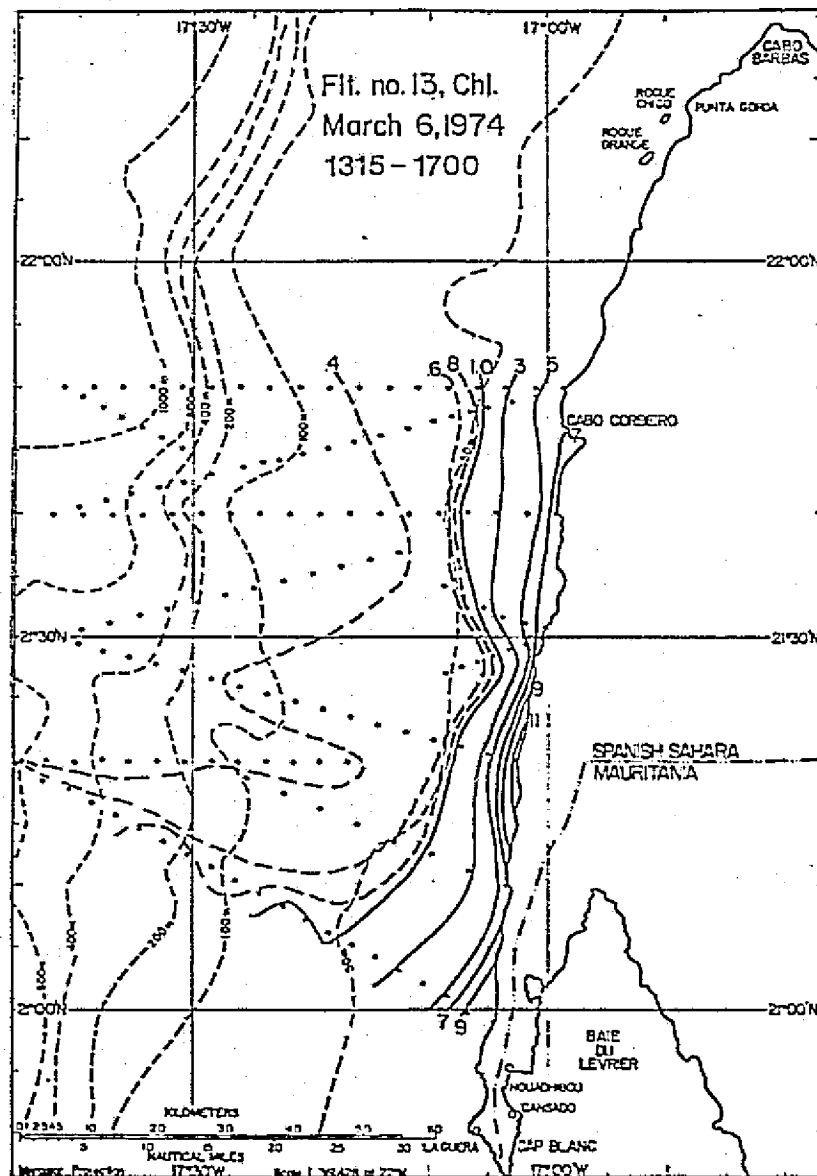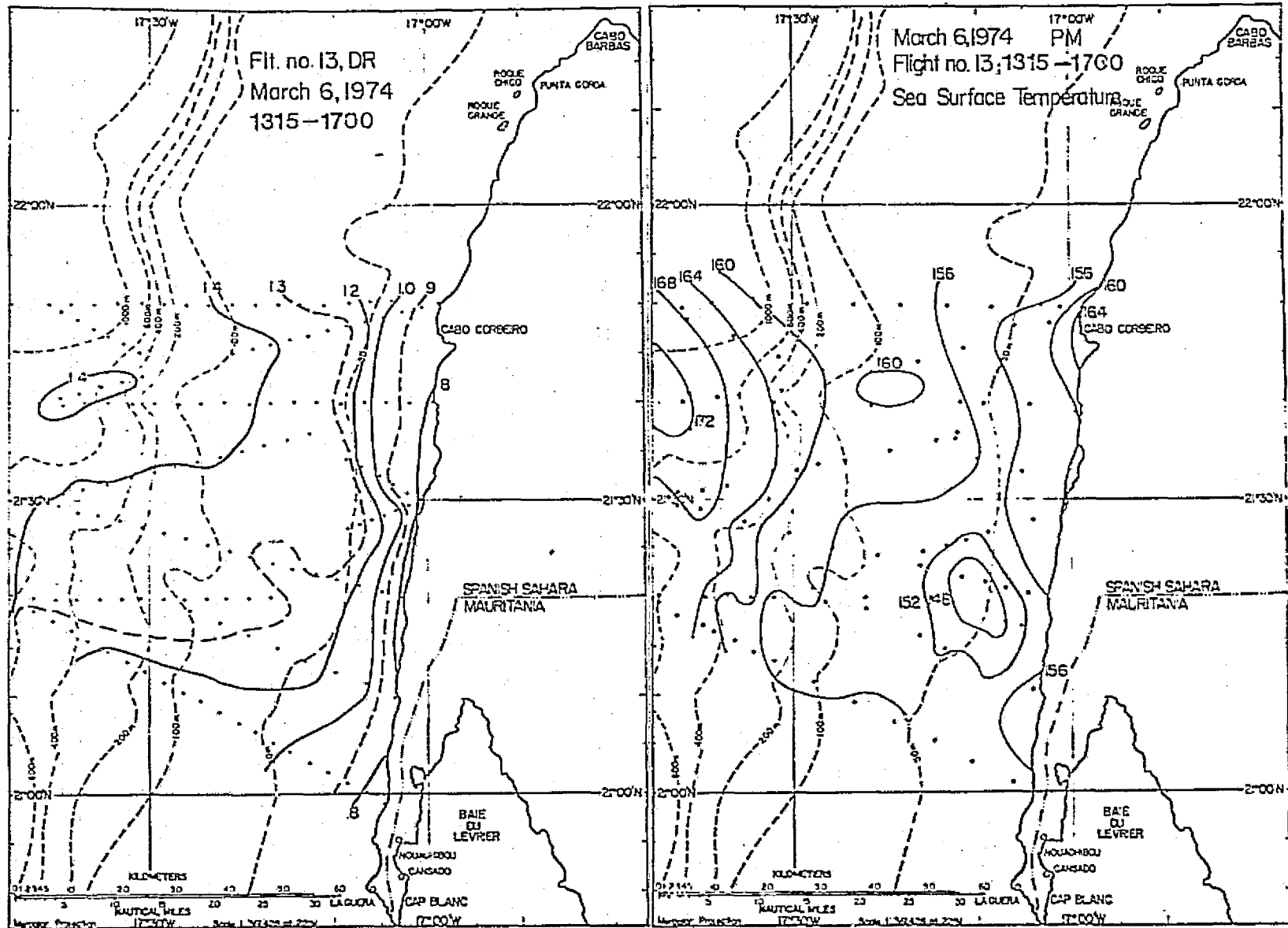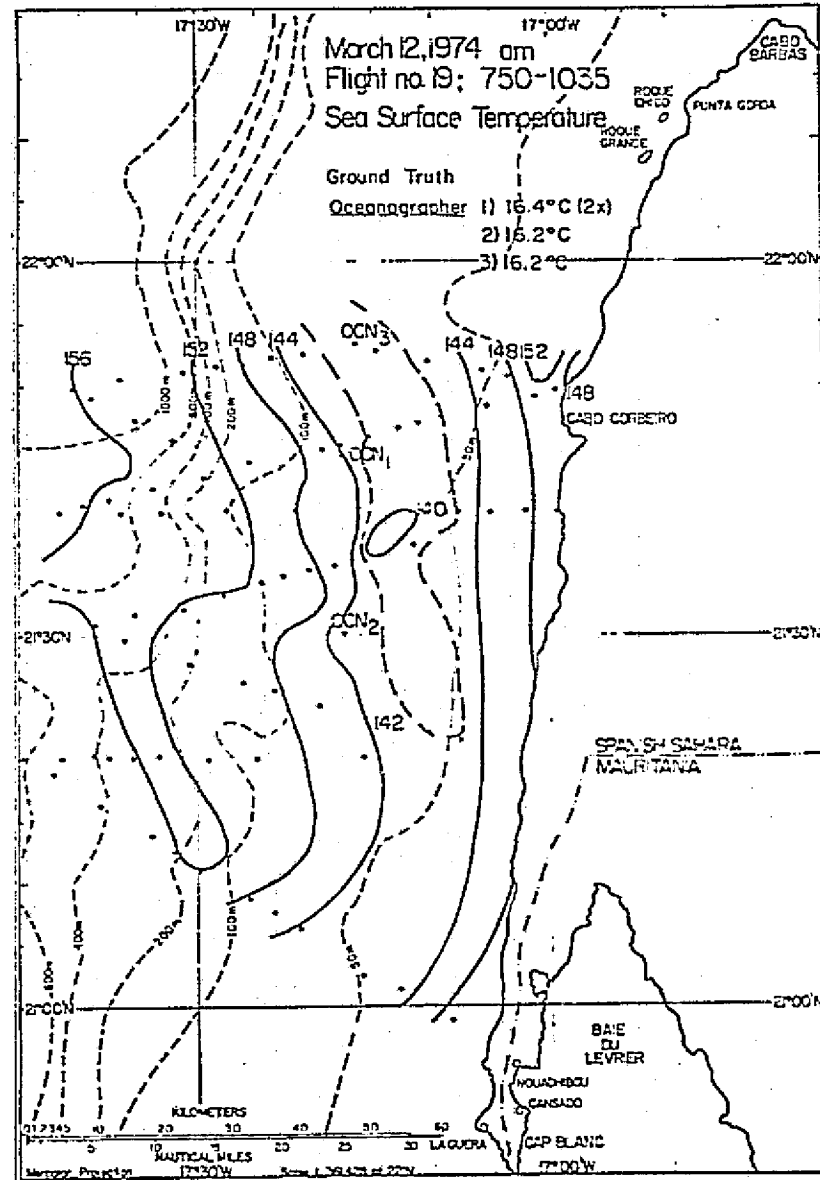
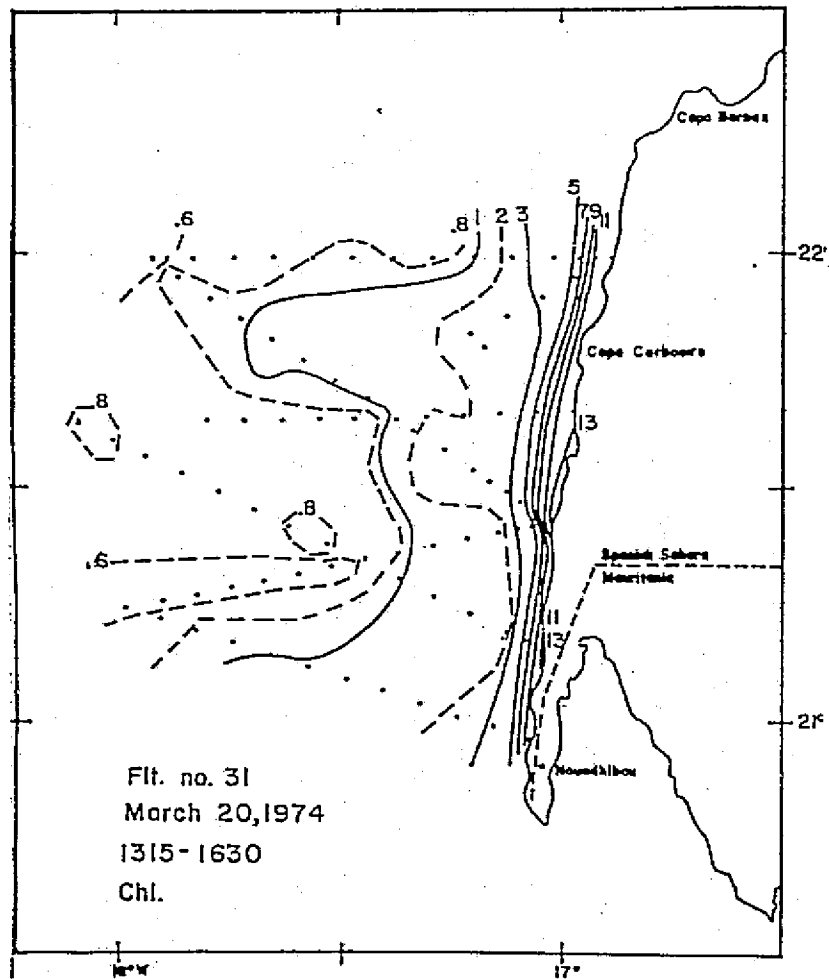Figure B.13c

Figure B.14a-c

Flt. no. 20
March 12,1974
1320-1640
Chl.

Flt. no. 20
March 12, 1974
1320-1640
 DR

Ground Truth (SST)
Gillis SST = 17.2°
Oceanographer 16.2°

Flt. no. 20
March 12, 1974; 1320-1640
Sea Surface Temperature

230

Figure B.15 a-c

Flt. no. 24
March 16,1974
1320-1450
Chl.

Flt. no. 24

March 16,1974

1320-1450

DR

Flt. no. 24
March 16,1974 pm 1320-1450
Sea Surface Temperature

March 20,1974
Flt. no. 30, Chl.
745-1130
Ground truth
Atlantis II 2.0mg/m³

Figure B.16a-c

233

Flight no. 30, D.R.
March 20, 1974
745-1130

March 20,1974   AM
Flight no. 30; 745-1130
Sea Surface Temperature

Ground Truth
Atlantis II 16.9°C

Flt. no. 31
March 20,1974
1315-1630
Chl.

Figure B.17a-c

Flt. no. 31
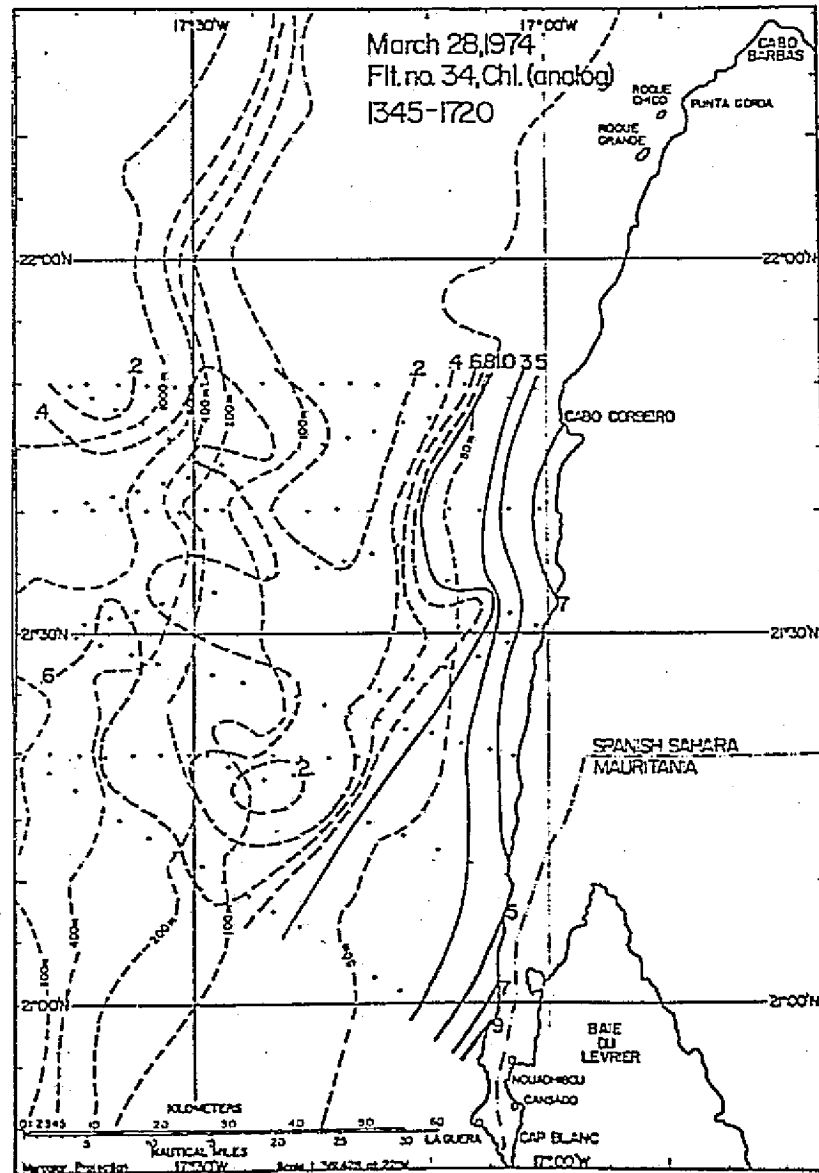March 20, 1974
1315-1630
DR.

Flt no. 31
March 20,1974
(pm) 1315-1630
Sea Surface Temperature

Figure B.18a

Figure B.18c